FLUORINE-18 AS A TRACER IN INORGANIC AND ORGANIC SYNTHESES AND ITS APPLICATION TO POSITRON EMISSION TOMOGRAPHY

BY

RAMAN V. CHIRAKAL, B.Sc., M.Sc.

A Thesis

Submitted to the School of Graduate Studies

in Partial Fulfilment of the Requirements

for the Degree

Doctor of Philosophy

McMaster University

March 1991

TO MY MOTHER C.V. PARVATHY WARRASYAR

AND IN THE MEMORY OF MY FATHER K.W. KRISHNA WARRIER

Doctor of Philosophy (1991) (Chemistry)

McMaster University, Hamilton, Ont.

TITLE: FLUORINE-18 AS A TRACER IN INORGANIC AND ORGANIC SYNTHESES AND ITS APPLICATION TO POSITRON EMISSION TOMOGRAPHY.

AUTHOR: Raman V. Chirakal, B.Sc. (Kerala University, India)

M.Sc. (Brock University)

SUPERVISOR: Professor Gary J. Schrobilgen

NUMBER OF PAGES: xxii, 254.

ABSTRACT

The application of fluorine-18 to the study of inorganic and organic reaction mechanisms has been investigated.

From the distribution of [^{18}F] among the decomposition products of $NF_4^+H^*F_2^-$ it has been shown that the attack of $H^*F_2^-$ on NF_4^+ occurred exclusively on the fluorine and not on the nitrogen contrary to predictions based on bond polarities.

An [^{18}F] exchange experiment between ClF_5 and [^{18}F]FNO showed complete randomization of the [^{18}F] between the two molecules. A ^{19}F NMR study using neat ClF_5 and ClF_5 in anhydrous HF solution in the presence and absence of excess CsF showed slow chemical exchange between ClF_5 and CsF in anhydrous HF at room temperature. Evidence from both [^{18}F] radiotracer and ^{19}F NMR studies has provided conclusive evidence for the existence of the ClF_6^- anion.

Fluorine-18 has also been used as a probe to study the selectivity of F_2 towards aromatic amino acids in different solvents. Differences in reactivity and selectivity of dilute fluorine towards tyrosine and protonated tyrosine in HF and HF/BF_3 respectively, have been exploited for the synthesis of 2- and 3-fluorotyrosine. Results from the radiofluorination of m-tyrosine in different solvents showed that anhydrous HF

is an ideal solvent for the synthesis of [^{18}F]fluoro-m-tyrosine.

Fluorine-18 labelled fluoro-m-tyrosine, has been synthesised and used, in conjunction with Positron Emission Tomography, to study striatal aromatic acid decarboxylase activity in living human brain. It has been demonstrated that [^{18}F]fluoro-m-tyrosine will probably supersede [^{18}F]fluorodopa as the compound of choice to study the dopaminergic pathway in man.

ACKNOWLEDGEMENTS

I would like to thank Dr. Gary J. Schrobilgen and Dr. E. Stephen Garnett for their excellent advice, guidance and encouragement. I very much appreciate the financial support provided by Dr. Garnett. I am grateful to Dr. E.S. Garnett, Director of Nuclear Medicine at Chedoke-McMaster Hospitals, and to the Department of Chemistry for permission to undertake this collaborative venture.

I would also like to thank the members of my supervisory committee, Drs. McGlinchey and McCarry for their support and useful suggestions.

Special thanks are due to Dr. Gunter Firnau and Dr. Claude Nahmias for their advice and the many discussions and assistance throughout my career in Nuclear Medicine. It is a pleasure to acknowledge Mr. Barry Bowen and Ms. Carole Ikeno, constant supporters during the past thirteen years.

Sincere gratitude must be given to Dr. Karl Christe, Rocketdyne, Rockwell International Corporation, Canoga Park, California, for his collaboration and for supplying the materials for inorganic exchange experiments. Thanks are extended to Dr. Jeremy C. P. Sanders for his expertise in variable temperature NMR experiments and the many helpful discussions during the past three years.

I gratefully acknowledge the co-operation of Mr. Brian Sayer and the excellent technical assistance on NMR from Dr.

Don Hughes. I wish to thank Mr. Adel Emara, Mr. Henry Harms and Ms. Kay Brown for their technical help.

My career would not have begun without the help and advice from my brother Dr. C.V. Krishnan and my friend Dr. P.S. Ramanathan.

I want to thank my dearest friend, Bev Kenyon, for his valued friendship that has lasted for so many years. His assistance in starting my career in the Department of Nuclear Medicine is gratefully acknowledged.

Above all, I wish to acknowledge the important contribution of my wife Janet for her patience, continued support and understanding.

TABLE OF CONTENTS

LIST OF TABLES

LIST OF FIGURES

CHAPTER 1

INTRODUCTION

A. General

Naturally occurring fluorine is monoisotopic. However, a number of radioactive isotopes of fluorine such as ^{17}F, ^{18}F, ^{20}F and ^{21}F have been produced since the 1930's. The inorganic chemistry of stable fluorine (^{19}F) has received increasing attention since elemental fluorine was first isolated and numerous inorganic fluorides were prepared and studied by Moissan over 100 years ago.[1] Virtually every aspect of modern life is in some way affected by compounds of fluorine.[2] For example, during the Manhattan Project, uranium hexafluoride was used for the enrichment of ^{235}U; sulphur hexafluoride because of its extraordinary stability and dielectric properties, is extensively used as an insulating gas for high voltage generators and switch gear. Other fluorine containing compounds have found their use in plastics, stable solvents, anaesthetics, lubricants and refrigerants. The great oxidizing strength of F_2 and many of its compounds with nitrogen and oxygen has been applied to the development of rocket propellants.

Despite the extensive chemistry of ^{19}F, only a limited amount of work has exploited the use of other isotopes of fluorine in the study of chemical reactions. This is mainly

due to the short half-lives of the radioactive fluorine isotopes which makes it a prerequisite to have isotope production facilities close to the research laboratories.

B. Isotopes of Fluorine

The radioactive isotopes of fluorine are all man made. They are listed in Table 1.1. ^{17}F and ^{18}F have a deficit of neutrons and decay by positron emission; ^{20}F and ^{21}F have a surfeit of neutrons and decay by negative beta emission. Only ^{20}F and ^{18}F have been used as radiotracers in chemical studies. The half-life of ^{20}F is only 10 sec. (Table 1.1) yet it has been used in neutron activation analysis to determine traces of fluoride impurity in barite and calcium phosphate.[3]

Fluorine-18 has a sufficiently long half-life (110 min.) to be useful as a radiotracer. However, a major limitation is that the production of ^{18}F and the subsequent experimental work must normally be carried out within 3 or 4 half-lives. The 511 keV γ-photons resulting from the annihilation of the 0.64 MeV positron emitted during the decay of ^{18}F can be easily detected using routine nuclear detectors making ^{18}F a useful isotope with which to study inorganic reaction mechanisms and metabolic pathways of biologically active fluoro-organics.

Table 1.1 Isotopes of Fluorine

Nuclide	Decay Mode	Product	Half-Life	Year of Discovery	Ref.
^{17}F	β^+	^{17}O	60 sec	1935	4
^{18}F	β^+	^{18}O	110 min.	1937	5
^{19}F	stable			1812	6
^{20}F	β^-	^{20}Ne	10 sec	1935	7
^{21}F	β^-	^{21}Ne	5 sec	1955	8

C. Production of ^{18}F

Several methods have been used to produce ^{18}F and they are compiled in a review by Worthington.[9] The most commonly used methods for the production of ^{18}F are given in Table 1.2.

Methods 1, 2 and 3 yield carrier-free ^{18}F. The product of the nuclear reaction $^{16}O(t,n)^{18}F$ (method 1) is contaminated with radioactive tritium because the initial reaction in this method involves $^{6}Li(n,\alpha)^{3}H$. Methods 4 and 5 yield ^{18}F without other radionuclidic impurities; however, because the target material contains ^{19}F, the product is not carrier free.

The $^{18}O(p,n)^{18}F$ reaction has a cross section of 200-700 mb for protons with energies 4-6 Mev. This method has proved to be the most efficient reaction for the production of large quantities of carrier-free ^{18}F in the form of ^{18}F-fluoride after the irradiation of $[^{18}O]H_2O$. However, its utility in producing large amounts of pure $[^{18}F]F_2$ gas is still being developed.[10] The reaction $^{20}Ne\ (d,\alpha)^{18}F$ produces pure $[^{18}F]F_2$ with low specific activity and a radiochemical yield that is dependant upon the energy of the deuteron beam and the target conditions. Usually, the $[^{18}F]F_2$ is extracted from the target by adding F_2 to the target gas; this method has been used for all the $[^{18}F]$ experiments described in this work.

Table 1.2. Methods for the Production of ^{18}F

Method	Nuclear Reaction	Source
1	$^{16}O(t,n)^{18}F$	Reactor, triton from $^{6}Li(n,\gamma)^{3}H$
2	$^{18}O(p,n)^{18}F$	Cyclotron, Accelerator
3	$^{20}Ne(d,\alpha)^{18}F$	Cyclotron, Accelerator
4	$^{19}F(n,2n)^{18}F$	Reactor, Neutron generators
5	$^{19}F(d,t)^{18}F$	Cyclotron, Accelerator

D. Applications of ^{18}F as a Radiotracer

1. Inorganic Chemistry

The use of ^{18}F for the determination of labilities of element-fluorine bonds and identification of reaction intermediates has been reviewed.[11] The use of ^{18}F is particularly important in experimental studies relating to syntheses of high-oxidation state hypervalent fluorine compounds of nitrogen and chlorine. These compounds are highly energetic and often may possess short lifetimes. Because of their highly corrosive nature, these unstable and reactive species may be difficult or impossible to identify using standard spectroscopic techniques and kinetic measurements. However, studies using ^{18}F-labelled compounds are very useful, and are often the only method for determining the nature of short-lived intermediates and the labilities of element-fluorine bonds.

For example, the relative distribution of ^{18}F in BF_3 and SF_4 after the decomposition of $B^*F_3SF_4$ adduct has provided evidence for the existence of fluorine bridging in $BF_4^-SF_3^+$ at low temperatures.[12] Moreover, the relative distribution of ^{18}F in BF_3 (83%) and in SF_4 (17%) proved that the fluorine bridge bonds are symmetrical (equation 1.1) as opposed to unsymmetrical fluorine bridge bonds (equation 1.2)

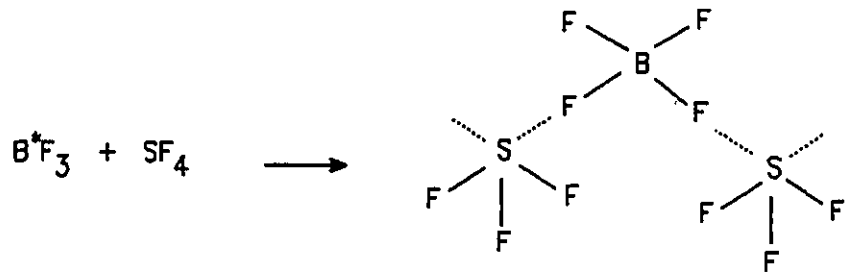

$B^*F_3 + S^*F_4$ (1.1)

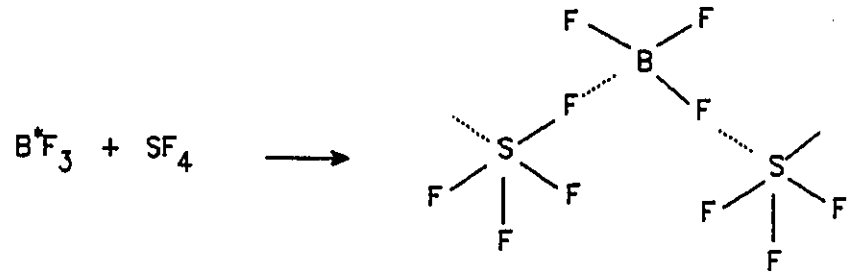

$B^*F_3 + S^*F_4$ (1.2)

In this work the distribution of ^{18}F in the products after the interaction of [^{18}F] labelled fluoride ion donors such as NO^*F with NF_4^+ and ClF_6^+ salts has been used to establish the existence or non-existence of hypervalent compounds of nitrogen and chlorine under a specific reaction condition.

2. Nuclear Medicine

One of the goals of medicine is to identify the abnormal biochemistry associated with a given pathology and to observe the abnormality directly and as early as possible in the afflicted organism. This is achieved, to a certain extent, by the standard techniques in nuclear medicine in which a patient is given a radioactively labelled substance and its fate in the body is followed by means of external detectors. Fluorine-18 was first used in nuclear medicine by Blau *et al.*[13] in 1962 when they replaced ^{87m}Sr with ^{18}F for bone scanning. Fluoride is irreversibly bound to bone and is totally extracted in a single passage of blood through bone. In addition, fluoride is rapidly excreted in the urine so that the non-osseous tissue background due to fluoride in the extracellular fluid falls rapidly. Together these properties enhance the target to background ratio. The image of the distribution of radioactivity produced by conventional imaging devices available to nuclear medicine fail to distinguish between regions of interest and regions containing radioactivity in front and behind them, i.e., these devices project information about the three-dimensional distribution of radioactivity on to a plane. The technique that combines early biochemical assessment of pathology achieved by nuclear medicine with the precise localization of radioactivity

achieved by computerized image reconstruction is known as Positron Emission Tomography (PET).

3. Positron Emission Tomography (PET)

Positron Emission Tomography employs the concepts of computerized tomography in combination with the use of specific molecules labelled with a positron emitter such as ^{18}F. When a positron is annihilated with an electron, pairs of 511 Kev photons are emitted in almost opposite directions. The image forming process in PET involves essentially three steps: (a) detection of γ-rays emitted during the process of the annihilation of positrons (b) identification of the source in the body from which the radiation is emitted and (c) presentation of the distribution of radioactivity in an accurate geometric image. It should be noted that tomographic images of the distribution of any γ-emitting radioisotope can be reconstructed and is referred to as Single Photon Emission Computerised Tomography (SPECT). However, a more faithful distribution of the radioactivity can be obtained if the γ-photons are derived from positrons. This is achieved by detecting pairs of 511 Kev photons in coincidence. Each coincidence defines a line along which a nuclear disintegration must have occurred, and hence, along which the radionuclide of interest must have been located. An array of detectors, usually placed along the circumference of a circle,

can establish the sources of all coincident pairs of γ-rays that originate within a volume defined by straight lines joining the pairs of detectors. A data acquisition system is used to collect all events recorded by the coincidence detectors and images are reconstructed from these raw data. The principle of image reconstruction is based on the fact that an object can be accurately reproduced from a set of its projections taken at different angles. The faithfulness of such a reconstruction is proportional to the number of projections. In a typical PET system around 300 projections will yield a spatial resolution of a few millimetres.

E. Use of Fluorine-18 as a Tracer for Biological Compounds

The early use of radiotracers to study the biomedical processes occurring in living organisms relied primarily on carbon-14 and tritium labelled molecules since these nuclides can be substituted for stable carbon and hydrogen in organic compounds without changing the biological properties of the molecule. Although much useful information on biomedical processes and their distribution within tissues can be obtained through the use of ^{14}C and ^{3}H in conjunction with autoradiography, the long half-life and short range of the emitted ß-particles has largely precluded their use in humans.

The short-lived positron emitting nuclides, ^{11}C, ^{13}N and ^{15}O can also be used to label organic molecules without changing their biological properties. In addition to their ready substitution for elements occurring naturally in organic molecules, there are three other characteristics that make these nuclides attractive tracers for studies in humans: (1) their short half-lives reduce the radiation dose to tissues, (2) the 511 Kev photons resulting from the annihilation of positrons with their antiparticles can be detected externally and (3) the much higher specific activities attainable with the short-lived nuclides (Table 1.3) make it possible to use them as labels for toxic molecules where the resulting labelled molecules show no measurable physiological effects. Simple labelled compounds such as $[^{15}O]O_2$, $[^{15}O]H_2O$, $[^{15}O]CO$ and $[^{11}C]$-CO can be obtained directly from the accelerators in which the radioactive nuclide is made and they have been used to study cerebral oxygen consumption, blood flow and blood volume.[14,15] In spite of these advantages just discussed, the relatively short half-lives of ^{11}C, ^{13}N and ^{15}O preclude their use in the study of mechanisms requiring measurements lasting more than an hour.

Table 1.3. Physical Properties of Tritium, Carbon-11 Carbon-14, Nitrogen-13, Oxygen-15 and Fluorine-18.

Nuclide	Half-life	Decay Mode	Maximum Energy (Mev)	Maximum Specific Activity (Ci/mole)
Tritium	12.35 y	β^-	0.0186	2.90×10^4
Carbon-14	5730 y	β^-	0.155	6.24×10^1
Carbon-11	20.4 m	β^+	0.96	9.22×10^9
Nitrogen-13	9.96 m	β^+	1.19	1.89×10^{10}
Oxygen-15	2.07 m	β^+	1.70	9.08×10^{10}
Fluorine-18	109.7 m	β^+	0.635	1.71×10^9

However, ^{18}F with its half-life of nearly 2 hrs allows complex or multi-step synthesis of organo-fluorine compounds. The maximum specific activity attainable with ^{18}F is similar to that of ^{11}C (Table 3). Further, the 110 min. half-life permits PET studies lasting up to six hours. Another advantage of ^{18}F is that unlike ^{11}C, ^{13}N and ^{15}O, it is readily available from both particle accelerators and nuclear reactors and a wide variety of nuclear reactions can be used for producing large quantities of ^{18}F (Table 1.2).

F. Effect of Fluorine Substitution on Biologically-Active Compounds

The substitution of fluorine for hydrogen in organic pharmaceuticals has a long and successful history and is currently widely practised. Filler[16] has outlined the advantages of fluorine substitution in biologically active molecules:

1. Fluorine, with its small atomic radius, closely mimics hydrogen with respect to steric requirements at enzyme receptor sites.
2. The strong electron-withdrawing effect of fluorine can significantly increase or decrease the reactivity and stability of functional groups and the reactivity of neighbouring reaction centres.

3. The substitution of fluorine for hydrogen at or near a reactive site frequently causes inhibition of metabolism. For example, the presence of fluorine instead of hydrogen (as in 5-fluorouracil) may actually block an essential biochemical reaction, i.e., the fluorine behaves as a "deceptor" group.
4. The replacement of hydrogen by fluorine usually increases the lipid solubility, thereby enhancing the rate of absorption and transport of the labelled agent *in vivo*. For some drugs, this may even be the most significant factor in improving their pharmacological activity.

Aromatic amino acids which are monofluorinated in the aromatic ring usually show biological activity that is closely related to that of the corresponding parent molecule.[17]

Aromatic amino acids are biologically important. They are used for protein synthesis in general, but in particular, a number of them serve as substrates from which the hormones thyroxin, adrenaline and noradrenaline and the neuro-transmitter dopamine are made. Because several neurological disorders are believed to be associated with imbalances in the

amounts of cerebral dopaminergic and noraderenergic activity, there has been a particular interest in the methods by which aromatic amino acids can be labelled with ^{18}F.

G. Synthesis of ^{18}F Labelled Radiopharmaceuticals

1. General Criteria for Synthesis

The following criteria need to be considered in the development of a successful synthesis of a fluorine-18 labelled radiopharmaceutical designed for *in vivo* studies using Positron Emission Tomography (PET). These are the radiochemical yield, purity, reactivity and selectivity of the fluorinating agent, regiospecificity, enantiomeric purity, specific activity, reproducibility and safety.

i. Radiochemical Yield

The most practical criterion is the radiochemical yield, since any method, used for the radiofluorination, must provide sufficient quantities of ^{18}F labelled product at the end of the synthesis. Radiochemical yield is the amount of radionuclide incorporated into the drug in its desired form. Radiochemical yields are usually reported after applying the correction for isotopic decay from the end of bombardment (EOB). In many instances it is also reported without correction for isotopic decay, instead it is expressed as the end of synthesis (EOS) yield. The decay corrected yield

indicates the efficiency of the chemical reaction, irrespective of the time taken to complete the synthesis. However, a high yield reaction may not be practical for the synthesis of a radiopharmaceutical for *in vivo* PET studies if the synthesis time is too long. It should be pointed out that the end of synthesis yield gives the same information as the decay corrected yield if the synthesis time is clearly stated.

ii. Purity of the Radiopharmaceutical

Chemical, radiochemical and radionuclidic purities of the final product must conform to the standards specified by the appropriate regulatory agency. In Canada this is the Health Protection Branch of National Health and Welfare. Chemical purity is a measure of the extent to which the final product is contaminated with chemicals other than the specified compound. Radiochemical purity is defined as the percentage of the total ^{18}F in the final product that is in the desired form. Recent advances in the chemical separation techniques and analytical methods for characterization of compounds have helped to develop rapid quality control procedures for radiopharmaceuticals.

The radionuclidic purity is a measure of the amount, if any, of other radionuclide contained in the final product. The radionuclidic purity depends on the method used to produce the

radionuclide. The nuclear reactions that use accelerators for the production of ^{18}F have been found to produce ^{18}F without radionuclidic contamination. Reactor-produced ^{18}F is different in that it is always contaminated with ^{3}H made by the $^{16}O(t,n)^{18}F$ reaction.

iii. Reactivity and Selectivity of Fluorinating Agent

Reactivity is a measure of the rate of a chemical reaction. Reactions involving the use of ^{18}F in the synthesis of radiopharmaceuticals must be fast to allow the necessary time for other synthetic procedures such as hydrolysis and/or HPLC separation of the product. While times up to 4 hours (two half-lives) have been considered acceptable for most chemical syntheses, reactions must also be selective so that high yields of the desired product can be obtained at the end of a synthesis. Selectivity of the reaction is the ability of the fluorinating agent to substitute fluorine for hydrogen in the parent molecule and produce predominantly mono fluorinated product. Higher selectivity of the fluorinating agent and fewer competitive reaction pathways will help obtain a higher radiochemical purity.

iv. Regioselectivity and Enantiomeric Purity

Regioselectivity is the ability of the fluorinating agent to produce predominantly one regioisomer of several possible

regioisomers. Because the biological activity of a molecule is often closely related to the stereochemistry of the substrate molecule, additional restrictions may be placed on the choice of the fluorinating procedure so that fluorinations may often need to be regioselective. For example, it has been shown that 6-fluoro-3,4-dihydroxyphenylalanine (6-FDOPA) is the ideal tracer to study the dopamine metabolism. Substitution of fluorine at 2- and 5- positions in 3,4-dihydroxyphenylalanine produce radically different rates of 3-O-methylation by the enzyme catechol-O-methyl transferase (COMT).[18,19]

Enantiomeric purity of the radiolabelled aromatic amino acid is crucial for tracer studies because the enzyme L-aromatic amino acid decarboxylase is stereospecific. The use of a racemic mixture would be equivalent to injection of two radiotracers with different biochemical and pharmacokinetic properties.

v. Specific Activity

Specific activity is the amount of radioactivity per unit mass of the labelled compound and it is often expressed as the number of millicuries of the labelled compound per millimole (or milligram) of the unlabelled compounds in the final product. It reflects the extent to which the labelled

compound is diluted with the unlabelled compound(s). In order for a labelled molecule to behave like a tracer, the specific activity of the labelled product must be as high as possible. Although a high radiochemical yield and purity can be obtained from a particular synthesis, the end product may have a low specific activity and therefore cannot be used for *in vivo* studies. This requirement will limit the choice of fluorinating agents, e.g., $[^{18}F]F_2$ and $[^{18}F]CH_3COOF$ are generally of low specific activity.

vi. Reproducibility and Safety

Synthetic schemes must be devised for routine use that will ensure reproducibility of yield and purity. Because the final product is to be used as a radiopharmaceutical it must also be sterile and pyrogen free.

An important consideration in any reaction involving ^{18}F is to minimise radiation exposure to the personnel involved in the process. This is especially pertinent when a synthesis involving high levels of radioactivity is carried out on a routine basis. Special attention must be paid to the technical aspects of the experimental setup such as radiation shielding, remote operations and elimination of non-essential manipulations.

The ultimate success of a chemical synthesis for routine radiofluorinations depends on its potential to satisfy all of the above criteria.

2. Role of Inorganic Fluorinating Agents in the Synthesis of Radiopharmaceuticals: An Overview

To date, direct fluorination and fluorodemercuration have been the most commonly used methods for the synthesis of [^{18}F] labelled aromatic amino acids. Other methods such as Balz-Schiemann, Wallach and other nucleophilic substitution reactions have been used for labelling aromatic compounds with [^{18}F]. However, the radiochemical yields of these reactions are low and the reasons for the low yields are discussed below.

i. Balz-Schiemann Reaction

Application of the Balz-Schiemann reaction[20] afforded the first carrier-added [^{18}F] labelled fluoroaromatics.[21] Fluorine-18 labelled analogues of four naturally occurring aromatic amino acids phenylalanine,[22] tyrosine,[23] tryptophan,[24] and 3,4- dihydroxyphenylalanine (DOPA)[25] were first prepared using the Schiemann reaction in which the fluorine in diazonium fluoroborate was labelled with [^{18}F] by reaction with [^{18}F]HF. The chemical yields of the Balz-Schiemann reaction are often low and a large number of side products may be

produced. Moreover, since the ^{18}F is introduced as labelled fluoroborate anion, the maximum possible radiochemical yield is 25% (1/4) (equation 1.3) and in practice, it ranges from 2 - 10%.

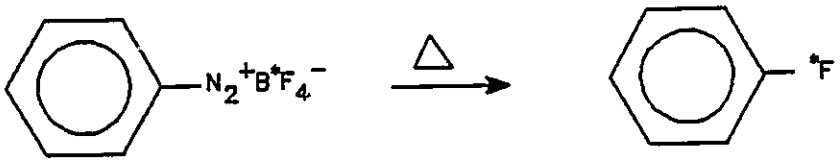

(1.3)

ii. Wallach Reaction

A slight modification of the Wallach reaction[26] was used to produce [^{18}F]-aryl fluorides with higher specific activity and radiochemical yield than the Balz-Schiemann reaction. No carrier-added ^{18}F-fluorobenzene and ^{18}F-fluorotoluene have been prepared, with 50% radiochemical yields, by the acid-catalized decomposition of aryl triazenes in the presence of $H^{18}F$ (equation 1.4).[2] Although this method was successful for the radio-fluorination of simple aromatic compounds, attempts to prepare ^{18}F-labelled butyrophenone neuroleptics such as haloperidol and spiperone produced very low yields (1 - 4%).[28] The modified Wallach reaction has also been used to produce [^{18}F]-fluorodopa; but again in unacceptably low yields (0.1 - 0.5%).[29]

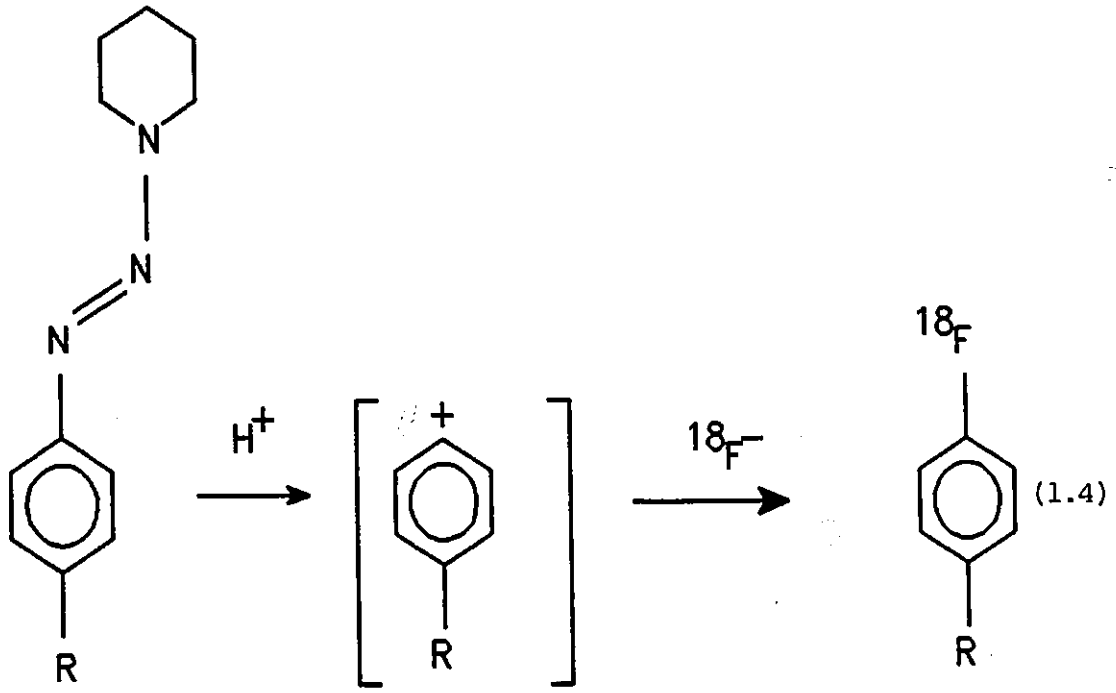

(1.4)

In general Balz-Schiemann and Wallach reactions have had limited success in the [^{18}F] labelling of simple aromatic compounds and their application to complex radiopharmaceuticals has been limited.

iii. Nucleophilic Substitution

Since the specific activity as well as the radiochemical yield at the end of the synthesis is low for both Schiemann and Wallach reactions, other nucleophilic substitution schemes have been explored to obtain [^{18}F] arylfluorides.[30] In general, nucleophilic substitution is possible when there is

sufficient activation of the aromatic ring by electron withdrawing groups in *ortho* or *para* positions (equation 1.5). It has been shown that ^{18}F could be substituted for ^{19}F on an aromatic ring.[31,32] The ^{18}F for ^{19}F exchange is useful only when the parent molecule already has a ^{19}F substituent. The high radiochemical yield (50 - 90%) and the potential for simple and rapid purification of the final product have been realised for model compounds only. No carrier added aryl [^{18}F]-fluorides have been obtained by performing essentially the same reaction as was used for ^{18}F for ^{19}F exchange, but using other leaving groups such as NO_2, Cl, Br (equation 1.5).[33,34]

Fluorine-18 labelled KF appeared to be the most efficient form of all fluoride ion sources, although other fluorides such as CsF, RbF, R_4NF are also useful.[35] So far, aromatic nucleophilic substitution has been used for the synthesis of [^{18}F] labelled simple substituted aryl fluorides which were subsequently used as precursors for the synthesis of complex molecules.[36]

iv. Limitation of Nucleophilic Substitution

In general the radiochemical yield of nucleophilic substitution is low. One reason for this is the severe reaction conditions. Often, the reactions were done at high

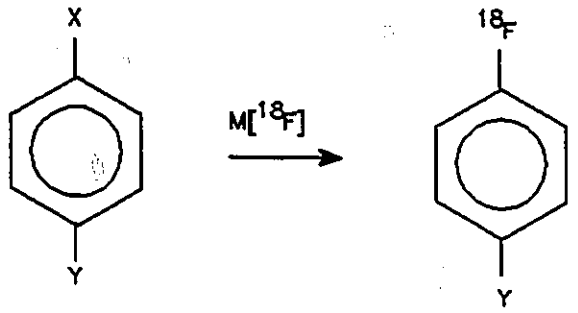

(1.5)

X = NO_2, F, Cl, Br, I, $(CH_3)_3N^+$

Y = CN, CHO, C=O, COOR, NO_2

M = Cs, Rb, K, $(alkyl)_4N^+$

temperatures. This obviously requires the substrate to be stable at high temperature. When they are not, nucleophilic methods for radiofluorination produce an extremely low yield of the desired product and large amounts of side products.

Another problem is the low solubility of fluorides. The low solubility of fluorides in standard solvents such as CH_3CN and DMSO reduces their reactivity thereby reducing the overall yield of the product. In many cases [^{18}F] fluoride ion is produced from [^{18}O]H_2O targets so that, in practice, to prepare truly anhydrous [^{18}F] fluoride is extremely difficult. Any water will reduce the nucleophilicity of fluoride ion.

Metallic ions may also reduce the nucleophilicity of fluoride ion. These metallic ions come from the target and their presence varies widely depending upon the nuclear reaction used to produce ^{18}F and the target design.[37] It has been reported that trace amounts of metal ions, present as impurities, considerably reduce the radiochemical yield of nucleophilic fluorinations. The adverse effect of metal ions on radiochemical yields can be reduced by the addition of crown ethers[38] and 2,2,2-crypt[39].

v. Electrophilic Substitution

In electrophilic fluorinations the fluorinating agent, usually containing a highly polarised ($X^{\delta-}$-$F^{\delta+}$), is allowed to react with an electron-rich aryl compound. It should be stressed that the species F^+ may never exist in solution.[40,41,42] However, the reactions of some fluorinating agents with organic substrates give fluorinated products whose orientations are usually explained by electrophilic fluorinations.

Fluorine-18 labelled electrophilic fluorinating agents such as perchlorylfluoride (ClO_3F)[43,44], N-fluoroalkyl sulphonamides[45] and N-fluoropyridinium triflates[46] have been made from $[^{18}F]F_2$. These agents were produced in moderate radiochemical yields and were used for the synthesis of [^{18}F]

labelled simple aromatic compounds. Their use to label biologically active organic compounds with [^{18}F] has not been evaluated.

Another electrophilic fluorinating agent Xenon difluoride (XeF_2) has been labelled with [^{18}F] both by the direct reaction of xenon and [^{18}F]F_2 gas[47] and by the isotopic exchange of XeF_2 with [^{18}F]HF[48] to give radiochemical yields of 70 and 30%, respectively. Xenon difluoride has been shown to be effective for the regiospecific fluorination of 3-O-methyl dopa,[49,50] but its utility for radiolabelling pharmaceuticals is limited because of isotopic dilution arising from the exchange between [^{18}F]XeF_2 and the catalyst, HF or BF_3, used in the fluorination reaction.

One of the most widely used electrophilic fluorinating agents is acetyl hypofluorite. Its synthesis and versatility as a mild fluorinating agent was originally reported by Rosen *et al.*[51] in 1981. Fowler *et al.*[52] reported the synthesis of [^{18}F]CH_3COOF by the reaction of [^{18}F]F_2 gas with acetyl salts in solution. This method was later simplified and made more reliable by the reaction of [^{18}F]F_2 gas with solid potassium acetate.[53] The use of [^{18}F]CH_3COOF for the radiofluorination of aromatic aminoacids has been reported by various groups.[54-57] In general, the fluorination is carried out using a derivative

of the amino acid and the desired product is isolated after the hydrolysis followed by HPLC (equation 1.6).

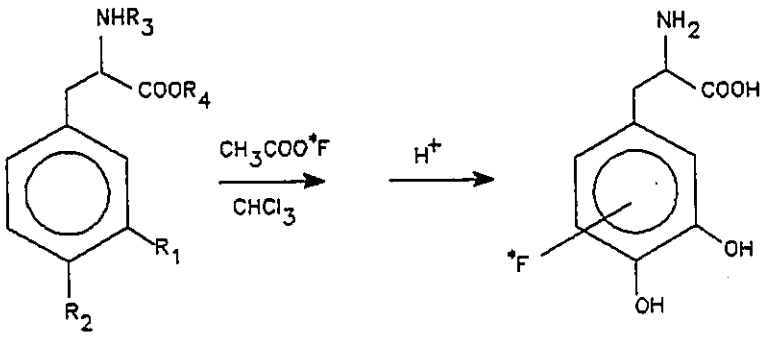

(1.6)

R_1 = OH, OCH_3 R_2 = OH, $OCOCH_3$

R_3 = H, $COCH_3$ R_4 = H, CH_3, C_2H_5

Acetylhypofluorite has also been used for regioselective fluorodemetallation reactions.[58] In these reactions, regioselectivity was achieved by prior functionalization of the aromatic ring followed by fluorination at that position. The success of the fluorodemetallation reaction was due to the weaker carbon-metal bond and the higher bond polarity compared to the corresponding carbon-hydrogen bond. Therefore, electrophilic attack was found to be faster and regioselective with high radiochemical yields. Organic derivatives of a number of elements such as silicon, tin, germanium, and mercury have been used in such fluorination reactions.[58]

Both $[^{18}F]F_2$ and $[^{18}F]CH_3COOF$ have been used for fluorodemetallation reactions. Comparison of the reactivities of these two fluorinating agents towards the aryl derivatives of silicon, tin, and germanium show that both F_2 and CH_3COOF produce satisfactory results for fluorodestannylation reactions while $[^{18}F]F_2$ is the preferred fluorinating agent for both silicon and germanium derivatives.[59] The radiochemical yields from the tin derivatives were 2 - 3 times higher than those obtained from silicon and germanium derivatives. The results were explained on the basis of a weaker Sn-C bond compared to Ge-C and Si-C bonds. These comparisons, however, were done for the synthesis of model compounds such as fluorobenzene and fluorotoluene.

An attempt to label 3,4-dihydroxyphenylalanine (DOPA) using the destannylation method failed because of the difficulty in synthesising the tin derivative.[58] However, fluorodemercuration, which employs $[^{18}F]CH_3COOF$, has been used successfully for the regiospecific synthesis of 6-$[^{18}F]$-fluorodopa (equation 1.7),[60] 4-$[^{18}F]$-fluorometatyrosine [61] and 6-$[^{18}F]$-fluorometaraminol.[62] The radiochemical yields for these reactions were ca. 40%. The demercuration reaction offers an advantage over the direct electrophilic fluorination by acetylhypofluorite in that it does not require separation of the isomers after the introduction of $[^{18}F]$. It should,

however, be stressed that electrophilic aromatic mercuration may produce isomeric mixtures of mercurated derivatives and it is necessary to separate the desired isomer before the radiofluorination reaction. It is also important to be scrupulously careful to remove all traces of mercury from the final product.

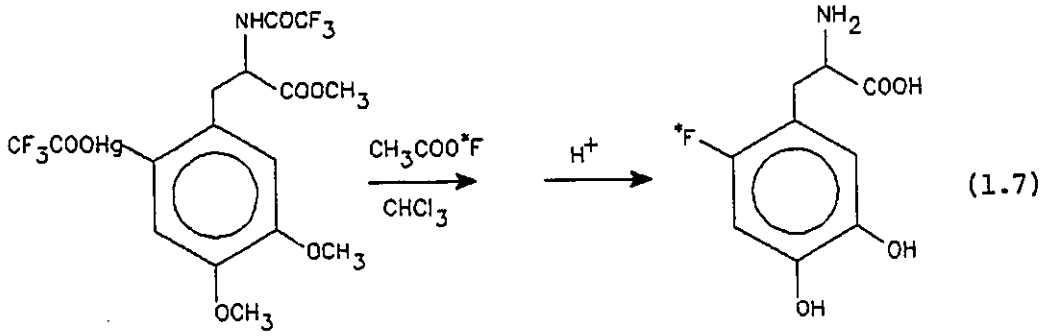

(1.7)

The original, and the simplest of all fluorinating agents is fluorine gas. It is the progenitor of most other electrophilic fluorinating agents. Since many particle accelerators can produce large quantities of $[^{18}F]F_2$ gas, it would be logical to develop and optimize synthetic routes that use $[^{18}F]F_2$ gas as the fluorinating agent. However, direct fluorination of organic compounds was thought to result in vigorous or explosive reactions, accompanied by charring. Accordingly, direct fluorination was not considered a viable method for the synthesis of organic fluorides.[63,64]

However, it has been shown that the reactivity of F_2 towards organic compounds can be moderated by diluting it with an inert gas.[65,66] Fortuitously, from the stand point of organic synthesis, $[^{18}F]F_2$ gas is made from fluorine/neon gas mixtures (typically 0.1 - 0.5% F_2 in neon). Cacece *et al.*[67] used $[^{18}F]F_2$ in neon to study the substrate selectivity and orientation of aromatic substitution by molecular fluorine. They established that, using dilute fluorine gas, molecular fluorination of substituted benzenes and toluenes proceed with similar selectivity and orientation as had been commonly observed for other halogens. Although direct fluorination with F_2 gas is logical and has been successful, the process has two important limitations: (a) the direct fluorination of organic compounds in solution is considerably restricted because of the lack of sufficiently inert solvents and (b) solvents like fluorocarbons are relatively inert to fluorine, but do not dissolve many of the organic compounds.

In the present work, a rapid yet efficient method for the radiofluorination of the amino acids tyrosine and m-tyrosine has been developed. In addition, the reactivity and selectivity of tyrosines towards fluorine in different solvents has been investigated.

CHAPTER 2

EXPERIMENTAL

(A) Vacuum Techniques

All vacuum manipulations involving fluorine, anhydrous hydrogen fluoride, arsenic pentafluoride, boron trifluoride, nitrosyl fluoride and nitric oxide were carried out on a metal vacuum line constructed from stainless steel and nickel and previously passivated with fluorine. A separate metal vacuum line fitted with a pressure transducer was used to prepare NMR samples containing known amounts of ClF_5. Solutions of aromatic amino acids in HF or HF/BF_3 were prepared using a third general purpose vacuum line constructed of 1/4" 316 stainless steel tube equipped with 316 stainless steel valves and Swagelok fittings. Pressures were measured in a calibrated portion of the vacuum line using a stainless steel Ashcroft Bourdon tube ("Duragauge" model 8439gauge) reading 0-30 lbs/in^2 absolute.

(B) Starting Materials and Solvents

Fluorine (Air Products) was passed through a NaF column to remove HF prior to use. Nitric oxide (Matheson) was used without further purification. Arsenic pentafluoride was prepared from AsF_3 and F_2 by Dr. Gary J. Schrobilgen.

Nitrosyl fluoride, prepared by the direct fluorination of NO (Matheson), was treated with fluorine by transferring 100 g of NOF into a previously passivated 250 mL Monel can and condensing sufficient fluorine at -196 °C to give a partial pressure of fluorine of 25 atm. at room temperature. After standing for several hours at room temperature, F_2 gas was removed under vacuum at -196 °C and the NOF was used directly from the can.

Research grade neon, 1% fluorine in neon, boron trifluoride (Matheson), anhydrous HF (Air Products), CF_3SO_3H, CF_3COOH (Aldrich) and HPLC grade CH_3CN (Caledon) were used without further purification.

Perfluoroammonium salts, $NF_4^+BF_4^-$ and $NF_4^+PF_6^-$, chlorine pentafluoride, and the hexafluorochlorine cation, $ClF_6^+AsF_6^-$, were provided by Dr. Karl O. Christe, Rocketdyne, a Division of Rockwell International Corporation, Canoga Park, California. The CsF (KBI) was dried by fusion in a platinum crucible and ground in the dry box.

L- Tyrosine, DL-m-tyrosine, 3-hydroxyphenyl-acetic acid, EDTA, sodium octane sulphonate (Aldrich), m-tyramine hydrochloride (Research Biochemicals), α-chymotrypsin, sodium

barbital, and ketamine hydrochloride (Sigma) were used without further purification.

Fluorine-13 labelled [^{18}F]6-fluorodopa and 3-O-methyl-[^{18}F]6-fluorodopa were prepared by the direct fluorination of DOPA (Sigma) and 3-O-methyl DOPA (Sigma) in HF/BF_3.[68]

(1) Preparation of L-m-Tyrosine

L-m-tyrosine was prepared by the stereospecific hydrolysis of DL-m-tyrosine ethyl ester by the action of α-chymotrypsin.[69] First DL-m-tyrosine was converted into its ethyl ester by passing HCl gas through cold solutions of m-tyrosine in ethanol. Hydrogen chloride gas was bubbled through until the tyrosine was completely dissolved and the resultant clear solution was stirred overnight. The solvent was then evaporated and the DL-m-tyrosine ethyl ester was washed with ethanol and dried. The L-enantiomer of the ester was stereospecifically hydrolysed by allowing the DL-ester to react with α-chymotrypsin (Sigma) at pH = 5 while the L-m-tyrosine was precipitated. HPLC analysis of the hydrolysis product, using waters Nova Pak™ C_{18} radial compression cartridge (mobile phase; 0.03M sodium hydrogen phosphate at pH 3.9 containing 1g/L octane sulphonate and 7% methanol and flow rate of 2 mL/min.), gave a u.v. peak at 8 min. and another at 65 min. By comparing the retention times of DL-m-tyrosine and

DL-m-tyrosine ethyl ester, these peaks were assigned to L-m-tyrosine and DL-m-tyrosine ethyl ester, respectively. The purity of L-m-tyrosine (92 ± 5%) was determined from the areas under the two peaks.

(2) Preparation of N-Acetyl-(4-acetoxyphenyl)L-alanine Methyl Ester A stream of HCl gas was bubbled through a cold (0 °C) suspension of L-tyrosine (3.9 g) in methanol for 1 - 2 min. The resultant clear solution was stirred overnight. The solvent was evaporated; the residue was redissolved in methanol and the methanol evaporated a second time and the residue dried overnight to give L-tyrosine methyl ester hydrochloride (4.9 g, 98% yield). The crude tyrosine methyl ester hydrochloride was stirred, with cooling, in a mixture of pyridine-acetic anhydride (1:1, 25 mL) for 10 min. and the mixture was poured into 1 M sulphuric acid (100 mL) followed by extraction with ethyl acetate (3 x 60 mL). Evaporation of the organic layer yielded a white solid (6.0 g, 100% yield). This was recrystallized from ethyl acetate, filtered and washed with hexane-ethyl acetate (1:2) to give 5.2 g (88% yield) of white solid, m.p. 98 - 100 °C. The ^{1}H NMR spectrum of the final product in $CDCl_3$ consisted of singlets at 1.90 (3H), 2.20 (3H) and 3.65 ppm for the three methyl groups. The spectrum of side-chain protons consisted of multiplets at 3.02 (2H, benzylic protons, AB part of the ABX spin system on the

side chain, J_{AB} = -13.70 Hz, J_{AX} = J_{BX} = 5.70 Hz) and 4.79 ppm (1H, CH, X part of the ABX spin system). A broad doublet was observed for the NH proton at 6.13 ppm. The aromatic region of the spectrum consisted of two doublets (AB pattern) at 7.03 and 6.93 ppm with $^3J_{AB}$ = 8.5 Hz. The high resolution mass spectrum of the compound gave the molecular ion at m/z = 280 $[m + H]^+$.

(C) Instrumentation

(1) Nuclear Magnetic Resonance Spectroscopy

i. NMR Instrumentation

The ^{19}F NMR spectra were recorded unlocked (field drift < 0.1 Hz h^{-1}) using a Bruker WM-250 or AM-500 spectrometer equipped with 5.8719 T and 11.744 T cryomagnets, respectively. On both instruments, spectra were obtained using 5-mm combination $^1H/^{19}F$ probes operating at 235.361 MHz (WM-250) or 470.599 MHz (AM-500).

The 5.8719 T ^{19}F spectra were typically accumulated in a 16K memory. Spectral width settings of 5 and 10 KHz were employed, yielding data point resolutions of 0.62 and 1.22 Hz and acquisition times of 1.638 and 0.819 s, respectively. No relaxation delays were applied. The number of free-induction decays accumulated was typically between 2000 and 10,000 transients.

The 11.744 T ^{19}F spectra were accumulated in a 16K memory. Spectral width settings of 5 and 30 KHz were employed, yielding data point resolutions of 0.61 and 3.59 Hz and acquisition times of 1.638 and 0.278 s, respectively. No relaxation delays were applied. Typically 80 to 1000 transients were accumulated.

On both instruments the pulse width corresponding to a bulk magnetization tip angle, θ, of approximately 90° was equal to 1 μs. No line broadening parameters were applied in the exponential multiplication of the free induction decays prior to the Fourier transformation. The spectra were referenced to neat $CFCl_3$. The chemical shift convention used was such that a positive (negative) sign signifies a chemical shift to high (low) frequency of the reference compound.

Low-temperature studies were carried out by using Bruker temperature controllers. The temperature was measured with a copper constantan thermocouple inserted directly into the sample region of the probe and was accurate to +1 °C.

Fluorine-19 spectra of fluoroaromatics were recorded at 235.36 MHz on a Bruker WM 250 spectrometer. Spectra were accumulated in 1500 scans in 16 K memories yielding a data point resolution of 0.244 Hz/Point. Spectra were run in 20

KHz spectral width (acquisition time 0.412 s) using a pulse width of 3 μs.

Proton and ^{13}C spectra were recorded on a Bruker AM 500 spectrometer at 500.135 MHz and 125.759 MHz, respectively, using a 5 mm dual frequency $^{1}H/^{13}C$ probe. Spectra were accumulated in 20 (^{1}H) and 3000 (^{13}C) scans in 32 K data points (^{1}H, 0.305 and ^{13}C, 1.795 Hz/data point) over a spectral width of 5.101 (^{1}H) and 2.941 KHz (^{13}C). Pulse widths of 5.0 (^{1}H) and 6.4 μs (^{13}C) (acquisition times were 1.605 s for ^{1}H and 0.555 s for ^{13}C) were used.

ii. NMR Sample Preparation

Fluorine-19 NMR samples were prepared in 25 cm-length of AWG 9 (ca. 4 mm o.d., 0.8 mm wall) FEP plastic tubing heat sealed at one end with the open flared (45° SAE) and joined, by means of a compression fitting, to a Kel-F valve. The assembly was seasoned overnight with ca. 1 atm. of F_2 gas, evacuated and weighed. A weighed amount of CsF was transferred into a sample tube in a dry box. Both ClF_5 and HF were distilled into NMR tubes through a metal line fitted with a pressure transducer that had been previously seasoned overnight with ca. 1 atm. ClF_5 vapour. The ClF_5 pressure was measured (to a ± 0.5% accuracy) in a calibrated portion of the metal vacuum line using a pressure transducer (0 - 1000 torr

range), whose wetted surfaces were Inconel, and the ClF_5 was condensed at -196 °C into the FEP NMR sample tube. The amount of HF solvent used was determined by direct weighing of the tube assembly. The FEP tube was heat sealed under dynamic vacuum with its contents frozen at -196 °C. The FEP sample tubes were placed in 5-mm thin-walled precision NMR tubes (Wilmad) in order to run their spectra.

The samples of fluorinated aromatic amino acids were prepared in D_2O.DCl and referenced at ambient temperature with respect to HDO (^1H, 4.60 ppm relative to external TMS), external neat $CFCl_3$ (^{19}F) and external TMS in D_2O (^{13}C).

Samples for low temperature ^1H and ^{13}C NMR were prepared by first dissolving 0.54 mmol of amino acid in approximately 5 mL of HF or HF/BF_3 (to maintain the same concentration used for the fluorination of aromatic amino acid) and transferring approximately 0.3 mL of the solution into a Teflon-FEP tube (Wilmad, 528 pp) kept at -70 °C. The Teflon-FEP tube was placed in a 5 mm thin-walled precision NMR tube (Wilmad) when the spectra were run.

(2) Mass Spectrometry

High-resolution mass spectra were obtained using a double focusing VG ZAB-E mass spectrometer under positive ion fast

atom bombardment conditions. Trifluoroacetic acid (20%) in glycerol was used as the matrix and xenon was the bombarding species (8 KeV). Accurate masses of the protonated molecular ions were obtained under high-resolution conditions using glycerol cluster ions as the reference.

(D) Studies with ^{18}F

(1) Production of ^{18}F

Fluorine-18 as $[^{18}F]F_2$ was produced using the nuclear reaction $^{20}Ne(d,\alpha)\ ^{18}F$. For the nuclear reaction $^{20}Ne(d,\alpha)\ ^{18}F$, the McMaster University Tandem Van de Graaff Accelerator (Super FN, High Voltage Engineering Corp., Burlington, Mass.) provided deuterons at 15 MeV in beam currents of up to 8 μA. The beam was well focused and its strike area was not greater than 2 mm in diameter.

The neon-fluorine gas target was constructed of nickel (Fig. 2.1). The inner surface was reamed out and polished. The seals were gold O-rings (0.5 mm in cross section). The window consisted of a nickel foil (0.025 mm thick) on the inside and aluminum foil (0.20 mm thick) on the outside (Advanced Alloy Inc., Toronto). The body of the target was cooled by chilled water (10 °C) that flowed through a cooling jacket made of aluminum. The pressure in the target was

Figure 2.1 $[^{18}F]F_2$ gas target. (A) Window, (B) Aluminum foil, (C) Nickel foil, (D) Gold O-ring, (E) Gas inlet, (F) Gas outlet, (G) Cooling water inlet and (H) Cooling water outlet.

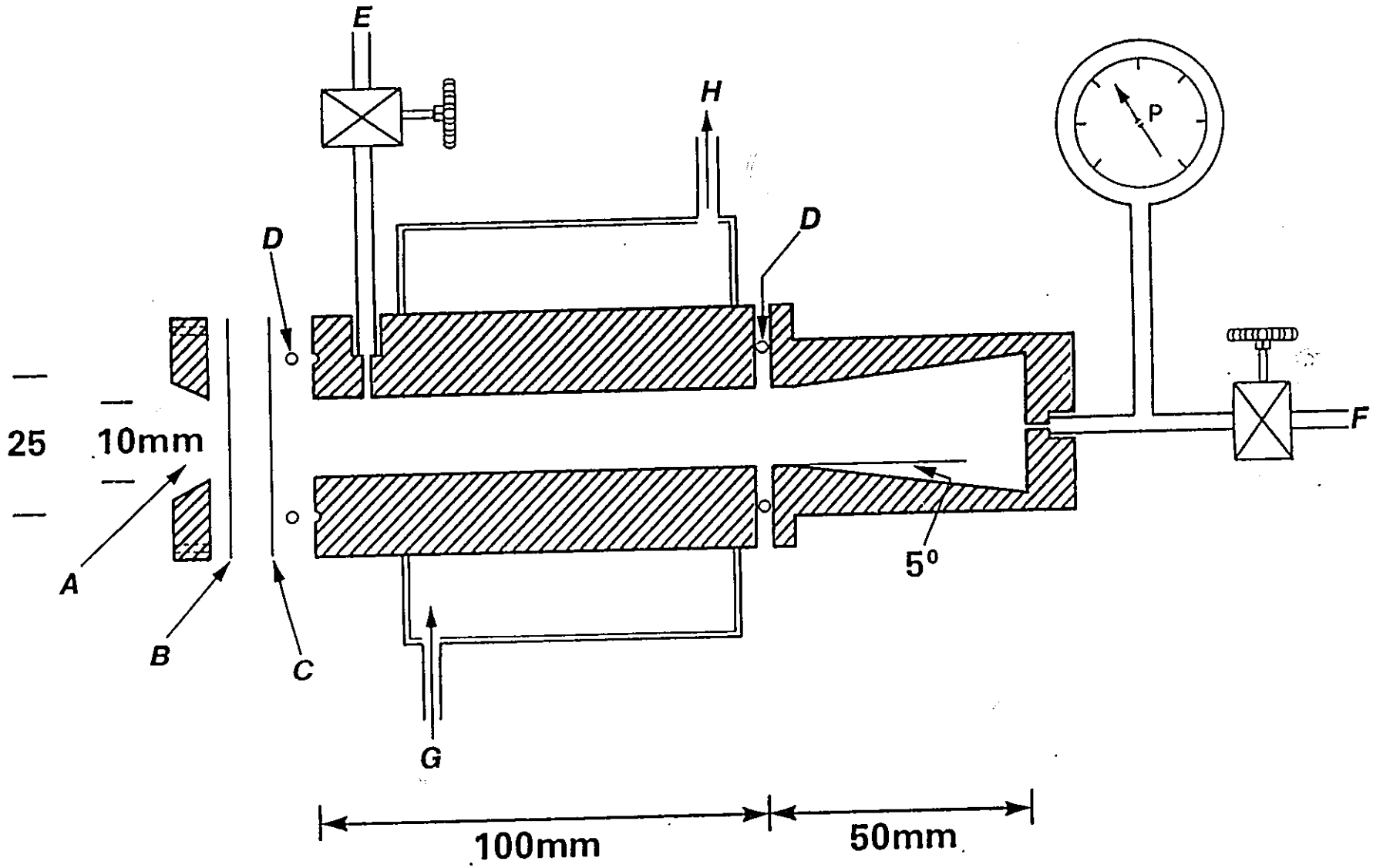
E
H
P
D
D
25
10mm
A
B
C
5°
F
G
100mm
50mm

monitored by a Monel Bourdon pressure gauge (Matheson). The gas inlet and outlet were closed by Monel bellows valves (Nupro). The internal volume of the target assembly, including the pressure gauge, was measured by using PVT-data and found to be 31.4 mL. A 36 ft length of 316 stainless steel tubing (1/8" o.d and 1/32" i.d.) was used to connect both the target inlet and outlet with the gas handling manifold in the chemistry laboratory. The manifold design was based on that described by Casella *et al.*[70], with the exception that 1/8" stainless steel tubing and stainless steel bellows valves were used in the present work.

The inner surface of the target was passivated first, heating to 300 °C for 24 hrs in dynamic vacuum followed by heating to 300 °C for 8 hrs with 3 atm. of hydrogen gas; and, finally, heating to 300° for 2 hrs with 2 atm. of pure fluorine gas. The transfer line and manifold were also passivated by repeating the above procedure except they were heated by occasional flaming.

The window side of the target was connected directly to the accelerator beam line. No special window cooling was found to be necessary under our irradiation conditions. The window foils attenuated the 15 MeV deuteron beam to 13.8 MeV.

Research grade neon gas and a mixture of 1% fluorine in neon (Matheson) were used. The gases were introduced into the target through the manifold. The total gas pressure in the target was 30.4 ± 0.7 atm. before and after bombardment. During bombardment the pressure always increased due to heating by the beam; for example, at 5 μA the pressure rose to 33.8 atm. The deuteron beam intensity on the target was measured with a "Keithley 414" microampere meter. Irradiation times were between 1. and 2 hrs.

(2) Measurement of ^{18}F

Fluorine-18 was measured using a radioisotope calibrator (Capintec CRC-12) manufactured by Capintec Inc. It consisted of a 6 cm. i.d. and 25 cm. deep measuring well surrounded by an ionization chamber filled with argon gas. The chamber walls are made of aluminum and the outside wall was shielded with 1/8" thick lead. The current produced in the ionization chamber, due to the interaction of photons with the gas molecules, was read using a digital readout. The sensitivity of the ionization chamber was determined using radioactivity standards supplied by the U. S. National Bureau of Standards (NBS) and/or by the Laboratoire de Métrologie de la Radioactivité (LMR), France. The accuracy of the calibrator was determined using ^{57}Co and ^{60}Co standard sources and it is reported to be ± 2% for γ-rays with ≥ 0.1 Mev energies. The

Capintec can measure radioactivity in the range 10 μCi to 2 Ci.

In the present work, the measured values for [^{18}F] were decay corrected back to the beginning of the experiment (t = 0). In experimental studies towards the syntheses of NF_3 and ClF_7 the activity of the reactants at zero time (t = 0) was measured in a 1/2" or 1/4" o.d., 6-8" long FEP reaction vessel. The FEP reaction vessel is equipped with Kel-F valves and attached to FEP U-tubes (heat-flared 45°) by means of compression fittings. The activity of the products was measured in 1/4" FEP U-tubes which are approximately 2 1/2" wide and 12" long. In order to correct for the differences in measured [^{18}F] activities due to differences in geometries and heights of the vessels, the following experiment was performed. A sample of [^{18}F] in 2 mL water in a 3/4" o.d. vial placed at the bottom of the measuring well was assayed to be 9.04 mCi. The same [^{18}F] sample 8" away from the bottom of the well gave a reading of 7.68 mCi (15% lower [^{18}F]). When the sample was transferred into an FEP U-tube the reading was 10.06 mCi; 10.6% more than the original reading in the 3/4" o.d. vial. It was found in all experiments that the [^{18}F] activities at the beginning and end of the experiments could be balanced if corrections were made for different geometries.

(3) Recovery of $[^{18}F]F_2$ from the Target

After bombardment, the target gas was emptied into a passivated cylindrical nickel vessel (height 150 mm o.d. 59 mm, wall thickness 6.25 mm, internal volume 193 mL) fitted with a grease-free high pressure stainless steel valve equipped with Teflon packing (Autoclave Engineering) at -196 °C. From the PVT data it was determined that 91% of total gas volume in the target was collected in the nickel vessel at -196 °C. The yield of $[^{18}F]F_2$ recovered from the target was determined by measuring the amount of radioactivity present in the nickel vessel. The yield of $[^{18}F]F_2$ was expressed as a percentage of the theoretical thick target yield for $[^{18}F]$ at the end of bombardment.

(E) Preparation of $[^{18}F]$Labelled Inorganic Fluorinating Agents

(1) Preparation of $[^{18}F]HF$ and $[^{18}F]HF_2^-$

$[^{18}F]HF$ was prepared by condensing $Ne/[^{18}F]F_2$ mixture onto 1 atm. of H_2 at -196 °C in the nickel vessel containing unlabelled anhydrous HF (2.35 mmol). The excess H_2 and Ne were pumped off at -196 °C and the radioactivity of $[^{18}F]HF$ remaining in the nickel can was measured. The $[^{18}F]HF$ was condensed at -196 °C into a Teflon reactor containing dry CsF (0.809 mmol) to produce $[^{18}F]HF_2^-$. The percentage (95.4%) of $[^{18}F]HF$ transferred from the nickel can was determined by

measuring the [^{18}F] contents in the nickel vessel and in the Teflon reactor.

(2) Preparation of [^{18}F]NOF

A 50 mL nickel can was heated to red heat four times with 2 atm. of H_2, followed each time by evacuation of the vessel while it was still hot. This procedure was then repeated four times with F_2 under static conditions, followed by treatment with 3 atm. of NOF at room temperature for one day and pumping for 4 hrs. The Ne/[^{18}F]F_2 mixture from the [^{18}F] target was condensed on top of nitric oxide (0.62 mmol) in the nickel vessel at -196 °C. The excess Ne was pumped off at -196 °C and F_2 (0.31 mmol) was added to the nickel can. The nickel vessel was briefly warmed to 20 °C to form [^{18}F]NOF. The vessel was cooled to -196 °C and excess fluorine, if any, was pumped off. The [^{18}F]NOF from the nickel vessel was directly condensed into the reaction vessel and used without further purification. For the ClF_5-[^{18}F]NOF exchange study, traces of HF were removed from [^{18}F]NOF by condensing [^{18}F]NOF into a U-tube containing 0.5 g of NaF at -196 °C followed by warming to -78 °C. Pure [^{18}F]NOF was recovered from U-tube by condensing it into an FEP reactor at -196 °C.

(F) Attempted Preparation of NF_5

(1) Pyrolysis of $[^{18}F]NOF + NF_4^+BF_4^-$

An FEP vessel equipped with a Kel-F valve that had been previously passivated with F_2 gas was loaded with $NF_4^+ BF_4^-$ (1.38 mmol) in the dry box. Fluorine-18 labelled NOF (1.38 mmol, 75 mCi) was condensed into the FEP reaction vessel at -196 °C and the total amount of $[^{18}F]$ in the reaction vessel was assayed. The reactor was gradually warmed to room temperature and kept at room temperature for 5 min. The volatile products from the reaction were separated by pumping through a series of U-tubes: a -196 °C trap, a soda lime trap and a -210 °C (N_2 slush) bath (Figure 2.2). The first trap at -196 °C contained unreacted $[^{18}F]NOF$ and traces of $[^{18}F]HF$ contaminants, the soda lime trap absorbed $[^{18}F]F_2$ and the third -210 °C trap contained $[^{18}F]NF_3$. The $[^{18}F]$ distribution after the reaction was determined by assaying each trap and the original reaction vessel. Identities of $[^{18}F]NOF$ and $[^{18}F]HF$ in the -196 °C trap were determined by condensing boron trifluoride (1.3 mmol) into the -196 °C trap and warming to -78 °C and maintaining at this temperature for 5 min. after which the contents were pumped through a soda lime trap. The amount of $[^{18}F]$ collected in the soda lime trap and $NO^+BF_4^-$ residue were assayed.

Figure 2.2 Apparatus for the separation of products after the pyrolysis of $NF_4^+BF_4^-$ and $NF_4^+HF_2^-$. (A). FEP Reaction vessel (1/2" o.d. x 3/8" i.d., 6-8'' long), (B). FEP U-tube (1/4" o.d. x 3/16" i.d., 2 1/2'' wide and 12'' long) at -130 °C (pentane slush), (C). FEP U-tube containing sodalime, (D). FEP U-tube at -210 °C (nitrogen slush), E. Kel-F valves and F. 1/4" o.d. x 1/3" i.d. Kel-F connectors.

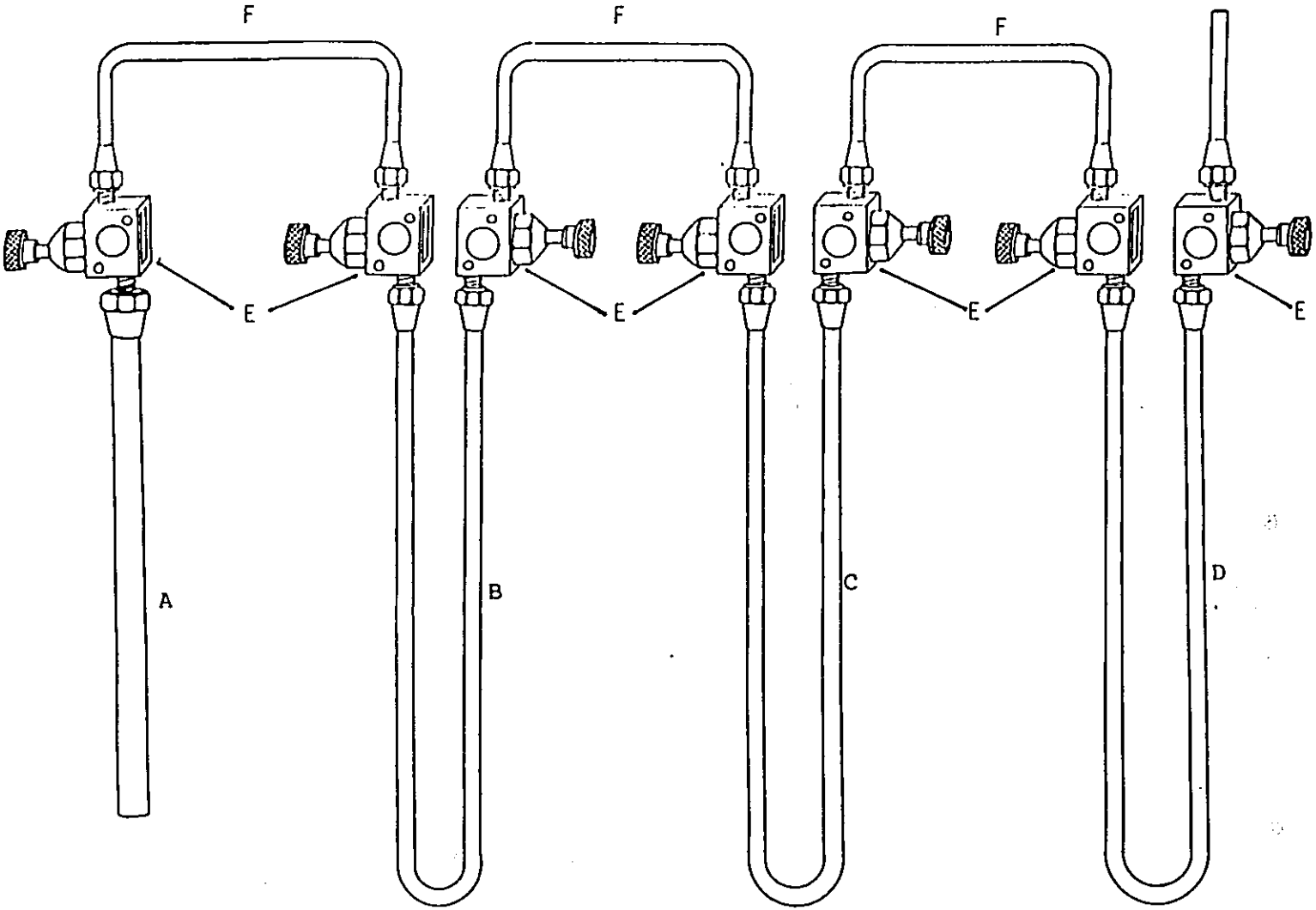
F
F
F
E
E
E
E
A
B
C
D

(2) Pyrolysis of $NF_4^+PF_6^-$ + $[^{18}F]HF_2^-$

An FEP tube equipped with a Kel-F valve was dried overnight, and passivated with F_2 for 24 hours. Dry CsF (0.809 mmol) and NF_4PF_6 (0.854 mmol) were loaded into the Teflon-FEP tube in the dry box. Fluorine-18 labelled HF was prepared by combining $[^{18}F]F_2$ and H_2 in a nickel can containing unlabelled HF (2.35 mmol). The $[^{18}F]HF$ was transferred into the Teflon reaction tube at -196 °C and the radioactivity (130.8 mCi) was measured. The reactants were first warmed to room temperature for 30 min. and excess HF was removed under vacuum from the reaction vessel and trapped at -196 °C in an FEP U-tube. The $[^{18}F]$ activity remaining in the reaction vessel (29.2 mCi) and excess HF (87.8 mCi) that had been trapped at -196 °C were assayed. The temperature was gradually raised to 100 °C over a period of 1 hour and at the same time the volatile products were pumped through an FEP cold trap at -130 °C to trap $[^{18}F]HF$ followed by a soda lime scrubber to absorb $[^{18}F]F_2$ and a -210 °C trap to condense $[^{18}F]NF_3$ (Figure 2.2). The $[^{18}F]$ contents in each trap and the Teflon reactor were assayed. Corrections were made for $[^{18}F]$ decay, but no corrections were made for differences in the geometries of the nickel vessel, in which the $[^{18}F]F_2$ was measured, and FEP vessels, in which the $[^{18}F]NOF$ and $[^{18}F]HF$ were measured.

(G) Attempted Preparation of ClF_7: $[^{18}F]NOF + ClF_6^+AsF_6^-$ System

Fluorine-18 labelled NOF (37 mCi) was condensed into an FEP reaction vessel containing $ClF_6^+AsF_6^-$ (0.315 mmol) at -196 °C. The $[^{18}F]NOF$ condensed on the walls of the reaction vessel was warmed and condensed into the bottom of the tube, by lowering the liquid nitrogen level, so that good mixing of the reactants could be achieved. An immediate bright orange-red colour appeared as NOF came in contact with $ClF_6^+AsF_6^-$. The colour disappeared when the reactants were warmed first to -78 °C and then to room temperature. The reactants were held at room temperature for 10 min and the contents of the reaction tube were pumped off through sodium fluoride and a cold trap at -196 °C followed by a soda lime trap at room temperature. The first trap containing 0.5 g of NaF, removed HF, the second trapped ClF_5 along with unreacted NOF and the sodalime trap absorbed F_2 (Figure 2.2). The radioactivity in each trap and the reaction tube was measured and corrected for the elapsed time from the beginning of the experiment. The amount of unreacted NOF was determined by condensing excess AsF_5 into the -196 °C trap, followed by warming to room temperature to form the complex $NO^+AsF_6^-$. The ClF_5 was then pumped back into the soda lime trap at -196 °C. The $[^{18}F]$ activity in $NO^+AsF_6^-$ was measured to determine the relative amount of unreacted NOF. The ClF_5 activity was calculated after measuring the soda lime trap at -196 °C and making corrections for the

residual activity that was present in the soda lime trap and for [^{18}F] decay.

(H) Identification of ClF_6^- as an Intermediate in the Exchange Between ClF_5 and [^{18}F]NOF

Fluorine-18 labelled NOF was prepared by condensing [^{18}F]F_2 (0.08 mmol) in neon into a nickel can, that had been previously passivated with F_2 and NOF, containing nitric oxide (0.62 mmol) and F_2 (0.30 mmol) at -196 °C. The can was briefly warmed to 20 °C and the [^{18}F]NOF formed was condensed into an FEP tube containing 0.5 g of NaF at -196 °C followed by warming to -78 °C. The [^{18}F]NOF (81 mCi), free of trace amounts of HF, was combined with ClF_5 (0.62 mmol) in a 1/4" o.d. FEP ampoule at -196 °C. The mixture was warmed to 20 °C for several minutes and then vacuum distilled through two U-tubes kept at -130 and -196 °C (Figure 2.3). The first trap contained ClF_5 and the second one contained NOF.

The radioactivity in each trap was measured and corrected for [^{18}F] decay. At the end of the experiment the trap containing ClF_5 (-130 °C) showed 84.9% of the original [^{18}F] and the remaining 15.1% was found in the second trap (-196 °C) containing NOF. The trapping efficiency for ClF_5 and NOF was checked by warming the ClF_5 trap to -78 °C and condensing the volatile gas into the NOF trap at -196 °C. The combined activities of [^{18}F]ClF_5 and [^{18}F]NOF were measured and AsF_5

Figure 2.3 Apparatus for the investigation of ClF_5-NO$^+$F exchange. (A) 1/2" o.d. x 3/8" i.d. FEP reaction vessel containing ClF_5 and NOF (B) FEP U-tube at -130 °C and (C) FEP U-tube at -196 °C. (D) Kel-F Valves and (E) 1/4" o.d. x 1/8" i.d. Kel-F connectors.

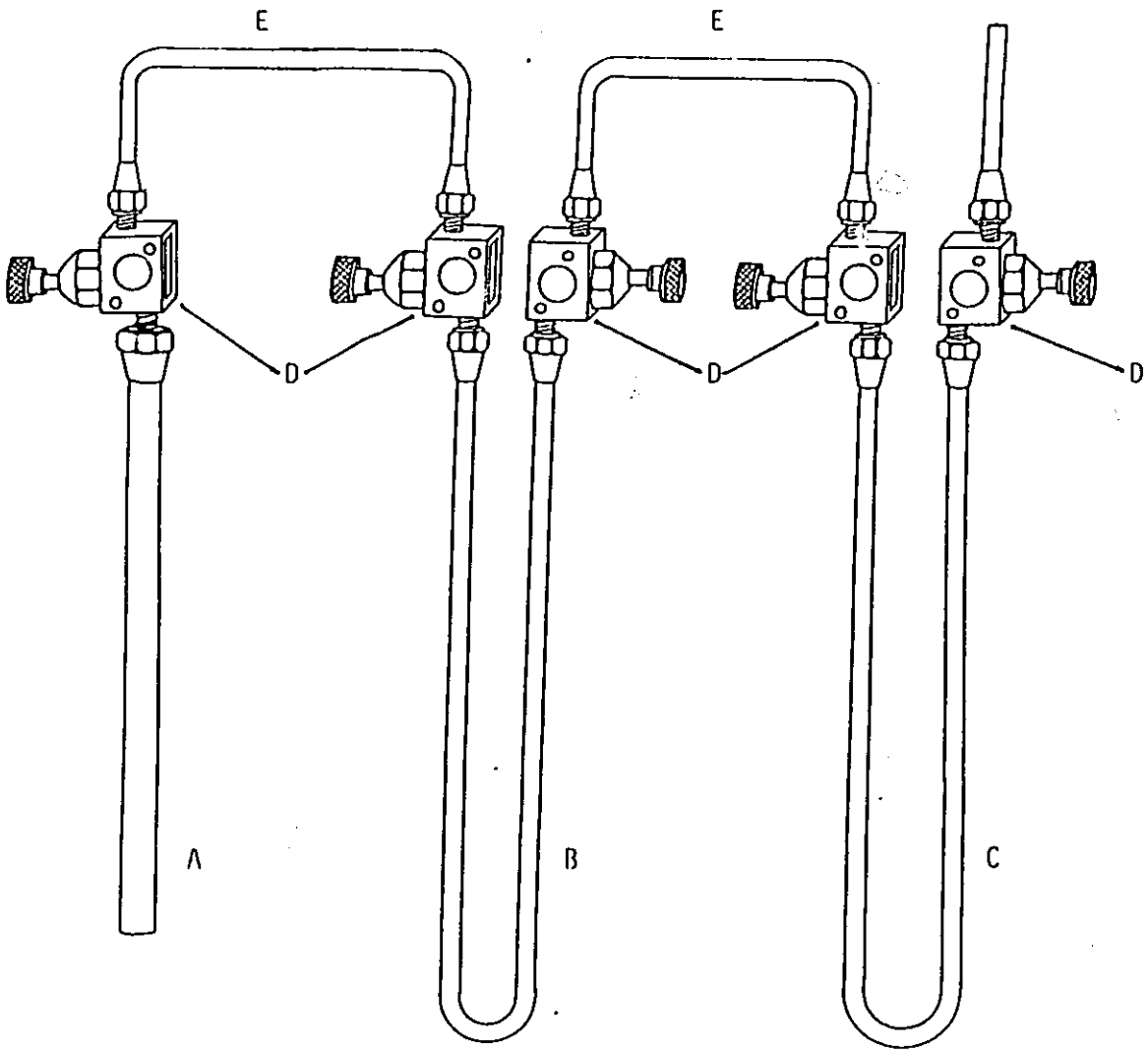
E
E
D
D
D
A
B
C

(1.22 mmol) was condensed into the trap. The contents were first warmed to -70 °C and then to room temperature and then pumped into a -196 °C trap where $ClF_4^+AsF_6^-$ was condensed. The relative distribution of the radioactivity in the $ClF_4^+AsF_6^-$ trap and the residue at room temperature ($NO^+AsF_6^-$) were measured and compared with calculated values for the random distribution of [^{18}F] among NOF, ClF_5 and AsF_5.

(I) Radiofluorination of Aromatic Compounds

(1) General Fluorination with [^{18}F]F_2

All fluorinations were carried out in a 3/4" Kel-F tube attached to a stainless steel assembly equipped with an inlet and an outlet valve (Figure 2.4). The valve assembly had a 1/4" Teflon inlet tube attached to the inlet valve for bubbling dilute fluorine gas through the solution of organic substrate in the Kel-F tube. The outlet gas was passed through a sodalime trap and charcoal filter before it was vented out through a flow meter. Solutions of aromatic compounds in HF were made by transferring a weighed amount (0.55 mmol) of the compound into the Kel-F tube and distilling in HF (≈ 5 mL) under vacuum at -196 °C. A known amount of boron trifluoride, if required, was condensed into the Kel-F vessel at -196 °C and the mixture was degassed. The HF or HF/BF_3 solution was equilibrated at - 70 °C before it was used for the fluorination reaction.

Figure 2.4 General Fluorination Apparatus. (A) 1/8" o.d. x 1/16" i. d. stainless steel tube from the target, (B) 3/4" o. d. Kel-F reaction vessel containing aromatic amino acid in HF at -70 °C, (C) 1/4" o. d. x 1/8" i. d. Teflon bubbling tube, (D) Sodalime trap, (E) Charcoal trap and (F) Flow meter. The Kel-F reaction vessel is connected to the sodalime and charcoal traps and flow meter, in series, by 1/8" o.d. x 1/16" i.d. Teflon tube using Swagelok fittings.

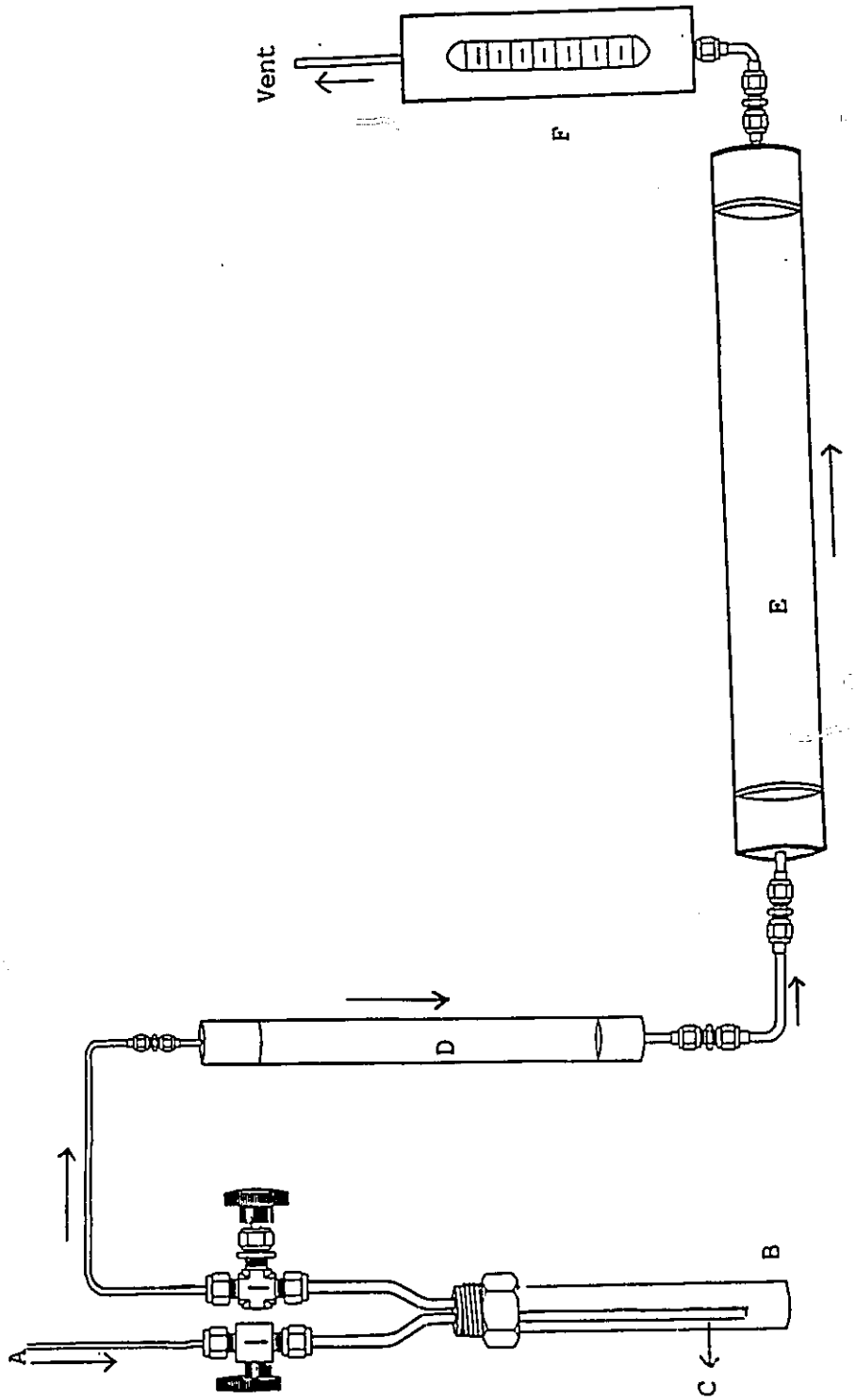
Vent
F
E
D
B
C

Fluorine-18 [F_2] (0.18 mmol) in neon (0.4% F_2 in neon) was bubbled through a solution of the substrate in anhydrous HF at -70 °C. The amount of [^{18}F]F_2 which reacted was determined by measuring the amount of radioactivity present in the crude reaction mixture after all the target gas had bubbled through. The HF solvent was pumped off under vacuum, the dry residue dissolved in water and transferred to a rotary evaporator and the water evaporated. The residue was redissolved in water and again evaporated to remove traces of acid. The final residue was dissolved in 2 mL of water and filtered through a 0.45 μ filter prior to HPLC analysis.

(2) Measurement of [^{18}F]F_2 Consumed in the Reaction

In order to assess the efficiency of a particular method for radiofluorination, it is necessary to know the total [^{18}F]F_2 available at the beginning of the reaction. This quantity depends on the efficiency of the nuclear reaction used to produce ^{18}F and the efficiency of the subsequent recovery of ^{18}F from the target. For the nuclear reaction $^{20}N(d,\alpha)^{18}F$, using an 11.5 Mev deuteron beam, the thick target yield at saturation has been experimentally determined to be 91 mCi/μA.[70] The amount of ^{18}F produced in the target is calculated using the equation (2.1)

$$^{18}F\ (mCi) = 91 \times i\ (1-e^{-\lambda t}) \qquad (2.1)$$

where t = time of irradiation, λ = decay constant for ^{18}F and i is the beam current in microamperes. For example, the amount of ^{18}F produced in the target after 110 min. irradiation at a beam current of 7 μA will be 318.5 mCi (equation 2.2)

$$^{18}F\ (mCi) = 91 \times 7\ (1-e^{(-0.693/110)110}) = 318.5\ mCi \qquad (2.2)$$

It has been shown that the maximum amount of $[^{18}F]F_2$ recovered under the present experimental conditions is 65% ± 8%.[47] However, the total $[^{18}F]F_2$ consumed in the reaction of F_2 with an organic substrate is dependent upon the solvent, the temperature and the reactivity of the organic substrate towards fluorine. In the present work, a measure of the total $[^{18}F]F_2$ used up in the reaction was obtained by assaying the ^{18}F present in the reaction mixture after the dilute $[^{18}F]F_2$ was bubbled through the solution of organic substrate and is reported as a percentage of the thick target yield of ^{18}F (i.e., ^{18}F produced in the target).

(3) Determination of Radiochemical Yield

The radiochemical yield is the amount of $[^{18}F]$-labelled organic compound produced relative to the total $[^{18}F]F_2$

available at the beginning of the experiment. In this work the radiochemical yield is determined by measuring the amount of [^{18}F] present in the labelled amino acid after separation from the reaction mixture using HPLC (decay corrected to the beginning of the experiment) and is reported as a percentage of the [^{18}F]F_2 obtained in the reaction mixture after all fluorine gas was bubbled through the amino acid solution.

It should be noted that the maximum radiochemical yield from [^{18}F]F_2 is at most 50% because only one fluorine atom in the fluorine molecule is radioactive and because there is an equal probability that the fluorine atom which reacts with the aromatic compound is the unlabelled fluorine (Equation 2.3).

$$Ar\text{-}H + 2^{*}F\text{-}F \longrightarrow Ar\text{-}F + Ar\text{-}^{*}F + HF + H^{*}F \qquad (2.3)$$

Therefore, for every two molecules of [^{18}F]F_2, only one molecule of labelled organic molecule is produced along with one molecule of labelled HF, giving a maximum radiochemical yield of 50%.

J. Preparation of [^{18}F]Labelled Biologically Active Aromatics

(1) Preparation of 3-Fluorotyrosine

3-Fluorotyrosine was prepared by the direct fluorination of tyrosine in HF (Scheme 1). Dilute [^{18}F]F_2 gas was bubbled

through a solution of 100 mg (0.54 mmol) of L-tyrosine in HF at -70 °C at 90 - 100 ml/min. for 35 - 40 min. A yellow colour immediately appeared as the $[^{18}F]F_2$ came in contact with the tyrosine/HF solution. The colour had turned bright orange-red after all of the F_2 gas had passed through. The temperature of the cold bath usually increased by 5 - 8 °C during the 35 - 40 min interval while the fluorination of tyrosine was taking place. The hydrogen fluoride was removed under vacuum and the reaction mixture was worked up as described earlier (see General Fluorination Procedure above). Direct fluorinations of L-tyrosine in CF_3COOH and CH_3CN/BF_3 were also done by a similar procedure.

Scheme 1

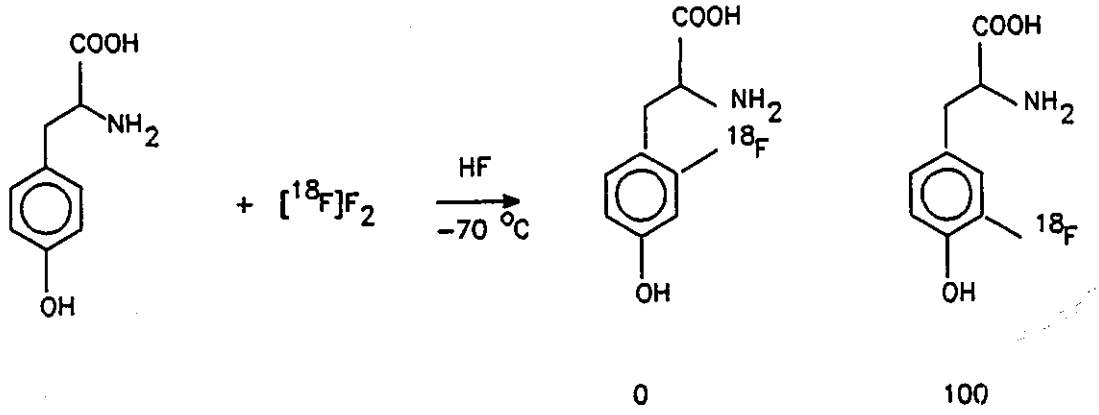

0 100

(2) Separation of 3-Fluorotyrosine

Fluorine-18 labelled 3-fluorotyrosine was isolated by passing the reaction mixture through two semi-preparative reverse phase columns (Waters μ BondaPak C_{18} 0.78 cm x 30 cm). The products were eluted with 0.1% acetic acid at 2 mL/min. The eluate from the columns was monitored using a UV detector (280 nm, preparative cell, Altec) and a NaI(Tl) scintillation detector. HPLC analysis of the reaction mixture gave a UV peak at 25 and 33 min (Figure 2.5 a). A comparison of the retention time as well as spiking the sample with authentic L-tyrosine allowed the earlier peak to be assigned to L-tyrosine. The fraction eluting at 33 min. had the same retention time and co-chromatographed with authentic 3-fluorotyrosine. It contained 30% of the total [^{18}F] found in the reaction mixture (Fig. 2.5 b). This fraction was collected for identification and characterization of the products using mass spectrometry and NMR spectroscopy (see Results Section).

(3) Preparation of 2-Fluorotyrosine

2-Fluorotyrosine was prepared by two different methods (reaction Schemes 2 and 3). For Scheme 2, 100 mg (0.54 mmol) of L-tyrosine dissolved in HF/BF_3 was fluorinated by passing dilute [^{18}F]F_2 gas through the solution at -70 °C. The reaction mixture was worked up as in Scheme 1.

Figure 2.5. HPLC trace of the reaction mixture obtained after the fluorination of L-tyrosine in HF (Scheme 1). (A) UV trace and (B) [^{18}F] trace.

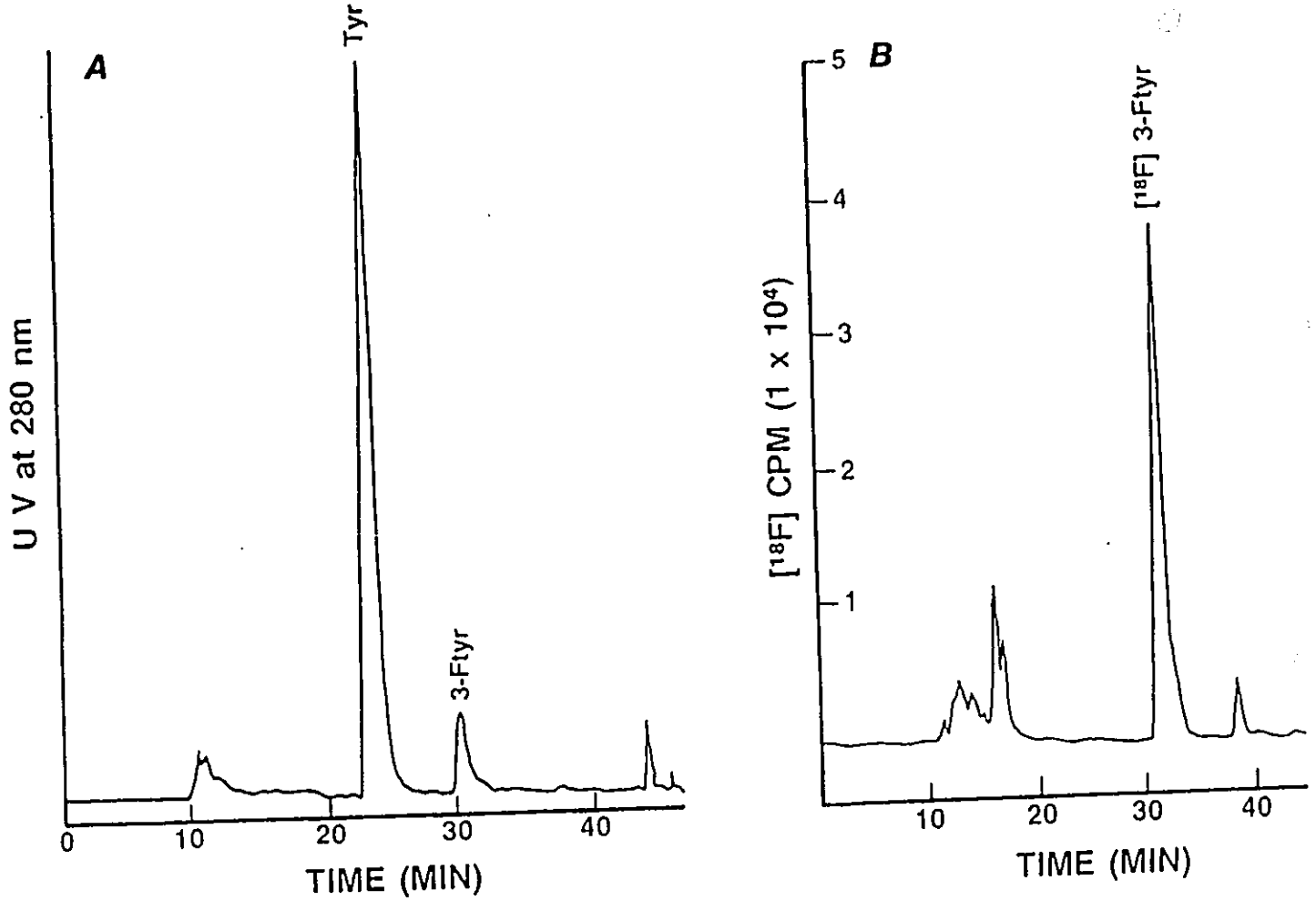
A
Tyr
3-Ftyr
U V at 280 nm
0
10
20
30
40
TIME (MIN)
B
[18F] 3-Ftyr
[18F] CPM (1 x 10⁴)
1
2
3
4
5
10
20
30
40
TIME (MIN)

Scheme 2

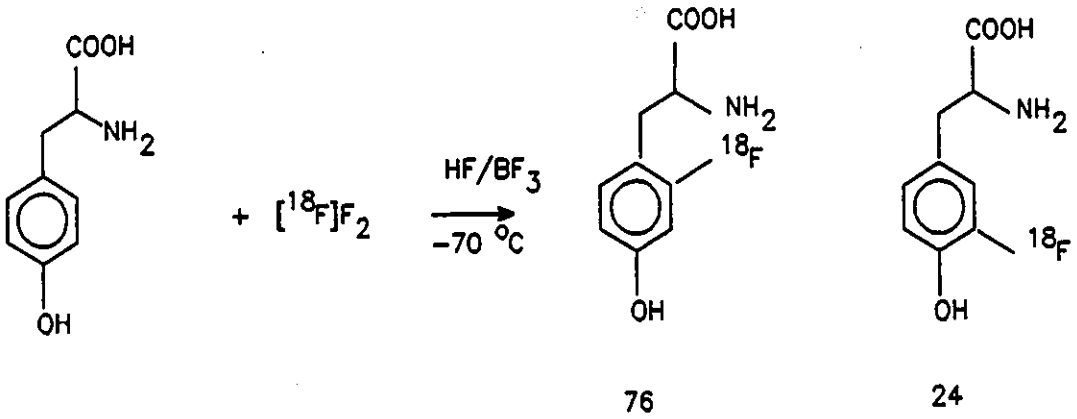

Scheme 3

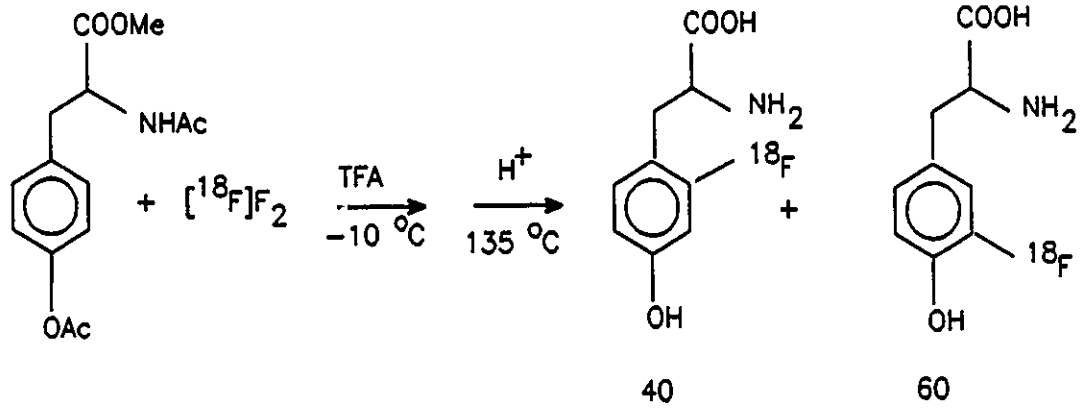

In reaction Scheme 3, N-acetyl-(4-acetoxyphenyl)alanine methyl ester (150 mg) was dissolved in 6 - 7 ml of trifluoroacetic acid and dilute $[^{18}F]F_2$ gas was bubbled through at -10 °C. After bubbling the gas for 35 - 40 min. at

90 - 100 mL/min., the reaction mixture was transferred into a round bottom flask and the solvent was evaporated under reduced pressure. The pale yellow oily residue that was obtained was dissolved in 48% HBr and refluxed for 25 min. at 145 °C. The HBr was evaporated, and the residue was washed with water (2 x 5 mL portions) and evaporated to remove any traces of acid. The final residue was dissolved in 2 mL water and filtered through 0.4 μ filter for HPLC analysis.

(4) Separation of 2-Fluorotyrosine

2-Fluorotyrosine was isolated along with 3-fluorotyrosine according to reaction Schemes 2 and 3. HPLC analysis of the reaction mixture (Scheme 2) showed peaks for tyrosine, 3-fluorotyrosine and another peak at 34 min (Figure 2.6 a). The radiochromatogram also contained peaks at 33 and 34 min. (Figure 2.6 b) and they together contained 26% of the total [^{18}F] activity found in the reaction mixture. The ratio of [^{18}F] activity in the peaks eluting at 33 and 34 min. was 24:76. Similar chromatograms were obtained when the reaction mixture from Scheme 3 was analyzed using HPLC except the ratio of [^{18}F] in the peaks eluting at 33 and 34 min. was 60:40 (Figure 2.7). Using the NMR data (see Results Section) and the [^{18}F] content of each of the peaks, the two products have been assigned to 3- and 2-fluorotyrosine.

Figure 2.6. HPLC trace of the products obtained after the direct fluorination of L-tyrosine in HF/BF_3 (Scheme 2). (A) UV trace and (B) [^{18}F] activity trace

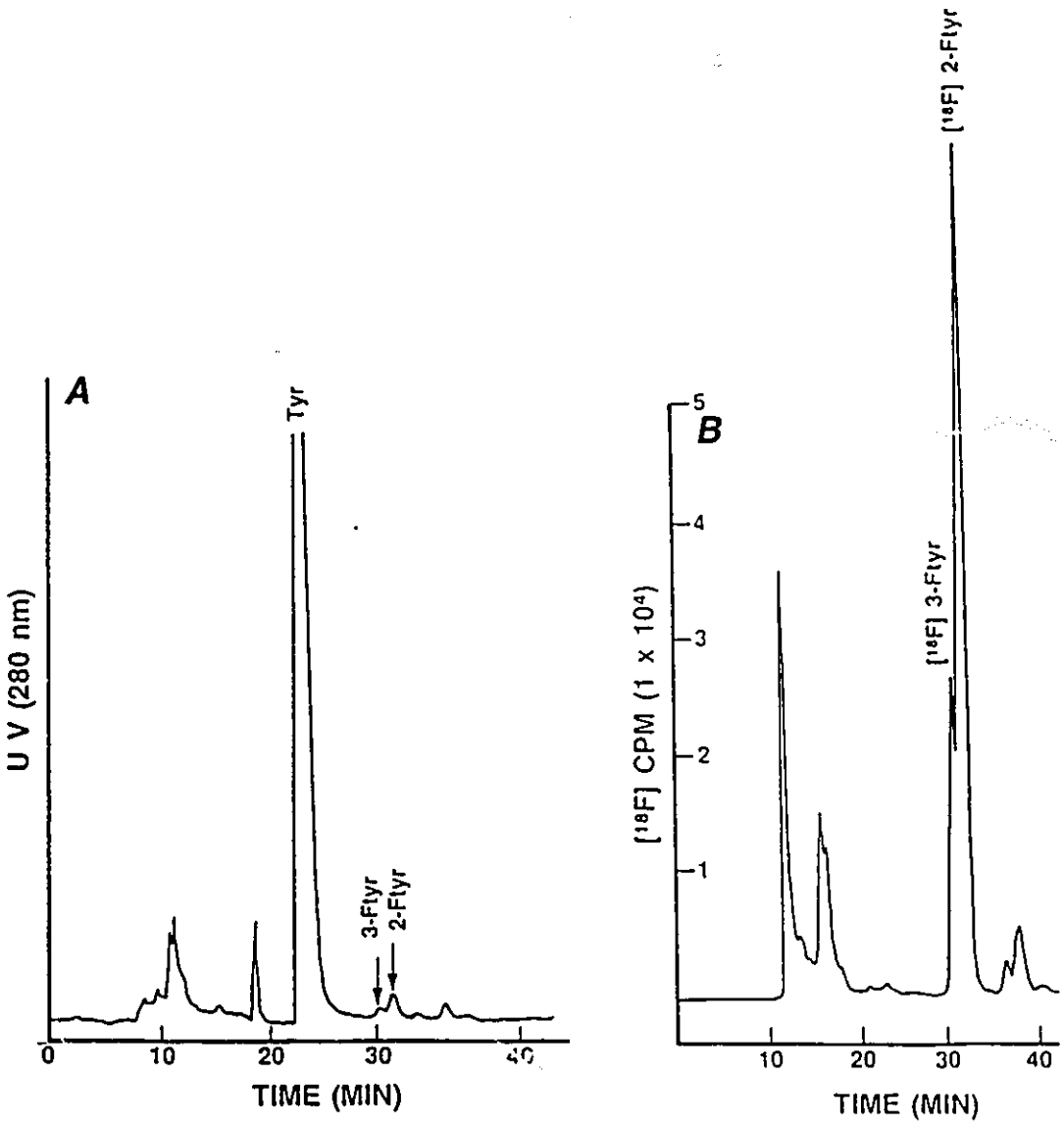
A
Tyr
3-Flyr
2-Flyr
U V (280 nm)
0
10
20
30
40
TIME (MIN)
B
[18F] 2-Flyr
[18F] 3-Flyr
[18F] CPM (1 x 10⁴)
1
2
3
4
5
10
20
30
40
TIME (MIN)

Figure 2.7. Radiochromatogram of the products obtained from Scheme 3. (A) UV trace and (B) [^{18}F] activity trace

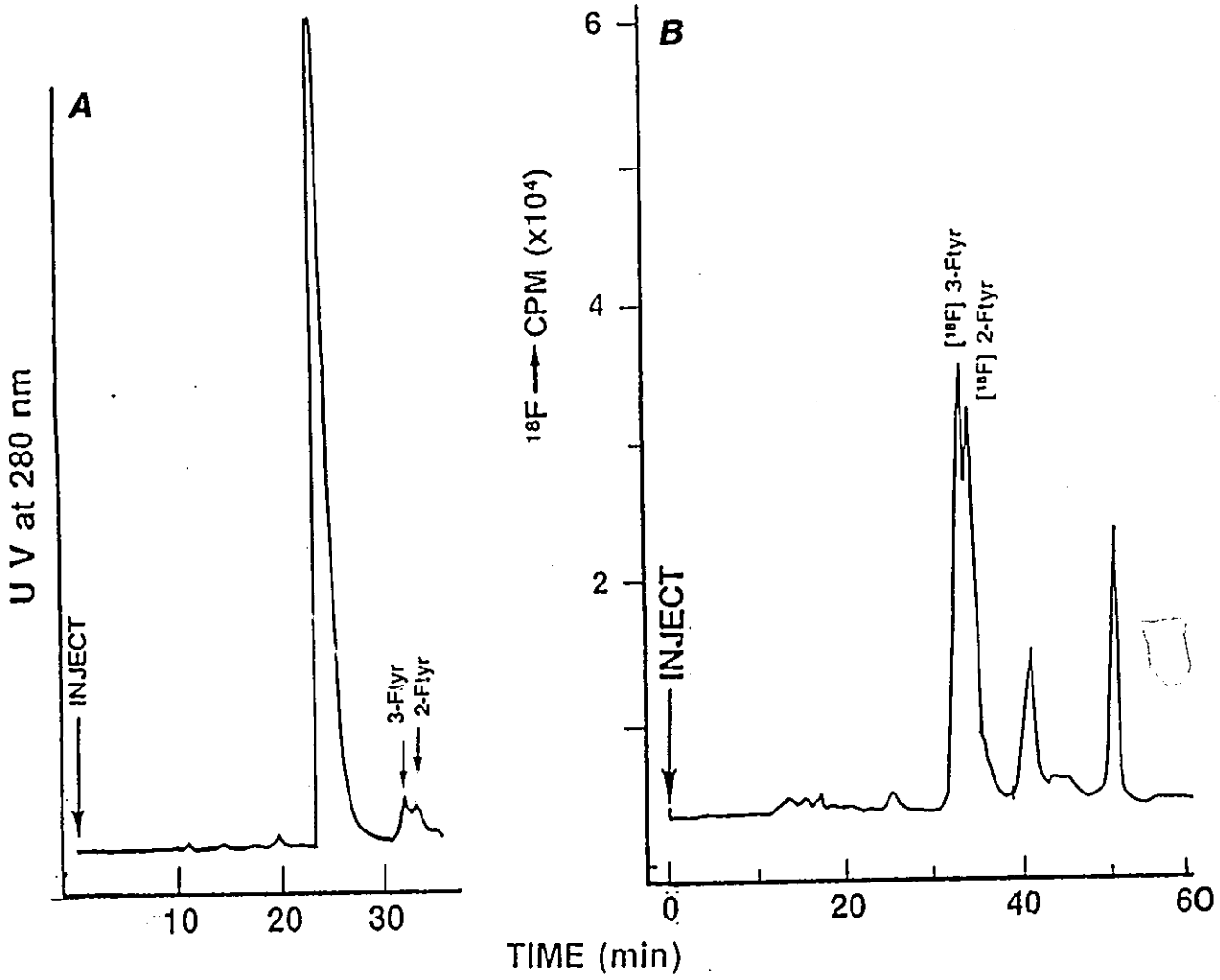
A
U V at 280 nm
INJECT
3-Flyr
2-Flyr
10
20
30
B
^{18}F → CPM (x10^4)
6
4
2
INJECT
[^{18}F] 3-Flyr
[^{18}F] 2-Flyr
0
20
40
60
TIME (min)

(5) Preparation of 2- and 6-Fluoro-m-Tyrosine

Fluorine-18 labelled fluorine (0.18 mmol) was allowed to react with m-tyrosine (0.47 mmol) in HF as described in the general fluorination procedure. Fluorine-18 labelled fluoro-m-tyrosine was isolated by passing the reaction mixture through two semipreparative reverse phase columns (Waters μ BondaPak C_{18} 0.78 cm x 30 cm). The products were eluted with 0.1% acetic acid in water containing 3% methanol at 2 mL/min. The eluate from the columns was monitored using a UV detector (280 nm) and a NaI(Tl) scintillation detector. HPLC analysis of the reaction mixture gave UV peaks at 20 and 23 min (Figure 2.8 a). A peak at 40 min. (Figure 2.8 a) containing unidentified products was obtained when the column was washed with methanol. A comparison of the retention time as well as spiking the sample with authentic DL-m-tyrosine allowed the earlier peak to be assigned to DL-m-tyrosine. The fraction eluting at 23 min. contained 43 % of the [^{18}F] activity (Figure 2.8 b) and was collected for identification and characterization of the products using mass spectrometry and NMR spectroscopy (see Results Section).

The radiochemical yields after the fluorination of m-tyrosine in other solvents were determined by analyzing the reaction mixtures using radio HPLC. The amount of [^{18}F]

Figure 2.8. HPLC chromatogram of the products obtained after the fluorination of m-tyrosine in HF at -70 °C. (A) UV trace and (B) [^{18}F] trac-

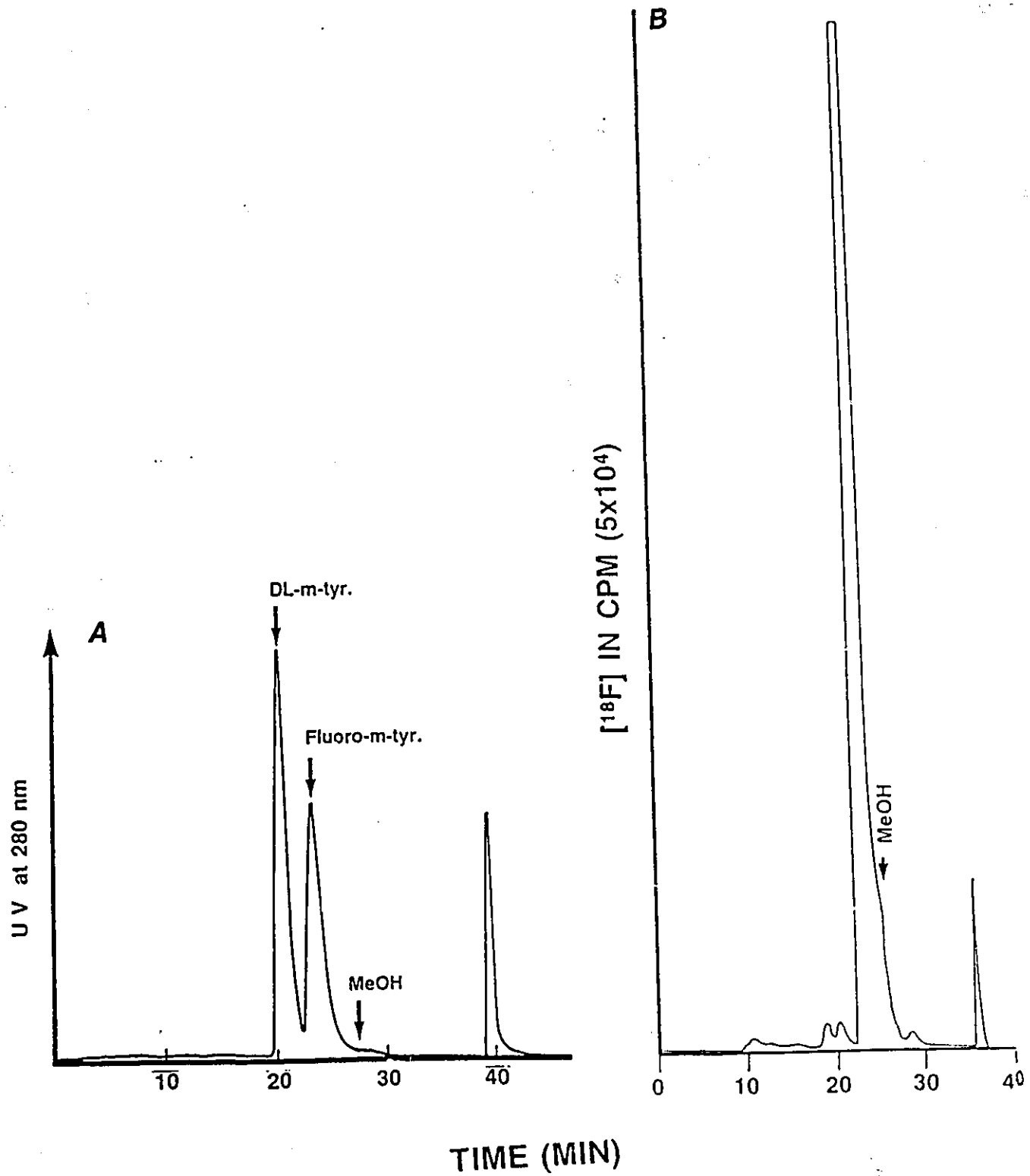
A
DL-m-tyr.
Fluoro-m-tyr.
MeOH
U V at 280 nm
10
20
30
40
B
[18F] IN CPM (5x10⁴)
MeOH
0
10
20
30
40
TIME (MIN)

present in the peak eluting at 23 min. was measured and it is expressed as percentage of the total [^{18}F] present in the bulk batch reaction mixture. The peak at 23 min. was also used for ^{19}F NMR to determine the orientation of fluorine in the aromatic ring.

(6) Separation of 2- and 6-Fluoro-m-Tyrosine

2- and 6-Fluoro-m-tyrosines were separated using reverse phase HPLC columns (Waters μ BondaPak C_{18} and Vydac C-18 columns connected in series) with an aqueous solution of trifluoroacetic acid (0.15%) and acetonitrile (4.5%) as the mobile phase and eluted at 2.5 mL/min. The radiochromatogram of the 2- and 6-[^{18}F]- fluoro-m-tyrosine gave peaks at 26 and 29 min. (Figure 2.9). The ratio of [^{18}F] activity in the samples eluting at 26 and 29 min. was 1 : 1.6. Using the ^{19}F NMR data and the [^{18}F] contents in the two peaks, the two products have been assigned to 2- and 6-fluoro-m-tyrosines, respectively. When the fluorination of m-tyrosine was done in HF/BF_3, the ratio of the [^{18}F] contents in the samples eluting at 26 and 29 min. was changed to 1:6 (Figure 2.10).

For routine production, the aqueous reaction mixture was applied to a Whatman M9 partisil 10/50-ODS-2 column. The fluorotyrosine was separated from the side products and the

Figure 2.9. (A) Radiochromatogram of the reaction mixture the obtained after the direct fluorination of m-tyrosine in HF at - 70 °C. (B) Radiochromatogram of the peak eluting at 23 min. in A (see text for HPLC conditions).

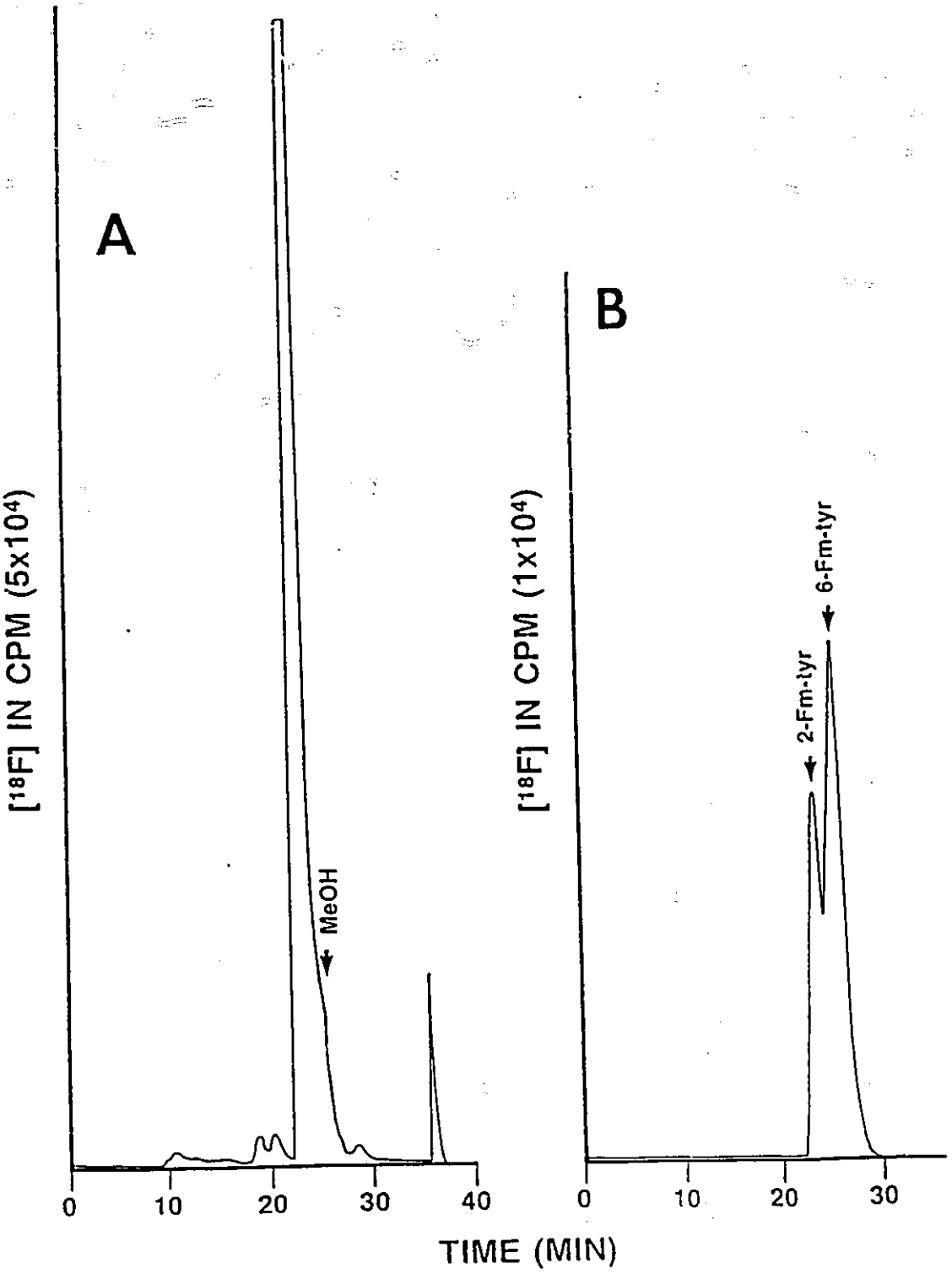
A
B
[18F] IN CPM (5x10⁴)
[18F] IN CPM (1x10⁴)
MeOH
2-Fm-tyr
6-Fm-tyr
0
10
20
30
40
TIME (MIN)

Figure 2.10. (A) Radiochromatogram of the reaction mixture after the direct fluorination of m-tyrosine in HF/BF_3 at - 70 °C (B) Radiochromatogram of the peak eluting at 23 min. in A (See text for HPLC conditions).

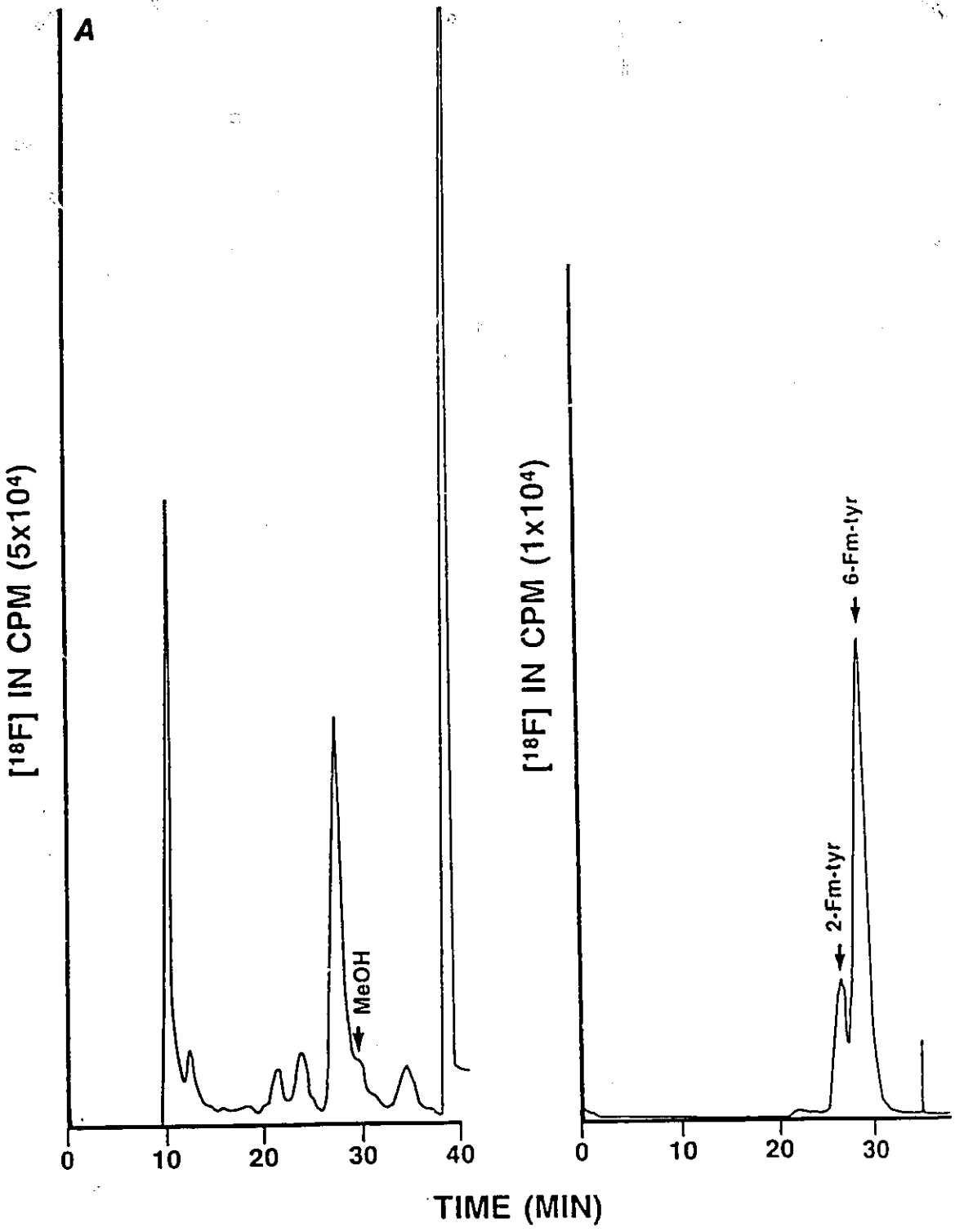
A
[18F] IN CPM (5x10⁴)
MeOH
0
10
20
30
40
[18F] IN CPM (1x10⁴)
2-Fm-tyr
6-Fm-tyr
0
10
20
30
TIME (MIN)

majority of m-tyrosine by eluting the sample with 0.1% acetic acid with 3% methanol at 4 mL/min. The fraction containing the majority of the radioactivity was collected, evaporated to dryness and redissolved in 1.5 mL water and the final product, a mixture of 2- and 6-fluoro-m-tyrosine, separated by HPLC as described above, giving a radiochemical purity of better than 98%. By using this procedure, 16 mCi of a mixture of [^{18}F]2- and 6-fluoro-m-tyrosine was produced from 100 mCi of [^{18}F]F_2 at the end of 150 min. synthesis time.

(7) Preparation of 2- and 6-Fluoro-m-Tyramine

Fluorine-18 labelled fluorine (0.18 mmol) was allowed react with m-tyramine.HCl (0.29 mmol) as described above. Fluorine-18 labelled fluoro-m-tyramine was isolated by passing the aqueous reaction mixture through two reverse phase semipreparative columns (Waters μ Bonda Pak C_{18} 0.78 x 30 cm). The products were eluted with 0.1% acetic acid in water at 2 mL/min. The major radioactive peaks was eluted at 20 and 22 min. and the ^{18}F content in these peaks were 36% and 64%, respectively (Figure 2.11 a). These fractions were combined and characterized by mass spectrometry and NMR spectroscopy (see Results Section).

Figure 2.11. (A) Radiochromatogram of the products obtained after the direct fluorination of m-tyramine in HF at -70 °C. (B) Radiochromatogram of the reaction mixture after the direct fluorination of 3-hydroxy phenylacetic acid HF at -70 °C (see text for HPLC conditions).

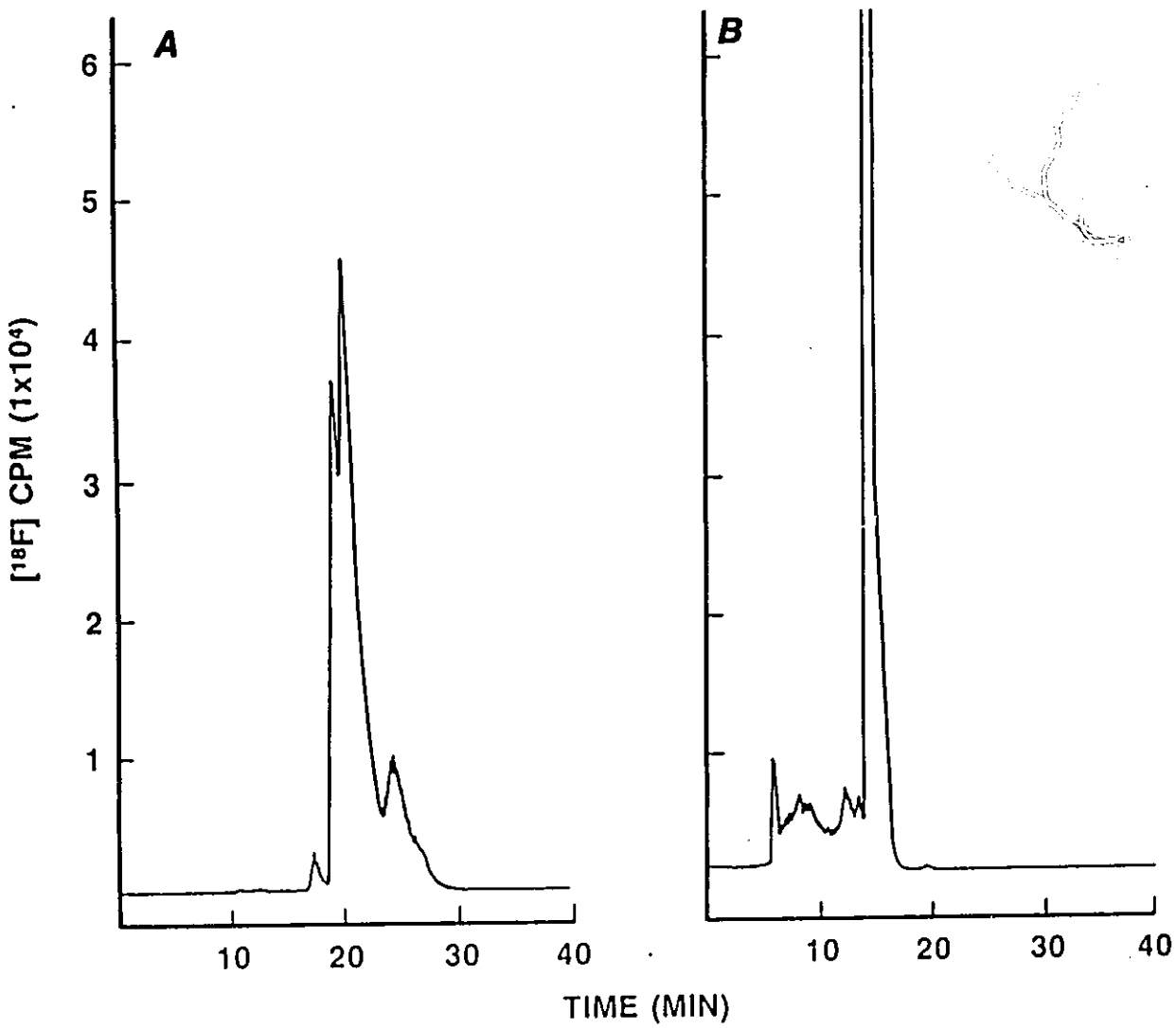
A
B
6
5
4
3
2
1
[18F] CPM (1x10⁴)
10
20
30
40
10
20
30
40
TIME (MIN)

(8) Preparation of 2- and 6-Fluoro-3-Hydroxyphenylacetic Acid

HPLC analysis of the reaction mixture (Waters μ BondaPak C_{18} column with 0.1% acetic acid in water containing 10% methanol; flow 2 mL/min) produced a major radioactive peak at 14 min. (Figure 2.11b). The mass spectrum and ^{1}H, ^{13}C, and ^{19}F NMR spectra of the fraction eluting at 14 min. showed that it contained 2-, 4- and 6-fluoro-3-hydroxyphenylacetic acid. No attempt was made to separate the 2-, 4- and 6-fluoro-isomers.

(K) Determination of the Selectivity of Molecular Fluorine

Fluorine-18 labelled F_2 (0.18 mmol) was allowed to react separately with equimolar quantities (F_2 : substrate, 1 : 2.6) of tyrosine/m-tyrosine, tyrosine/DOPA and m-tyrosine/DOPA. Each reaction was carried out in HF or HF/BF_3 at -70 °C. After the fluorination, the reaction mixture was worked up as described before (see general fluorination) and the products were analyzed using reverse phase HPLC. The eluate from the column was monitored using a UV detector (280 nm) and a NaI(Tl) scintillation detector.

(L) Radiofluorination of Aromatic Amino Acids in Trifluoro-methane Sulphonic Acid Solution of trifluoromethane-sulphonic acid (1 M) in trifluoroacetic acid was prepared in a bag under dry nitrogen atmosphere. Fluorination of DL-m-tyrosine or L-DOPA were carried out by bubbling dilute $[^{18}F]F_2$

gas (0.4% in neon) through a solution of m-tyrosine (0.47 mmol) and L-DOPA (0.54 mmol) in CF_3COOH/CF_3SO_3H at 0 - 4 °C (ice slush). After the reaction, the amount of [^{18}F] present in the reaction mixture was assayed and the solvent was evaporated on a rotary evaporator. The oily residue was washed with water (3 mL) and evaporated again. The final residue was dissolved in water and filtered through a 0.2 μ filter prior to HPLC analysis.

(M) Biological Studies with ^{18}F

(1) Measurement Distribution of ^{18}F in the Monkey Brain

All animal experiments were carried out by Dr. Gunter Firnau, Professor of Radiology at McMaster Medical Centre. Three *macacca mulatta* of unknown age were used. They weighed 3.1, 5.6 and 8.2 kg, respectively. Before a study, an animal was deprived of food for 12 hours. It was immobilized by an inter muscular injection of ketamine hydrochloride (10 mg/kg). Anaesthesia was induced and maintained with sodium barbital. [^{18}F]Fluoro-L-m-tyrosine (2.4 - 11.3 mCi) in 5 mL of saline was injected intravenously. An animal was killed by an intravenous injection of euthanyl (100 mg/kg) at either 20, 45 or 90 min. after it had been given [^{18}F]fluoro-L-m-tyrosine. The brain was exposed immediately by craniotomy, quickly removed, placed on an ice cold plate and cut coronally at the level of the superior precentral sulcus. The caudate nucleus,

putamen, thalamus, hypothalamus and substantia nigra were identified dissected out as described by Szabo and Cowan.[71] Cortical samples were taken from the occipital pole, superior cingulate gyrus and the parietal lobe. A blood sample was also taken at the time of death. The ^{18}F content of aliquots (0.3 - 1.6 g) of these tissues was measured with a NaI(Tl) well counter.

(2) Analysis of ^{18}F-Containing Metabolites in the Monkey Brain and Plasma

Brain samples were suspended in approximately 6 mL of 7% perchloric acid that contained 1 mmol of sodium EDTA and 10 mmol of sodium bisulphite. The suspension was homogenized first by a mechanical tissue grinder and then by sonication for 30 sec. It was next centrifuged at 3,000 g for 30 min. The supernatant was separated, concentrated to a volume of 0.5 - 1.0 mL by rotary evaporation, and passed through a membrane filter (pore size 0.45 μm). The resulting solution was taken for chromatographic analysis. The plasma samples were processed similarly.

The ^{18}F-labelled metabolites in the supernatant from brain and plasma samples were separated by reversed phase liquid chromatography using a Waters NOVO PAK™-C_{18} Radial Compression Cartridge (4 μm; 8 x 100 mm; mobile phase 0.03 M sodium

hydrogen phosphate in water at pH 2.9, containing 1g/l sodium octanesulfonate and 7.4% acetonitrile and a flow rate of 2 mL/min). The effluent from the column was collected into 1-mL fractions using an automatic fraction collector. The ^{18}F radioactivity in each fraction was measured with a NaI(Tl) well counter. The ^{18}F-containing peaks were identified by comparing their retention times with those of authentic ^{18}F labelled fluoro-m-tyrosine, fluoro-m-tyramine and fluoro-3-hydroxyphenyl acetic acid. A fourth radioactive peak present in the chromatogram was assigned to the 3-O-sulphocongugate of fluoro-m-tyramine as reported by Melega *et al.*[72]

The recovery of each metabolite during the extraction procedure and chromatographic analysis was determined as follows. A known amount of authentic metabolite was added to brain and plasma and the spiked tissues were processed and analyzed as described above. The fraction of each metabolite that was recovered after the total procedure was determined (Table 2.1).

(3) Measurement of ^{18}F in the Human Brain

Measurements of [^{18}F] in the human brain were done using McMaster Positron Emission Tomograph. A detailed description of the design and construction of the tomograph have been

Table 2.1 Fraction of ^{18}F Metabolite Recovered After Extraction from Tissue and HPLC Analysis

Metabolite	Brain	Plasma
[^{18}F]Fluoro-L-m-tyrosine	0.58 ± 0.04	0.67 ± 0.01
[^{18}F]Fluoro-m-tyramine	0.70 ± 0.13	0.64 ± 0.06
[^{18}F]Fluoro-3-hydroxy-phenylacetic acid	0.45 ± 0.01	0.49 ± 0.05

described elsewhere.[73,74,75] Briefly, it is a single slice tomograph consisting of 160 bismuth germanate scintillation detectors arranged along the circumference of a circle, 535 mm in diameter. The size of each crystal was 1 x 25 x 45 mm^3 and each detector is attached directly to photomultiplier tube. The transaxial spatial resolution of the tomograph is 8 mm (fwhm) and each section is 15 mm thick. The sensitivity, measured using a cylindrical phantom, 200 mm in diameter, is 16,000 cps/uCi/cc.

Using external landmarks and a rigid head holder, it was possible to reposition the subjects reproducibly within the tomograph. Typically, five overlapping sections of brain each containing striatum were obtained. Each section overlapped its predecessor by 10 mm. This insured that the section containing the greatest volume of striatum could be identified and used for measuring [^{18}F] content in selected regions of the brain. This procedure minimizes partial volume effects. Regions of interest were defined over the striata and over a portion of the occipital cortex. The amount of [^{18}F] in each region was expressed as the average cpm/pixel within the region normalized to the amount of [^{18}F] radioactivity injected.

CHAPTER 3.

APPLICATION OF [^{18}F] TO THE INVESTIGATION OF HYPERVALENT COMPOUNDS OF NITROGEN

A. GENERAL

"Hypervalent" or "hypercoordinated" compounds belong to an interesting class of compounds because they violate the traditional concepts of valence. In these compounds the number of electrons in the valence shell of the central atom exceeds eight. Shriver *et al.*[76] have defined hypervalent compounds as "those compounds in which Lewis octet structures demand more than an octet of electrons around at least one atom". The nature of bonding in hypervalent compounds is still an open controversy.[77a,b] The bonding in these compounds has been explained in two ways: (a) by allowing the violation of the Lewis octet rule through promotion of electrons into vacant higher lying d orbitals and (b) by modifying the Lewis rule of localized bonding pairs to allow bonds of more ionic character thus preserving the octet rule and circumventing the necessity of expanding the valence shell to include the d orbitals. The development of three-centre four electron bond model (as in XeF_2) has lent plausibility to the latter explanation.

In 1968, Olah *et al.*[78] presented experimental evidence for the penta-coordinated carbonium ion of the type CH_5^+. They

observed hydrogen-deuterium scrambling after methane-d_4 was treated with a ten-fold excess of 1:1 HSO_3F:SbF_5 solution at room temperature. The results were explained by the protonation of methane to give the methanonium ion CH_5^+ which can undergo reversible protonation leading to hydrogen exchange. They suggested that the preferred structure of CH_5^+ has C_s symmetry in which the carbon atom maintains approximately tetrahedral hybridization, with one sp^3 orbital bound simultaneously to two hydrogen s orbitals forming a three-center two-electron bond.

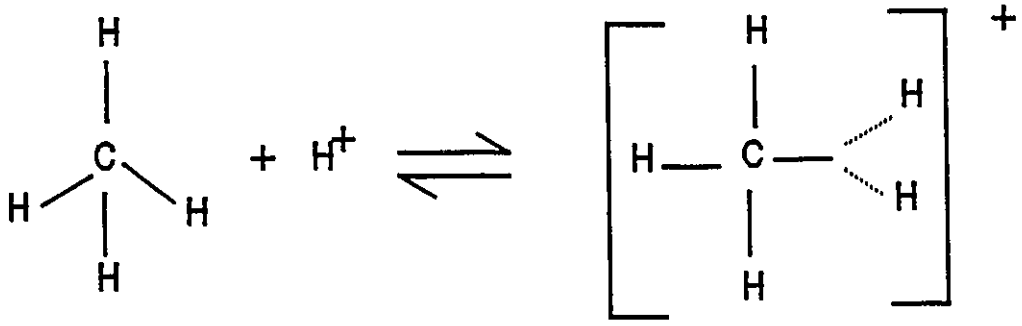

The isoelectronic boron analog of CH_5^+, BH_5, has also been postulated as the intermediate during the aqueous protolysis of borohydride carried out in deuterium oxide.[79] The formation of HD as the main product and about 4% H_2 as the minor product was explained by the possible attack of D^+ on the B-H bond

itself allowing subsequent scrambling in BH_4D prior to cleavage into BH_3 and HD

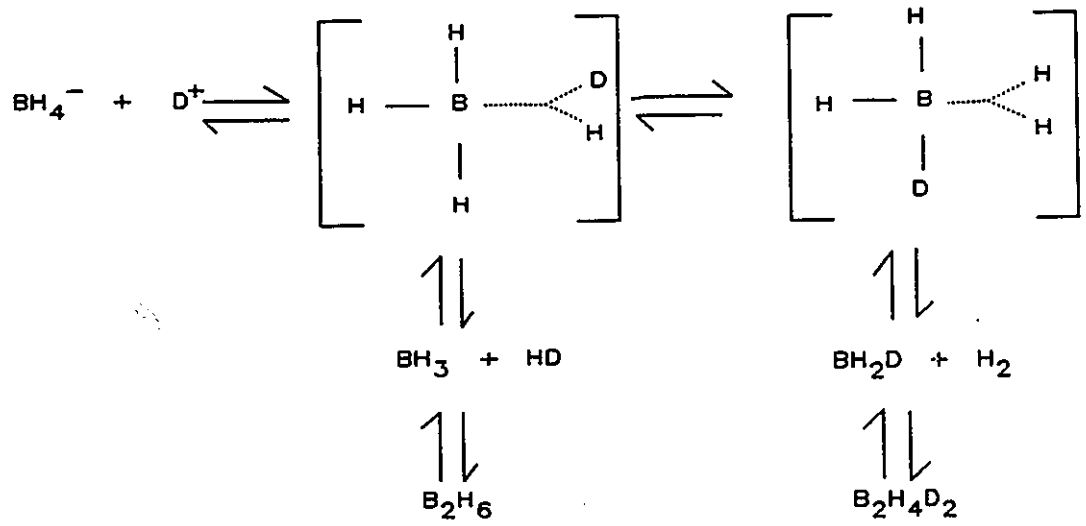

Whereas the above experimental data indicate the existence of hypercoordinated carbon and boron, convincing experimental evidence for penta-coordinated nitrogen compounds such as NF_nH_{5-n} has not been presented. For example, low-temperature UV irradiation of NF_3 and F_2 produced small amounts of a white solid residue after the reactants were pumped off at 113 K.[80] The white solid volatilized at 143 K and only NF_3 was detected in the mass spectrum. It was postulated that the white solid might be $NF_4^+F^-$ but not enough sample could be

produced to obtain conclusive evidence for the presence of NF_5.

It was suggested that the decomposition of $NF_4^+AsF_6^-$ into NF_3, F_2 and AsF_5 might proceed via an equilibrium dissociation step involving NF_5 followed by the irreversible decomposition of the unstable NF_5 into NF_3 and F_2 (equations (3.1) and (3.2)).[81]

$$NF_4^+AsF_6^- \rightleftharpoons [NF_5] + AsF_5 \qquad (3.1)$$

$$[NF_5] \longrightarrow NF_3 + F_2 \qquad (3.2)$$

However, infrared matrix isolation studies of the thermal decomposition of $NF_4^+AsF_6$- gave no evidence for the formation of NF_5.[81]

An isotopic exchange study using $NF_4^+AsF_6^-$ and $[^{18}F]AsF_5$, $[^{18}F]NF_3$ and $[^{15}N]NF_3$ gave ambiguous evidence for the existence of NF_5.[82] For example, partial fluorine exchange between $NF_4^+AsF_6^-$ and $[^{18}F]NF_3$ was observed while no nitrogen exchange was observed between $NF_4^+AsF_6^-$ and $[^{15}N]NF_3$.[82] Based on the observed results the authors have postulated an intermediate NF_4^*F species where the labelled fluorine is not equivalent to the other four fluorine atoms.

In 1973 Olah *et al.*[83] postulated the existence of penta-coordinated nitrogen based on the results obtained from heating lithium deuteride and ammonium trifluoroacetate in a melt (equation (3.3)).

$$D^- + 2NH_4^+ \longrightarrow [NH_4D] \longrightarrow \underset{85\%}{NH_3} + \underset{15\%}{NH_2D} + \underset{66\%}{H_2} + \underset{21\%}{HD} + \underset{13\%}{D_2} \quad (3.3)$$

In order to account for the formation of H_2 and D_2 they proposed nucleophilic attack by D^- at the quaternary nitrogen causing exchange to occur via a penta-coordinated nitrogen intermediate NH_4D (equation (3.4)).

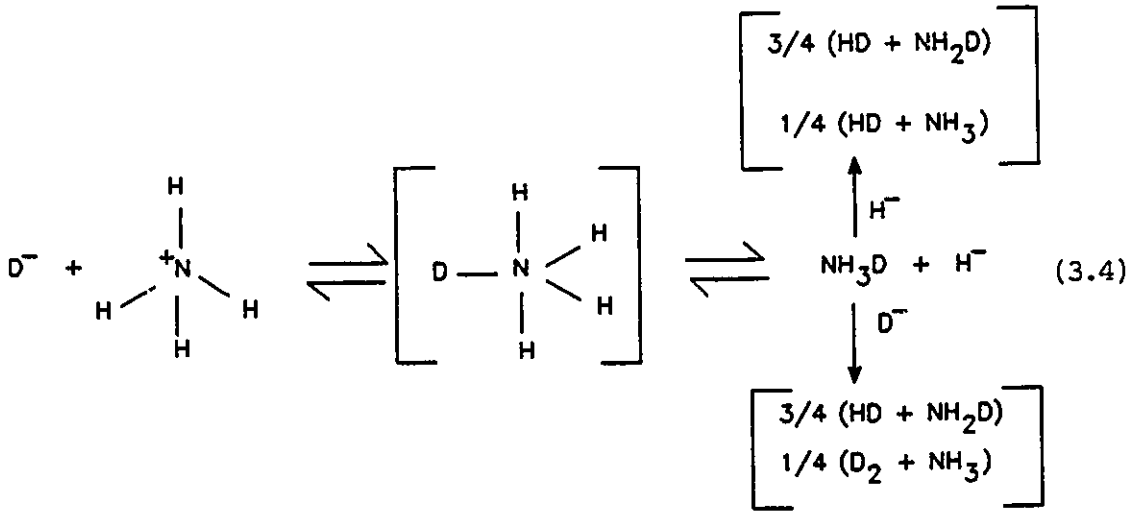

(3.4)

The deuterated ammonium ion can react with H^- and D^- giving ammonia and hydrogen appropriately labelled with deuterium. However, it was subsequently shown that the observed H_2 to D_2 ratio greatly exceeded those expected for the formation of an intermediate NH_4D and a catalytic isotope exchange reaction of the HD gas must be involved.[84]

Theoretical calculations have been carried out for NF_5 [85], NH_3F_2 [86] and NH_5.[87] which showed that the penta-coordinated NX_5 species are unstable with respect to decomposition to $NX_3 + X_2$ and are less stable than the corresponding $NX_4^+X^-$ salt. However, more recent high-level theoretical calculations indicate that NF_5 will be stable with five independent linkages to the central nitrogen atom.[88] Moreover, the vibrational frequencies for NF_5 have been calculated and they have all been found to be positive.[89] These theoretical studies combined with previous experimental results indicate that the existence of a stable penta-coordinated nitrogen species is pausible. Therefore, it is possible that penta-coordinated nitrogen species could exist as short-lived unstable intermediates. In this work the interaction of NF_4^+ with the fluoride ion donors $[^{18}F]NOF$ and $[^{18}F]HF_2^-$ have been studied in order to possibly establish the existence of NF_5.

B. RESULTS AND DISCUSSION

1. Radiochemical Yields of [^{18}F]Fluorinating Agents

Results of [^{18}F]F_2 recovery from the target and the radiochemical yields of [^{18}F]NOF and [^{18}F]HF produced from [^{18}F]F_2 are summarized in Table 3.1

The recovery of [^{18}F]F_2 from the target was reproducible and the usable [^{18}F]F_2 was 65% ± 8% of theoretical thick target yield for [^{18}F]. Casella *et al.*[70] have obtained similar quantities of [^{18}F] with the same nuclear reaction using a 15 MeV deuteron beam.

The radiochemical yield of [^{18}F]HF was 74% at the end of the synthesis. To date, reported syntheses for [^{18}F]HF involved removing the [^{18}F] activity from the target walls by heating to 500 - 1000 °C and flushing the target with hydrogen.[90,91] Another method has been described by Tewson and Welch[92] who added 2% hydrogen to the neon-fluorine target gas resulting in the in-target formation of [^{18}F]HF. The [^{18}F]HF formed was collected by passing the gas over Cs_2CO_3 or CsF coated on a silver wool. The method described in this work is simpler and more reproducible and the reaction of F_2 with H_2 is instantaneous and quantitative.

Table 3.1 Radiochemical Yields of [^{18}F]NOF and [^{18}F]HF

[^{18}F]F, Recovered (mCi)	[^{18}F]NOF (mCi)	[^{18}F]HF (mCi)	Synthesis Time (min)	Radiochemical Yield
153	75.0		88 min	49%
107	80.3		30 min	75%
95	36.4		40 min	38%
176		130.8	77 min	74%

The radiochemical yields of [^{18}F]NOF varied from 38 to 74%. Other reported synthesis of [^{18}]NOF were carried out by adding NO to the neon target gas in a flow system and the radiochemical yield (decay corrected to the end of bombardment) of [^{18}F]NOF was reported to be 60%.[93] Lambercht *et al.*[94] have added NO to the neon target gas (thick target conditions) and found that the radiochemical yield was 7% relative to the [^{18}F]F_2 yield. In the present work some variations in the yield (end of synthesis yield) of [^{18}F]NOF have been observed. This is partly due to the loss of [^{18}F] when excess fluorine is pumped off from the reaction vessel and due to the longer synthesis time. It was also observed that the amounts of [^{18}F] retained on the surface of the nickel can during the preparation of [^{18}F]NOF varied with each preparation.

2. On the Existence of NF_5

A major drawback of the NH_4^+ system for the investigation of penta-coordinated nitrogen species is the unfavourable polarity of the N-H bond for the $H^-(D^-)$ attack on the quaternary nitrogen. Since in NH_4^+ the positive charge resides on the protons and the negative charge on the nitrogen, the negatively charged H^- anion should attack on proton (equation (3.5)) and not on the nitrogen (equation (3.6)) as required for a penta-coordinated nitrogen transition state.

$$D^- + NH_4^+ \longrightarrow NH_3 + HD \quad \text{(attack on H)} \qquad (3.5)$$

$$D^- + NH_4^+ \longrightarrow NH_3D^+ + H^- \quad \text{(attack on N)} \qquad (3.6)$$

For the formation of penta-coordinated nitrogen, reaction (3.6) must compete with the more favourable acid-base reaction (3.5).

This drawback can be overcome in the NF_4^+-F^- system where, due to the higher electronegativity of fluorine, the N-F bond will be polarized placing the positive charge on the central nitrogen atom. Christe *et al.*[95] have calculated the force constants and bond orders in the isoelectronic series of BF_4^-, CF_4, and NF_4^+ and have concluded that the decrease in bond order in going from CF_4 to NF_4^+ (1.13 and 0.85, respectively) may be due to considerable polarization of the N-F bond in NF_4^+. However, theoretical analyses of charge distributions show that in NF_4^+ the negative charge resides predominantly on the fluorines whereas in NH_4^+, the positive charge is more evenly distributed.[96] Therefore, nucleophilic attack by the anion at the nitrogen will be favoured in the NF_4^+-F^- system compared to the NH_4^+-H^- system.

Use of $[^{18}F]F^-$ would confirm the possible existence of NF_5 as an intermediate by comparing the $[^{18}F]$ contents in NF_3 and F_2. The nucleophilic attack of $[^{18}F]F^-$ on nitrogen would cause isotopic scrambling among the five fluorines and therefore 60% (3/5) of the original $[^{18}F]$ should be found as NF_3 and 40% (2/5) should be found as F_2 (equation (3.7)). If the $[^{18}F]F^-$ attacks on the fluorine then no $[^{18}F]$ will occur as NF_3 and 100% of the original ^{18}F will be found as F_2 (equation (3.8)).

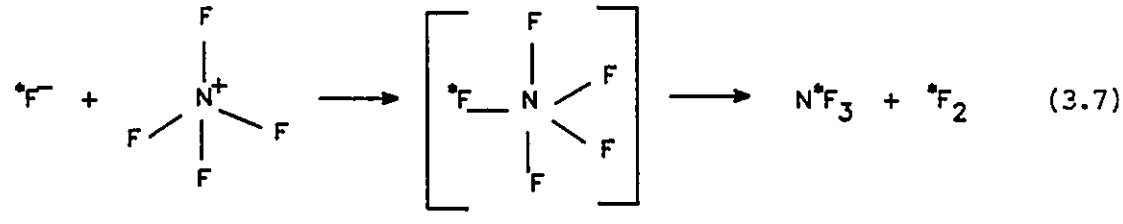

(3.7)

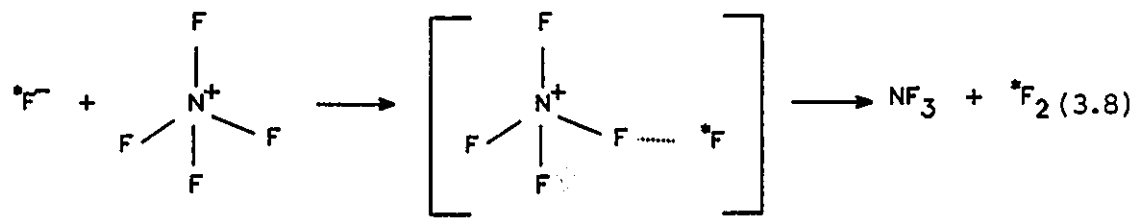

(3.8)

3. Pyrolysis of $NF_4^+BF_4^-$ + [^{18}F]NOF

The radiochemical yield of [^{18}F]NOF recovered from the direct reaction of [^{18}F]F_2 and NO was 75%. The distribution of [^{18}F] after the displacement reaction between $NF_4^+BF_4^-$ and [^{18}F]NO^+F^- and subsequent pyrolysis of the product is given in Table 3.2. The expected distribution of [^{18}F] among the reactants and products after the nucleophilic attack of F^- at quaternary nitrogen in NF_4^+ (equation (3.7)) and at the fluorine (equation (3.8)) are also shown in Table 3.2.

The total [^{18}F] activity found among the reactants and products after the decomposition of $NF_4^+BF_4^-$ was 68.7 mCi (decay corrected). This was 8.4% lower than the starting activity (75 mCi). However, this difference could be accounted for when a correction of 10 ± 2% in [^{18}F] measurements, due to different geometries of FEP reactors and FEP U-tubes, was applied. In the present work the relative distributions of [^{18}F] in F_2 and NF_3 were measured in vessels having the same geometries, eliminating the need for geometrical corrections.

As seen from Table 3.2, no [^{18}F] (no more than the background activity) was observed in the soda lime (F_2) or in the -210 °C trap (NF_3). All the original activity was distributed between the initial reaction vessel and the

-196 °C trap containing [^{18}F]NOF and [^{18}F]HF. The activity in $NF_4^+BF_4^-$ may result from traces of HF present in the reaction mixture causing isotopic scrambling (equation (3.9) and (3.10)).

$$HF + NO^*F \longrightarrow NO^+ + H^*F_2^- \qquad (3.9)$$

$$H^*F + BF_4^- \longrightarrow B^*F_3 + H^*F_2^- \qquad (3.10)$$

The presence of HF in the reaction mixture was confirmed after the reaction of BF_3 with the fluorine-containing species trapped in the -196 °C vessel. If the trap contained only [^{18}F]NOF, 100% retention of the activity in the $NO^+BF_4^-$ was expected. It was found that 22% of the [^{18}F] was volatile at -78 °C and it could be trapped on the soda lime and it can be argued that this activity arose from [^{18}F]HF present in the -196 °C trap.

Since no [^{18}F] was found on the soda lime and in the -210 °C trap, the initial displacement reaction (equation (3.11))

$$NO^+F^- + NF_4^+BF_4^- \longrightarrow NO^+BF_4^- + [NF_5] \longrightarrow F_2 + NF_3 \qquad (3.11)$$

Table 3.2. Distribution of [^{18}F] After the Thermal Decomposition of $NF_4^+BF_4^-$ and [^{18}F]NOF

	Relative Distribution of ^{18}F Activities (mCi)		
	Observed	Predicted Values for Attack on	
		F	N
Reaction tube[a]	28.9	60	33.3
-196 °C Trap[b](HF/ NOF)	39.7	0	0
Sodalime (F_2)	0.0018	15	16.7
-210 °C Trap (NF_3)	0.0035	0	25.0

[a] Assumed ^{18}F scrambling with F on BF_4^-

[b] Contained both unreacted $NO^{18}F$ and $H^{18}F$ contaminant (see text).

could not have taken place. The $NF_4^+BF_4^-$ salt has been reported to be stable at room temperature and decomposes irreversibly to NF_3 and F_2 at 200 °C.[97]

4. Pyrolysis of $NF_4^+PF_6^-$ + $[^{18}F]HF_2^-$

The pyrolysis of $NF_4^+HF_2^-$ was chosen because of its low thermal stability[98] and the linear, highly polar structure of HF_2^- presents no steric hindrance for the attack of F^- on the quaternary nitrogen in NF_4^+. Moreover, the preparation of $[^{18}F]HF_2^-$ was straight forward and reproducible (equation (3.12)).

$$[^{18}F]HF + CsF \longrightarrow Cs^+[^{18}F]HF_2^- \qquad (3.12)$$

The $NF_4^+[^{18}F]HF_2^-$ was prepared from $NF_4^+PF_6^-$ and $Cs^+[^{18}F]HF_2^-$ in a minimal amount of anhydrous HF as a solvent (equation (3.13)).

$$NF_4PF_6 + Cs[^{18}F]HF_2 \xrightarrow{HF} CsPF_6 + NF_4[^{18}F]HF_2 \qquad (3.13)$$

The decomposition of NF_4HF_2 salt, a stable compound at room temperature in excess HF, was carried out at 25 - 100 °C under dynamic vacuum after the removal of excess HF (equation (3.14)).

$$NF_4HF_2 \xrightarrow[vac]{\Delta} NF_3 + F_2 + HF \qquad (3.14)$$

The decomposition products were trapped in three separate traps. The relative distribution of [^{18}F] products in each trap allowed one to distinguish between attack of HF_2^- on the nitrogen or fluorine of NF_4^+. If nitrogen can coordinate to five fluorine atoms, the HF_2^- should attack at nitrogen because of more favourable Coulomb forces and hence result in a statistical scrambling of [^{18}F] among NF_3, F_2 and HF. If, however, nitrogen can coordinate to only four fluorine atoms, then HF_2^- must attack on the fluorine in NF_4^+. In this case all the activity should be found in F_2 and HF and none in NF_3. Since the PF_6^- anion can readily exchange with the labelled HF_2^- anion in HF solution, the $CsPF_6$ residue is expected to contain a statistical amount of [^{18}F] activity. The observed [^{18}F] distribution after the pyrolysis of $NF_4^+[^{18}F]HF_2^-$ is reported in Table 3.3.

The balance between the amounts of [^{18}F] in the reactants (29.2 mCi) and the products (28.65 mCi) was excellent when geometrical corrections were applied to these values. The quantitative nature of the reaction (3.14) was confirmed in a separate cold experiment by our collaborators, Christe and

Table 3.3 Distribution of [^{18}F] After the Pyrolysis of $NF_4^+PF_6^-$ + [^{18}F]HF_2^-

	Relative Distribution of ^{18}F Activity (mCi)		
	Observed	Predicted Values for Attack on	
		F	N
Reaction tube[a] [b]	17.6	16.4	12.8
-130 °C trap (HF)	8.2	8.7	6.2
Sodalime (F_2)	2.85	2.95	4.2
-210 °C trap (NF_3)	0.0012	0	6.4

[a] Assuming random distribution of ^{18}F between F^- and PF_6^-.

[b] Include activity in PF_6^- anion

coworkers at Rockwell International, by material balance measurements using unlabelled reagents under identical conditions.

The results in Table 3.3 indicate excellent material balances for [^{18}F] assays and are in accord with nucleophilic attack of HF_2^- on the fluorine and not on the nitrogen atom of NF_4^+. The fact that a small amount of [^{18}F] activity was observed in NF_3 should not be interpreted as a small contribution of competing attack on nitrogen but can be explained by slight variations of the background radiation level and the associated difficulties in measuring very small amounts of radioactivities accurately.

5. Mechanisms for the Decomposition of $NF_4^+HF_2^-$

Christe *et al.*[99] have considered four different schemes for the decomposition of NF_4^+ salts in a closed system.

Scheme 1

$$NF_3 + AsF_5 \rightleftharpoons NF_2^+AsF_6^-$$

$$F_2 \rightleftharpoons 2F\cdot$$

$$NF_2^+AsF_6^- + F\cdot \rightleftharpoons NF_3\cdot^+AsF_6^-$$

$$NF_3\cdot^+AsF_6^- + F\cdot \rightleftharpoons NF_4^+AsF_6^-$$

Scheme 2

$$F_2 \rightleftharpoons 2F\cdot$$

$$F\cdot + AsF_5 \rightleftharpoons AsF_6\cdot$$

$$AsF_6\cdot + NF_3 \rightleftharpoons NF_3\cdot{}^+AsF_6^-$$

$$NF_3\cdot{}^+AsF_6^- + F\cdot \rightleftharpoons NF_4^+AsF_6^-$$

Scheme 3

$$F_2 \rightleftharpoons 2F\cdot$$

$$F\cdot + NF_3 \rightleftharpoons NF_4\cdot$$

$$NF_4\cdot + F\cdot \rightleftharpoons NF_5$$

$$NF_5 + AsF_5 \rightleftharpoons NF_4^+AsF_6^-$$

Scheme 4

$$F_2 \rightleftharpoons 2F\cdot$$

$$F\cdot + NF_3 \rightleftharpoons NF_4\cdot$$

$$NF_4\cdot + AsF_5 \rightleftharpoons NF_3\cdot{}^+AsF_6^-$$

$$NF_3\cdot{}^+AsF_6^- + F\cdot \rightleftharpoons NF_4^+AsF_6^-$$

Schemes 1, 2 and 3 were ruled out mainly because they do not comply with the following experimental observations:

(a) NF_3 does not form stable adducts, even at low temperature, with BF_3, PF_5, AsF_5 and SbF_5.

(b) The decomposition of NF_4^+ salts is strongly suppressed by BF_3 or AsF_5.

(c) ESR measurements have shown that the $NF_3^{\cdot+}$ radical cation is a crucial intermediate in both the low-temperature UV photo-synthesis and γ-irradiation-induced decomposition of NF_4^+ salts. Furthermore, the fluorination of $NF_3^{\cdot+}$ to NF_4^+ appears to require F atoms.

(d) ESR flow-tube experiments gave no indication of interaction between $F^{\cdot}$ atoms as expected for the reaction step

$$AsF_5 + F^{\cdot} \longrightarrow AsF_6^{\cdot}.$$

(e) There is no evidence for the existence of NF_5 as an intermediate.

(f) There is strong indication that during the formation of NF_4^+ salts, the first step must be the dissociation of F_2 into two fluorine atoms.

Christe *et al.*[96] suggested that Scheme 4 complied with all of the above experimental observations and therefore should be the preferred mechanism. However, if $NF_4^{\cdot}$ radical is present in the decomposition of the $NF_4^+H^*F_2^-$ salt, as is required for Scheme 4, then one of the fluorines would be radioactive. This would result in a statistical distribution of $^*F$ between NF_3 and $F^{\cdot}$ and therefore the relative distribution of [^{18}F] in NF_3 and F_2 would be 75% and 25%, respectively. Contrary to

this prediction, the present results showed no [^{18}F] in NF_3 indicating that the mechanism shown in Scheme 4 does not apply to the decomposition of the $NF_4^+HF_2^-$ salt.

The present findings may be explained by the mechanism shown in the following scheme (Scheme 5) which is similar to Scheme 2 above.

Scheme 5

$$NF_4^+H^*F_2^- \longrightarrow NF_3\cdot^+H^*F_2^- + F\cdot$$

$$NF_3\cdot^+H^*F_2^- \longrightarrow NF_3 + H^*F_2\cdot$$

$$H^*F_2\cdot \longrightarrow H^*F + {}^*F\cdot$$

$${}^*F\cdot + F\cdot \longrightarrow {}^*F\text{-}F$$

Scheme 5 accounts for the fact that there is no NF_5 or $NF_4\cdot$ radical present as an intermediate during the decomposition of $NF_4^+HF_2^-$ salt and therefore no [^{18}F] can be expected in NF_3. Unlike the AsF_6^- or BF_4^- salts, where the formation of AsF_5 or BF_3 suppress the decomposition rate in a closed system, the formation of HF does not affect the thermal decomposition of the $NF_4^+HF_2^-$ salt.

C. CONCLUSION

The present work shows that HF_2^- attack on NF_4^+ occurs exclusively on the fluorine atom. Since the polarities of the bonds in both NF_4^+ and HF_2^- would favour attack on nitrogen,

the lack of attack on nitrogen is likely to be due to steric reasons. Because of its small size and high electronegativity, fluorine is the ideal ligand for achieving maximum coordination around a central atom.

In a recent theoretical study it was suggested that the reaction between NF_3 and F_2 is more likely to form NF_5 than from the reaction of NF_4^+ and F^-.[85] This is because the latter reaction is in competition with the significantly more exothermic reaction that produces NF_3 and F_2 (equation (3.15)).

$$NF_4^+ + F^- \longrightarrow NF_3 + F_2 \qquad (3.15)$$

In the light of these arguments it would be interesting to investigate the reaction of NF_3 with $[^{18}F]F_2$ at low temperatures. In the low-temperature reaction molecular fluorine is thermally dissociated into F atoms which would then be allowed to impinge upon a surface of cold NF_3. Thermal dissociation could be achieved using a specially constructed hot-wire reactor similar to that used for the preparation of KrF_2[100] and photolytic dissociation by means of a focused UV source.[80] If the reaction between F atoms and NF_3 forms either NF_5 or $NF_4\cdot$ radical as an intermediate, then the use of $[^{18}F]F_2$ would provide conclusive evidence for the existence of either of these intermediates. For example,

after reaction, the excess $[^{18}F]F_2$ can be pumped off and trapped on the sodalime. The intermediate, if it can be formed along with NF_3, will be retained on the frozen walls of the reactor. The reactor could subsequently be warmed, and the products NF_3 and F_2 separated using a -196 °C trap a and sodalime trap. The relative distribution of $[^{18}F]$ in NF_3 and F_2 would be 75% and 25%, respectively, for an $NF_4\cdot$ radical intermediate, but the relative distribution of $[^{18}F]$ in NF_3 and F_2 would be 60 and 40%, respectively, for the NF_5 intermediate. There will be no $[^{18}F]$ in NF_3 if no reaction occurs between NF_3 and F_2.

CHAPTER 4

APPLICATION OF ^{18}F TO THE INVESTIGATION OF HYPERVALENT COMPOUNDS OF CHLORINE

A. INTRODUCTION

Elemental fluorine combines with other halogens to form halogen fluorides of varying stoichiometries: XF, XF_3, XF_5 and XF_7.[101] The syntheses and characterization of mono, tri and pentafluorides of Cl, Br and I have been reported. However, among the heptafluorides, IF_7 [102] and TeF_7^- [103] are the only main-group examples. In fact, IF_7 is one of the two neutral heptafluorides in the periodic table; the other one being ReF_7 [104] (the synthesis of OsF_7 [105] and AuF_7 [106] have been reported but are unsubstantiated and suspect). Fogle and Rewick[107] have reported the preparation of small quantities of BrF_7 by heating a mixture of BrF_5 and F_2 to 110 - 340 °C in the presence of CsF. Bromine heptafluoride was reported to be stable up to temperatures as high as 250 °C.[107] Attempts by other workers to make BrF_7 [108] and ClF_7 [109,110] by low temperature displacement reactions using BrF_6^+ and ClF_6^+ salts, respectively, with NOF failed; instead only the pentafluorides and F_2 were obtained (equations (4.1) and (4.2)).

$$ClF_6^+PtF_6^- + NOF \xrightarrow{-78\ ^\circ C} NO^+PtF_6^- + ClF_5 + F_2 \qquad (4.1)$$

$$BrF_6^+AsF_6^- + 2NOF \xrightarrow{-78\ ^\circ C} NO^+AsF_6^- + NO^+BrF_6^- + F_2 \qquad (4.2)$$

Recent Raman spectroscopic studies[111] of the tetramethyl ammonium salts of IF_6^- and BrF_6^- salts in CH_3CN show that the free valence electron pair in IF_6^- is sterically active whereas in BrF_6^- it is not. This difference in steric activities of the free valence electron pairs is attributed to the difference in size of the central I and Br atoms. Since in a rigid molecule the spacial requirement of a sterically active free valence electron pair slightly exceeds that of a fluorine ligand,[112] one would predict that iodine can accommodate seven fluorine atoms (or six fluorines plus a sterically active lone pair) around it, but bromine cannot. Therefore, unlike IF_7, the existence of stable BrF_7 and ClF_7 is unlikely for steric reasons. However, the above displacement reactions (equations (4.1) and (4.2)) might proceed through the unstable intermediates BrF_7 and ClF_7, and are unstable toward decomposition to the +5 oxidation state and F_2. Use of [^{18}F]NOF in displacement reactions involving ClF_6^+ and BrF_6^+ could provide evidence for the presence of the intermediate heptafluorides. The relative activities of [^{18}F] in the products, $XF_5 + F_2$, would give a statistical distribution if the observed products are formed via an XF_7 intermediate.

B. RESULTS AND DISCUSSION

1. On the Existence of ClF_7

Displacement reactions involving ClF_6^+/BrF_6^+ and NOF produce the pentafluorides of Br and Cl along with F_2. It is possible that these pentafluorides and F_2 result from the decomposition of the unstable heptafluoride intermediates. Of these two heptafluorides, BrF_7 is more likely to exist than ClF_7 for steric reasons. However, the investigation of the possible existence of BrF_7 was not given priority in this study for the following reasons: (1) The build up in nuclear charge which occurs across the first transition series and the comparatively weak screening power of 3d electrons will have the effect of increasing the ionization energies of the 4s electrons. (2) Although BrF_7 is expected to be more stable than ClF_7 from a steric point of view, BrF_7 is expected to be thermodynamically less stable than ClF_7. This is exemplified by the fact that the bromine +7 oxidation state (eg. BrO_4^-) is more difficult to prepare than its chlorine analogue (ClO_4^-). (3) A [^{18}F] tracer study is not suitable for investigating the existence of BrF_7 as an unstable intermediate because BrF_5 is a fluoride-ion acceptor and the products obtained from the BrF_6^+ reaction are $NO^+BrF_6^-$ and F_2 and not BrF_5 and F_2. Fluorine-18 tracer studies were deemed to be ideal for the investigation of ClF_7 because ClF_5 and F_2 can be readily separated and the relative distribution of labelled fluorines

in both products can be measured. Moreover, $NO^+ClF_6^-$ and the ClF_6^- anion were not known to be stable.[113]

The quantitative nature of the reaction between $ClF_6^+AsF_6^-$ and NOF was confirmed in a separate cold experiment by our collaborators Christe *et al.* using unlabelled reagents under identical conditions. The distribution of [^{18}F] among all the species resulting from the displacement reaction between $ClF_6^+AsF_6^-$ and [^{18}F]NOF is summarized in Table 4.1. In order to compare the experimental data with the theoretical values for the attack of [^{18}F] fluoride ion on the Cl (equation (4.3)) or F (equation (4.4)) in ClF_6^+, the expected [^{18}F] distributions for all the fluorine-containing species have been calculated. The calculations are based on the total [^{18}F] found among all the species after the experiment and they are shown in Table 4.2. Also shown in Table 4.2 are the relative amounts of [^{18}F] expected for random exchange of fluorine atoms including AsF_6^-.

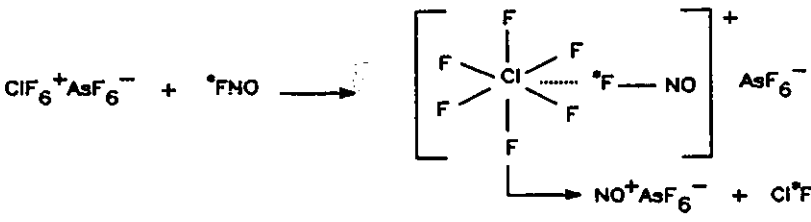

(4.3)

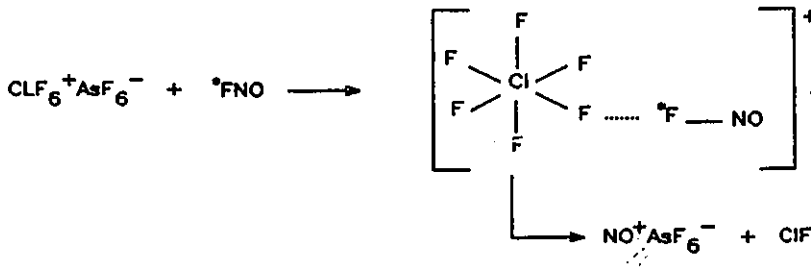

(4.4)

As can be seen from Table 4.1, 7.1% of the total [^{18}F] remained in the original FEP reactor. This radioactivity was due to the presence of [^{18}F] in $NO^+AsF_6^-$ and unreacted $ClF_6^+AsF_6^-$ since all other products are volatile and were pumped off. The 7.1% radioactivity associated with the residue is considerably lower than the expected value for total isotopic scrambling of fluorines followed by attack of the fluoride ion at chlorine (46%) or fluorine (75%) in ClF_6^+ (Table 4.2). It can therefore be argued that [^{18}F] exchange between NOF and AsF_6^- does not take place to a significant extent under the present reaction conditions. The observed results can be accounted for if small amounts of HF are present in the system. Any HF present, however, will be absorbed on the sodium fluoride and therefore the NaF trap is also expected to be radioactive. The 6.7% [^{18}F] observed in the sodium fluoride (Table 4.1) confirmed the presence of HF impurity in the system. The [^{18}F] present in AsF_6^- can be attributed to exchange reactions such as

$$HF + NO^*F \longrightarrow H^*F + NOF \qquad (4.5)$$

$$H^*F + AsF_6^- \longrightarrow HF + As^*F_6^- \qquad (4.6)$$

In principle, it should be possible to obtain evidence for the existence of ClF_7 as a transient species, using [^{18}F]

Table 4.1. Distribution of [^{18}F] (mCi) in $ClF_6^+AsF_6^-$ + NO^+F Displacement Reaction.

F containing species	[^{18}F] Found	% of the total[^{18}F]
Reaction tube ($NO^+AsF_6^-$)	2.94	7.1
Sodium fluoride (HF)	2.79	6.7
-196 °C trap (ClF_5 + NOF)	30.10	72.4
Sodalime (F_2)	5.95	14.3
ClF_5 (separated as ClF_4^+)[a]	19.91	47.9
NOF (separated as NO^+)[a]	10.10	24.3

[a] Separated as the AsF_6^- salt (see text).

Table 4.2. Theoretical [^{18}F] Distribution for Equations (4.3) and (4.4).

Species	% Distribution of ^{18}F Resulting From Attack on Cl		% Distribution of ^{18}F Resulting From Attack on F	
	Random Exchange	No Exchange	Random Exchange	No Exchange
$NO^+AsF_6^-$	46.2	0	75.0	0
ClF_5	38.5	71.4	0	0
F_2	15.4	28.6	25.0	100

exchange studies, by comparison of the the relative distribution of [^{18}F] in ClF_5 and F_2 and decomposition products. The predicted values for the relative distribution of [^{18}F] in ClF_5 and F_2, as shown in Table 4.2, will be lower than the true values expected for this reaction. This is because the data in Table 4.2 is based on the total [^{18}F] present among all the fluorine-containing species including unreacted [^{18}F]NOF and [^{18}F]HF impurity. The observed relative distributions of [^{18}F] in ClF_5 (19.91 mCi) and F_2 (5.95 mCi) were 77% and 23%, respectively, and are in qualitative agreement with the theoretical values for ClF_5 (5/7 x 100 = 71.4%) and F_2 (2/7 x 100 = 28.6%) for the attack of [^{18}F]F^- on the chlorine in ClF_6^+ (equation (4.3)). For the alternative mechanism, where [^{18}F]F^- attacks one of the fluorine ligands of ClF_6^+ followed by the elimination of F_2 and ClF_5 (equation (4.4)), the theoretical [^{18}F] distribution would be zero and 100%, respectively, for ClF_5 and F_2.

Although the [^{18}F] distribution in ClF_5 and F_2 appears to indicate the presence of ClF_7 as an intermediate, the discrepancy between the predicted value and observed value should be accounted for. Furthermore, it is possible that the exchange of ClF_5, produced after the attack of fluoride ion on the fluorine ligand, with other fluorine containing species

such as [^{18}F]HF, [^{18}F]NOF and [^{18}F]F_2 would also show the presence of [^{18}F]ClF_5.

Rogers and Katz[114] have reported that [^{18}F] exchange between [^{18}F]HF and halogen fluorides such as ClF_3, BrF_3, BrF_5 and IF_5 at room temperature was complete in 10 min. in the liquid phase and in 3 min. in the gas phase. Therefore, it is likely that ClF_5 would undergo random exchange with [^{18}F]HF that was present in the system. This exchange alone cannot account for the 47% of the total [^{18}F] found in the ClF_5, but it may explain the higher percentage of ^{18}F in ClF_5 compared to the predicted value for [^{18}F] in ClF_5 if ClF_7 was an intermediate (equation (4.3)).

The exchange between ClF_5 and [^{18}F]F_2 can be ruled out because the previous [^{18}F] investigations involving the gas-phase exchange between halogen fluorides and elemental fluorine were found to be negative.[115] The rates of isotopic exchange between elemental fluorine and ClF_3, BrF_5 and IF_7 were zero in all cases up to 100 °C in Cu, Al and Ni reaction vessels. It can therefore be argued that the ^{18}F in ClF_5 could not have been due to [^{18}F]F_2-ClF_5 exchange.

Isotopic exchange between [^{18}F]NOF and ClF_5 could also account for the observed data. However, the mechanism for

such an exchange would involve the hitherto unknown ClF_6^- anion. A previous study using [^{18}F]CsF showed no evidence for fluorine exchange in the heterogeneous ClF_5/CsF system.[113] The lack of exchange could have been due to the very low solubility of CsF in ClF_5. Consequently, the gas-phase exchange between ClF_5 and [^{18}F]NOF was investigated in the present study.

2. The Existence of ClF_6^- Anion

Among the interhalogen compounds, polyfluorocations, XF_2^+, XF_4^+ and XF_6^+ and polyfluoroanions, XF_2^- and XF_4^- are well established compounds.[116] However, in the series XF_6^-, only BrF_6^- and IF_6^- are known.[117,118] These compounds belong to the AX_6E class possessing six fluorine ligands, X, and a free valence electron pair, E. As stated before, due to the larger size of the iodine atom the free valence electron pair in the valence shell of iodine, the lone pair of IF_6^- is stereochemically active whereas in BrF_6^- it is not. By analogy, the free valence electron pair in ClF_6^- is expected to be sterically inactive and therefore no steric restrictions will be involved in ClF_6^- anion. Yet, attempts to make ClF_6^- using alkali metal fluorides and ClF_5 failed and the only products observed were ClF_3 and F_2.[119] Furthermore, an [^{18}F] radiotracer study of the CsF-ClF_5 system did not provide any evidence for fluorine exchange and for the formation of ClF_6^- as an

intermediate.[113] Since the existence ClF_6^+ cation[120] and ClF_6 radical[121] have been well established, and the fact that the free valence electron pair in ClF_6^-, by analogy with BrF_6^-, is expected to be stereochemically inactive, the lack of success of the above experiments in isolating the ClF_6^- anion is most likely due to the weak Lewis acidity of ClF_5 and the low solubilities of CsF and $CsClF_6$ in ClF_5. However, an ^{18}F radiotracer study of the ClF_5-NOF system in the gas phase would eliminate solubility problems and possibly provide a conclusive answer as to the existence of ClF_6^- anion. In this study evidence is presented, using ^{19}F NMR and a ^{18}F radiotracer study, for the existence of the ClF_6^- anion.

3. ^{19}F NMR Study of Chemical Exchange Behaviour Between F^- and ClF_5.

Chlorine pentafluoride has previously been shown in two ^{19}F NMR studies to possess a square pyramidal (C_{4v}) AX_4E structure in the liquid state[122,123] as predicted by the VSEPR model.[124] Alexandre and Rigny[123] demonstrated that, unlike the equatorial X_4 part of the ^{19}F NMR spectrum, which showed a secondary isotopic shift arising from ^{19}F bonded to ^{35}Cl and ^{37}Cl, the axial A part of the spectrum was broadened significantly and showed no evidence for an isotopic shift. This study concluded that chemical exchange between the axial (F_{ax}) and equatorial (F_{eq}) fluorines could be disregarded and

that the line broadening of F_{ax} arises from partially quadrupole collapsed scalar couplings between $^{19}F_{ax}$ and the spin-3/2 quadrupolar nuclei ^{35}Cl and ^{37}Cl, $^{1}J(^{19}F_{ax}-^{35,37}Cl)$, which are significantly larger than $^{1}J(^{19}F_{eq}-^{35,37}Cl)$. Nuclear relaxation time measurements in the same study have confirmed this and have provided estimates of the magnitudes of the scalar couplings ($^{1}J(^{19}F_{ax}-^{35}Cl)$ = 192 Hz and $^{1}J(^{19}F_{eq}-^{35}Cl) \leq 20$ Hz). The larger value for $^{1}J(F_{ax}-^{35}Cl)$ is in accord with the shorter F_{ax}-Cl bond observed in this molecule.[125] The temperature behaviour of the ^{19}F NMR spectrum of liquid ClF_5 was investigated in the previous study, but does not report any variations of linewidths as a function of temperature. In the present study the ^{19}F NMR of neat ClF_5, ClF_5-HF and ClF_5-CsF/HF have been investigated and the data obtained from these studies are summarized in Table 4.3

Fluorine-19 NMR spectra of neat ClF_5 at 25, -56 and -90 °C are shown in Figure 4.1. While there is little effect upon the linewidth of the F_{eq} resonance on lowering the temperature, a significant narrowing of the F_{ax} resonance linewidth is observed together with partial resolution of its chlorine isotopic shift. The observed line narrowing for the F_{ax} resonance is attributable to the increased quadrupolar relaxation rates of ^{35}Cl and ^{37}Cl at low temperatures where the

Table 4.3. ^{19}F NMR Data for Neat ClF_5 and ClF_5/HF and ClF_5-CsF/HF Solutions

Sample Composition	T (°C)	Chemical Shift δ(ppm)[a]		$^2J(F_{ax}-F_{eq})$ (Hz)	Linewidth (Hz)		Secondary Isotopic Shift[b] $^1\Delta^{19}F(^{37/35}Cl)$ (ppm)	
		F_{eq}	F_{ax}		F_{eq}	F_{ax}	F_{eq}	F_{ax}
Neat ClF_5	24.4	259.8	428.8	133	3.5	≈110	-0.079	e
	-56.4	257.2	426.9	133	4.0	44	-0.088	-0.1977
	-90.0	256.4	426.6	133	5.2	26	-0.091	-0.199
ClF_5 in HF Solv't[c]	25	256.4	424.6	130	5.7	≈140	-0.078	e
	-56.3	253.9	422.6	130	2.5	71	-0.087	e
ClF_5/CsF in HF Solv't[d]	25	253.6	420.9	123	28	≈110	e	e
	-56.3	250.8	418.8	124	6.9	18	-0.085	-0.189

[a] Spectra were referenced with respect to external $CFCl_3$ at 25 °C.

[b] $^1\Delta^{19}F(^{37/35}Cl)$/ppm = $\delta F(^{37}Cl) - \delta F(^{35}Cl)$.

[c] Concentration of ClF_5, 0.536 m.

[d] Concentrations of ClF_5, 0.619 m and CsF, 5.60 m.

[e] Isotopic shift not resolved.

isotropic molecular tumbling correlation time (τ_c) for ClF_5 is greater.[126] This behaviour is consistent with the dominant contribution of scalar relaxation of the second kind, via $^1J(F_{ax}-^{35/37}Cl)$, to the spin-spin relaxation time (T_2) of the F_{ax} nuclei, as found in the previous study.[123]

The ^{19}F NMR spectra of a solution of ClF_5 (0.536 m) in anhydrous HF and a solution of ClF_5 (0.619 m) in anhydrous HF containing CsF (5.60 m) were also investigated. The ^{19}F NMR spectrum of ClF_5 recorded in HF solvent at 25 °C consists of two well-resolved doublets corresponding to equatorial fluorines on ^{35}Cl and ^{37}Cl spin coupled to the axial fluorine environment (Figure 4.2). The latter environment, as in the neat sample of ClF_5 at 24.4 °C, is broadened significantly owing to partial quadrupole collapse of the $^1J(^{35,37}Cl-^{19}F)$ scalar couplings so that resolution of the isotopically shifted quintets (Figure 4.2; c.f. Figure 4.1) is precluded. The line broadening on the quintets is again dominated by scalar coupling and not by fluorine exchange, as has been established for neat ClF_5 in the present and earlier studies.[123] The addition of F^- to HF solutions of ClF_5 results in pronounced broadening of the doublet resonances at 25 °C, preventing resolution of the isotope shift, whereas the appearance of the axial fluorine resonance remains essentially

Figure 4.1 Variable-temperature ^{19}F NMR spectra (470.599 MHz) of neat ClF_5. A and E denote resonances for axial and equatorial fluorine environments, respectively; asterisks (*) denote resonances arising from the ^{37}Cl isotopomer.

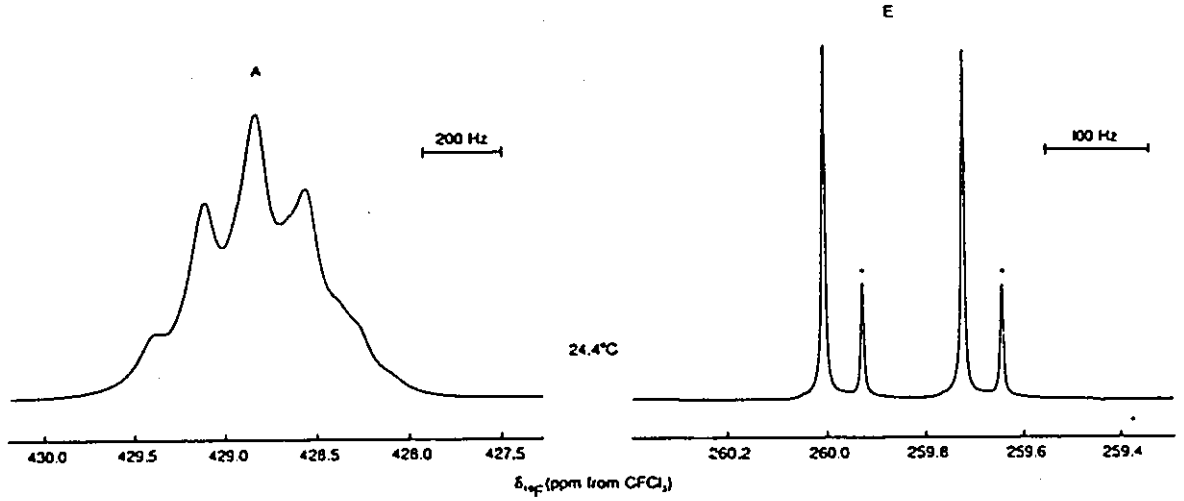
A
200 Hz
E
100 Hz
24.4°C
430.0
429.5
429.0
428.5
428.0
427.5
260.2
260.0
259.8
259.6
259.4
δ1H (ppm from CFCl3)

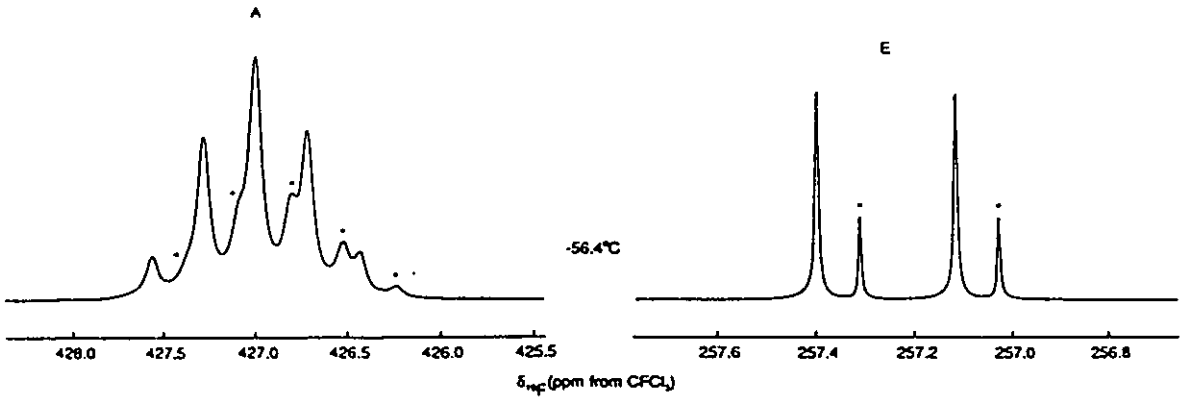
A
E
-56.4°C
428.0
427.5
427.0
426.5
426.0
425.5
257.6
257.4
257.2
257.0
256.8
δ1H (ppm from CFCl3)

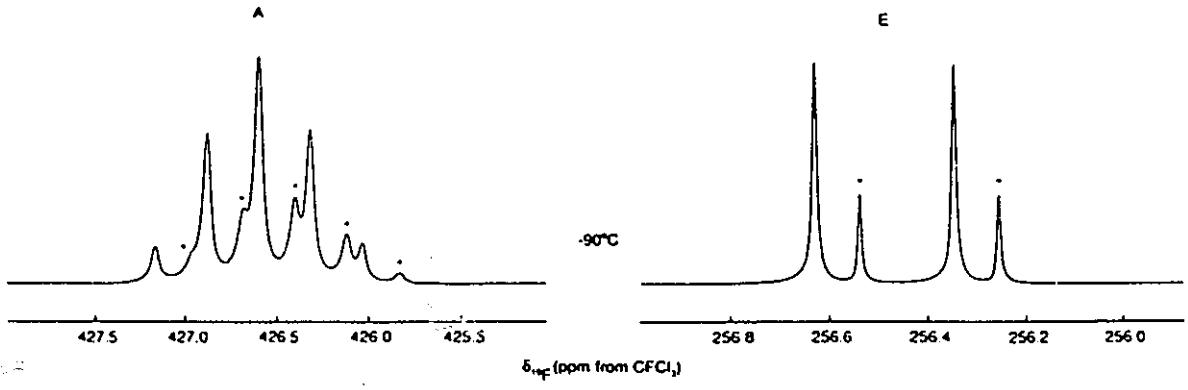
A
E
-90°C
427.5
427.0
426.5
426.0
425.5
256.8
256.6
256.4
256.2
256.0
δ1H (ppm from CFCl3)

Figure 4.2 Variable-temperature ^{19}F NMR spectra (235.36 MHz) of ClF_5 (0.536 m) in HF solution. A and E denote resonances for the axial and equatorial fluorine environments, respectively; asterisks (*) denote resonances arising from the ^{37}Cl isotopomer.

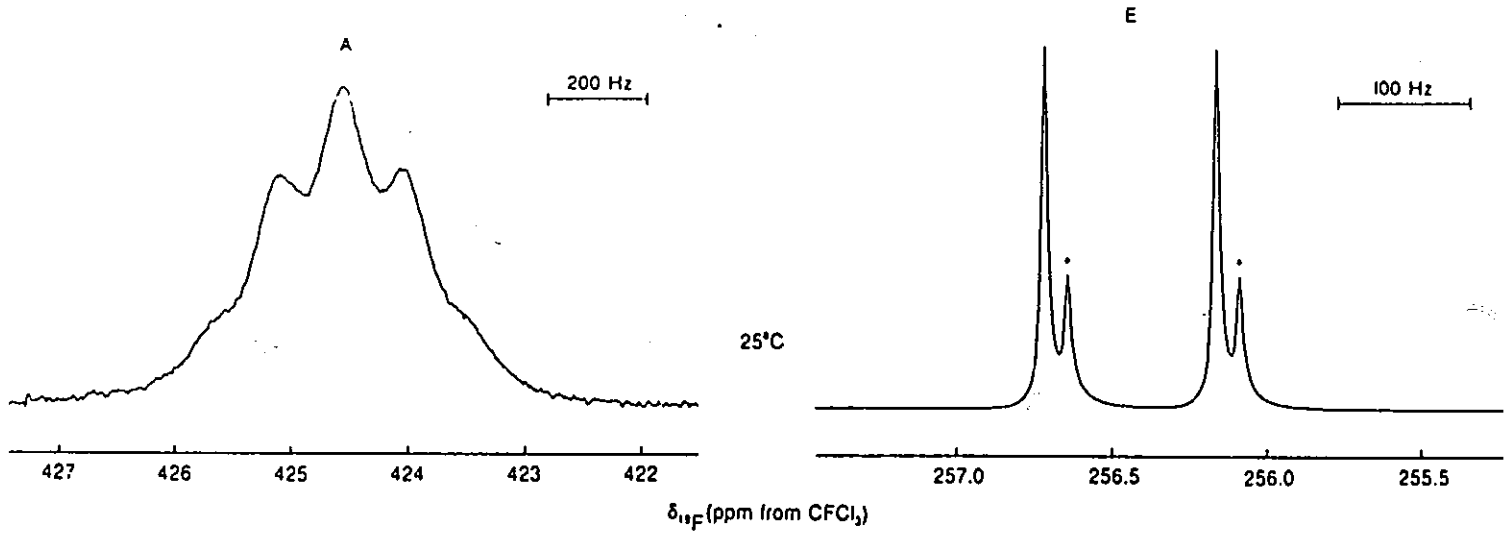
A
200 Hz
E
100 Hz
25°C
427
426
425
424
423
422
257.0
256.5
256.0
255.5
$\delta_{^{19}F}$(ppm from $CFCl_3$)

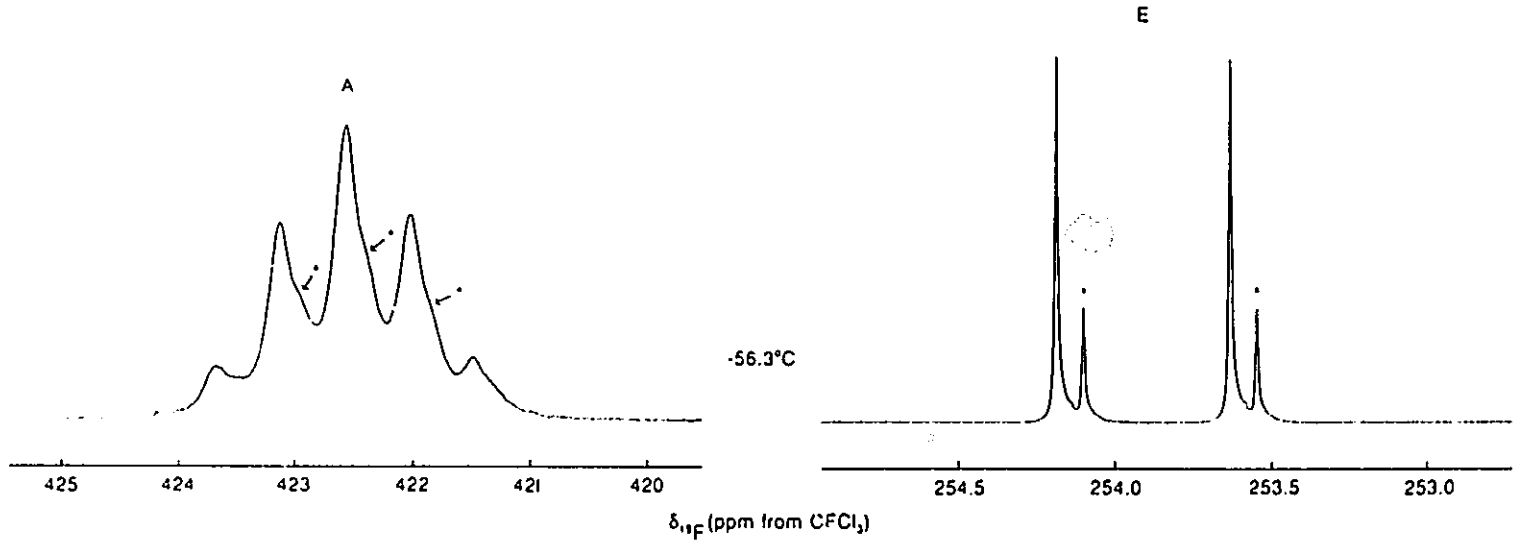
A
E
-56.3°C
425
424
423
422
421
420
254.5
254.0
253.5
253.0
$\delta_{^{19}F}$(ppm from $CFCl_3$)

Figure 4.3 Variable-temperature ^{19}F NMR spectra (235.361 MHz) of ClF_5 (0.619 m)-CsF (5.60 m) in HF solution. A and E denote resonances for the axial and equatorial fluorine environments, respectively; asterisks (*) denote resonances arising from the ^{37}Cl isotopomer.

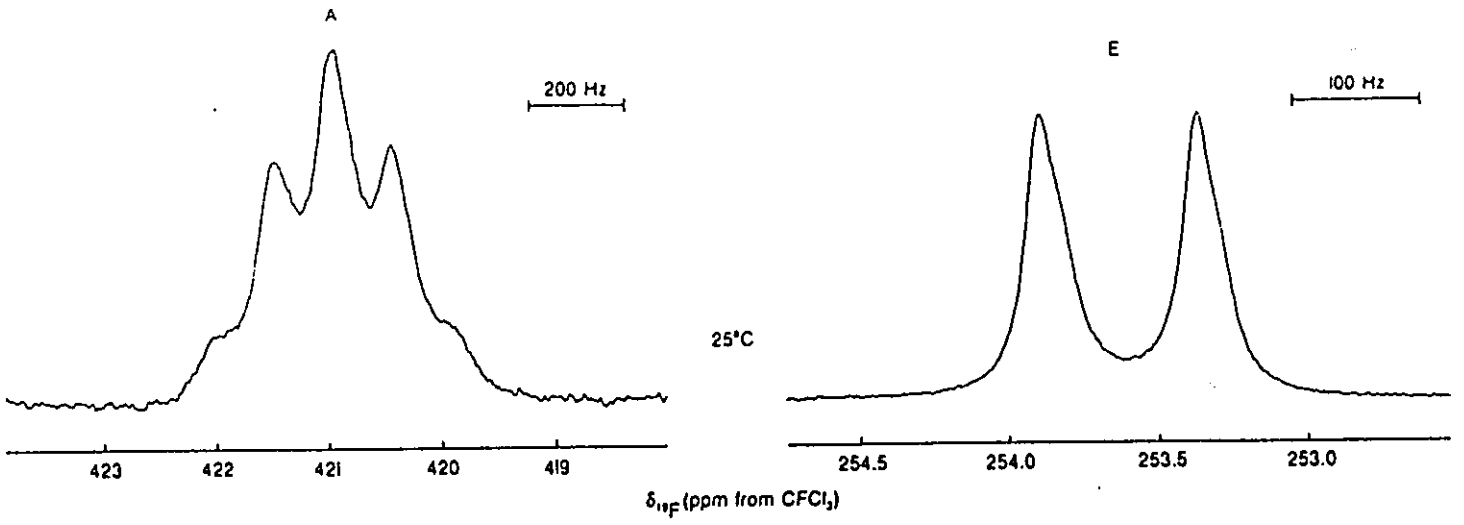
A
200 Hz
E
100 Hz
25°C
423
422
421
420
419
254.5
254.0
253.5
253.0
$\delta_{^{19}F}$ (ppm from $CFCl_3$)

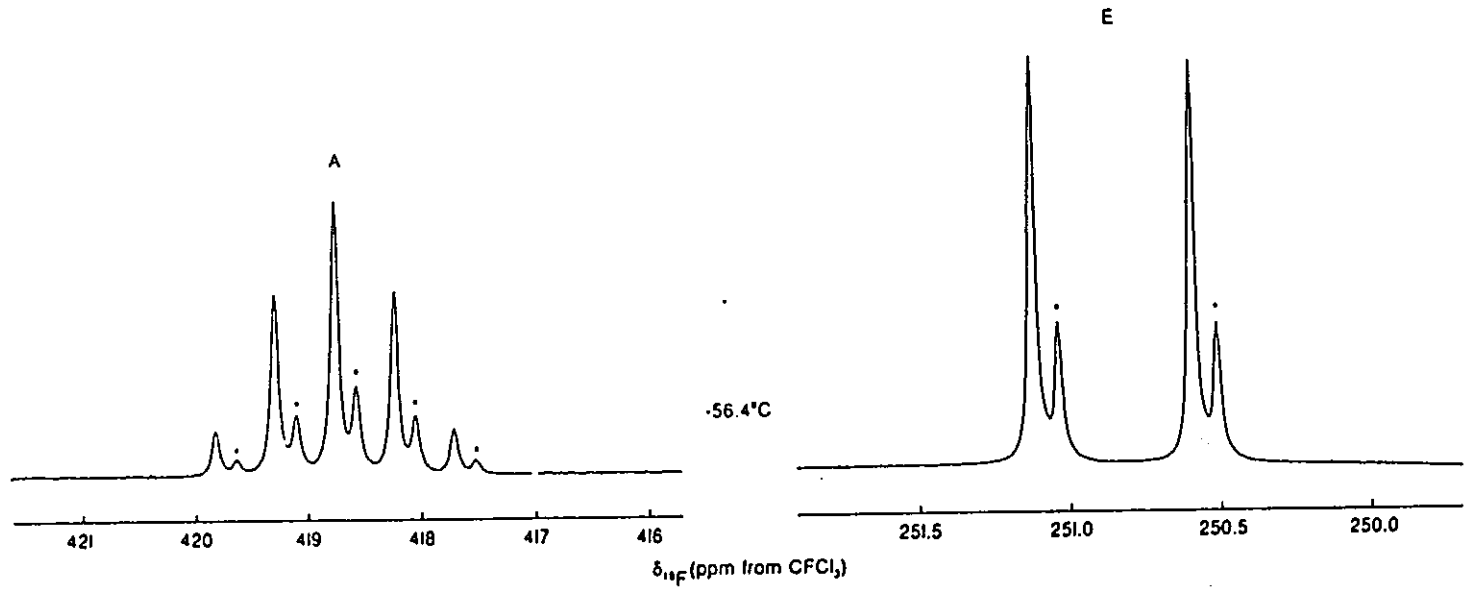
E
A
-56.4°C
421
420
419
418
417
416
251.5
251.0
250.5
250.0
$\delta_{^{19}F}$ (ppm from $CFCl_3$)

unchanged (Figure 4.3). The line broadening is consistent with slow intermolecular ^{19}F exchange arising from equilibrium (equation (4.7)) and the intermediacy of ClF_6^- in the exchange process.

$$ClF_5 + F(HF)_x^- \rightleftharpoons ClF_6^- + xHF \qquad (4.7)$$

Cooling of the ClF_5/F^- sample to -56 °C slowed ^{19}F chemical exchange sufficiently to allow resolution of the equatorial fluorine doublets (Figure 4.3) and the axial fluorine quintets. This is the first time the two quintet patterns arising from the $^{35}Cl/^{37}Cl$ secondary isotope effect have been observed in ClF_5. The sharpening of the axial fluorine resonance is not, however, attributed to slowing of the ^{19}F chemical exchange process, but is primarily attributed to the dominant effect of the increased quadrupole relaxation rates of the ^{35}Cl and ^{37}Cl nuclei on $^1J(^{35,37}Cl-^{19}F)$ at low temperatures where τ_c for ClF_5 is greater. The addition of CsF presumably increases the viscosity of the solvent medium owing to $F(HF)_x^-$ formation, and hence increases τ_c for ClF_5, leading to collapse of the $^1J(^{35,37}Cl-^{19}F)$ couplings. In contrast, the ^{19}F resonances associated with ClF_5 dissolved in HF do not sharpen as significantly, although the quintet pattern clearly possesses a narrower linewidth than at 25 °C (Figure 4.2). The broader lines can be attributed to the low viscosity of the HF solvent

medium, even at -56 °C, allowing the partially collapsed $^{1}J(^{35,37}Cl-^{19}F)$ couplings to persist in the slow chemical exchange limit.

The secondary isotope shifts, $^{1}\Delta^{19}F_{ax}(^{37/35}Cl)$ = -0.189 ppm and $^{1}\Delta^{19}F_{eq}(^{37/35}Cl)$ = -0.085 ppm for ClF_5/CsF in HF at -56 °C (Figure 4.4), follow the usual trend and are negative, i.e., the observed NMR nucleus bonded to the heavier of two isotopes has its NMR resonance to lower frequency.[127] They are comparable in magnitude to those for closely related species in the same row of the periodic table, i.e.; ClF_6^+, $^{1}\Delta^{19}F(^{37/35}Cl)$ = -0.15 ppm;[128] SF_6, $^{1}\Delta^{19}F(^{34/32}S)$ = -0.0552 ppm[129] and SF_4, $^{1}\Delta^{19}F_{ax}(^{34/32}S)$ = -0.0690 and $^{1}\Delta^{19}F_{eq}(^{34/32}S)$ = -0.0330 ppm[129] with the ^{19}F bonded to the heavier isotope occurring at lower frequency. The relative sizes of isotopic shifts are known to be larger for shorter bonds[130] and this is also true for the secondary isotopic shifts of ClF_5 [r(Cl-F_{ax}) = 1.58, r(Cl-F_{eq}) = 1.67 Å [125] and f_{Rax} = 3.01, f_{Req} = 2.57 mdyne Å^{-1}][131] and BrF_5 [r(Br-F_{ax}) = 1.689, r(Br-F_{eq}) = 1.774 Å [132] and f_{Rax} = 4.07, f_{Req} = 3.19 mdyne Å^{-1}][129], where $^{1}\Delta\ ^{19}F_{ax}(^{81/79}Br)$ = -0.030 and $^{1}\Delta^{19}F_{eq}(^{81/79}Br)$ = -0.015 ppm.[133] Moreover, the ratio $^{1}\Delta^{19}F_{ax}(^{37/35}Cl)/^{1}\Delta^{19}F_{eq}(^{37,35}Cl)$ = 2.22 is remarkably similar to those found for the axial and equatorial secondary isotopic shifts of SF_4, $^{1}\Delta^{19}F_{ax}(^{34/32}S)/^{1}\Delta^{19}F_{eq}(^{34/32}S)$ = 2.09 and BrF_5, $^{1}\Delta^{19}F_{ax}(^{81/79}Br)/^{1}\Delta^{19}F_{eq}(^{81/79}Br)$ = 2.0.[133]

4. ^{18}F Radiotracer study.

Results from the [^{18}F] exchange study of ClF_5-NOF system shows that the exchange is complete within 10 min. The observed distribution of [^{18}F] is in agreement with the predicted values for random exchange of fluorines between ClF_5 and NOF (Table 4.4). After combining [^{18}F]ClF_5 and [^{18}F]NOF followed by complexation with AsF_5, it was found that 37.7% of the total activity was isolated as $NO^+AsF_6^-$ and 62.3% of the activity was associated with $ClF_4^+AsF_6^-$. This is in excellent agreement with the predicted values of 37.5 and 62.5%, respectively, resulting from reaction (4.8)

$$NOF + ClF_5 + 2AsF_5 \longrightarrow NO^+AsF_6^- + ClF_4^+AsF_6^- \qquad (4.8)$$

and therefore confirms that the only volatile products condensed in the two low-temperature baths were ClF_5 and NOF. Our experimental data also confirmed that the previous failure to obtain evidence for ClF_6^- anion as an intermediate, when $Cs^{18}F$-ClF_5 was used, is due to the lack of solubility of CsF in ClF_5.

The distribution of [^{18}F] in ClF_5 and NOF after the exchange show, within experimental error, random exchange of fluorines between NOF and ClF_5 at room temperature via equilibrium (equation (4.9))

$$ClF_5 + NO^*F \longrightarrow Cl^*F_5 + NOF \qquad (4.9)$$

Two different mechanisms could account for the observed results. The first is the dissociation of ClF_5 into ClF_3 and F_2 followed by the [^{18}F] exchange between F_2 and [^{18}F]NOF (equation (4.10) and (4.11)).

$$ClF_5 \longrightarrow ClF_3 + F_2 \qquad (4.10)$$

$$F_2 + NO^*F \longrightarrow {}^*F_2 + NOF \qquad (4.11)$$

$$^*F_2 + ClF_3 \longrightarrow Cl^*F_5 \qquad (4.12)$$

This is unlikely because a previous [^{18}F] study[115] indicated no exchange between ClF_3 and F_2 and therefore cannot account for the observed radioactivity in ClF_5. Moreover, the formation and decomposition of F_3NO must be reversible for random exchange between [^{18}F]F_2 and FNO and this is unlikely under the present experimental conditions, i.e., F_3NO is prepared either by the low-temperature electric discharge[134] of O_2 and NF_3 or by the action of IrF_6 with FNO,[135] not by the direct fluorination of NO.

Rogers and Katz[114] have proposed an intermediate complex, $HClF_4$, with one of the lone pairs on the chlorine in

Table 4.4. Distribution of [^{18}F] after the exchange between ClF_5 and [^{18}F]NOF for 10 min. at 25 °C.

Material	[^{18}F] Found (mCi)	[^{18}F] Predicted for Random Exchange
Reaction tube	5.4	---
-196 °C trap (NOF)	12.7 (14.4%)	14.7 (16.7%)
-130 °C trap (ClF_5)	75.6 (85.6%)	73.6 (83.3%)

equatorial position, to explain the gas-phase exchange between ClF_3 and HF. A similar mechanism with ClF_6^- as an intermediate appears to give a satisfactory explanation for the observed fluorine exchange between ClF_5 and NOF (equation (4.13)).

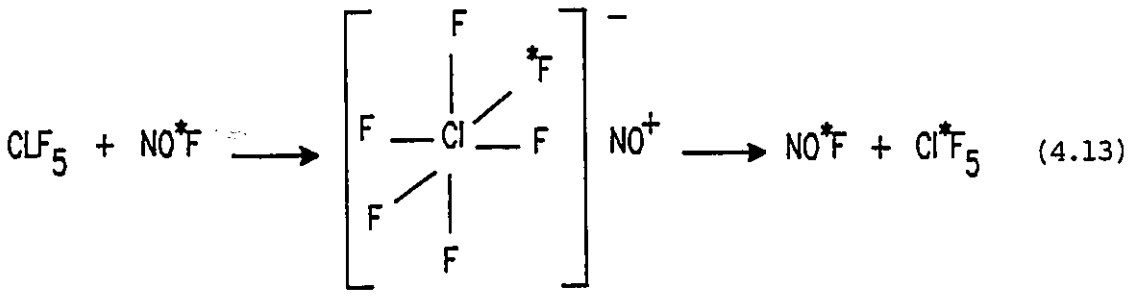

(4.13)

Evidence for the existence of the ClF_6^- anion from the present [^{18}F] study lead to a further study by Christe *et al.* to stabilize and isolate the ClF_6^- anion.[136] It was found that the bulky $(CH_3)_4N^+$ cation can be used to stabilize the highly reactive ClF_6^- anion. Moreover, $(CH_3)_4N^+ClF_6^-$ is soluble in CH_3CN at -30 °C, allowing its synthesis and characterization by Raman spectroscopy according to equation (4.14)

$$(CH_3)_4N^+F^- + ClF_5 \xrightarrow[-30\ °C]{CH_3CN} (CH_3)_4N^+ClF_6^- \qquad (4.14)$$

C. CONCLUSION

Conclusive evidence for the existence of ClF_6^- anion has been obtained. The exchange results led to the subsequent isolation and characterization of this anion and demonstrates the usefulness of [^{18}F] as a tracer to investigate inorganic reaction mechanisms. Although the exchange between ClF_5 and NO*F can account for the results of the [^{18}F] study in the $ClF_6^+AsF_6^-$ + NO*F displacement reaction, the possible intermediacy of ClF_7 cannot be completely ruled out. Based on the present findings, it seems necessary to devise another experiment where the ClF_5 formed from the displacement reaction can be separated before it can come in contact with NO*F in the system. One approach may be to conduct a flow experiment in which [^{18}F]NOF is passed through a solid bed of $ClF_6^+AsF_6^-$ under dynamic pumping through a -130 °C cold trap followed by sodalime (ambient temperature) and -196 °C traps. An alternate approach may be to measure the rates of exchange between [^{18}F]NOF and ClF_5 at different temperatures. The results could then be used to predict the relative distribution of [^{18}F] in NOF and F_2 due to exchange alone during the displacement reaction between ClF_6^+ salt and NOF.

CHAPTER 5

SYNTHESIS OF 2- AND 3-FLUOROTYROSINE

A. Introduction

Tyrosine (4-hydroxyphenylalanine) is a non-essential aromatic amino acid derived in animal cells by the hydroxylation of phenylalanine. It is a precursor of thyroxine and of the neurotransmitter hormones adrenaline and noradrenaline. It is also a precursor of the central neurotransmitter dopamine. In addition, it is a constituent of many proteins. Therefore, an ^{18}F labelled fluorotyrosine would be a useful tracer, in positron emission tomography, to study hormone, neurotransmitter or protein synthesis.

The pharmacology and toxicology of 3-fluorotyrosine have been the subjects of detailed investigations since 1930.[137] Prior to 1944, 3-fluorotyrosine was used in Germany as a pharmaceutical for the treatment of hyperthyroidism.[138] The first synthesis of 3-fluorotyrosine was actually reported by Schiemann and Winkemuller in 1933.[139] Palmer *et al.*[140] reported the synthesis of [^{18}F]3-fluorotyrosine using the Schiemann reaction, a time consuming multi-step synthesis, with a radiochemical yield of 1 - 3%. Its application as a pancreas immaging agent has also been reported.[141] The

syntheses of [^{18}F]2-fluorotyrosine or 2-fluorotyrosine had not been reported prior to the present work.

The aim of this research project was, in part, to develop a rapid yet efficient synthesis for [^{18}F]2- and 3-fluorotyrosine for routine use in Nuclear Medicine. In order to achieve this goal the differences in reactivity and selectivity of fluorine gas towards L-tyrosine in HF and HF/BF_3 have been exploited for the synthesis of 2- and 3-fluorotyrosine. 2-Fluorotyrosine has also been prepared by the direct fluorination of N-acetyl-(4-acetoxyphenyl)L-alanine methyl ester.

B. Results

1. 3-Fluorotyrosine

The mass spectrum of the compound eluting at 33 min. (see Chapter 2, separation of 3-fluorotyrosine) gave a protonated molecular ion at m/z = 200 $[M + H]^+$. The proton NMR spectrum of the sample revealed one less proton in the aromatic region when compared to the ^{1}H NMR spectrum of L-tyrosine. The ^{1}H chemical shifts and coupling constants were also similar to those of the authentic 3-fluorotyrosine (Table 5.1). The ^{19}F NMR spectrum was identical to that of the authentic compound and it consisted of a doublet of doublets at -136.6 ppm ($J_{(H-F)ortho}$ = 11.63 Hz and $J_{(H-F)meta}$ = 6.85 Hz) (Figure 5.1). The ^{13}C

chemical shifts agreed with the values predicted for substitution of fluorine at position 3 (Table 5.2). The ^{13}C chemical shifts of 3-fluorotyrosine were calculated using the emperically derived substituent parameters[142] for fluorine and the ^{13}C shifts of tyrosine in D_2O.DCl.

2. 2-Fluorotyrosine

The peak eluting at 34 min. during the HPLC analysis of the reaction mixture from both Schemes 2 and 3 has been ascribed to 2-fluorotyrosine on the basis of the following evidence: the high-resolution mass spectrum of the combined peaks was identical to that of the 3-fluorotyrosine; the ^{19}F NMR spectrum of the sample gave a doublet of doublets at -136.6 ppm (3-fluorotyrosine) and a triplet at -115.8 ppm (Figure 5.1); the areas under these multiplets agreed with the distribution of [^{18}F] in the radiochromatogram; the ^{13}C spectrum of the mixture gave signals well resolved from those arising from 3-fluorotyrosine and their chemical shifts agreed with the values predicted for 2-fluorotyrosine (Table 5.2).

During the production runs, Scheme 1 (page 57) yielded 5 - 6 mCi of [^{18}F]3-fluorotyrosine, after 125 min. of synthesis time, from 70 mCi of [^{18}F] in the reaction mixture. The radiochemical purity was greater than 98%. Scheme 2 (page 60)

Figure 5.1. ^{19}F NMR spectrum of (235.361 M Hz) 2- and 3-fluorotyrosine in D_2O.DCl. (A) 2-Fluorotyrosine and (B) 3-Fluorotyrosine.

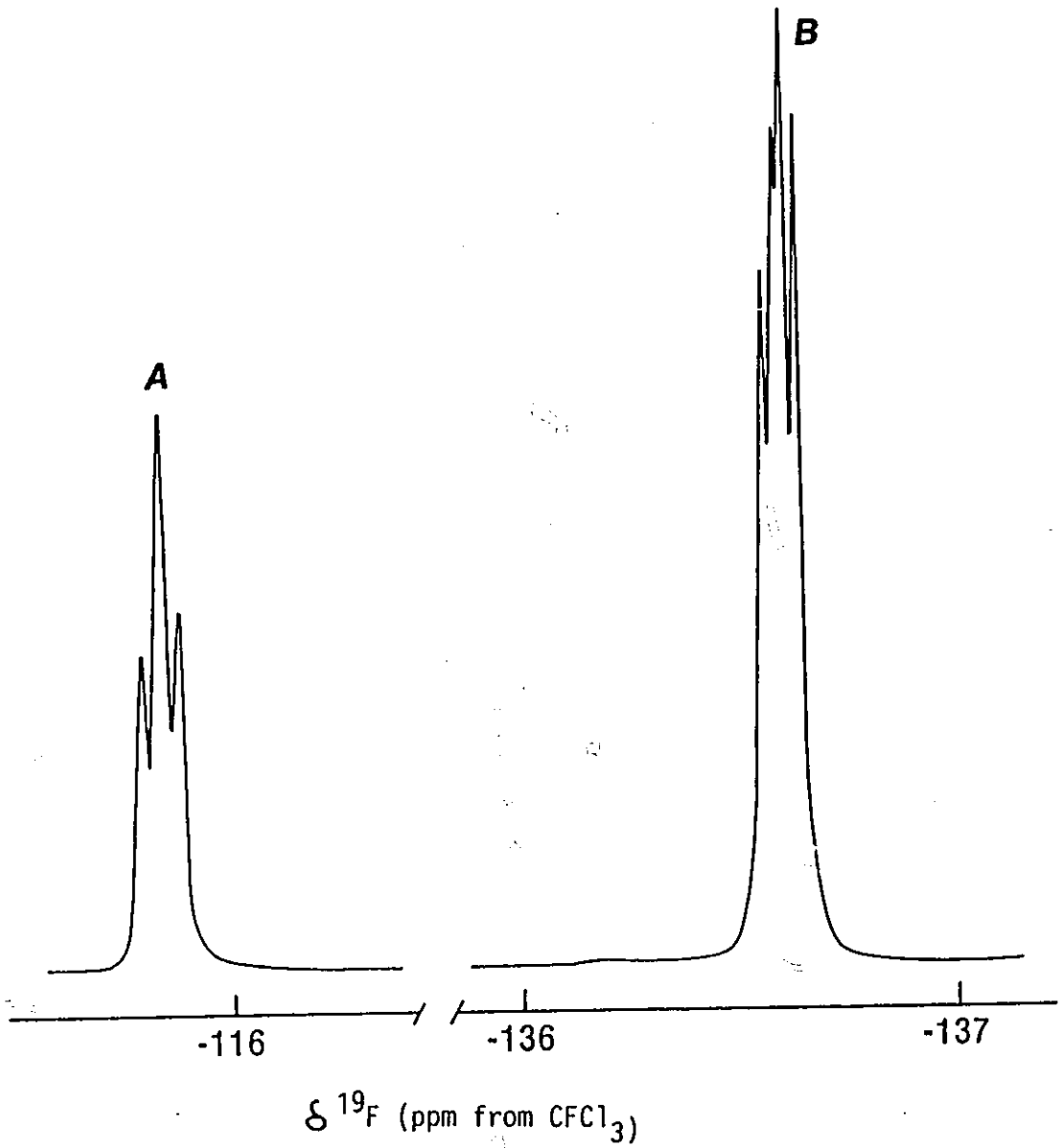
A
B
-116
-136
-137
δ 19F (ppm from CFCl3)

Table 5.1 ^1H NMR data for 3-Fluorotyrosine.

	δ (^1H) ppm [a]	Coupling Constants (Hz)	
H-α	4.10	$^3J(AX)$	5.7
H-β	3.05	$^3J(BX)$	7.5
	2.94	$^2J(AB)$	-14.8
H-2	6.86	$^4J(H_2H_6)$	1.9
H-5	6.77	$^3J(H_5H_6)$	8.2
H-6	6.75	$^3J(H_2F)$	12.0
		$^3J(H_5F)$	8.2

[a] Referenced with respect to external neat TMS at 30 °C

Table 5.2. ^{13}C NMR data for 3- and 2-Fluorotyrosine.

$\delta(^{13}C)$, ppm[a]	3-Fluorotyrosine	2-Fluorotyrosine
COOH	172.3	172.3
C_α	55.1	54.6
C_β	35.7	30.6
C_1	127.6 (127.6)[b]	113.5 (112.5)[b]
C_2	118.2 (117.8)	162.9 (167.1)
C_3	152.5 (152.3)	104.4 (102.9)
C_4	144.0 (142.1)	158.2 (157.2)
C_5	119.4 (118.0)	113.1 (112.7)
C_6	127.0 (127.6)	133.6 (132.9)

Coupling Constants (Hz)			
$^3J_{1,F}$	5.7	$^2J_{1,F}$	16.1
$^2J_{2,F}$	18.4	$^1J_{2,F}$	243.8
$^1J_{3,F}$	240.7	$^2J_{3,F}$	25.0
$^2J_{4,F}$	12.8	$^3J_{4,F}$	12.3
$^3J_{5,F}$	---	$^4J_{5,F}$	2.3
$^4J_{6,F}$	2.6	$^3J_{6,F}$	5.7

[a] Referenced with respect to neat external TMS.

[b] Calculated values using fluorine substituent parameters and ^{13}C chemical shifts of tyrosine in D_2O.DCl.

produced 1.0 mCi of [^{18}F]2-fluorotyrosine from 18 mCi of [^{18}F] in the reaction mixture after 125 min. of synthesis time while Scheme 3 (page 60) gave 1.7 mCi of [^{18}F]2-fluorotyrosine from 95 mCi of [^{18}F] in the reaction mixture after a synthesis time of 165 min. The radio-chemical purities of [^{18}F]2-fluorotyrosine from Schemes 2 and 3 were 85 ± 2% and 75 ± 3%, respectively.

3. <u>^{1}H and ^{13}C Spectra of Tyrosine in HF and HF/BF$_3$</u>

The ^{1}H NMR spectrum of tyrosine in HF at -79 °C consisted of an AB pattern at 6.94 and 6.75 ppm (4H, aromatic), a broad singlet at 6.11 ppm (NH_3^+) and multiplets at 4.23 ppm (X part of the ABX spin system on the side chain) and at 3.17 and 2.90 ppm (AB part of the ABX spin system). The ^{1}H spectrum of tyrosine in HF/BF$_3$ was similar to that of tyrosine in HF except that all signals were shifted to higher frequencies (Table 5.3). In addition, there was a signal at 10.21 ppm which was assigned to the carboxylic acid proton.

At higher temperatures no changes in the ^{1}H and ^{13}C spectra of tyrosine in and HF/BF$_3$ were apparent except that all signals were shifted to higher frequencies and the high frequency signal at 10.21 ppm started to collapse at -33 °C and had disappeared completely into the base line at 0 °C.

Table 5.3. ^1H NMR Parameters for Tyrosine in HF and HF/BF_3

$\delta(^1H)$, ppm[a]

	HF	HF/BF_3		
	-79 °C	-79 °C	-33 °C	-1 °C
H-2,6	6.94	7.27	7.31	7.33
H-3,5	6.72	7.12	7.18	7.21
CH	4.23	4.75	4.79	4.81
CH_2	3.17	3.37	3.42	3.44
	2.90	3.17	3.25	3.29
NH_{3+}	6.11	6.67	6.70	6.69
OH	---	---	---	---
COOH	---	10.21	10.19	---

Coupling Constants (Hz)

$^3J_{H2-H3} = 8.70$, $^2J_{A-B} = -14.94$, $^3J_{A-X} = 6.18$, $^3J_{B-X} = 9.14$

[a] Referenced with respect to the residual proton in acetone-d_6 (99.99 atom % deuterium ($\delta(^1H$) 2.04 ppm).

The ^{13}C spectrum of tyrosine in HF/BF_3 was quite distinct from that of the tyrosine in HF (Table 5.4) which showed the signals expected from all the carbons, whereas the spectrum of tyrosine in HF/BF_3 showed only one signal for the quaternary carbons. Furthermore, the signal from the carboxylic acid group was not observed.

C. DISCUSSION

1. NMR Spectroscopy

It has been reported that aromatic compounds containing a ring activating substituent, OR, are protonated at the ring carbon *para* to the OR group and not at the oxygen atom when dissolved in strong acids.[143] This is because the positive charge in the protonated species can be delocalised resulting in a quinonoid structure (equation 5.1).

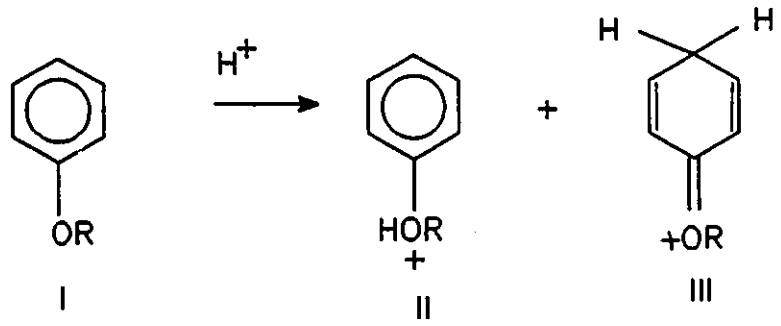

(5.1)

Table 5.4. ^{13}C Chemical Shifts[a] of Tyrosine in HF and HF/BF_3 at -79 °C and in $D_2O.DCl$ (30 °C).

	HF	HF/BF_3	$D_2O.DCl$
C_1	129.3	146.3[b]	126.7
C_2	134.0	131.7	132.0
C_3	119.3	117.2	117.1
C_4	155.4	146.3[b]	156.3
C_5	119.3	117.2	117.1
C_6	134.0	131.7	132.0
CH_2	37.4	33.9	35.7
CH	58.9	55.2	55.2
COOH	176.8	--	172.4

[a] Referenced with respect to neat external TMS at 21 °C.

[b] Only one signal was observed for quaternary carbons.

Olah and Mo[144] used super acids with varying acidities (1:1 $HF:SbF_5$ in SO_2ClF, 1:1 $HSO_3F:SbF_5$ in SO_2ClF, 4:1 $HSO_3F:SbF_5$ in SO_2ClF and HSO_3F in SO_2ClF) to show that the ratio of ring protonation to oxygen protonation is dependent upon the acidity of the medium. Specifically, using low-temperature ^1H NMR they showed that the ratio of C-protonation to O-protonation decreased when the acidity of the medium was decreased.[144] Brouwer *et al.*[145], using a solution of anisole in HF saturated with BF_3, reported evidence for the protonation of both the oxygen and ring carbon at low temperatures. However, the protonation of *para* methyl anisole in HF/BF_3 occurred exclusively at the oxygen atom and this was attributed to the considerable reduction in basicity at the para position when a methyl group is substituted for hydrogen at that position.

The ^1H NMR spectrum of tyrosine in HF/BF_3 at -78 °C showed no evidence for the ring protonation of tyrosine. This could be due to two factors: (1) the concentration of BF_3 in HF used in the present study is 0.97 M compared to the saturated solution of BF_3 in HF used by Brouwer *et al.*;[145] it is known that ring protonation is favoured when the acidity of the solvent is higher, (2) protonation of tyrosine (a zwitterion) in strong acids will occur at the carboxylate group before occuring at any other site. The presence of the acidic proton

at 10.21 ppm in the -79 °C spectrum of tyrosine in HF/BF_3 clearly supports this view.

It has also been reported that the ratio of ring protonation to oxygen protonation of anisole in HF/BF_3 increased from 1.5 at -80 °C to 50 at 0 °C.[145] In the present study no ring protonated species were observed for tyrosine in HF/BF_3 from -80 to +1 °C. The disappearance of the signal at 10.21 ppm could be due to fast exchange between the carboxylic proton and the solvent HF.

Results from the present ^1H NMR studies also show that the oxygen in the phenolic group is protonated in the tyrosine HF/BF_3 solution because the chemical shifts of aromatic protons are shifted to higher frequencies compared to the chemical shifts observed for tyrosine in HF (Table 4.3). The differences in chemical shifts indicate that all proton environments are deshielded when tyrosine is dissolved in HF/BF_3. The deshielding of aromatic protons may be explained by the deactivation of the aromatic ring as a result of the protonation of the hydroxyl group.

2. Radiofluorination of Tyrosine HF and HF/BF_3

i. General Features

Results from the radiofluorination of tyrosine in HF, HF/BF_3, CF_3COOH and CH_3CN are shown in Table 5.5. Three important points which depend upon the solvent used for radiofluorination should be noted. These are namely (a) the fraction of $[^{18}F]F_2$ retained in the reaction vessel, (b) the radiochemical yield and (c) the regio-selectivity of fluorination. These points are discussed in more detail later in this chapter.

ii. Retention of $[^{18}F]F_2$ in the Reaction Mixture

The fraction of $[^{18}F]F_2$ retained in the reaction mixture after the fluorination of tyrosine in HF/BF_3 was 12%. This is considerably less than the 55%, or more, of the $[^{18}F]F_2$ retained when other solvents are used for the fluorination. Since $[^{18}F]F_2$ does not exchange with the fluorine in HF/BF_3, and since HF/BF_3 is expected to be inert to attack by fluoride ion it can be argued that most of the fluorine escaped unreacted during the fluorination of tyrosine in HF/BF_3. In other words the aromatic ring of tyrosine in HF/BF_3 is deactivated with respect to electrophilic attack by fluorine. Protonation at the oxygen of the hydroxyl group when tyrosine is dissolved in HF/BF_3 would cause deactivation of the aromatic ring.

Table 5.5. Results from the Radiofluorination of Tyrosine in Different Solvents.

Solvent	Temp. (°C)	%[^{18}F]F_2 Recovered	Radiochemical yield (%)	Regioselectivity 2-F(%)	3-F(%)
CH_3CN/BF_3	-30	21	8	0	100
CF_3COOH	-10	51	12	0	100
HF	-70	62	27	0	100
HF/BF_3	-70	12	19	78	22

Similar results were obtained during the direct fluorination of 3,4-dihydroxyphenylalanine (DOPA) in HF and HF/BF_3.[68] However, the difference between the $[^{18}F]F_2$ consumed during the fluorination of dopa in HF (62%) and in HF/BF_3 (37%) was much smaller when compared to the fluorination of tyrosine in HF (62%) and HF/BF_3 (12%). In the case of dopa, this is to be expected because the two hydroxyl groups on the aromatic ring would make the ring sufficiently activated, even in HF/BF_3, for electrophilic attack by fluorine.

The low-temperature ^1H NMR study of tyrosine in HF/BF_3 showed evidence for the protonation of tyrosine at the oxygen of the hydroxyl group (see NMR results above). As a consequence, the reactivity of tyrosine in HF/BF_3 towards electrophilic fluorination or the $[^{18}F]F_2$ retained in the reaction mixture would be predictably low.

iii. Radiochemical Yield

The radiochemical yield of 3-fluorotyrosine increased as the acidity of the reaction medium increased from CH_3CN/BF_3 to CF_3COOH to HF. This is consistent with the observation, in a previous study in which DOPA was fluorinated using $[^{18}F]F_2$ gas,[68] that the yield of fluorine-substituted products increased with increasing acidity of the reaction medium. However, unlike fluorodopa whose radiochemical yield was more

than doubled in going from HF to HF/BF_3, the radiochemical yield of fluorotyrosine was decreased when the acidity of HF was increased by the addition of BF_3. One explanation may be that, as discussed above, the reactivity of DOPA in HF/BF_3 towards electrophilic fluorination was not reduced to the same extent as was the case with tyrosine in HF/BF_3.

It is possible that the direct fluorination in CH_3CN/BF_3 and CF_3COOH may cause competitive reactions such as the oxidation of the hetero atoms (O and N) in the amino acid and consequently the yield of the 3-fluorotyrosine would be relatively low. It is known that at higher temperatures, reactions of fluorine are initiated by the $F^{\cdot}$ atoms[66] and therefore fluorination in CH_3CN/BF_3 and CF_3COOH at relatively high temperatures will produce more side products. When either of these solvents was used, the amount of $[^{18}F]F_2$ retained in the reaction vessel (55%) was comparable to that obtained for the fluorination using HF as the solvent. It can therefore be concluded that the lower radiochemical yield after the reaction in CH_3CN/BF_3 and CF_3COOH is due to the higher, but nonselective reactivity of fluorine towards tyrosine in these solvents. This in turn would reduce the radiochemical yield of the substitution product.

The 10% radiochemical yield of 3-fluorotyrosine after the direct fluorination of tyrosine in CF_3COOH (Table 5.5) is considerably lower than that reported by Coenen *et al.* [146] who, using the same method, obtained a 30% radiochemical yield for 3-fluorotyrosine. A possible explanation could be the lower concentration (50 μmoles) and higher dilution (0.2% F_2 in neon) of fluorine that is used for the fluorination reaction by Coenen *et al.*[146] compared to the total amount of fluorine (180 μmoles and 0.4% in neon) in the present study.

iv. Regioselectivity of Radiofluorination

In all solvents used in the present study, except in HF/BF_3, the direct fluorination of L-tyrosine is regiospecific. This is surprising. Given the extreme reactivity of elemental fluorine with hydrocarbons, one would expect little or no selectivity in reactions involving molecular fluorine. Misaki[147,148] has reported similar results for the fluorination of p-cresol and p-hydroxy benzoic acid in which 3-fluoro-4-hydroxytoluene and 3-fluoro-4-hydroxy benzoic acid are produced, respectively. Cacace and Wolf[149] have studied the reactivity and orientation of the direct liquid phase fluorination of substituted benzenes and have suggested that the fluorination proceeds through a mechanism similar to that of the ionic halogenation reactions of aromatic compounds. The formation of 3-fluorotyrosine after the direct

fluorination of tyrosine is consistent with this latter mechanism because the electron releasing property of the hydroxyl group would make position 3 (*ortho* to the hydroxyl group) more susceptible to electrophilic attack.

The regioselectivity of fluorination is also dependant upon the concentration of BF_3 in HF (Table 5.6, Figure 5.2). Table 5.6 shows that as the concentration of BF_3 in HF was increased from 0 M to 0.96 M, i.e., as the acidity of the medium was increased, the ratio of 2-fluorotyrosine to 3-fluorotyrosine increased from 0 to 3.2. This is consistent with observation that the ratio of protonated to unprotonated species increases with increasing acidity of the solvent.[142]

The present finding relating to the differences in orientation of electrophilic fluorination of tyrosine in HF and HF/BF_3 is in contrast with the previous studies relating to the direct fluorination of DOPA in which no such changes in orientation were observed.[69] It is difficult to rationalize the fluorination results of dopa because of the presence of three ring activating substituents on the aromatic ring. However, the differences in reactivity and selectivity of $[^{18}F]F_2$ towards tyrosine in HF and HF/BF_3 may be explained by the differences in reactivity of $[^{18}F]F_2$ towards tyrosine (equation 5.2) and protonated tyrosine (equation 5.3).

Figure 5.2. Radiochromatogram of the products obtained from the direct fluorination of L-tyrosine in HF containing different concentrations of BF_3. $[BF_3]$: (A) 0 M, (B) 0.32 M, (C) 0.96M.

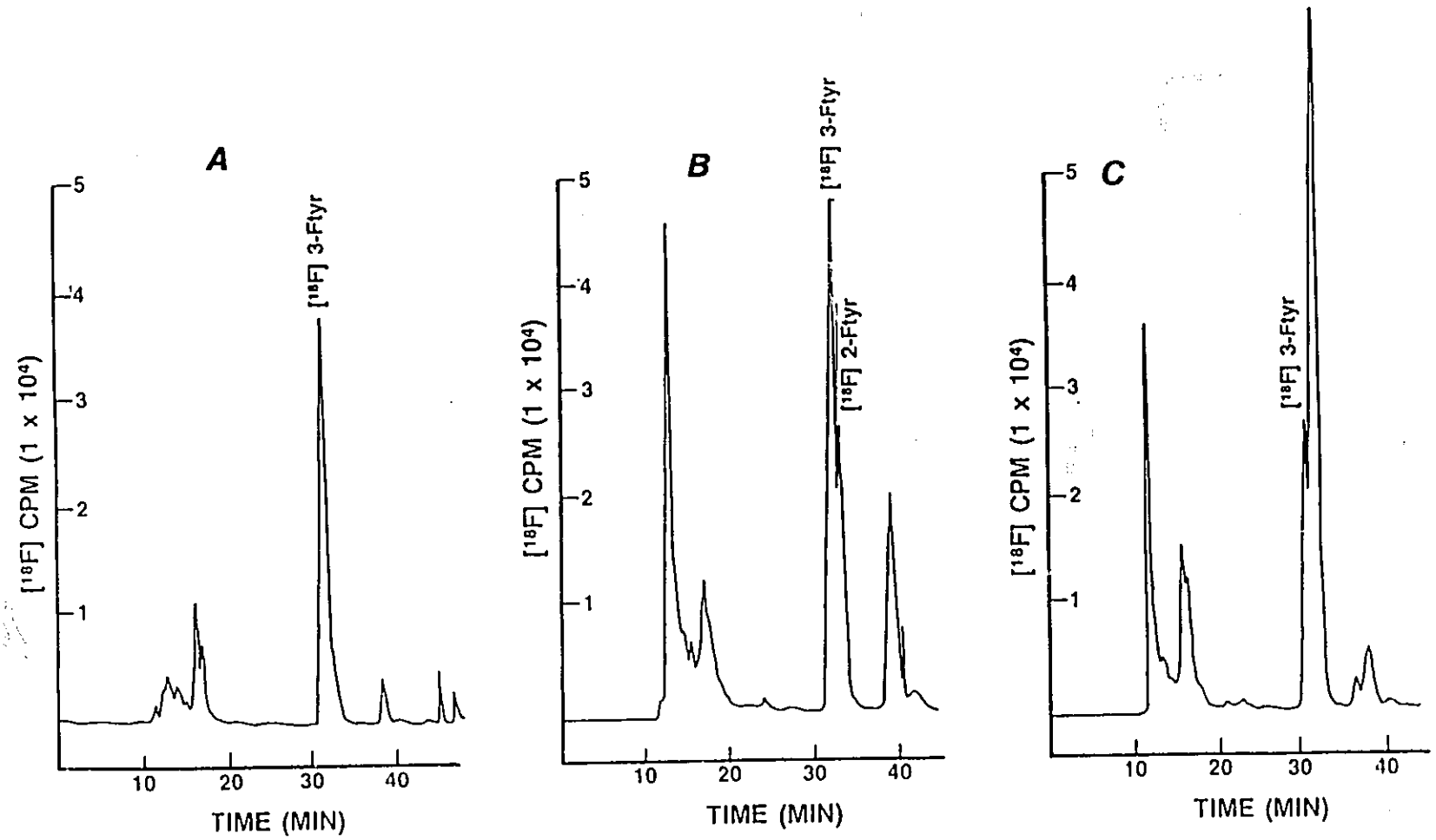
A
B
C
[18F] 3-Ftyr
[18F] 2-Ftyr
[18F] CPM (1 x 10⁴)
TIME (MIN)
1
2
3
4
5
10
20
30
40

Table 5.6. Isomer Distribution vs Concentration of BF_3 in HF for Direct Fluorination of Tyrosine

Molar Conc. of BF_3 in HF	% $[^{18}F]F_2$ Retained	Radiochemical Yield (%)	Isomer Distribution % 2-F	% 3-F
0	62	27	0	100
0.32	17	12	66	34
0.55	9	18	78	24
0.96	12	19	78	22
0.96	9	32	80	20

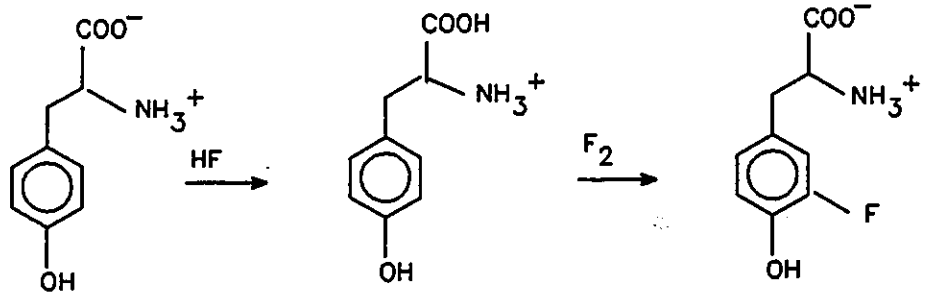

(5.2)

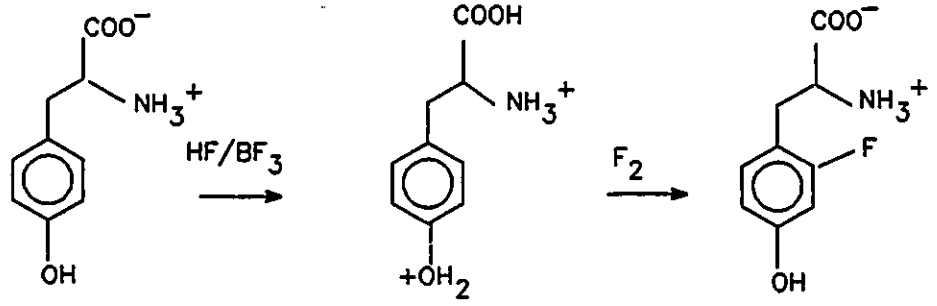

(5.3)

Other workers have compared the reactivity and selectivity of $[^{18}F]F_2$ and $[^{18}F]CH_3COOF$, a mild electrophilic fluorinating agent, towards tyrosine in CF_3COOH at +4 °C and have shown that both fluorinating agents produce no more than 7% of 2-fluoro tyrosine.[144] These results are in contrast to the present study where direct fluorination of tyrosine in CF_3COOH at -10 °C produced 100% 3-fluorotyrosine. The higher selectivity obtained in this study may be due to the relatively lower reaction temperature and higher substrate to fluorine ratio (3 : 1 compared to 1.3 : 1) used for the direct fluorination.

3. Reaction Scheme 3

Protection of the phenolic group in tyrosine by the electron withdrawing acetyl group, should favour the formation of 2-fluorotyrosine during the electrophilic fluorination of tyrosine. Indeed, the direct fluorination of O,N-acetylated tyrosine methyl ester in all solvents studied, except HF, produced 2- and 3-fluoro-tyrosine (Table 5.7). When HF was used as the solvent, 98% of the monofluorinated product was 3-fluorotyrosine. This may be due to hydrolysis of the acetyl group by HF, after which the fluorination reaction becomes similar to Scheme 1.

In Scheme 3, the fraction of $[^{18}F]F_2$ retained in the reaction mixture is similar in all solvents studied (Table 5.7). The radiochemical yields are relatively low in CH_3CN/BF_3 and $CHCl_3/CFCl_3$ (1 : 1). The trend in radiochemical yield is in agreement with the trend observed for Scheme 1 which showed a higher yield as the acidity of the solvent was increased. In general, the higher $[^{18}F]F_2$ retention in the reaction mixture and lower radiochemical yield, observed for Scheme 3, indicate higher reactivity but lower selectivity of fluorine towards the tyrosine derivative.

If the fluorination proceeds predominantly by a 'polar substitution mechanism', then the protection of the phenolic

Table 5.7 Results from the Radiofluorination of N-Acetyl-(4-Acetoxyphenyl)L-Tyrosine Methyl Ester

Solvent	Temperature °C	%[^{18}F]F_2 Retained	Radiochemical Yield(%)	Regioselectivity % 2-F	%3-F
HF	-70	46	15	2	98
CF_3COOH	0	40	10	48	52
CF_3COOH	-10	35	13	38	62
CH_3CN/BF_3	-30	46	8	44	56
$CHCl_3/CFCl_3$	-45	36	3	25	75

group by the acetyl group should have resulted in the formation of 2-fluorotyrosine as the major product. So far, no systematic study has been reported showing the contribution from the side chain of aromatic amino acid to the orientation of electrophilic fluorinations. For example, it has been reported that the fluorination of O-acetyl tyrosine (no protection on the amine or acid group) in CF_3COOH resulted in 71% and 29% of 2- and 3-fluoro tyrosine, respectively, with a combined radiochemical yield of 15%. It appears that the carboxyl group and/or the amino group on the side chain may be involved in the elimination of the developing fluoride ion, as HF, during or after the formation of the carbon-fluorine bond at C-2. The results fron the direct fluorination of tyrosine in HF/BF_3 with similar regioselectivity and radiochemical yield supports such an involvement by the side chain.

D. Conclusions

Direct fluorination of tyrosine in HF provides an efficient and rapid method for the synthesis of [^{18}F]3-fluoro tyrosine. Two different methods for the synthesis of 2-fluoro tyrosine have been developed. The direct fluorination of tyrosine in HF/BF_3 is the preferred method because no synthesis of the organic precursor is necessary and therefore no time is lost in removing the protecting groups after the initial fluorination reaction. The protonation of tyrosine in

HF/BF_3 makes it less susceptible, not only to electrophilic attack by F_2, but also makes it less susceptible to oxidative attack of fluorine at other sites. Clear evidence for this can be seen from the $[^{18}F]F_2$ retained after the fluorination of O-acetyl derivative, a compound which is also deactivated for electrophilic attack in CF_3COOH. The radiochemical yields in both reactions are comparable indicating a cleaner reaction when HF/BF_3 is used as the solvent.

CHAPTER 6

SYNTHESIS OF [^{18}F] LABELLED FLUORO-m-TYROSINE, FLUORO-m-TYRAMINE AND FLUORO-3-HYDROXYPHENYLACETIC ACID

A. INTRODUCTION

Since the introduction of Position Emission Tomography there has been an ongoing search for new ^{18}F-labelled tracers that can be used to study presynaptic dopaminergic functions. Garnett *et al.*[150] using PET showed that [^{18}F]6-FDOPA could be used to visualize dopamine metabolism in the living human brain. However, after the administration of [^{18}F]6-FDOPA, there is some non-specific accumulation of [^{18}F] activity in the brain, probably due to the 3-O-methyl-[^{18}F]6-FDOPA formed in the blood by the action of catechol-O-methyltransferase.[151,152] An accurate determination of dopamine turnover rate using PET data will therefore need to account for the O-methylated derivative. The [^{18}F]6-FDOPA technique showed the feasibility of assessing aromatic amino acid decarboxylase (AADC) activity *in vivo*.[153] Now it is necessary to develop a tracer that will act only as a substrate for AADC. This will thereby simplify the mathematical model used to explain the time course of the ^{18}F in the brain following an intervenous injection of the tracer and thereby improve its veracity.

It has been shown that m-tyrosine is a good substrate for AADC and that its Km (Michaelis-Menten constant) value is almost identical to that of L-dopa.[154] m-Tyrosine also crosses the blood brain barrier with a brain uptake index approximately twice that of L-dopa.[155] However, unlike dopa, m-tyrosine is not a substrate for catechol-O-methyltransferase.[156] Consequently, ^{18}F-labelled m-tyrosine should be an ideal tracer to study AADC activity in the brain as was first suggested by DeJesus *et al.*[157]

In this chapter, a general method the direct fluorination in anhydrous hydrogen fluoride is demonstrated for m-tyrosine and its metabolites m-tyramine and 3-hydroxy-phenylacetic acid. A comparative study of the recovery of $[^{18}F]F_2$ from the target and the radiochemical yields for the direct fluorination of m-tyrosine in HF, HF/BF_3, HF/CsF, CF_3COOH and CH_3CN/BF_3 is also reported.

B. RESULTS

1. ^{1}H and ^{13}C Spectra of m-Tyrosine

^{1}H NMR parameters of m-tyrosine in D_2O.DCl, HF and HF/BF_3 are listed in Table 6.1. The ^{1}H NMR spectrum of m-tyrosine in D_2O.DCl consisted of a triplet at 6.57 (1H), two doublets at 6.16 (1H) and 6.14 (1H) and a broad singlet at 6.10 ppm (1H). These were assigned to H-5, H-6, H-4 and H-2, respectively.

Assignments of H-5 (triplet due to spin-spin couplings to H-6 and H-4) and H-2 (broad singlet with residual couplings to *meta* protons) were based on the multiplicities of their signals. Both H-6 and H-4 are expected to give a doublet with small couplings to H-2. The assignment of H-6 is based on a proton-proton nuclear Overhauser enhancement (NOE) experiment in which the irradiation of one of the benzylic protons at 2.46 ppm increased the intensity of the doublet at 6.16 and the singlet at 6.10 ppm (Figure 6.1). Consequently the doublet at 6.16 ppm was assigned to H-6. The signals from the protons on the side-chain consisted of multiplets at 3.66 (X part of the ABX spin system), 2.58 and 2.46 ppm (AB part of the ABX spin system).

The ^1H NMR spectrum of m-tyrosine in HF at -79 °C consisted of a triplet at 6.90 (1H, H-5) and singlets at 6.52 (2H, H-4, H-6) and 6.42 ppm (1H, H-2) (Figure 6.2A). The signals from the protons on the side chain consisted of a broad singlet at 5.95 (NH_3^+) and multiplets at 4.08 (X part of the ABX spin system), 3.01 and 2.75 ppm (AB part of the ABX spin system). The ^1H spectrum of m-tyrosine in HF/BF_3 (0.96 M BF_3, Figure 6.2b) was different from that of m-tyrosine in HF and showed the following features: (a) the chemical shifts of all protons were moved to higher frequencies, (b) the

Figure 6.1 (A) ^1H NMR spectrum (500.135 MHz,) of m-tyrosine in D_2O.DCl at 30 °C. (B) The proton-proton NOE difference spectrum after the irradiation of the proton at 2.46 ppm. In Figure 6.1 only the aromatic region is shown.

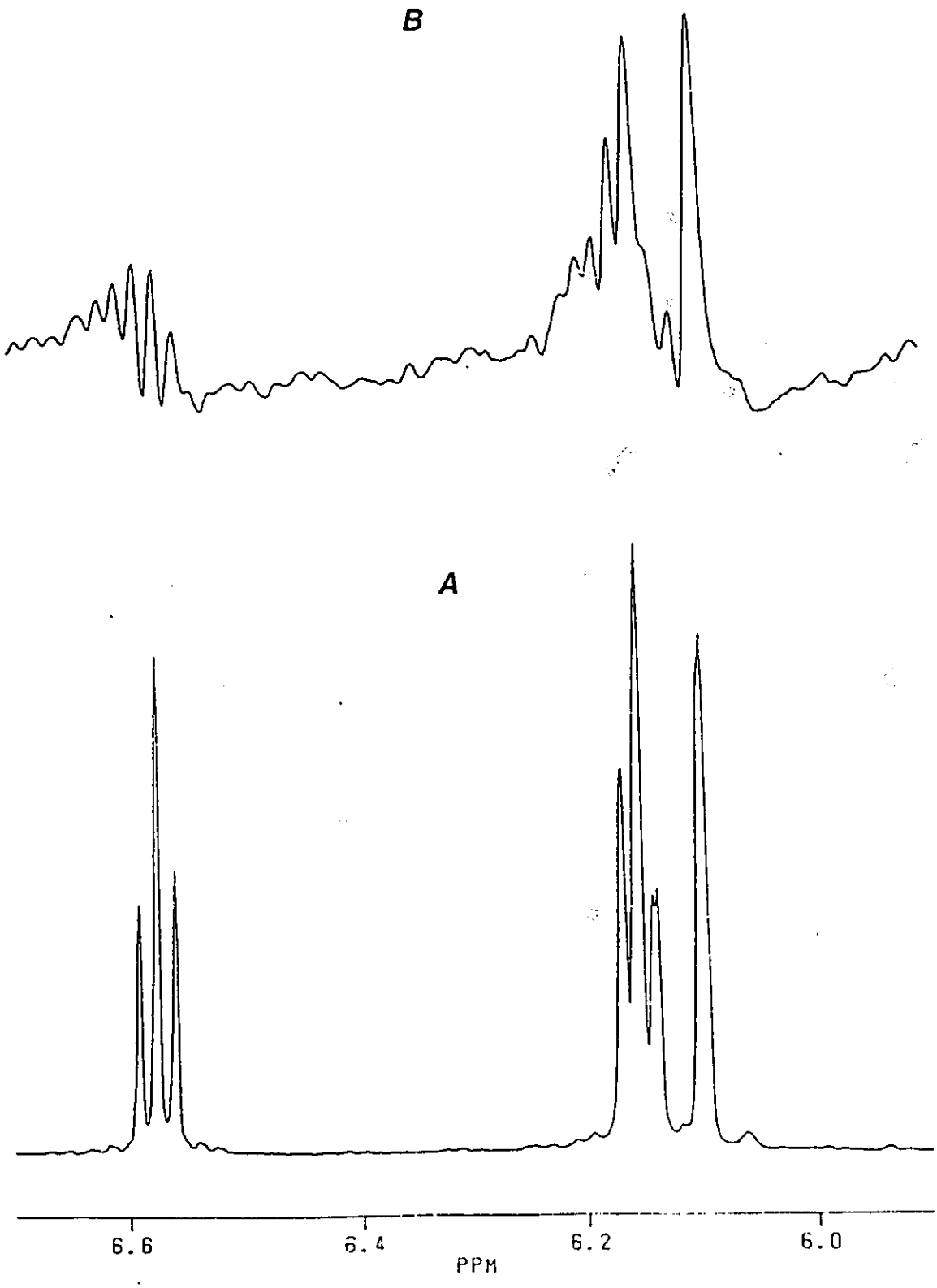
B
A
6.6
6.4
6.2
6.0
PPM

signals due to H-4 and H-6 were well resolved and appeared as doublets due to spin-spin couplings between H-5 and H-6 and H-5 and H-4 and (c) additional signals at 9.83 and 10.21 ppm were observed. The areas under the high-frequency signals were 1.67 and 3.19, respectively, and they were assigned to protonated hydroxyl and carboxyl groups, respectively. The intensities of these signals were reduced considerably when the concentration of BF_3 was 0.16 M.

The ^1H NMR spectrum of m-tyrosine in CH_3CN/BF_3 (Figure 6.3) consisted of signals at δ = 2.84 and 3.05 (AB portion of the ABX spin system on the side chain), 4.04 (X portion of the ABX spin system), singlets at 6.33 (NH_2) 6.52 (H-2), 9.17 (OH) and 10.83 (COOH), doublets at 6.58 and 6.59 (H-4, H-6) and a triplet at 7.03 (H-5). In addition, there were two extra singlets at 7.12 and 7.36 ppm that had not been identified (Figure 6.3). The signal at 7.36 ppm had disappeared and the intensity of of the signal at 7.12 ppm was reduced when the temperature was raised to -1.5 °C. The temperature dependence of these additional signals indicates that they arise from the donor-acceptor complex of BF_3 with m-tyrosine.

Figure 6.2 ^{1}H NMR spectrum (500.135 MHz) of m-tyrosine at -79 °C (A) in HF and (B) in HF/BF_3

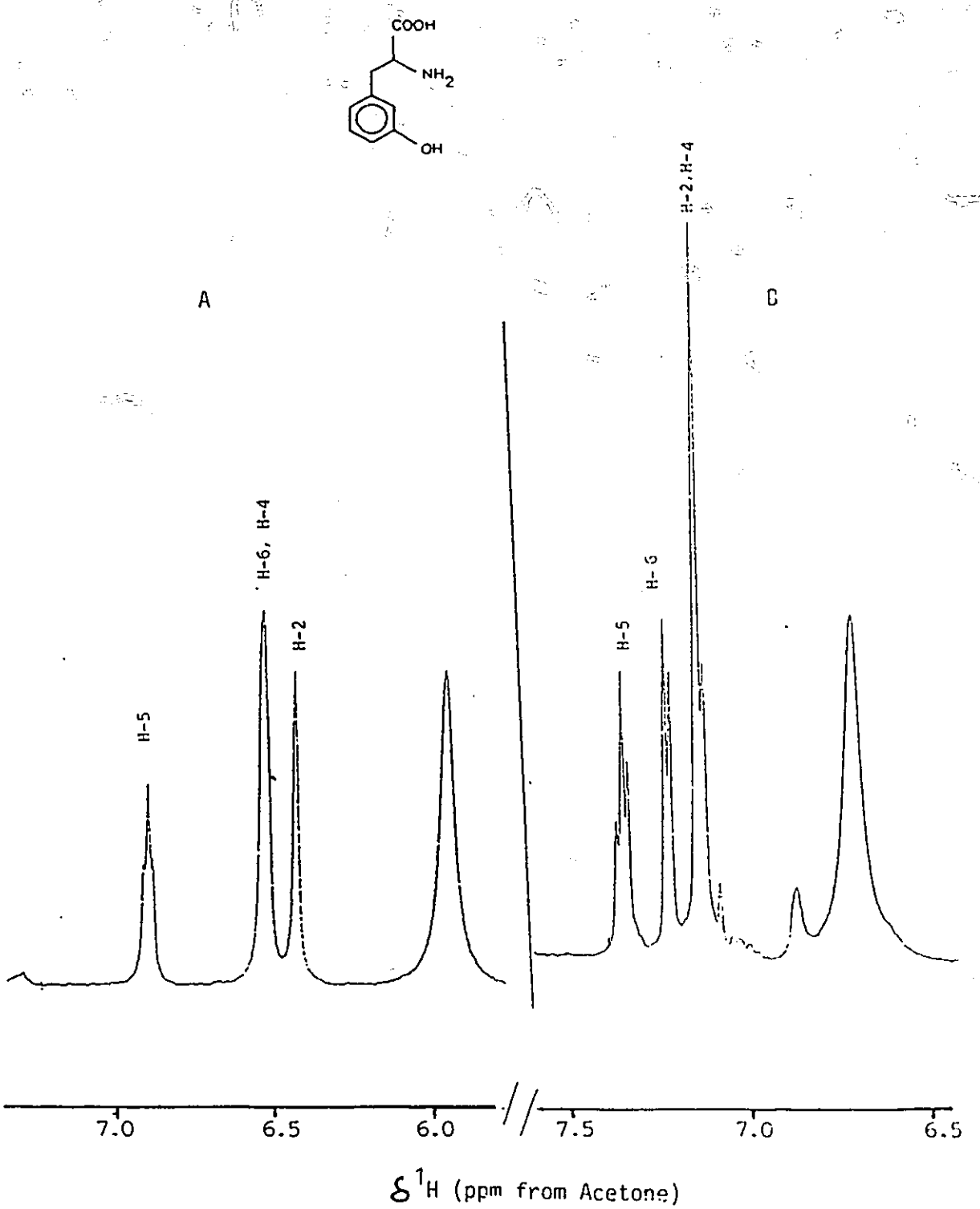
COOH
NH2
OH
A
C
H-5
H-6, H-4
H-2
H-5
H-6
H-2,H-4
7.0
6.5
6.0
7.5
7.0
6.5
δ1H (ppm from Acetone)

Figure 6.3 ^1H NMR spectrum (500.135 MHz) of m-tyrosine in CH_3CN/BF_3 at -30 °C. Asterisks (*) denote additional signals (see text).

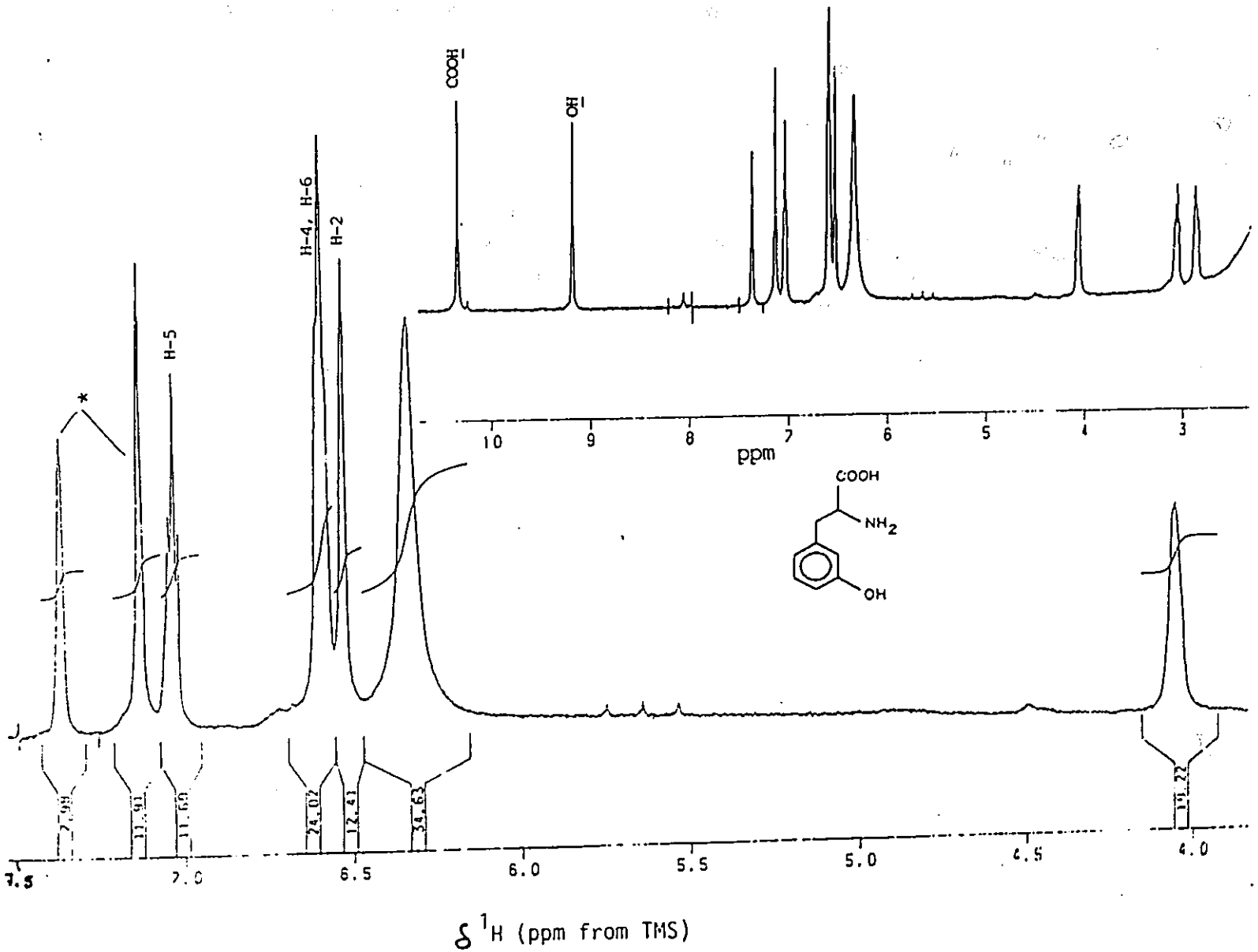
COOH
OH
H-4, H-6
H-2
H-5
*
10
9
8
7
6
5
4
3
ppm
COOH
NH2
OH
7.5
7.0
6.5
6.0
5.5
5.0
4.5
4.0
7.98
11.91
11.68
24.02
12.41
34.63
10.22
δ 1H (ppm from TMS)

Table 6.1. ^1H Chemical Shifts (ppm) and Coupling Constants (Hz) of m-Tyrosine in D_2O.DCl (30 °C), HF and HF/BF3 at -79 °C

Chemical Shifts[a]				Coupling Constants[b]	
	HF	HF/BF_3	D_2O.DCl		
H-2	6.42	7.15	6.10	$^3J_{H5,6}$	7.88
H-4	6.52	7.17	6.14	$^3J_{H5,4}$	7.78
H-5	6.90	7.37	6.57	$^4J_{H6,2}$	----
H-6	6.52	7.25	6.16	$^4J_{H4,2}$	----
NH_3^+	5.95	6.73	--		
CH	4.08	4.82	3.66	$^2J_{HA,B}$	-14.58
CH_2	3.01 2.75	3.39 3.23	2.58 2.46	$^3J_{HA,X}$	7.58
				$^3J_{HB,X}$	5.65
$-OH_{2+}$	--	9.81	---		
$-COOH_{2+}$		10.19	---		

[a] Referenced with respect to residual proton in acetone d_6 at 2.04 ppm.

[b] Coupling constants obtained from the spectrum in D_2O.DCl at 30 °C.

Carbon-13 chemical shifts of m-tyrosine in D_2O.DCl, HF and HF/BF_3 are listed in Table 6.2. In general, ^{13}C signals shifted to higher frequencies when BF_3 was added to the m-tyrosine/HF solution. Maximum deshielding was observed for C-6 ($\Delta\delta$ = 10.7 ppm). The assignment of the ^{13}C signals is based on a selective hetero nuclear decoupling experiment in which the irradiation of the protons at 7.37 (triplet, H-5) and 7.25 ppm (doublet, H-6) increased the intensity of the ^{13}C signal at 135.8 and 133.4 ppm, respectively,. Consequently, the ^{13}C chemical shifts were assigned to C-5 and C-6, respectively. Similarly the irradiation of the protons at 7. 15 and 7.17 ppm (H-2, H-4) increased the intensity of the ^{13}C signals at 121.0 and 120.8 ppm. These were assigned to C-2 and C-4, respectively.

Another feature of the ^{13}C spectrum of m-tyrosine in HF/BF_3 was that no separate signals for quaternary carbons were observed as the concentration of BF_3 was increased. In addition, the signal from the carboxylic carbon was not observed when the concentration of BF_3 was increased to 0.96 M. Both of these effects can be expected if O-protonated tyrosine is the predominant form in m-tyrosine/HF/BF_3 solution. Relaxation times of C-3 and the carboxylic carbon would be longer in the O-protonated tyrosine.

Table 6.2. ^{13}C Chemical Shifts[a] of m-Tyrosine in $D_2O.DCl$ (30 °C), HF and HF/BF_3 at -79 °C

	$D_2O.DCl$	HF	HF/BF_3	
			0.25 M BF_3	0.96 M BF_3
C_1	136.49	132.3	137.7	150.1[a]
C_2	115.88	114.3	120.7	121.0
C_3	156.77	151.4	150.7	150.1[a]
C_4	117.14	114.1	120.3	120.8
C_5	131.52	130.3	135.6	135.8
C_6	122.43	122.7	132.7	133.4
CH_2	54.78	33.5	38.0	38.0
CH	36.20	54.3	58.8	59.0
-COOH	171.89	172.2	182.2	--

[a] Referenced with respect to neat external acetone.

[a] Only one signal observed for quaternary carbons

2. Identification of Fluoro-m-tyrosine

The mass spectrum of the compound eluting at 23 min. (see HPLC conditions on page 66) gave a protonated molecular ion at m/z = 200 $[M + H]^+$. The proton NMR spectrum showed a multiplet at 6.53 - 6.81 ppm (3H, aromatic), 4.1 ppm (X part of the ABX spin system on the side chain) and 2.91 and 3.17 ppm (AB part of the ABX spin system). The ^{19}F NMR spectrum (Figure 6.4) showed a seventeen-line multiplet at -129 ppm (60% by integration) and a doublet of doublets at -142 ppm (35% by integration). The latter was assigned to 2-fluoro-m-tyrosine since the fluorine on carbon-2 is expected to couple to both meta protons to give a doublet of doublets. The fluorine on carbon-6 of the 6-fluoroisomer is expected to be split by three non-equivalent protons and the two protons of the $-CH_2$ group on the side chain and should consist of 8 triplets ($ABCM_2X$ spin system). The spectrum was simulated using the program Laocoon PC NMR Simulation.[158] The results from the simulated $ABCM_2X$ spectrum after iteration were in excellent agreement with those of the observed spectrum. The ^{13}C spectrum consisted of signals that are in agreement with the calculated values[142] for the 2- and 6-fluoroisomers (Table 6.3). The 4- and 5-fluoroisomers were assigned to weak signals at -137.2 and -138.7, respectively, and have combined intensities of less than 5% (see Figure 6.4).

Figure 6.4 ^{19}F NMR spectrum of fluoro-m-tyrosine obtained after the direct fluorination of m-tyrosine in HF at -70 °C

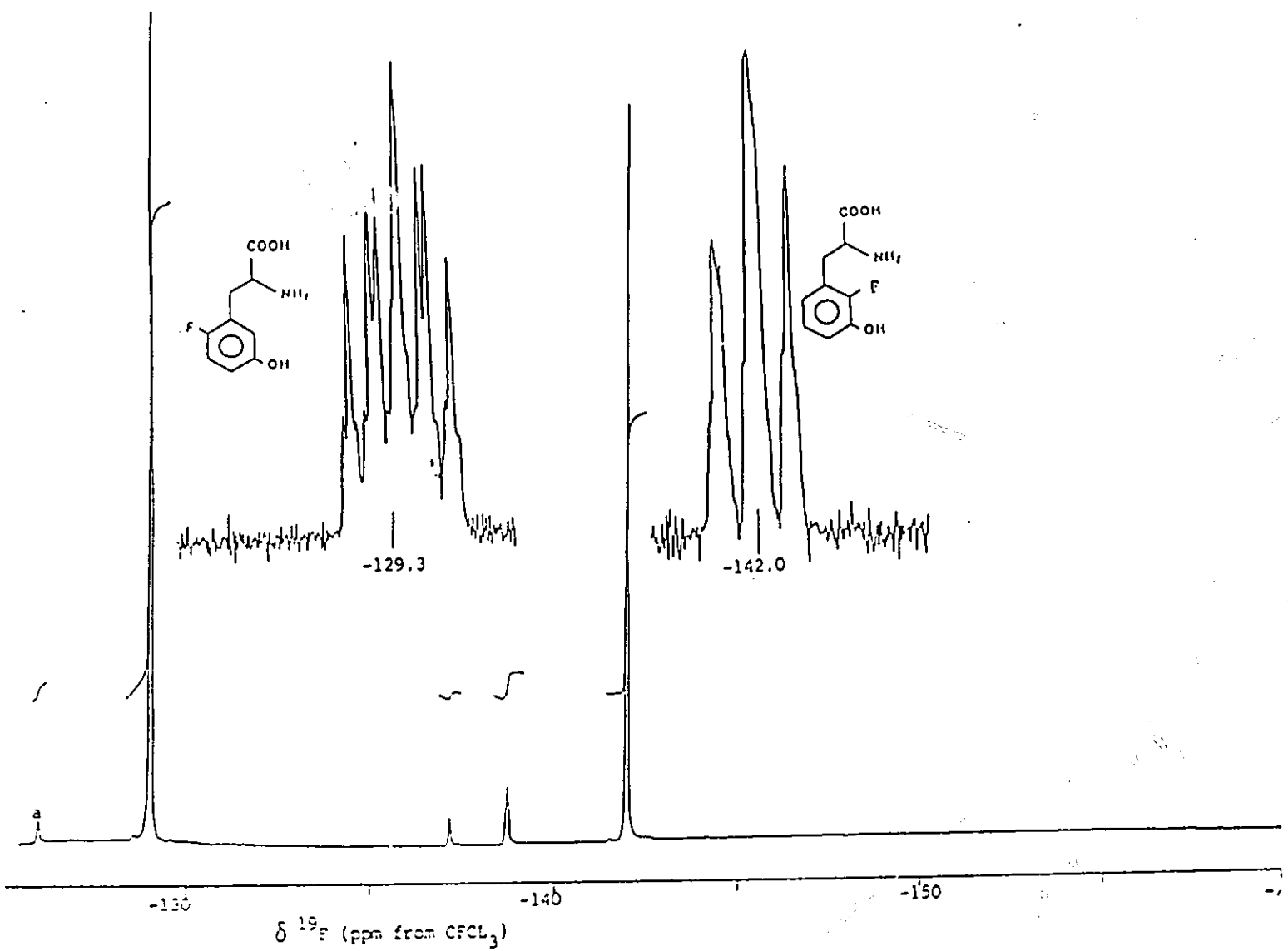
COOH
NH2
F
OH
-129.3
COOH
NH2
F
OH
-142.0
a
-130
-140
-150
δ 19F (ppm from CFCl3)

Table 6.3. ^{13}C Chemical Shifts (ppm) (a) and ^{13}C-^{19}F Coupling Constants (Hz) (b) of 2- and 6-Fluoro-DL-m-Tyrosine

(a) Chemical Shifts

	6-Fluoro-m-Tyrosine	2-Fluoro-m-Tyrosine
-COOH	172.2	172.2
-C	55.1	55.1
-C	35.9	35.9
C_1	122.8 (122.6)[a]	122.8 (122.6)[a]
C_2	117.5 (117.1)	151.4 (151.4)
C_3	152.9 (152.7)	144.7 (144.9)
C_4	118.8 (118.4)	118.9 (118.3)
C_5	117.6 (117.6)	126.4 (127.4)
C_6	155.6 (157.6)	123.6 (123.4)

(b) Coupling Constants

$^2J_{1,F}$	17.8	$^2J_{1,F}$	17.8
$^3J_{2,F}$	--	$^1J_{2,F}$	238.9
$^4J_{3,F}$	--	$^2J_{3,F}$	--
$^3J_{4,F}$	10.2	$^3J_{4,F}$	10.2
$^2J_{5,F}$	20.2	$^4J_{5,F}$	--
$^1J_{6,F}$	236.0	$^3J_{6,F}$	--

[a] Calculated values using fluorine substituent parameters are shown in brackets.

Reaction of $[^{18}F]F_2$ with L-m-tyrosine in HF gave a major radioactive product that had a retention time of 23 min. (two C_{18} μ Bondapak columns, 0.1% acetic acid containing 3% methanol at 2 mL/min). The ^{19}F NMR spectrum of the compound eluted at 23 min was identical to that of the mixture of 2- and 6-fluoro-m-DL-tyrosine, described above.

The enantiomeric purity of the compound was determined by the procedure described by Gil-Av *et al.*[159] The final product was injected onto a reverse phase analytical column (μ BondaPak C-18; 3.9 x 300 mm) and eluted with a chiral mobile phase (L-proline 0.017 M, $Cu(OAc)_2$ 0.5 H_2O 0.008 M at pH 5) at 1.5 mL/min. The radiochromatograms of [^{18}F]fluoro-L-m-tyrosine (Figure 6.5A) and [^{18}F] fluoro-DL-m-tyrosine (Figure 6.5B) contained peaks at 15 and 20 min. ([^{18}F]2- and 6-fluoro-D-m-tyrosine) and 36 and 41 min. ([^{18}F]2- and 6-fluoro-L-m-tyrosine). From the amounts of [^{18}F] present in each peak, the enantiomeric purity of L-fluoro-m-tyrosine was found to be 96 $\pm$ 1%.

3. Identification of Fluoro-m-Tyramine

High-resolution mass spectrometry of the product isolated using HPLC gave a molecular ion peak at m/z = 156 $[M + H]^+$. The ^1H NMR spectrum gave multiplets at 6.64 - 6.91 (3H,

Figure 6.5. Chiral HPLC trace of (A) 2- and 6-fluoro-L-m-tyrosine and (B) 2- and 6-fluoro-DL-m-tyrosine.

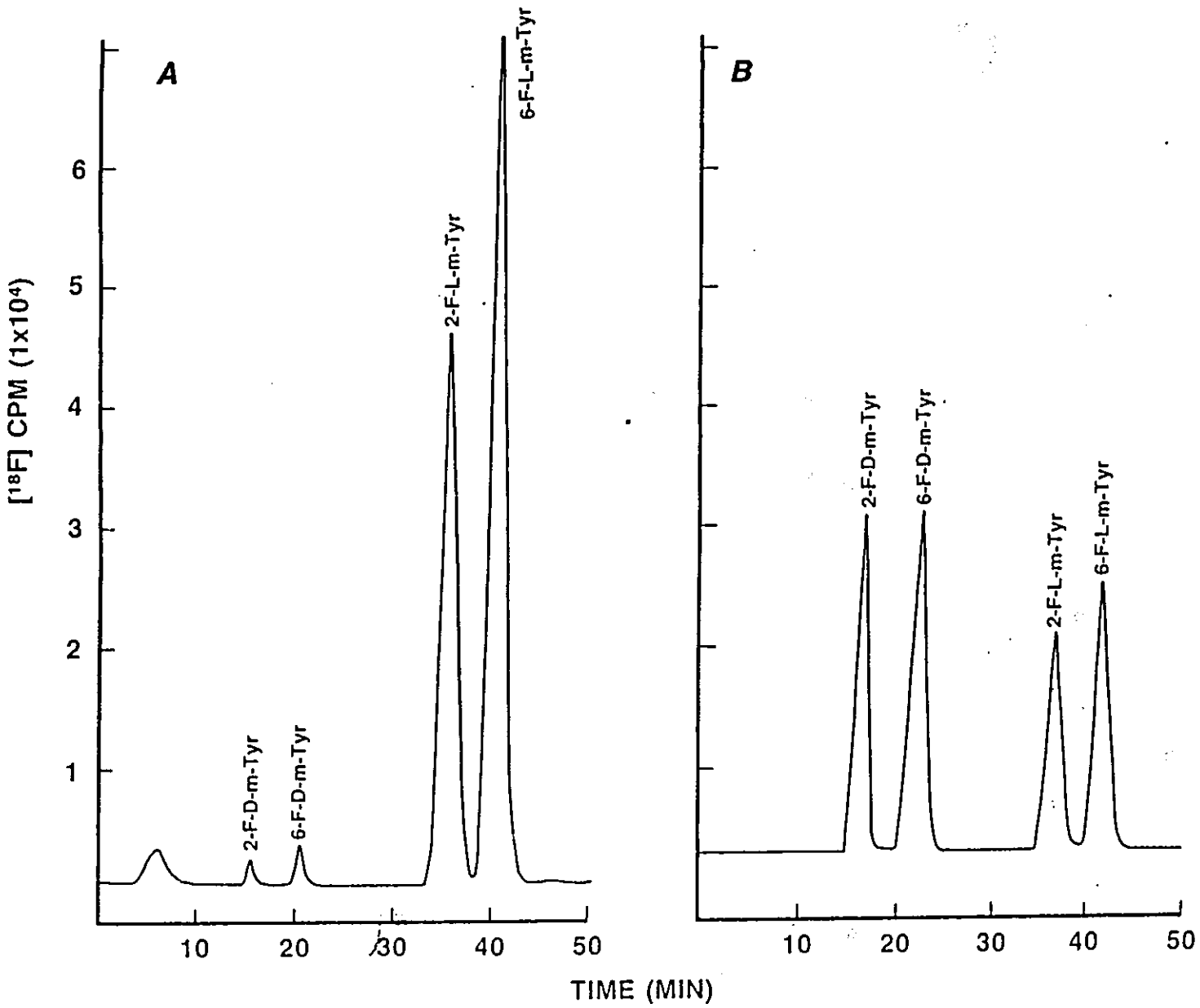
A
B
[18F] CPM (1x10⁴)
1
2
3
4
5
6
2-F-D-m-Tyr
6-F-D-m-Tyr
2-F-L-m-Tyr
6-F-L-m-Tyr
10
20
30
40
50
TIME (MIN)

aromatic) and triplets at 3.11 ppm (2H $\underline{CH_2}NH_2$) and at 2.83 ppm (2H, benzylic protons). The ^{19}F NMR spectrum of the compound gave two seven-line multiplets (ABCX spin system) at -130.4 ppm (62%) and at -140.1 ppm (8%), a doublet at -138.6 ppm (3%) and a doublet of doublets at -143.4 (15%). These were assigned to the respective 6- ,4- ,5- and 2-fluoroisomers. In addition, there were unidentified signals at -127.2, -129.4 and -150.6 ppm having combined intensities of 12%. The ^{13}C spectrum consisted of signals that are in agreement with the calculated values for the 6-fluoroisomer (Table 6.4). Additional signals were observed at 123.1, 122.2, 125.9 ppm which may arise from other isomers in the sample.

4. Identification of Fluoro-3-Hydroxyphenylacetic Acid

The mass spectrum of the compound eluting at 14 min. showed a molecular ion peak at m/z = 171 $[M + H]^+$. The ^{19}F NMR spectrum consisted of a sixteen-line multiplet (arising from an $ABCM_2X$ spin system) at -129.33 ppm (64%), an eight-line multiplet (ABCX spin system) at -139.88 ppm (9%) and a doublet of doublets at -142.12 ppm (27%); these were assigned to the 6-, 4- and 2-fluoro isomers, respectively. The ^{13}C NMR spectrum showed signals corresponding to the calculated chemical shifts in the 6-fluoroisomer (Table 6.4). There were other weak signals at 117.5, 118.2, 119.9, 123.3, 123.7 and

Table 6.4. ^{13}C Chemical Shifts (ppm) (a) and ^{13}C-^{19}F Coupling Constants (Hz) (b) of 6-Fluoro-m-Tyramine and 6-Fluoro-3-Hydroxyphenylacetic Acid

(a) Chemical shitfs

	6-Fluoro-m-Tyramine	6-Fluoro-3-Hydroxy-phenylacetic Acid
-COOH	--	176.9
$-CH_2-\underline{CH_2}NH_2$	41.6	40.9
$-\underline{C}H_2$	33.2	--
C_1	125.4 (126.3)[a]	123.1 (123.6)[a]
C_2	118.4 (118.8)	119.0 (119.3)
C_3	152.8 (152.9)	152.6 (152.6)
C_4	116.7 (117.3)	116.8 (117.2)
C_5	117.5 (118.3)	117.9 (117.9)
C_6	156.5 (157.1)	156.3 (157.6)

(b) Coupling Constants

$^2J_{1,F}$	17.9	$^2J_{1,F}$	18.0
$^3J_{2,F}$	4.5	$^1J_{2,F}$	2.5
$^4J_{3,F}$	--	$^2J_{3,F}$	--
$^3J_{4,F}$	7.9	$^3J_{4,F}$	7.5
$^2J_{5,F}$	--	$^4J_{5,F}$	20.1
$^1J_{6,F}$	235.0	$^3J_{6,F}$	236.1

[a] Calculated values using fluorine substituent parameters are shown in brackets.

125.7 presumably arising from other fluoro-isomers in the sample.

C. DISCUSSION

1. NMR Spectroscopy

Birchall *et al.*[143] have reported that m-cresol, when dissolved in fluorosulphuric acid, is protonated at the ring carbon *para* to the OH group. The protonation at this ring carbon allows delocalization of the positive charge and as a result protonation at the ring carbon is preferred to protonation at the oxygen. Subsequently it has been shown that the site of protonation (oxygen versus carbon) depends on the acidity of the solvent.[144] Brouwer *et al.*[160], using HF/BF_3 as the solvent, showed that the site of protonation was dependent upon the basicity of the ring carbon and the temperature.

It has been established that tyrosine, when dissolved in HF/BF_3, is protonated at the oxygen and not at the ring carbon. But, unlike tyrosine, the carbon atom *para* to the OH group in m-tyrosine would be activated for protonation because of the absence of an alkyl substituent. However, the low-temperature ^1H and ^{13}C NMR spectra of m-tyrosine in HF/BF_3 showed no evidence for the ring protonation. The additional low-field signals in the proton spectrum and the high

frequency-shifts of ^{1}H and ^{13}C signals in the m-tyrosine/HF/BF_3 spectrum, compared to the chemical shifts of m-tyrosine in HF, indicate the presence of O-protonated species. When the spectrum of m-tyrosine/HF/BF_3 in a sealed 5 mm tube was recorded, new signals were observed at 11.89, 12.04 and 12.89 ppm. (Figure 6.6). These have been assigned to the two conformations for the protonated carboxyl groups structure IV (11.89 and 12.04 ppm) and structure V (12.89 ppm). Similar results have been reported for the formic acid/HF/BF_3 system.[161]

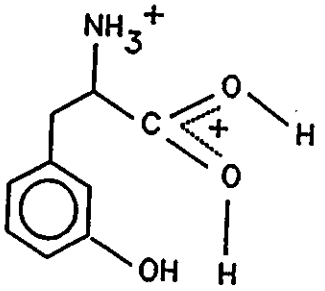

IV

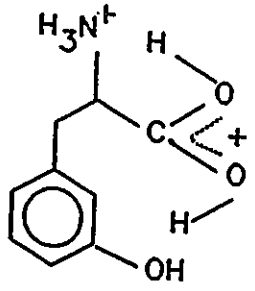

V

2. <u>^{18}F Radiotracer Study.</u>

Direct fluorination of m-tyrosine, m-tyramine and 3-hydroxyphenylacetic acid with $[^{18}F]F_2$ in anhydrous hydrogen fluoride mainly produced mixtures of 2- and 6-fluoro derivatives as the major products (Scheme 6.1)

Figure 6.6 ^{1}H NMR spectrum (500.135 MHz) of m-tyrosine in HF/BF_3 at -81 °C.

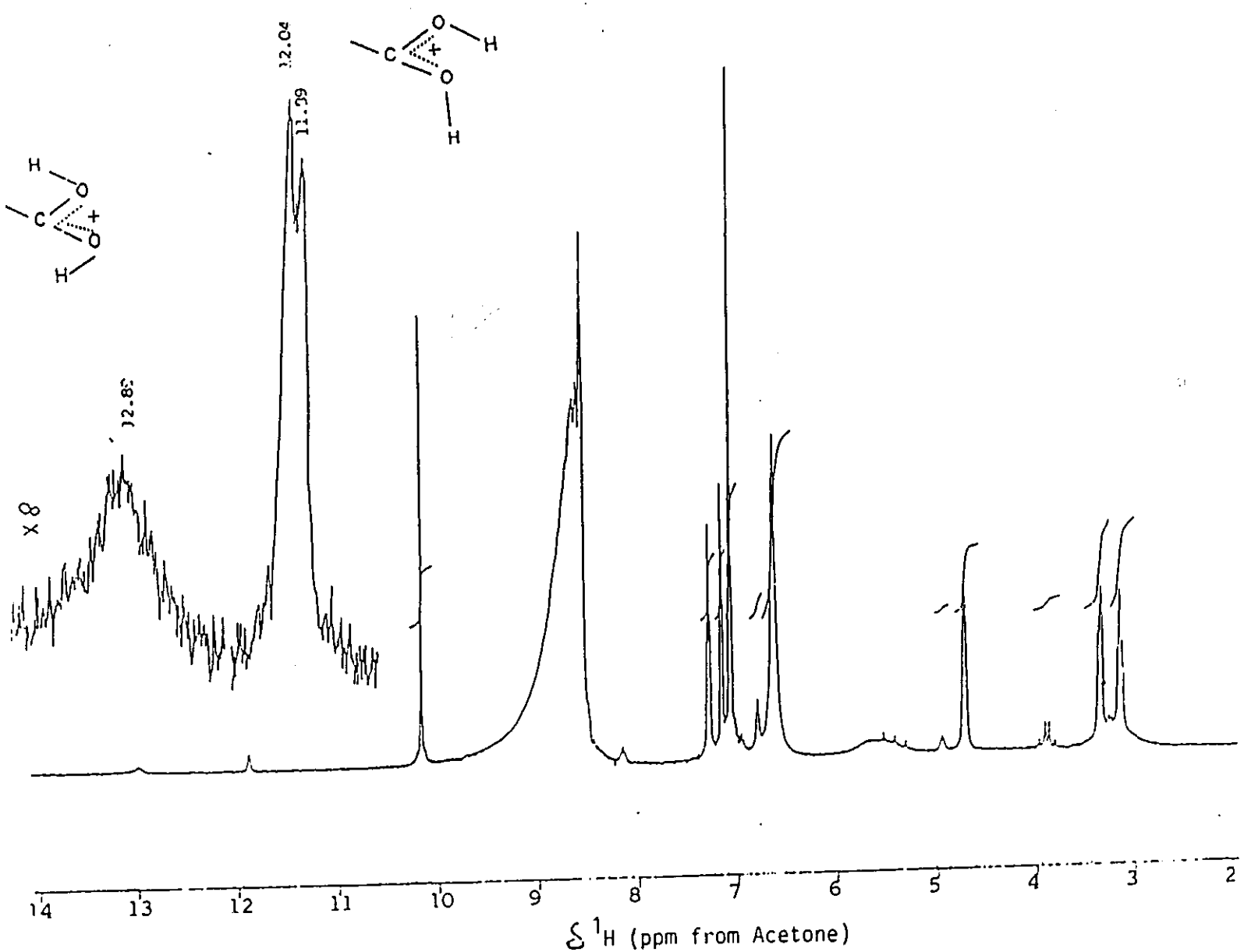
12.04
11.39
12.85
x8
14
13
12
11
10
9
8
7
6
5
4
3
2
δ ¹H (ppm from Acetone)

The radiochemical yield with respect to $[^{18}F]F_2$ of each reaction was 43%, 30% and 37% respectively (Table 6.5).

Scheme 6.1

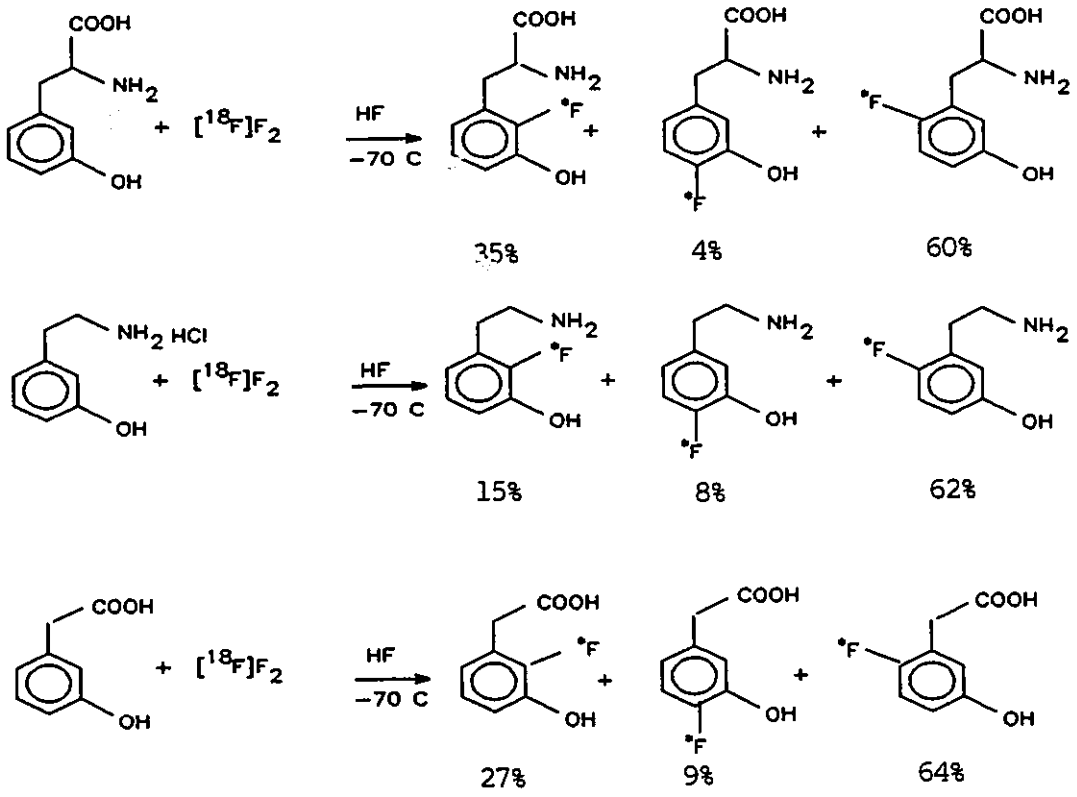

Table 6.5 Results from the Radiofluorination of m-Tyrosine, m-Tyramine and 3-Hydroxyphenylacetic Acid in HF at -70 °C

	Fluoro-m-tyrosine			Fluoro-m-tyramine				Fluoro-3-hydroxyphenylacetic Acid		
Radiochemical yield (%)	43			31				37		
$\delta^{19}F$ (ppm)	-142.0	-138.7	-129.3	-143.4	-140.1	-138.6	-130.4	-142.1	-139.9	-129.3
Relative intensity (%)	35	4	60	15	8	3	62	27	9	64
Position of fluorine on the aromatic ring	2	4	6	2	4	5	6	2	4	6
Coupling Constants (Hz)	4.6	-	5.8	7.1	8.1	-	5.6	7.0	7.8	5.5
$^4J_{HF}$			4.4		4.3		4.5		4.3	4.7
			1.3*							1.5*
$^3J_{HF}$			9.9		11.7	8.6	6.9	6.9	11.6	9.6

* Coupling to the side chain proton

From the results of radiofluorination of m-tyrosine and its metabolites (Table 6.5) it is clear that, except for the reaction of m-tyramine hydrochloride, the major radioactive product isolated after direct fluorination was a monofluorinated derivative. The somewhat lower radiochemical yield of fluoro-m-tyramine in comparison to m-tyrosine and 3-hydroxyphenylacetic acid may be due to the susceptibility of m-tyramine to oxidation. The effect of higher F_2 : substrate ratio (1 : 1.7) in this reaction, compared to 1 : 2.26 for m-tyrosine and 3-hydroxyphenylacetic acid, would be to increase the polymerization and addition reactions. Such competitive reactions have been shown to be characteristic of fluorinations involving high F_2 : substrate ratios.[66] Finally, the low radiochemical yield of fluoro-m-tyramine could also be due to the presence of HCl in m-tyramine hydrochloride which would reduce the acidity of the reaction medium and this, in turn, would reduce the radiochemical yield of fluorination.

3. Radiofluorination of m-Tyrosine

Results from the radiofluorination of m-tyrosine in different solvents are summarized in Table 6.6. This table highlights the observation that the fraction of $[^{18}F]F_2$ consumed during the reaction, the radiochemical yield and the regioselectivity of fluorination all depend upon the solvent used.

Table 6.6. Effect of Solvents on the Radiochemical yield and Isomer Distribution of Fluoro-m-tyrosine

Solvent	Temp. (°C)	% ^{18}F Recovered[a,b] From the Target	Radiochemical Yield	Isomers 2	4	5	6
CH_3CN/BF_3	-35	53	20	23	28	2	35
CF_3COOH	+ 4	55	15	35	9	5	49
HF/CsF	-70	55	44	36	8	3	50
HF	-70	60	43	35	4	-	60
HF/BF_3	-70	14	5	14	-	-	86

[a] % ^{18}F Recovered from the target = $\frac{[^{18}F]mCi \text{ Measured in the Reaction Vessel} \times 100}{91.5 \text{ mCi (saturation yield)} \times (1-e^{-t})}$.

[b] Maximum ^{18}F that can be recovered from the target = 65 ± 8% (See ref. 47 for details).

i. Recovery of $[^{18}F]F_2$

The fraction of $[^{18}F]F_2$ retained in the reaction vessel is similar in all solvents except in HF/BF_3. The high recovery of $[^{18}F]F_2$ in CH_3CN/BF_3 and CF_3COOH could arise from the reaction of $[^{18}F]F_2$ with trace amounts of water present in the solvent to produce $[^{18}F]HF$. It is also possible that the relatively high temperatures (-35 and +4 °C) used in these reactions may promote competitive reactions either by the oxidation of hetero atoms (O and N) in the aromatic amino acid or by free radical initiated reactions. Both processes would increase $[^{18}F]F_2$ in the reaction vessel, and both would reduce the radiochemical yield (see next section).

The drastic reduction in the recovery of $[^{18}F]F_2$ in HF/BF_3 strongly suggests that m-tyrosine in HF/BF_3 is not activated for electrophilic fluorination. This is in agreement with the low-temperature ^1H and ^{13}C NMR results which showed that m-tyrosine in HF/BF_3 is protonated at the oxygen and, as a result, the aromatic ring is expected to be less suceptible to electrophilic substitution.

ii. Radiochemical Yield

The radiochemical yield of $[^{18}F]$fluoro-m-tyrosine ranged from moderate (15%) in CF_3COOH to excellent (43%) in HF. The increase in radiochemical yield with increasing acidity of the

reaction medium follows the general trend for radiochemical yields of fluorotyrosine and fluorodopa. The higher radiochemical yield and higher recovery of $[^{18}F]F_2$ in HF indicate that fluorine substitution is most efficient when HF is the solvent. The efficiency of direct fluorination can be explained on the basis of the following: (a) low reaction temperatures and polar solvents enhance the electrophilic substitution, (b) HF, being a fluoride acceptor, would be expected to facilitate electrophilic fluorinations by removing the developing fluoride ion when the carbon-fluorine bond formation taken place on the aromatic ring; (Both of these conditions have been postulated by Rozen[162] to describe the different characteristics of a variety of electrophilic fluorinations using fluorine and acetylhypofluorite) and (c) in strong acids the amino group in m-tyrosine is strongly protonated and therefore it is less susceptible to oxidation by the powerful oxidising agent F_2. Similar arguments have been used to explain the high and low radiochemical yields when L-methyl-N-acetyl-[ß-(3-methoxy-4-acetoxyphenyl)] alaninate and 3,4-dihydroxyphenylalanine were fluorinated with acetyl hypofluorite.[163]

The drastic reduction in radiochemical yield in HF/BF_3 can only be explained by the reduced reactivity of $[^{18}F]F_2$ towards the O-protonated m-tyrosine present in the solution

(see NMR results). However, this is in contrast to the previously observed results for tyrosine in HF/BF_3 where only a moderate reduction in the yield of fluorotyrosine was observed. In both compounds, the aromatic ring is activated by the OH group therefore protonation of this group is expected to have a similar effect on ring fluorination. Assuming the mechanism of fluorination is the same in both cases, it is not clear why the radiochemical yield of fluoro-m-tyrosine is drastically different in HF (43%) and HF/BF_3 (5%) from the radiochemical yield of fluorotyrosine in HF (27%) and HF/BF_3 (17%).

The fluorination of m-tyrosine in CH_3CN/BF_3 and CF_3COOH at relatively higher temperatures may promote competitive reactions either by oxidation of hetero atoms (O and N) or by the free radical initiated reactions. Both processes could account for the reduced radiochemical yields in these solvents. It should be pointed out that the present results are consistent with results obtained for tyrosine (Chapter 5) and dopa.[68]

It has been shown that [^{18}F]labelled acetyl hypofluorite ([^{18}F]CH_3COOF) can be used for the direct fluorination of m-tyrosine in 10% CF_3COOH in glacial acetic acid.[164] The 71% radiochemical yield obtained from this reaction is much higher

than that obtained in the present work with $[^{18}F]F_2$ and m-tyrosine in CF_3COOH (for comparison with $[^{18}F]F_2$ the radiochemical yield obtained from the $[^{18}F]CH_3COOF$ reaction needs to be divided by 2). This is surprising because, a comparison of direct electrophilic fluorination of phenyl alanine, tyrosine, O-acetyl tyrosine and dopa in CF_3COOH produced in each case a lower radiochemical yield with $[^{18}F]CH_3COOF$ than with $[^{18}F]F_2$.[146] The higher radiochemical yield of [^{18}F]fluoro-m-tyrosine from the $[^{18}F]CH_3COOF$ reaction may be explained by the fact that acetyl hypofluorite is known to be a mild fluorinating agent compared to F_2 and therefore, it is expected to produce less side products. Since the radiochemical yields are a measure of the efficiency of fluorine substitution, it can be argued that acetyl hypofluorite is more selective towards m-tyrosine than towards other aromatic amino acids such as phenyl alanine, tyrosine and dopa.

iii. Regioselectivity of Fluorination

Table 6.6 also shows that the regioselectivity of fluorination depends on the reaction conditions. In m-tyrosine, the hydroxyl group, being the most activating substituent, is expected to direct the incoming electrophile to *ortho* and *para* positions. In the present study this general trend in orientation is observed only when the

fluorination is carried out in CH_3CN/BF_3 when the ortho (2- + 4-fluoro) to para (6-fluoro) ratio is 1.5 to 1. In all other solvents used in this study, the major product is 6-fluoro-m-tyrosine. This is in contrast to the results reported for electrophilic fluorinations, using F_2, for phenylalanine,[146] phenol and m-cresol.[147] In each of these cases fluorine substituted preferentially at the position ortho to the activating substituent and ortho : para ratios of 6.4 : 1, 3.3 : 1 and 2.5 : 1, respectively, were observed.

It should be pointed out that 4-fluoro-m-tyrosine is the minor product in all direct fluorination of m-tyrosine except in CH_3CN/BF_3. A similar substitution pattern has been observed during the electrophilic fluorination of m-tyrosine[164] and ß-fluoro-methylene-m-tyrosine[165] using $[^{18}F]CH_3COOF$ and during the electrophilic bromination of m-tyrosine using Br_2.[166] These results are all surprising because, from the steric considerations, substitution of fluorine at C-4 would be more favoured than at C-2.

As the acidity of the reaction medium is increased, the *ortho* : *para* ratio was decreased (Table 6.6). For example, the direct fluorination of m-tyrosine in HF shows that the ortho (2-fluoro + 4-fluoro) to para (6-fluoro) ratio is 1 : 1.5. When the reaction is carried out in HF/BF_3, the ortho to

para ratio increases to 1 : 6. A similar effect has been observed for the fluorination of phenol where the ratio of ortho : para fluorophenols were reduced from 1.03 in 65% HF to 0.97 in anhydrous HF.[145]

iv. Acidity of HF vs Reactivity and Orientation of Fluorination

The acidity of HF can be increased or decreased by addiing acid (BF_3) or a base (F^-) to HF. Proton transfer reactions of weak bases and their conjugate acids in HF have been studied.[167] It has been shown that the concentration of weak bases and their conjugate acids in HF can be adjusted by adding NaF or BF_3 to the solution. Since the reactivity and orientation of fluorination differs in solvents of different acidities, it is of interest to study the effect of F^- and BF_3 on the radiofluorination of m-tyrosine in HF. Results from this study are summarized in Table 6.7.

The reactivity of $[^{18}F]F_2$ towards m-tyrosine was determined by measuring the $[^{18}F]$activity recovered from the target after the reaction. The orientation of the products was determined from the ratio of the $[^{18}F]$ content in the peaks eluting at 26 and 29 min.(Figure 6.7) and they were corroborated with the results from ^{19}F NMR.

Table 6.7. Reactivity and Selectivity of $[^{18}F]F_2$ Towards m-Tyrosine in HF with Varying Acidities.

Conc. F^- or BF_3 in HF	Solvent	$[^{18}F]F_2$ Recovered	Radiochemical Yield (%)	Distribution of Isomers 2-F	4-F	5-F	6-F
0.90	HF/CsF	55	44	36	8	3	50
0	HF	60	43	35	4	-	60
0.16	HF/BF_3	47	35	36	-	-	64
0.31	HF/BF_3	35	20	31	-	-	69
0.67	HF/BF_3	18	5	14	-	-	86
0.96	HF/BF_3	20	5	14	-	-	86

It is clear that the presence of CsF in HF has no noticeable effect on the reactivity of F_2 ($[^{18}F]F_2$ recovered) and the radiochemical yield. The 5% difference in the recovery of $[^{18}F]F_2$ in HF and HF/CsF can be considered marginal because the recovery can vary ±8% depending upon the irradiation conditions. However, both $[^{18}F]F_2$ recovery and radiochemical yield are reduced considerably when 0.6 - 0.9 M BF_3 is present in HF. As the concentration of BF_3 is increased, and hence the acidity of the reaction medium, the concentration of protonated tyrosine will also be increased (see NMR Resuts). As a consequence, the reactivity of m-tyrosine in HF/BF_3 towards electrophilic fluorination would be expected to be reduced, thereby causing a reduction in the radiochemical yield (Table 6.7). This is in agreement with a previous study on phenol[145] where a substantial reduction in the yield of fluorophenols was reported when anhydrous HF (35% yield) was used instead of 65% HF as the solvent during fluorination.

The change in acidity in going from HF to HF/BF_3 has no effect on the orientation of fluorination. This is in contrast to the results from the fluorination of tyrosine in which the substitution of fluorine changed from the carbon *ortho* to the hydroxyl group to the *meta* position when BF_3 was added to the reaction mixture. ^1H and ^{13}C NMR data of both

Figure 6.7. Radiochromatograms of the products obtained after the fluorination of m-tyrosine in HF containing different concentrations of BF_3. (A) 0 M, (B), 0.31 M, (C) 0.96 M

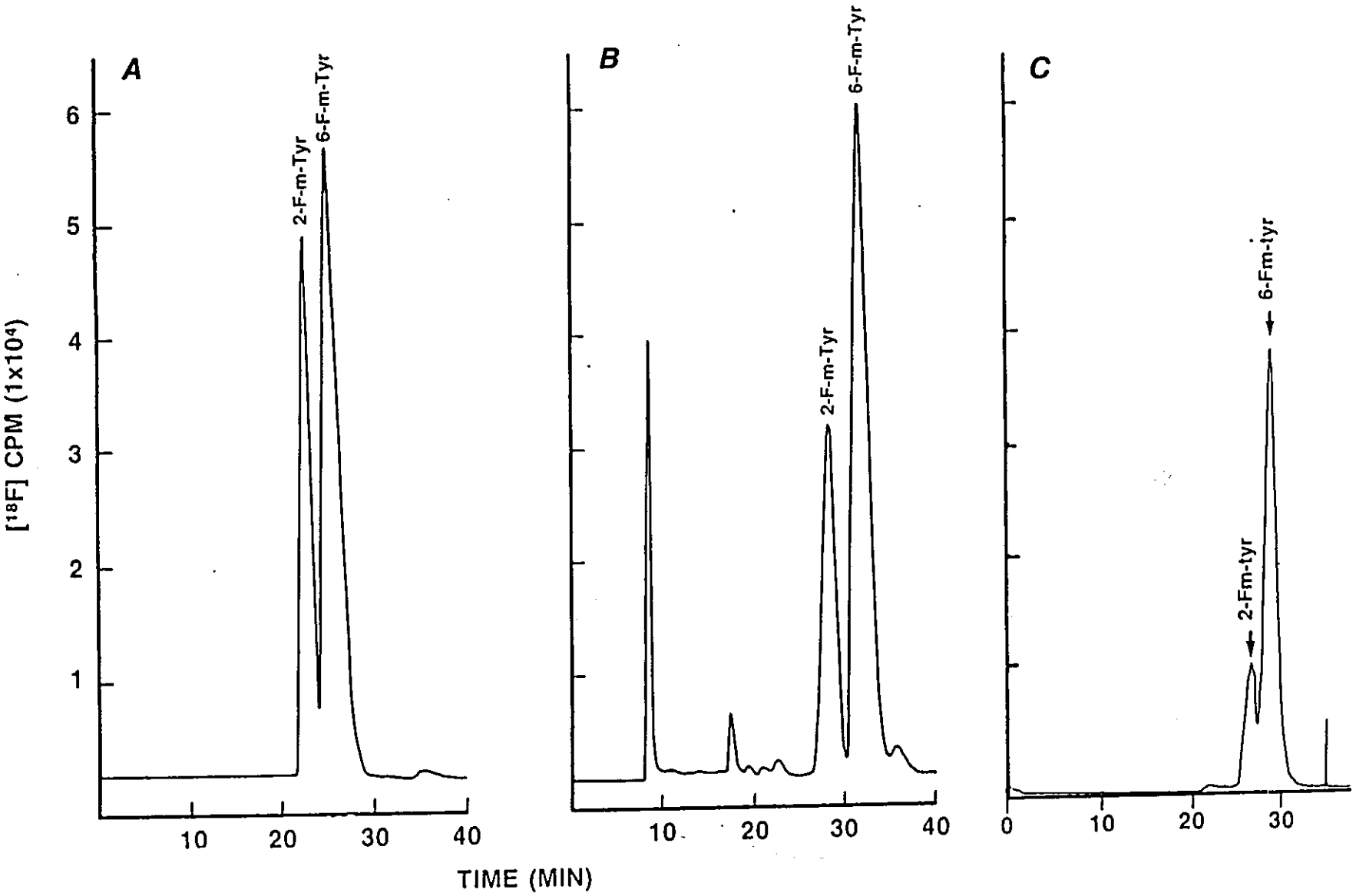
A
B
C
2-F-m-Tyr
6-F-m-Tyr
2-Fm-tyr
6-Fm-tyr
[18F] CPM (1x10⁴)
TIME (MIN)
1
2
3
4
5
6
0
10
20
30
40

tyrosine and m-tyrosine in HF/BF_3 showed the hydroxyl group is protonated by HF/BF_3. In addition, the $[^{18}F]F_2$ recovered from the target during the fluorination was reduced,in both cases, largely due to deactivation of the aromatic ring. By analogy with the reaction of F_2 with tyrosine in HF/BF_3 (see equation 5.3), ring fluorination of m-tyrosine is therefore expected to produce 5-fluoro-m-tyrosine as the major product. It should also be pointed out that in the ^{13}C spectrum of m-tyrosine in HF/BF_3 the maximum high frequency shift ($_{\Delta}\delta$) was observed for C-6 (10.7 ppm) compared to C-2 (6.7 ppm), C-4 (6.7 ppm) and C-5 (5.3 ppm). It is therefore surprising that 86% of the ring fluorinated product is 6-fluoro-m-tyrosine.

v. Preferential Substitution of Fluorine at Carbons 2- and 6- in m-Tyrosine

The preferential substitution of fluorine at 2- and 6-position of m-tyrosine can only be explained if we assume some involvement of the side chain. It is possible that in strong acids protonation of the hydroxyl group causes its *ortho-para* directing properties to be less effective and therefore the side chain becomes the most effective ring activating substituent. However, this does not explain the lack of substitution at carbon-4. An alternative explanation may be a neighbouring group effect from the carboxyl group on the side chain. Taylor *et al.*[168] first demonstrated the effect of

the neighbouring carboxylic group in electrophilic thallation and subsequently have explained the results of direct fluorination of phenyl alanine by a similar neighbouring group effect from the side chain. An intermediate involving the carboxylic group on the side chain (Structure VI) similar to that observed for electrophilic thallation (Structure VII) can be proposed to explain the observed orientation of fluorination of m-tyrosine in strong acids.

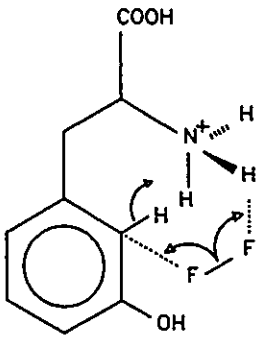

VI

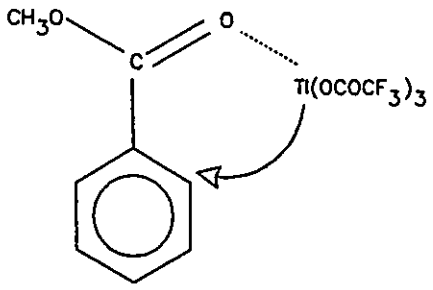

VII

The formation of higher percentages of 4- and 5- fluoro-m-tyrosine, when the acidity of the reaction medium is progressively decreased in going from HF/BF_3 to CF_3COOH(see Table 14), would support this proposed mechanism. Further support for this mechanism is obtained from the fluorination of m-tyrosine in CH_3CN/BF_3, which resulted in almost equal proportion of 2-, 4- and 6-fluorotyrosine. In this case the amine is not protonated.

D. Conclusions

The aim of this work has been to develop a relatively fast and efficient method for the radiofluorination of m-tyrosine. To that end the present work has shown that anhydrous hydrogen fluoride is an ideal solvent for this purpose. Since the general fluorination method does not require protection of the functional groups, no elaborate synthesis of precursors is necessary and no time is lost in removing the protecting groups after the initial fluorination reaction. Automated systems for the separation of 2- and 6-fluorodopas have been established[169] and a similar system could be developed for the production and routine use of [^{18}F]6-fluoro-m-tyrosine.

CHAPTER 7

AROMATIC SUBSTITUTION BY MOLECULAR FLUORINE: REACTIVITY AND SELECTIVITY

A. Introduction

Despite the recent renewed interest in the direct fluorination of biologically active aromatic compounds, there have been no studies reported relating to the mechanisms and kinetics of the reactions of fluorine with these compounds. There have been reports that the reactions of fluorine with organic compounds are violent and uncontrollable, frequently leading to explosions and almost invariably to the destruction of the organic substrates when they are not adequately moderated by dilution and temperature. It has been shown in the previous two chapters that direct fluorination of tyrosine and m-tyrosine in anhydrous HF is an efficient method for the introduction of [^{18}F] into the aromatic ring. In a previous study it has been reported that the direct fluorination of DOPA and 3-O-methyl-DOPA in HF/BF_3, rather than HF, is the most efficient method for the introduction of [^{18}F] into the aromatic ring.[68] The efficiency of ring fluorination was evident from the radiochemical yield of each reaction in HF, HF/BF_3 and CF_3COOH (Table 7.1).

A trend in radiochemical yields, similar to that observed for the direct fluorination of aromatic amino acids in CF_3COOH (Table 8.1), was also observed for [^{18}F]fluoro-m-tyrosine

Table 7.1. Radiochemical Yields of Direct Fluorination of Aromatic Amino Acids.

Substrate	Product	Radiochemical Yield (%) HF	HF/BF_3	TFA
m-Tyrosine	F-m-Tyrosine	43	5	15
Tyrosine	F-Tyrosine	27	19	12
DOPA	F-DOPA	18	43	8
3-O-methyl-DOPA	F-DOPA[a]	22	38	12[b]

[a] Obtained after the hydrolysis of O-methyl compounds (Ref. 68)

[b] Unpublished result, this laboratory.

(71%), [^{18}F]fluorotyrosine (15%) and [^{18}F]fluorodopa after direct fluorination of m-tyrosine,[164] tyrosine[146] and DOPA[146], respectively, using acetylhypofluorite as the fluorinating agent. It is interesting to note that the reaction of fluorine or acetylhypofluorite with m-tyrosine produced fluoro-m-tyrosine in excellent yield compared to similar reactions with other aromatic amino acids. Such selectivity for ring substitution in m-tyrosine by fluorine or acetylhypofluorite is unexpected because in all compounds listed in Table 7.1 the aromatic ring is activated mainly by the hydroxyl or methoxy group for electrophilic substitution. The aromatic ring in DOPA and 3-O-methyl-DOPA will be activated more than either of the tyrosines and consequently they are expected to be more susceptible to electrophilic attack. Cacace and Wolf[67] have reported that the relative reactivity of aromatic substrates with F_2 increased with increasing activation of the aromatic ring i.e., in the order nitrobenzene << benzene < toluene << anisole. Since the radiochemical yields of fluoro aromatics are indicative of the efficiency of substitution by fluorine on the aromatic ring, the results in Table 7.1 show that reaction of F_2 with simple aromatic molecules does not serve as model for the reactivity of F_2 with biologically active aromatic amino acids. Therefore a series of competition experiments involving [^{18}F]F_2 and pairs of different aromatic amino acids were carried out

to determine the relative reactivity of $[^{18}F]F_2$ towards tyrosine, m-tyrosine and DOPA in HF at -70 °C.

B. Results

1. Reaction of $[^{18}F]F_2$ with Tyrosine/DOPA

HPLC analysis (two waters μbonda Pak C^{18} 0.7 x 30 cm. with 0.1% acetic acid in water as mobile phase and a flow rate of 2 mL/min.) of the reaction mixture, obtained after the competitive fluorination of tyrosine and DOPA in HF, showed major radioactive peaks at 25 and 33 min (Figure 7.1a). The two peaks were identified as fluorodopa and fluorotyrosine, respectively, by comparing their retention times with that of authentic samples. The ratio of $[^{18}F]$ contents in the two peaks was 1.2 : 1. The identities of both compounds were verified by the ^{19}F NMR of both samples combined. The relative intensities of the ^{19}F NMR signals due to fluorodopa and to fluorotyrosine (1.3 : 1) agreed with the value obtained from the $[^{18}F]$ assay.

When the same reaction was carried out in HF/BF_3, HPLC analysis showed one major radioactive peak ($[^{18}F]$fluorodopa) at 20 min. No $[^{18}F]$ peak that could be assigned to $[^{18}F]$fluorotyrosine was observed in the radiochromatogram (Figure 7.1b).

2. Reaction of $[^{18}F]F_2$ with Tyrosine/m-Tyrosine

HPLC analysis (two Waters μ-bonda Pak C_{18} 0.7 x 30 cm. with 0.1% acetic acid in water containing 3% methanol as mobile phase and a flow rate of 2 mL/min.) of the products after the reaction of $[^{18}F]F_2$ with a mixture of tyrosine and m-tyrosine in HF produced two major radioactive peaks at 21 min. and 25 min (Figure 7.2). The two peaks were identified as $[^{18}F]$fluorotyrosine and $[^{18}F]$fluoro-m-tyrosine after comparing the retention times of authentic fluorotyrosine and fluoro-m-tyrosine under the same HPLC conditions. The relative amount of $[^{18}F]$ in the two peaks at 21 and 25 min. was 1: 6. The combined radiochemical yield of $[^{18}F]$fluorotyrosine and $[^{18}F]$fluoro-m-tyrosine was 33%.

3. Reaction of $[^{18}F]F_2$ with m-Tyrosine/DOPA

HPLC analysis of the products (same conditions as above) produced two radioactive peaks at 19 and 25 min. which were assigned to $[^{18}F]$Fluorodopa and $[^{18}F]$fluoro-m-tyrosine, respectively, by comparing their retention times with the authentic samples of fluorodopa and fluoro-m-tyrosine under the same HPLC conditions. The two peaks contained 7.2% and 25.8% of the total radioactivity injected and the relative ratio of $[^{18}F]$ in the two peaks were 1 : 3 (Figure 7.3).

Figure 7.1. [^{18}F]HPLC trace of the reaction mixture obtained after the radiofluorination of tyrosine and DOPA in HF (A) and HF/BF_3 (B).

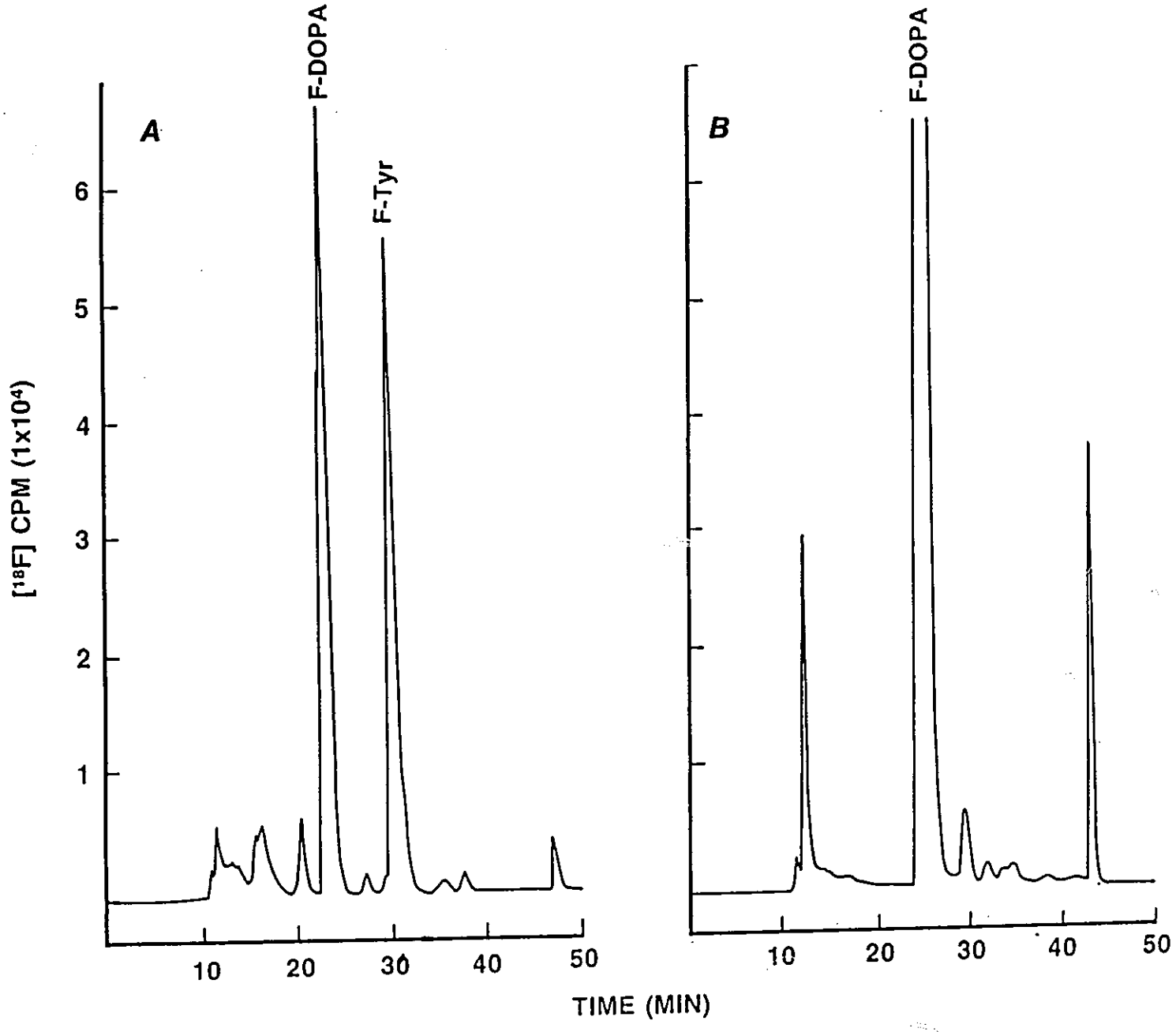
A
B
F-DOPA
F-Tyr
F-DOPA
[18F] CPM (1x10⁴)
1
2
3
4
5
6
10
20
30
40
50
TIME (MIN)

Figure 7.2. Radiochromatogram of the reaction mixture obtained after competitive fluorination of tyrosine and m-tyrosine in HF at -70 °C.

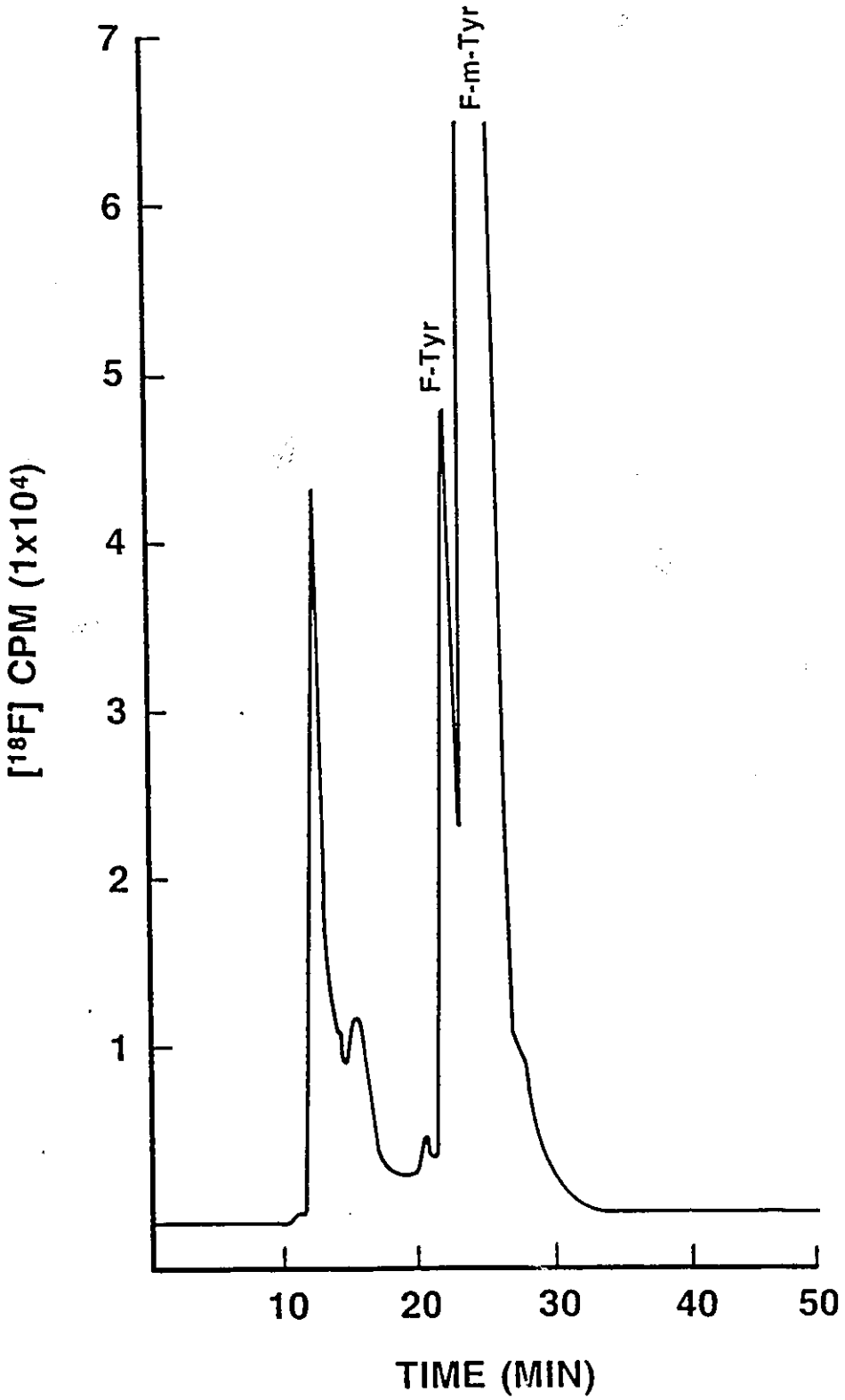
7
6
5
4
3
2
1
[18F] CPM (1x10⁴)
F-Tyr
F-m-Tyr
10
20
30
40
50
TIME (MIN)

Figure 7.3. Radiochromatogram of the products obtained after the direct fluorination of m-tyrosine and DOPA in HF at -70 °C

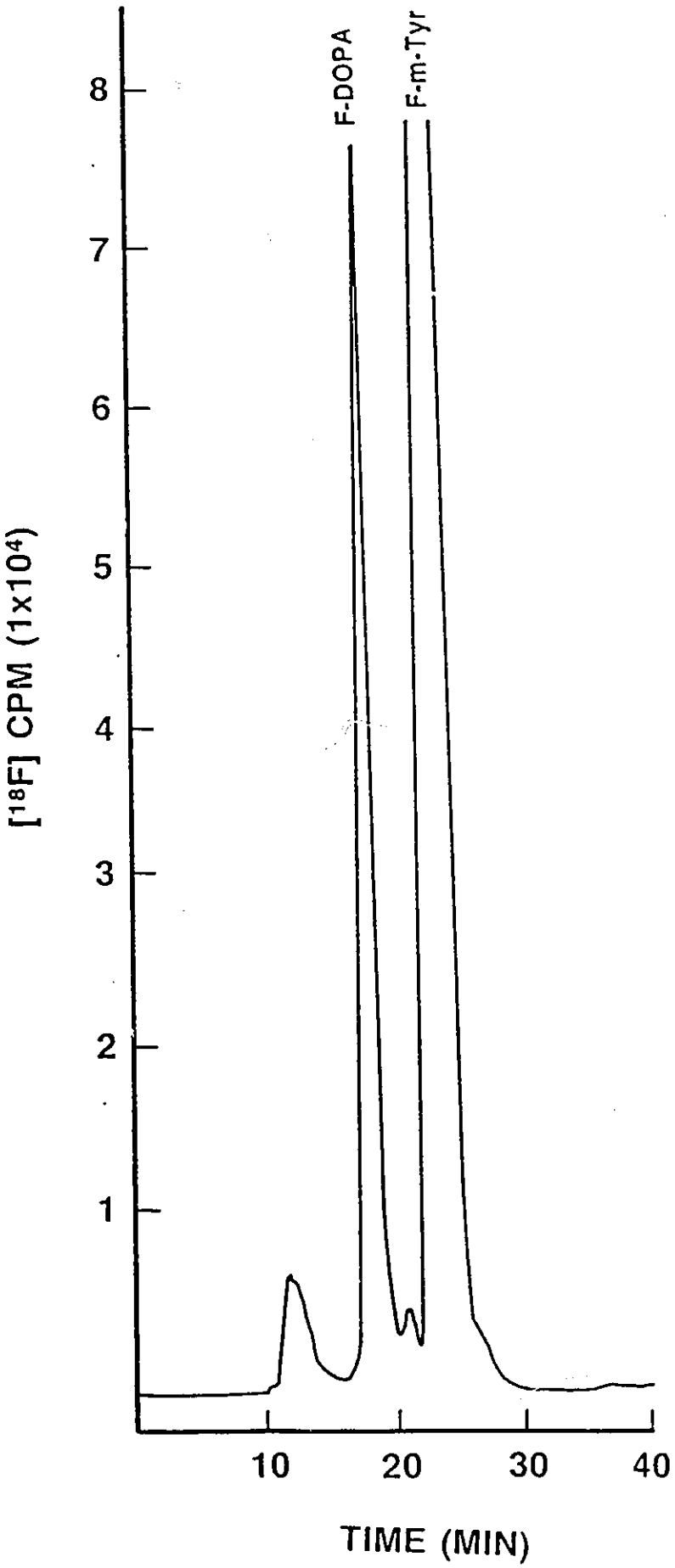
F-DOPA
F-m-Tyr
8
7
6
5
4
3
2
1
[18F] CPM (1x10⁴)
10
20
30
40
TIME (MIN)

C. DISCUSSION

Results from the study of the relative reactivity of $[^{18}F]F_2$ towards tyrosine, m-tyrosine and DOPA indicate that, in HF, m-tyrosine is more susceptible to substitution by fluorine than tyrosine and DOPA (Scheme 7.1).

Scheme 7.1

Selectivity of $[^{18}F]F_2$ towards Tyrosines and DOPA.

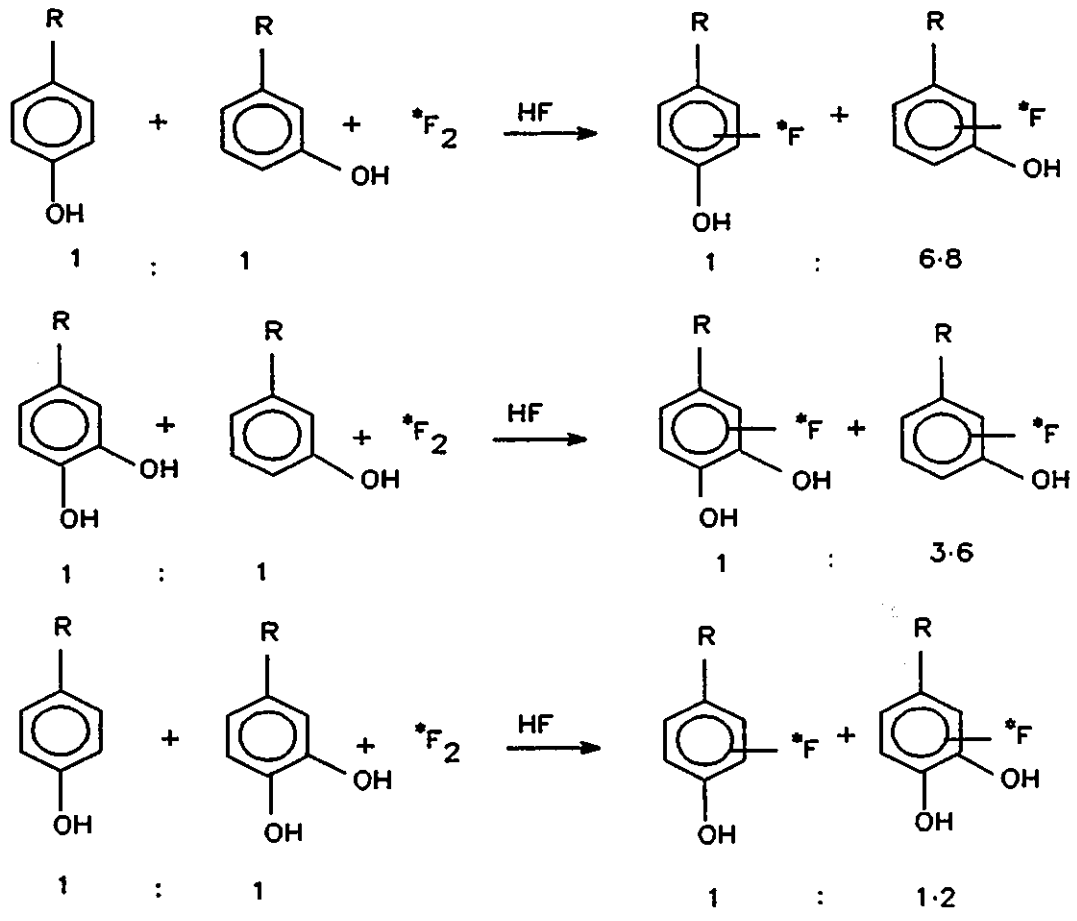

R = $-CH_2-CH(NH_2)COOH$

Competitive fluorination of tyrosine and DOPA in HF/BF_3 show that $[^{18}F]F_2$ is 100% selective to DOPA (Scheme 7.2)

Scheme 7.2

Selectivity of $[^{18}F]F_2$ Towards DOPA and Tyrosine in HF/BF_3

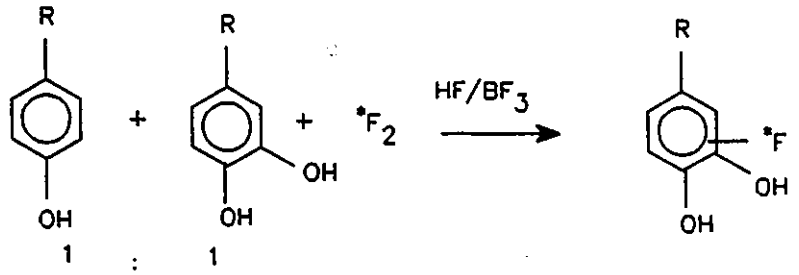

R = $-CH_2-CH(NH_2)COOH$

It should be emphasized that the reaction conditions employed in this study were similar to the preparative conditions that have been used for aromatic radiofluorination, i.e., the ratio of $[F_2]$:[substrate] was 1 : 2.5. An entirely different product pattern may be obtained if the ratio of $[F_2]$: [substrate] was changed. The relative distribution of the products in Scheme 7.1 followed the trend in radiochemical yield for each individual reaction (Table 7.1) except for the reaction of $[^{18}F]F_2$ with tyrosine and DOPA in HF. In the latter reaction, the ratio of fluorotyrosine to fluorodopa

(1 : 1.2) was higher than that would be predicted from the radiochemical yields (1 : 0.64). However, it seems reasonable that fluorine would react more rapidly with the electron-rich aromatic ring in DOPA and that consequently more fluorodopa should be formed.

The relative distribution of fluorotyrosine and fluoro-m-tyrosine (1 : 6.8) was much higher than the relative radiochemical yields of fluorotyrosine and fluoro-m-tyrosine (1 : 1.6). In both compounds the aromatic ring is activated mainly by the OH group and therefore both were expected to show similar reactivity to $[^{18}F]F_2$. However, in tyrosine there is only one favoured site (*ortho* to the OH group) that is available for the electrophilic attack whereas in m-tyrosine there are three favoured sites (*ortho* and *para* to the OH group) for the attack by an incoming electrophile. Even if the number of active sites for electrophilic attack on the aromatic ring of tyrosine (1) compared to that of m-tyrosine (3) is taken into account, the amount of fluoro-m-tyrosine produced was still much more than expected.

The relative distribution of fluorodopa and fluoro-m-tyrosine (1 : 3.2) is even more surprising because the presence of a second hydroxyl group in DOPA is expected to make dopa more susceptible to electrophilic attack. This has

been found to be true in the reaction of F_2 with tyrosine and DOPA. It can be argued that because of the electron-rich aromatic ring in DOPA, it would also be more susceptible to oxidation by F_2 and consequently a higher yield for fluorodopa cannot be expected. However, this explanation alone cannot account for the observed result because the combined radiochemical yield of fluorodopa and fluoro-m-tyrosine (33%) after the competitive fluorination of m-tyrosine and DOPA. In contrast, the reaction of $[^{18}F]F_2$ with DOPA has been shown to produce [^{18}F]FDOPA with a radiochemical yield of 18%. The results from the competitive fluorination of DOPA and m-tyrosine indicate that the ring substitution of m-tyrosine is the preferred reaction pathway to the oxidation of DOPA by fluorine.

The exclusive substitution of fluorine on DOPA during the fluorination of a 1 : 1 mixture of DOPA and tyrosine in HF/BF_3 can be explained by the deactivation of the aromatic ring due to protonation of the OH group by HF/BF_3. The result is also predictable from the radiochemical yield for fluorinated amino acid in HF/BF_3 (Table 7.1). Since the efficiency of fluorination of m-tyrosine in HF/BF_3 is significantly lower than the fluorination of DOPA in HF/BF_3 it can be predicted that exclusive substitution of fluorine on DOPA would occur during the competitive fluorination of m-tyrosine and DOPA.

It appears that the presence of an additional OH substituent on DOPA, compared to tyrosines, would make it sufficiently active, even in HF/BF_3, for substitution by fluorine.

It should be stressed that these reactions were done at a higher $[F_2]$: [substrate] ratios and only the radiochemical yields of ring substituted products have been measured. Consequently, the reactivity of F_2 towards the substrate may not be accurately represented owing to the formation of fluorine-containing side-products. Since the ring substituted products are of great interest, the present results represent a true, though qualitative, trend in reactivity and selectivity of F_2 for ring substitution of the aromatic amino acids. At present it is uncertain as to what factors are influencing the much higher selectivity of F_2 towards m-tyrosine. It is possible the selectivity is kinetically controlled and the reaction of fluorine with m-tyrosine is more rapid compared to the reactions of F_2 with tyrosine and DOPA.

D. Conclusions

The present study has shown that fluorine, despite its reputation as a poor reagent (due to its high reactivity) for high-yield and selective fluorination of organics, has significant selectivity towards aromatic substrates.

Moreover, the reactivity and selectivity of fluorine can be controlled by the judicious selection of the solvent.

CHAPTER 8

USE OF TRIFLUOROMETHANESULPHONIC ACID IN THE RADIOFLUORINATION OF AROMATIC COMPOUNDS

A. Introduction

It has been shown that the radiochemical yield of ring fluorinated compounds from the direct fluorination of aromatic amino acids increased with increasing acidity of solvent. This was particularly true for the direct fluorination of L-DOPA in which the radiochemical yield of [^{18}F]FDOPA was increased from 8% in CF_3COOH to 43% in HF/BF_3.[1] Furthermore, the orientation of the products was considerably different after the fluorination of L-DOPA in CF_3COOH and HF/BF_3. While the fluorination of L-DOPA in HF/BF_3 produced 6-FDOPA as the major product, the same reaction in CF_3COOH produced no 6-fluorodopa,[170] but it produced 2- and 5-fluorodopa in 75 and 25% yields, respectively. Although the direct fluorination of aromatic amino acids in HF and HF/BF_3 have been successful, it is still desirable to develop a solvent that can be handled safely for the routine production of [^{18}F]labelled compounds in less specialized laboratory environments, i.e., the use of HF or HF/BF_3 requires special equipment such as a metal vacuum line and Kel-F or PTFE vessels which are expensive and difficult to fabricate.

The acidity of trifluoromethane sulphonic acid (CF_3SO_3H, commonly known as triflic cid) is comparable to that of HF.[171] It has been used in a variety of organic reactions and the protonation of many aromatic compounds in CF_3SO_3H has been studied.[172,173] The only limitation is its high boiling point which makes it less suitable as a solvent for the synthesis of labelled compounds with short-lived isotopes. This study was undertaken to explore the use of CF_3SO_3H for the direct fluorination of m-tyrosine and L-DOPA.

B. RESULTS

1. NMR spectra of m-Tyrosine and L-DOPA

^1H and ^{13}C Chemical shifts of m-tyrosine in CF_3COOH and CF_3COOH/CF_3SO_3H are summarized in Table 8.1. Unlike the spectrum of m-tyrosine in CF_3COOH, the ^1H spectrum of m-tyrosine in CF_3COOH/CF_3SO_3H showed well resolved signals for the aromatic protons. In addition, the spin-spin couplings between H-5 and H-6 and H-5 and H-4 were resolved. The coupling between benzylic protons and the CH on the side-chain was not resolved in either spectrum. A comparison of the ^{13}C chemical shifts of m-tyrosine in CF_3COOH/CF_3SO_3H with that of m-tyrosine in CF_3COOH showed that the aromatic carbons, C-2, C-5 and C-6 are further deshielded presumably due to protonation of m-tyrosine by CF_3SO_3H.

Table 8.1. ^{1}H and ^{13}C Chemical Shifts of m-Tyrosine in CF_3COOH and CF_3COOH/CF_3SO_3H at -11 °C

^{13}C Chemical Shifts[a]

	CF_3COOH	CF_3COOH/CF_3SO_3H
C_1	135.5	136.2
C_2	117.8	123.3
C_3	156.1	151.8
C_4	117.6	122.8
C_5	133.0	133.3
C_6	124.5	130.5
CH_2	57.3	57.4
CH	36.7	36.6
-COOH	175.1	175.0

^{1}H Chemical Shifts[b]

	CF_3COOH	CF_3COOH/CF_3SO_3H
H-2	6.71	6.62
H-4	6.71	6.72
H-5	6.71	6.88
H-6	6.71	6.59
NH_{3+}	6.35	6.35
CH_2	2.99 2.71	2.99 2.76
CH	4.04	4.04

[a] Referenced with respect to internal trifluoroacetic acid at 164.2 PPM at 21 °C.

[b] Referenced with respect to neat TMS at 21 °C.

Proton NMR data of L-DOPA in CF_3COOH and CF_3COOH/CF_3SO_3H at -11 °C are summarized in Table 8.2. Signals arising from the aromatic protons of L-DOPA in CF_3COOH consisted of a broad singlet at 6.5 ppm and two doublets at 6.53 and 6.37 ppm (Figure 8.1 a). These were assigned to H-2, H-5 and H-6, respectively. The coupling between H-2 and H-6 was not resolved, but the broadening of the doublet at 6.37 ppm was presumably due to a small coupling between H-2 and H-6. The signals from the benzylic protons and the CH on the side-chain showed the expected ABX pattern and the NH_3^+ was observed as a broad line at 6.83 ppm.

The ^1H spectrum of L-DOPA in CF_3COOH/CF_3SO_3H was similar to that observed in CF_3COOH except that the signals from the aromatic protons were shifted to higher frequencies. An extra set of signals having the same pattern was also observed at 6.75 (s), 6.74 (d) and 6.73 (d) ppm (Figure 8.1 b). These are likely due to the presence of aromatic protons of the protonated DOPA present in the solution.

A comparison of the ^{13}C spectrum of L-DOPA in CF_3COOH/CF_3SO_3H with that in CF_3COOH showed that the signals due to aromatic carbons were shifted to higher frequencies. In addition, there were extra signals arising from the

Figure 8.1. ^1H NMR spectrum of L-DOPA in (A) CF_3COOH and (B) CF_3COOH/CF_3SO_3H at -11 °C. In Figure 8.1 only the aromatic regions are shown.

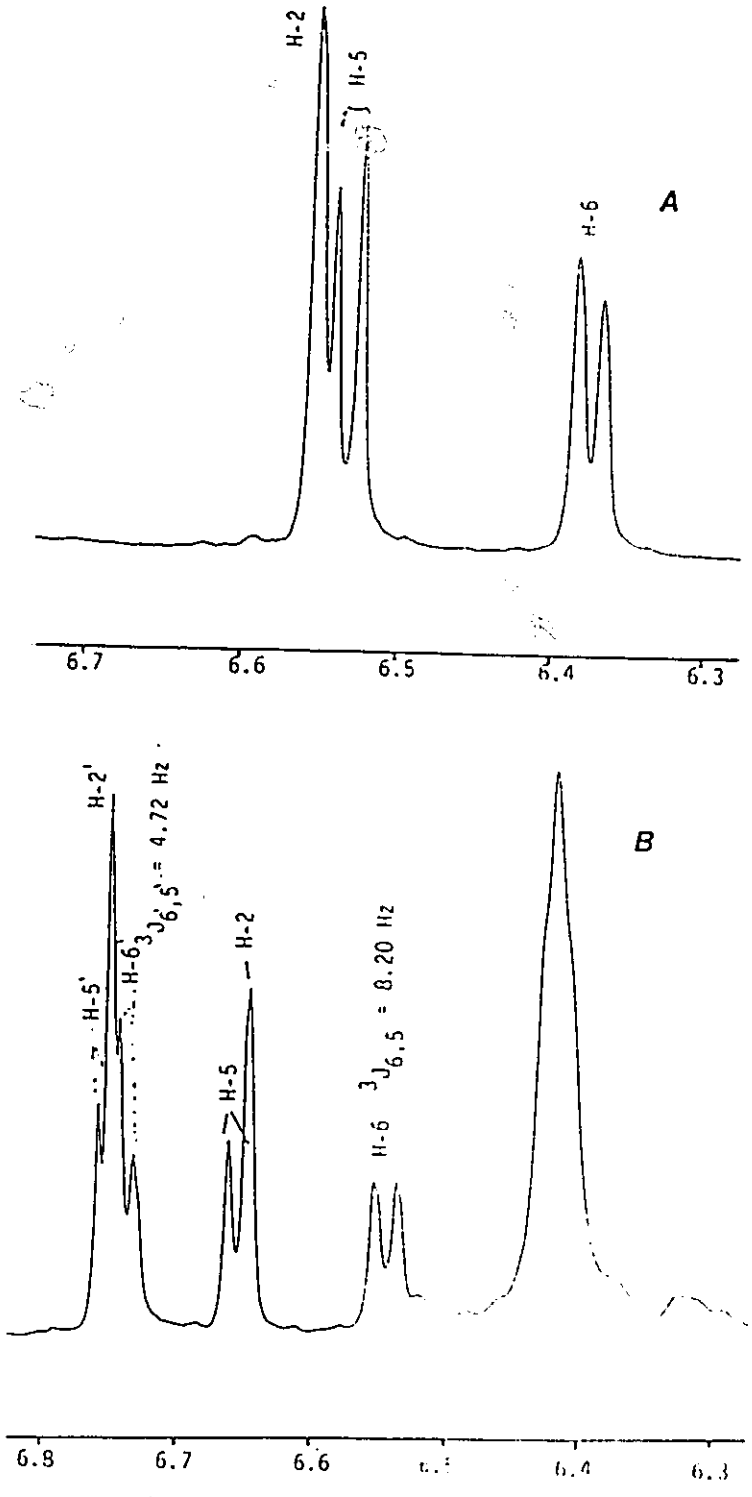
H-2
H-5
H-6
A
6.7
6.6
6.5
6.4
6.3
H-2'
H-5'
H-6'
$^3J_{6',5'}$ = 4.72 Hz
H-2
H-5
H-6
$^3J_{6,5}$ = 8.20 Hz
B
6.8
6.7
6.6
6.4
6.3
δ ^{1}H (ppm from acetone at 2.04 ppm)

Table 8.2. ^{1}H NMR Data of L-DOPA in CF_3COOH and CF_3COOH/CF_3SO_3H at -11 °C

Chemical Shifts

	CF_3COOH	CF_3COOH/CF_3SO_3H
H-2	6.55	6.64 6.74[a]
H-5	6.37	6.54 6.75[a]
H-6	6.53	6.65 6.73[a]
CH_2	3.05 2.76	3.04 2.80
CH	4.12	3.83
NH_3^+	6.83	6.41

Coupling Constants (Hz)

$^3J_{H5,H6}$ = 8.8 (4.7)[b] $^2J_{AB}$ = -15.2, $^3J_{AX}$ = 8.9 and $^3J_{BX}$ = 5.7

[a]Extra signals from the protonated species.

[b]Coupling between H-5 and H-6 in the protonated species.

Table 8.3. ^{13}C Chemical Shifts[a] of L-DOPA in CF_3COOH and CF_3COOH/CF_3SO_3H at - 11 °C

	CF_3COOH	CF_3COOH/CF_3SO_3H
C_1	132.4	135.1 139.8
C_2	119.6	121.2 125.4
C_3	145.6	148.2
C_4	145.2	147.8
C_5	119.3	121.1 125.2
C_6	125.3	128.3 131.9
CH_2	36.7	36.3 36.7
CH	57.7	57.6 57.6
COOH	175.5	175.0 175.1

[a] Referenced with respect to internal trifluoroacetic acid at 116.4 ppm.

protonated dopa present in the sample (Table 8.3). The additional ^{13}C signals for the aromatic carbons complemented the additional high-frequency signals observed in the ^{1}H spectrum.

2. Radiofluorination of m-Tyrosine and L-DOPA in CF_3COOH/CF_3SO_3H

HPLC Analysis of the reaction mixture, obtained after the radiofluorination of m-tyrosine in CF_3COOH/CF_3SO_3H or CF_3COOH showed a major [^{18}F] peak at 25 min. The peak eluting at 25 min. was assigned to [^{18}F]fluoro-m-tyrosine after comparing with the retention time of authentic fluoro-m-tyrosine. The identity and orientation of fluoro-m-tyrosine were confirmed using ^{19}F NMR (Table 8.4).

HPLC Analysis of the reaction mixture obtained after the radiofluorination of L-DOPA in CF_3COOH/CF_3SO_3H showed a major [^{18}F] peak at 21 min. (Figure 8.2). For comparison, the radiochromatogram of the products from the same reaction in CF_3COOH is also given Figure 8.2. The ^{19}F NMR spectrum of the compound eluting at 21 min. consisted of a doublet of doublet at -126.2 (53%), a doublet at -135.3 (15%) and a singlet -139.5 (32%)ppm. The ^{19}F chemical shifts agreed with previously reported values for 6-, 5- and 2-fluorodopa.[69]

Figure 8.2. Radiochromatogram of the reaction mixture obtained after the direct fluorination of L-DOPA in (A) CF_3COOH and (B) CF_3COOH/CF_3SO_3H.

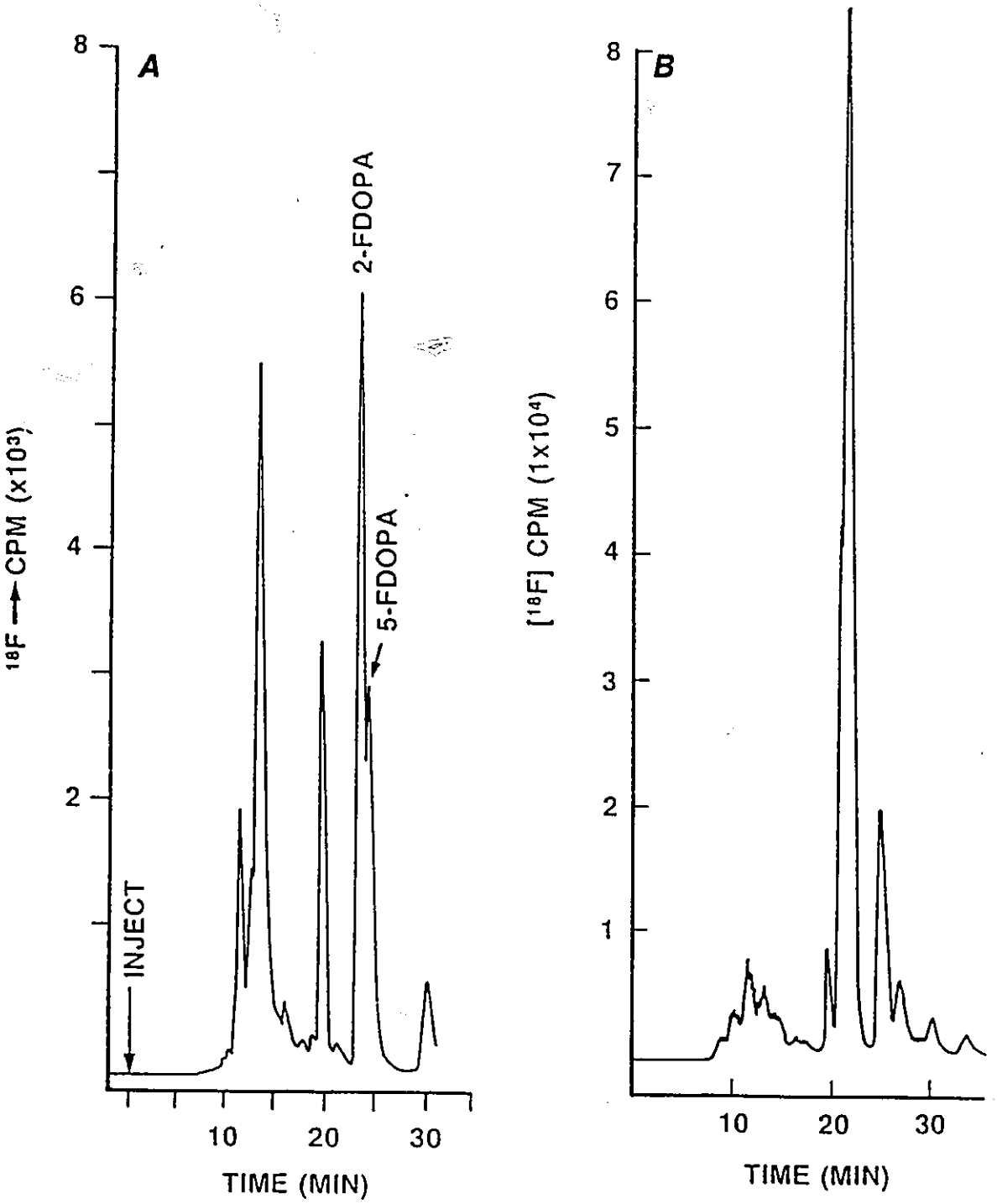
A
B
8
7
6
5
4
3
2
1
^{18}F — CPM (x10^3)
[^{18}F] CPM (1x10^4)
INJECT
2-FDOPA
5-FDOPA
10
20
30
TIME (MIN)

C. DISCUSSION

Results from the radiofluorination of m-tyrosine and L-DOPA in CF_3COOH and CF_3COOH/CF_3SO_3H are summarized in Table 7.3.

The relative distributions of 2-, 4-, 5- and 6- fluoro-m-tyrosine were similar after the direct fluorination of m-tyrosine in either CF_3COOH or CF_3COOH/CF_3SO_3H. However, results in Table 7.3 show that the radiofluorination of m-tyrosine in CF_3COOH and CF_3COOH/CF_3SO_3H produced marked differences in the amount of fluorine consumed ($[^{18}F]F_2$ recovery) and the radiochemical yield. While the amount of $[^{18}F]F_2$ recovered from the target was reduced by almost 50%, the radiochemical yield of [^{18}F]fluoro-m-tyrosine was doubled during the radiofluorination in CF_3COOH/CF_3SO_3H. It can be argued that the reduction in $[^{18}F]F_2$ recovery is presumably due to the reduced reactivity of F_2 towards protonated m-tyrosine in CF_3SO_3H solvent. This is supported by the observed high frequency shifts of ^1H and ^{13}C signals of m-tyrosine in CF_3COOH/CF_3SO_3H, which in turn, indicate that the aromatic ring is deactivated. The higher radiochemical yield of fluoro-m-tyrosine in going from CF_3COOH to CF_3COOH/CF_3SO_3H is to be expected because such a trend in radiochemical yields with increasing acidity of the solvent has already been established (Chapter 6).

Table 8.4. Effect of CF_3SO_3H in the Radiofluorination of m-Tyrosine and L-DOPA

Substrate	Solvent	%[^{18}F]F_2 Recovered	Radiochemical Yield (%)	Isomer Distribution 2	4	5	6
m-Tyrosine	CF_3COOH	55	15	35	9	5	49
	CF_3SO_3H/CF_3COOH	30	30	30	7	9	53
L-DOPA	CF_3COOH	60	8	65	-	35	-
	CF_3SO_3H/CF_3COOH	7	16	32	-	15	53

Results from the radiofluorination of L-DOPA in CF_3COOH and CF_3COOH/CF_3SO_3H (Table 8.4) show that the presence of CF_3SO_3H has a considerable effect on the recovery of $[^{18}F]F_2$, radiochemical yield and the isomer distribution.

The drastic reduction in the recovery of $[^{18}F]F_2$ strongly suggests that L-DOPA is protonated in CF_3COOH/CF_3SO_3H. Low-temperature ^1H and ^{13}C spectra of L-DOPA in CF_3COOH/CF_3SO_3H indicated the presence of DOPA and O-protonated DOPA in the sample. However, it is not clear why $[^{18}F]F_2$ reacts preferentially with the protonated L-DOPA in which the aromatic ring is deactivated (Scheme 8.1)

Higher radiochemical yields of $[^{18}F]$fluorodopa resulting from fluorinations in CF_3COOH/CF_3SO_3H indicate that the substitution of fluorine is the preferred route when the acidity of the solvent is increased. The results in Table 8.3 also indicate that, unlike the fluorination of L-DOPA in CF_3COOH, 6-fluorodopa is the major product when CF_3SO_3H is present in the reaction mixture. This result further confirms that $[^{18}F]F_2$ reacts preferentially with the protonated species in solution. Therefore, the differences in $[^{18}F]F_2$ recovery and orientation of fluorination in L-DOPA in CF_3COOH and CF_3COOH/CF_3SO_3H solvents can be explained by differences in reactivity and selectivity of $[^{18}F]F_2$ towards L-DOPA and protonated DOPA in the two solvents (Scheme 8.1).

Scheme 8.1

Selectivity of F_2 towards DOPA in TFA and TFA/Triflic Acid

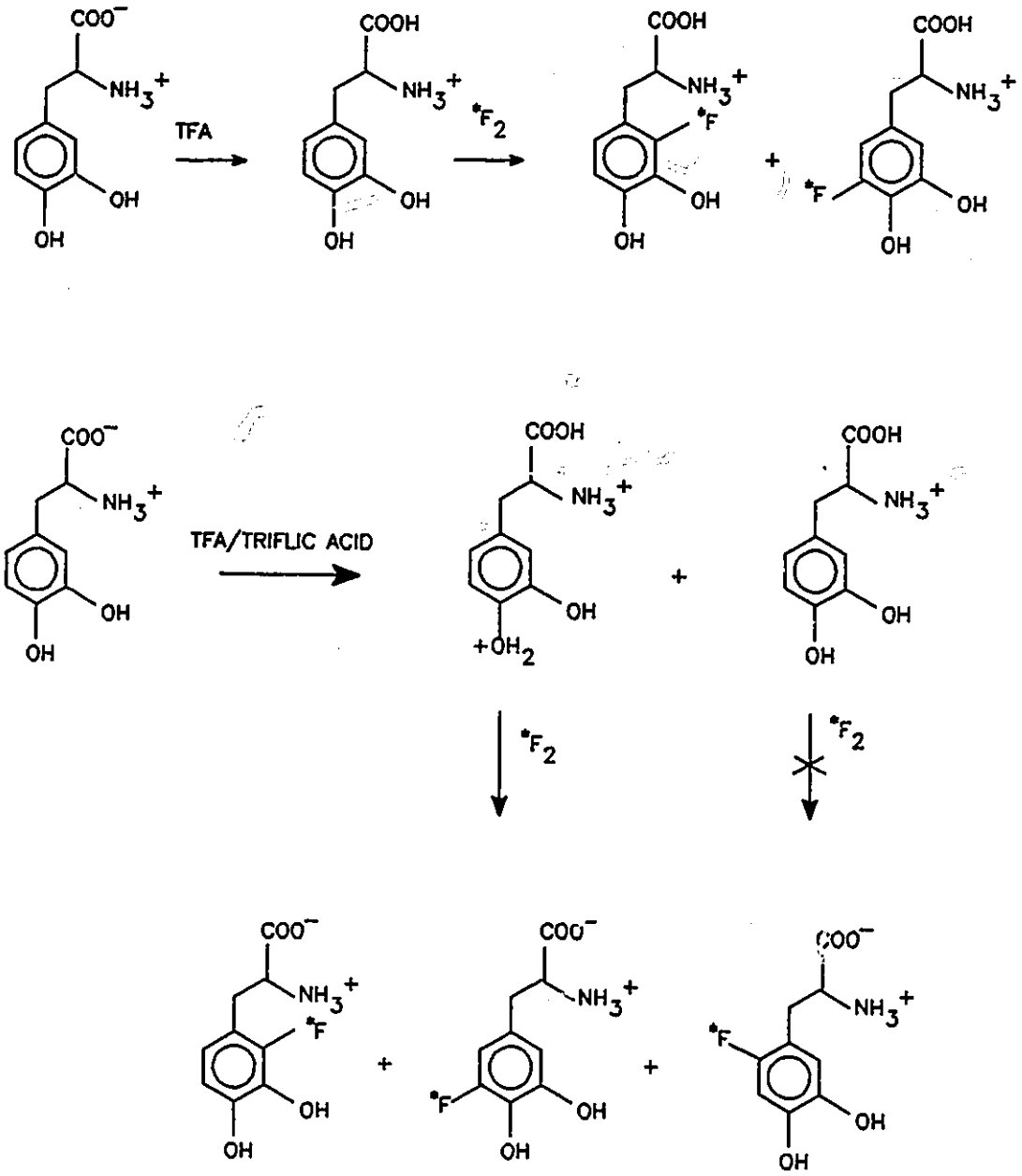

D. Conclusions

Results from the present study show that CF_3COOH/CF_3SO_3H may be used as a solvent for the synthesis of [^{18}F]6-fluorodopa and [^{18}F]fluoro-m-tyrosine. Its potential to replace HF/BF_3 for the routine production of [^{18}F]fluorodopa needs further investigation to establish the conditions for higher [^{18}F]F_2 recovery from the target. The reactivity of [^{18}F]F_2 and the radiochemical yield of [^{18}F]fluoro-m-tyrosine indicate that HF is a much better solvent than a CF_3COOH/CF_3SO_3H mixture for the direct fluorination of m-tyrosine.

CHAPTER 9

APPLICATION OF [^{18}F] LABELLED FLUOROTYROSINE AND [^{18}F]FLUORO-m-TYROSINE IN POSITRON EMISSION TOMOGRAPHY

A. Introduction

Of all the intracerebral catecholaminergic pathways in the human brain, those that use dopamine as their neurotransmitter contain the largest amounts of this amine. The majority of the dopaminergic nerve terminals, unlike the noradrenergic terminals which ramify diffusely throughout out the cortex, are found in the striata. The striata (left and right) are well defined collections of nerve cells situated in the centre of each cerebral hemisphere (Fig 9.1). They are connected directly to the cerebral cortex, the mantle of nerve cells that covers the brain, and to the brain stem. Each striatum is divided into two parts: the caudate nucleus, connected to the front part of the cerebral hemisphere, and the putamen, connected to the sensori motor cortex in the more lateral regions. It is the high local concentration in the striata of dopamine and the enzymes that synthesise it that lend themselves to study by PET.

It is known that the clinical features of Parkinson's disease, muscular rigidity, immobility, flexed posture and

Figure 9.1 Horizontal section of the human brain at the level of striata. This cross section is about 4 cm above and parallel to a plane through the bridge of the nose and the earholes of the subject. (A) Caudate nucleus, (B) Thalamus and (C) Putamen.

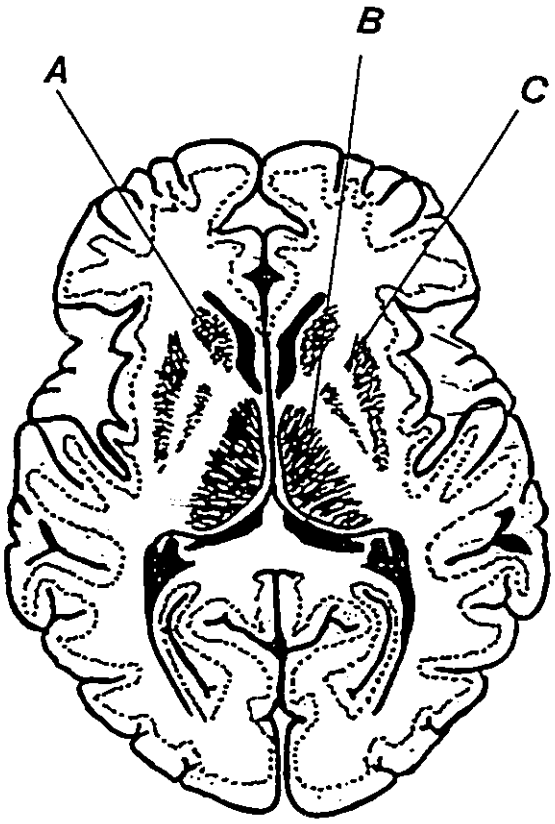
A
B
C

tremor, are associated with marked deficiencies of striatal dopamine.[174] These observations, corroborated many times from autopsy examinations,[175] lead to the use of L-DOPA to alleviate the symptoms of Parkinson's disease. Garnett *et al.*[150] pioneered the use of [^{18}F]6-fluorodopa, in conjunction with PET, to visualise the regional distribution of intracerebral dopamine in human brain during life. Subsequently, [^{18}F]6-fluorodopa was also used to show that the accumulation of [^{18}F] was reduced in the contralateral putamen of patients suffering from hemiparkinsonism.[153] These findings were the first demonstration, during life, of a disturbance of intrastriatal dopamine metabolism in Parkinson,s disease.

Inspite of the obvious usefulness of the qualitative studies such as those above, the quantitative analysis of PET data from [^{18}F]6-fluorodopa is difficult. Attempts to quantitate the uptake of [^{18}F]6-fluorodopa from blood and its retention in the striatum have produced conflicting results on the age related impairment of nigrostriatal nerve endings.[176,177] One reason for this difficulty is the complex *in vivo* chemistry of the tracer (Scheme 9.1). Specifically, studies have shown that [^{18}F]fluorodopa, once injected, is metabolised in the blood to 3-methoxy-[^{18}F]6-fluorodopa by catechol-O-methyl transferase (COMT). The presence of 3-O-methoxy-[^{18}F]6-fluorodopa, which also crosses the blood-brain barrier (the

continuous sheet of cells that lines the cerebral blood vessels and regulates the transport of all chemicals entering or leaving the brain), increases the nonspecific accumulation of radioactivity in the brain.

Scheme 9.1

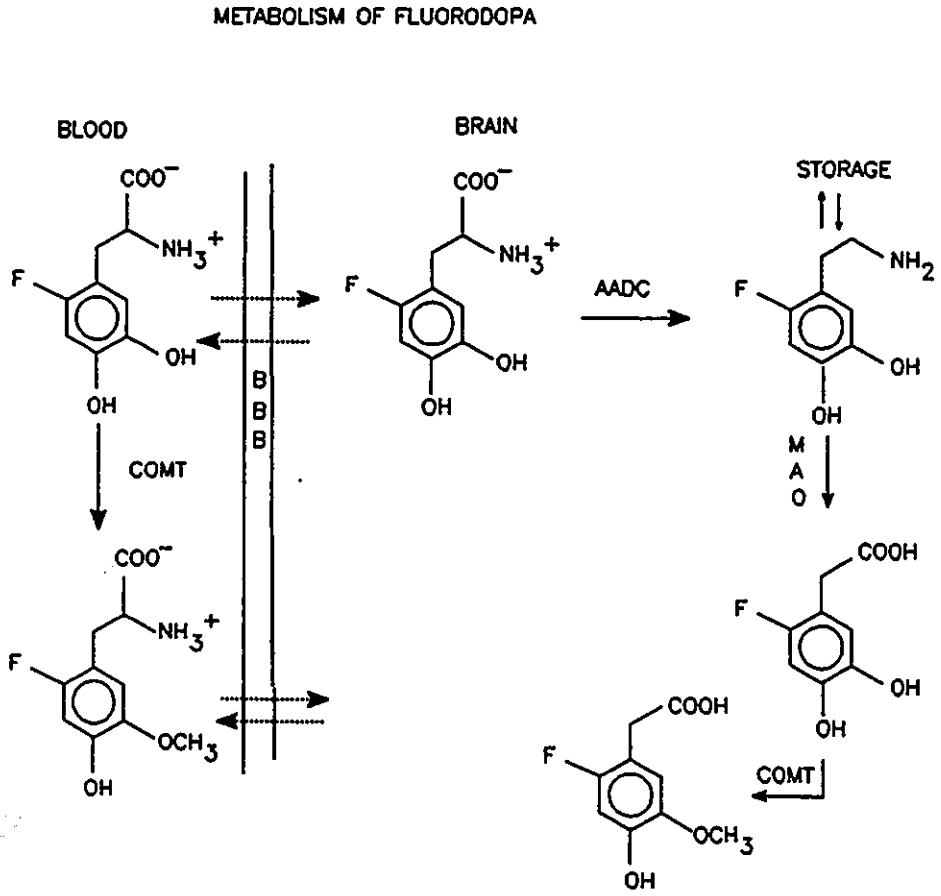

Consequently, the development of any mathematical model to determine, from PET data, the rate of dopamine synthesis should take into consideration the nonspecific accumulation of ^{18}F in the brain. It is, therefore, desirable to use some other ^{18}F labelled substrate that would reduce the non specific accumulation of ^{18}F in the brain while still measuring decarboxylase activity in the dopaminergic structures in the brain.

In this chapter the striatal distribution of [^{18}F] in the human brain after a normal volunteer was injected with [^{18}F] fluorotyrosine and [^{18}F]fluoro-m-tyrosine was measured and results were compared with results from a similar study using [^{18}F]6-fluorodopa. The use of [^{18}F] fluorotyrosine and [^{18}F]fluoro-m-tyrosine for the study of dopamine metabolism using PET will be discussed.

B. RESULTS

1. Studies with [^{18}F]2-and 3-Fluorotyrosine

On separate occasions a 48 year old male volunteer was injected with 5 mCi and 2.7 mCi of [^{18}F]3- and 2-fluoro-tyrosine, respectively. Figure 9.2 shows the distribution of[^{18}F] in a cross section of the brain of this volunteer, at the level of striatum, 120 min after injection of [^{18}F]2-

Figure 9.2 PET study of a normal individual two hours after the injection of [^{18}F]2-fluorotyrosine. This cross section is at the level of striatum. In this figure the person's nose is towards the top and his left is on the reader's right. The pink colour represents maximum accumulation of [^{18}F], followed by the red, yellow, green and blue.

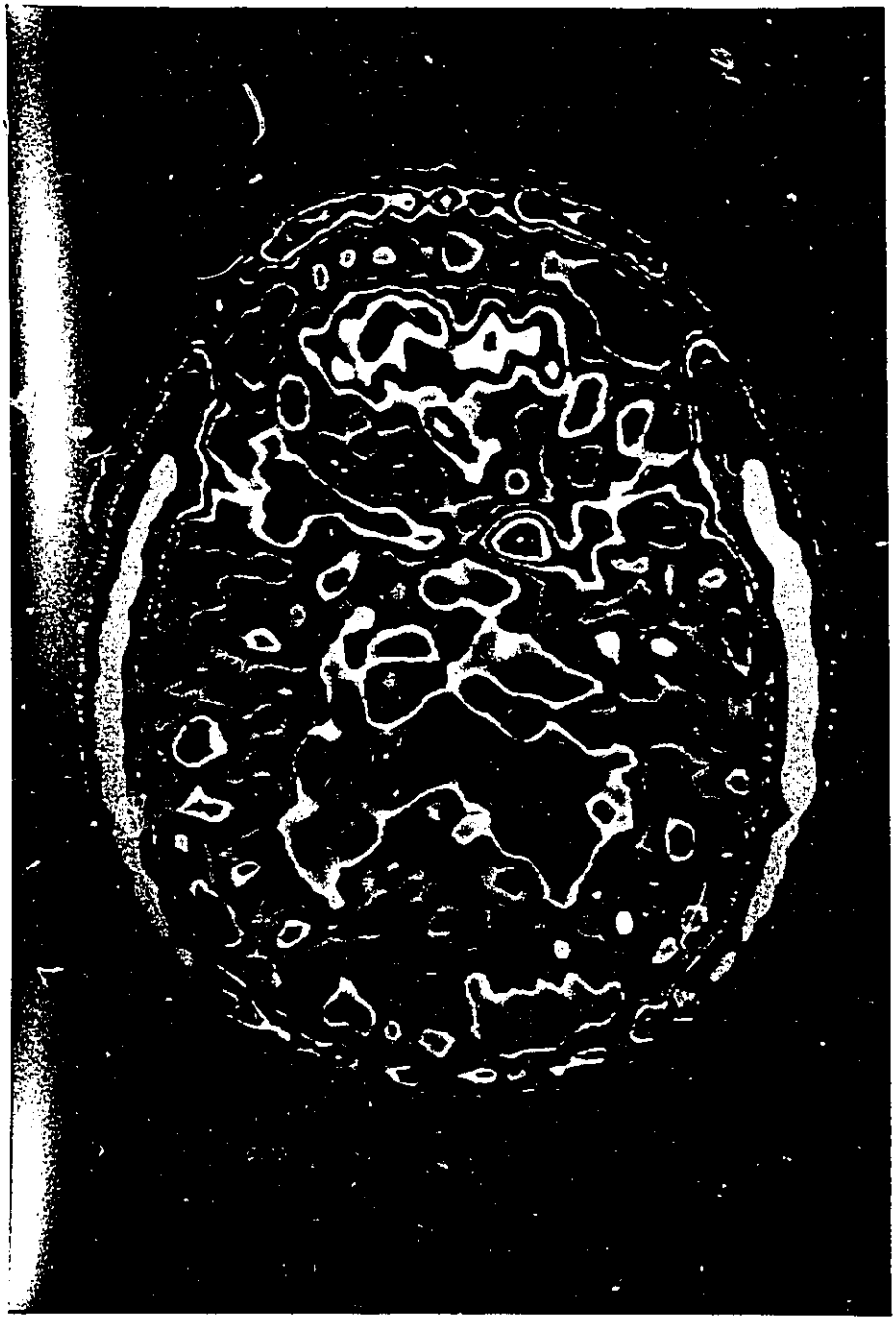

Figure 9.3 PET study of a normal individual two hours after the injection of [^{18}F]3-fluorotyrosine. This cross section is at the level of striatum. In this figure the person's nose is towards the top and his left is on the reader's right. The pink colour represents maximum accumulation of [^{18}F], followed by the red, yellow, green and blue.

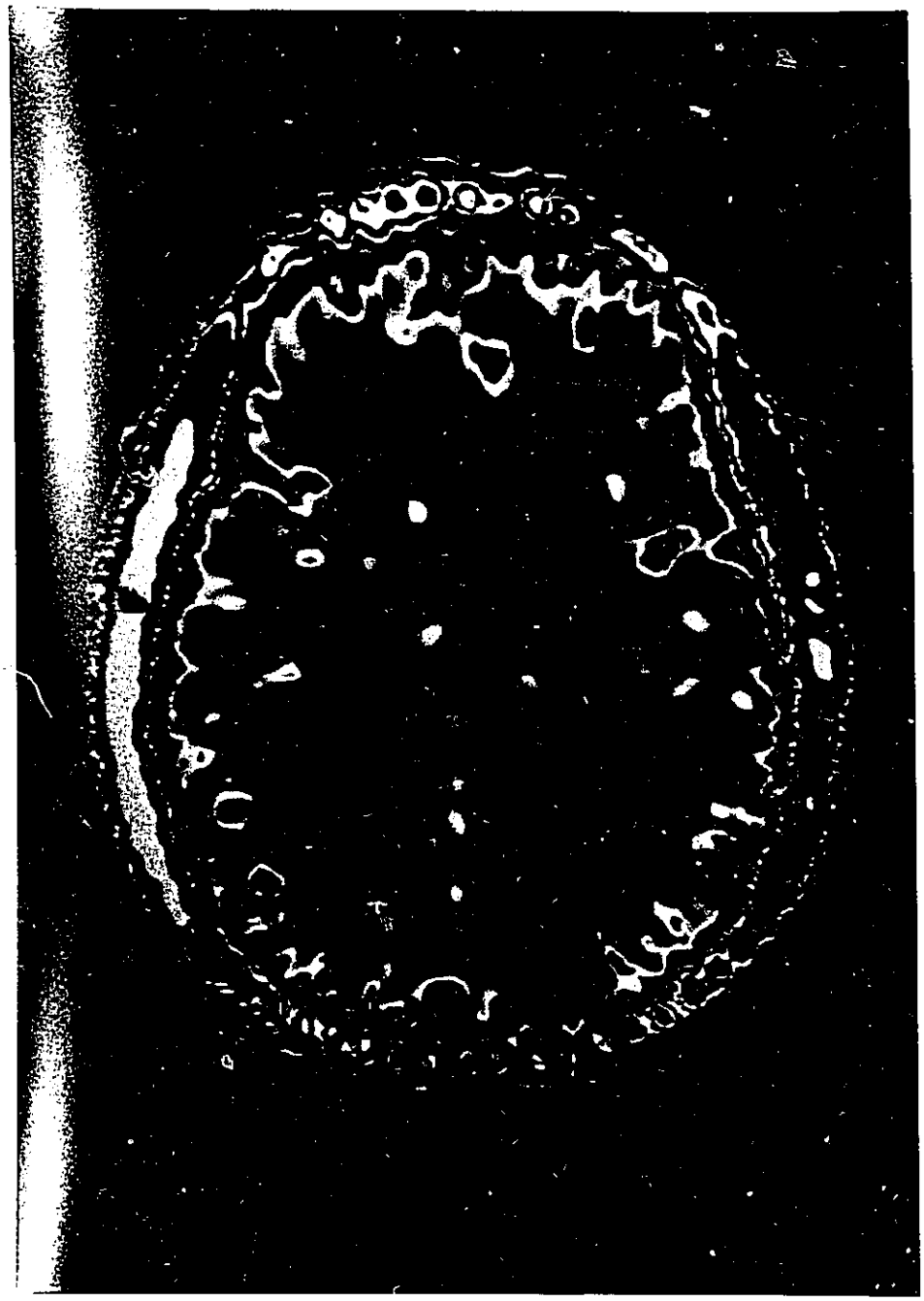

Figure 9.4 Time course of [^{18}F] in the brain of a normal individual after the injection of (A) [^{18}F]2-fluorotyrosine and (B) [^{18}F]6-fluorodopa.

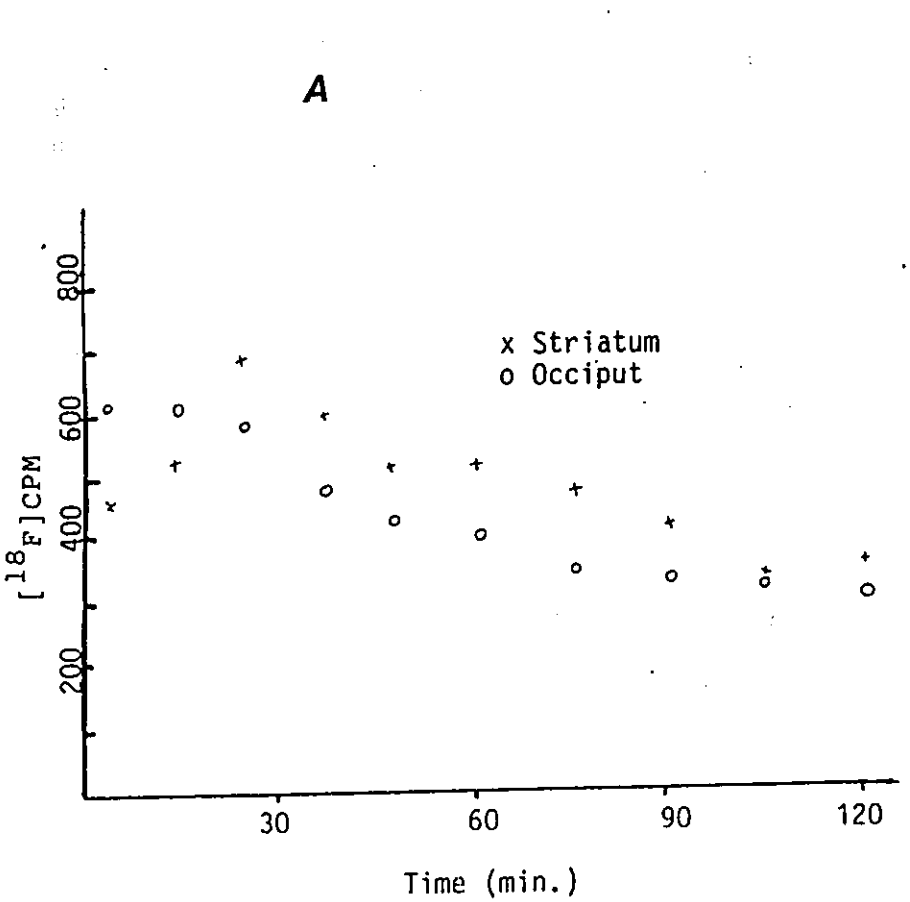
A
x Striatum
o Occiput
[18F]CPM
800
600
400
200
30
60
90
120
Time (min.)

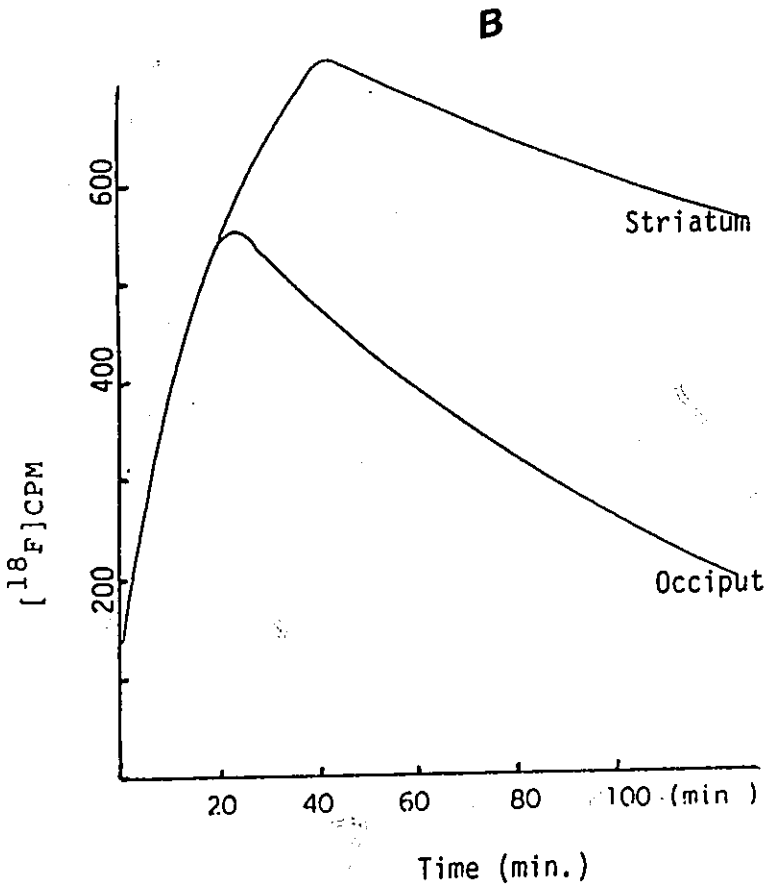
B
Striatum
Occiput
[18F]CPM
600
400
200
20
40
60
80
100 (min)
Time (min.)

fluorotyrosine and Figure 9.2 shows the distribution of [^{18}F] in the same cross section 60 min after injection of [^{18}F]3-fluorotyrosine. The striatal and occipital accumulation of [^{18}F] at different times after the injection of [^{18}F]2-fluorotyrosine are shown in Figure 9.4 a. For comparison, the time activity curve obtained after the same individual was injected with [^{18}F]6-fluorodopa is shown in Figure 9.4 b.

2. Studies with [^{18}F]Fluoro-m-Tyrosine and [^{18}F]6-Fluorodopa

Two individuals were studied. One was a 50 year old male, free of any movement disorders, and the other was a 48 year old male patient with well documented hemiparkinsonism. On separate occasions they were each given 3.0 mCi doses of [^{18}F]fluoro-L-m-tyrosine and [^{18}F]6-fluorodopa.

Figure 9.5 a shows the distribution of ^{18}F in the brain, at the level of the striatum, in the normal subject 2 hours after injection of [^{18}F]6-fluorodopa. Figure 9.5 b, shows the distribution of ^{18}F in the same subject 2 hours after receiving [^{18}F]fluoro-L-m-tyrosine. The accumulation of ^{18}F in the striatum was measured to be 1.7 times that in the occipital cortex after [^{18}F]6-fluorodopa and 4.4 times after [^{18}F]-fluoro-L-m-tyrosine .

Figure 9.6 shows that the initial striatal and occipital accumulation of ^{18}F (cpm/pixel/mCi) after [^{18}F]6-fluorodopa (Figure 9.6 a) is very similar to that after [^{18}F]fluoro-L-m-tyrosine (Figure 9.6 b). Approximately 30 minutes after injection the time activity curves from striatum and occiput diverge noticeably. The major difference between the studies is that the ^{18}F content of the occiput 120 minutes after [^{18}F]fluoro-m-L-tyrosine was injected falls to approximately 25% of the maximum while it only falls to 60% of the maximum after fluorodopa.

Figure 9.7 a shows the distribution of ^{18}F in the brain of the parkinsonian patient 2 hours after [^{18}F]6-fluorodopa. Figure 9.7 b shows the distribution of ^{18}F in the same patient after [^{18}F]fluoro-L-m-tyrosine. Note that the pattern of retention of radioactivity in the striatum and especially the reduction of ^{18}F in the left putamen is similar in both cases.

3. Studies with [^{18}F]Fluoro-3-hydroxyphenylacetic Acid and 3-Methoxy-[^{18}F]6-fluorodopa

A 50 year old male volunteer was studied after he was injected, on separate occasions, with 3 mCi doses of [^{18}F]fluoro-3-hydroxyphenylacetic acid and 3-methoxy-[^{18}F]6-fluorodopa. Figure 9.8 a shows the distribution of ^{18}F in the brain of this normal individual 1 hour after receiving

Figure 9.5 PET study of a normal individual two hours after the injection (A) [^{18}F]6-fluorodopa and (B) [^{18}F]fluoro-L-m-tyrosine. This cross section is at the level of striatum. In figure 9.5 the person's nose is towards the top and his left is on the reader's right. The pink colour represents maximum accumulation of [^{18}F], followed by the red, yellow, green and blue.

TOP

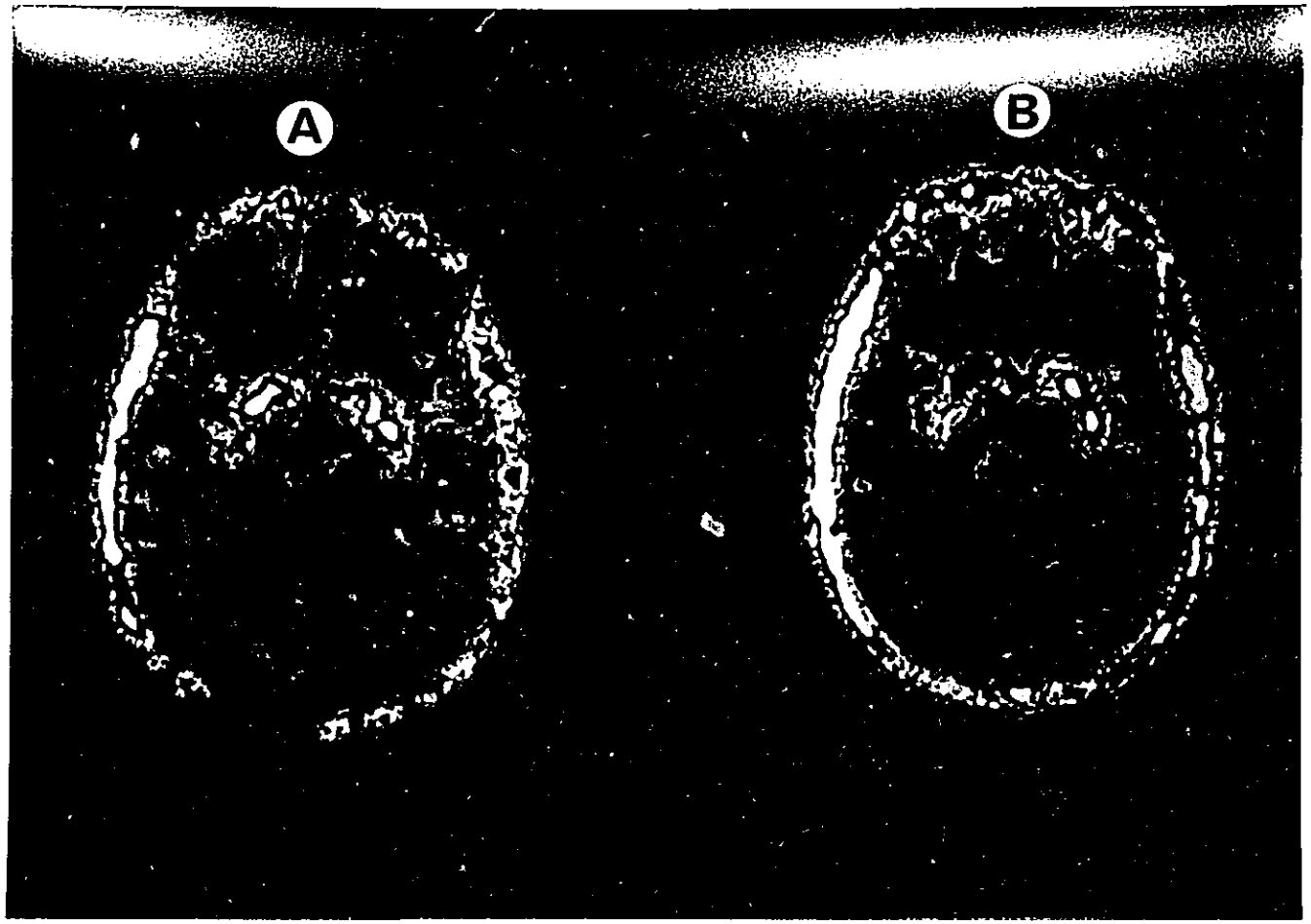

BOTTOM

Figure 9.6 Striatal and occipital accumulation of [^{18}F] in the brain of normal volunteer after the injection of (A) [^{18}F]6-fluorodopa and (B) [^{18}F]fluoro-L-m-tyrosine.

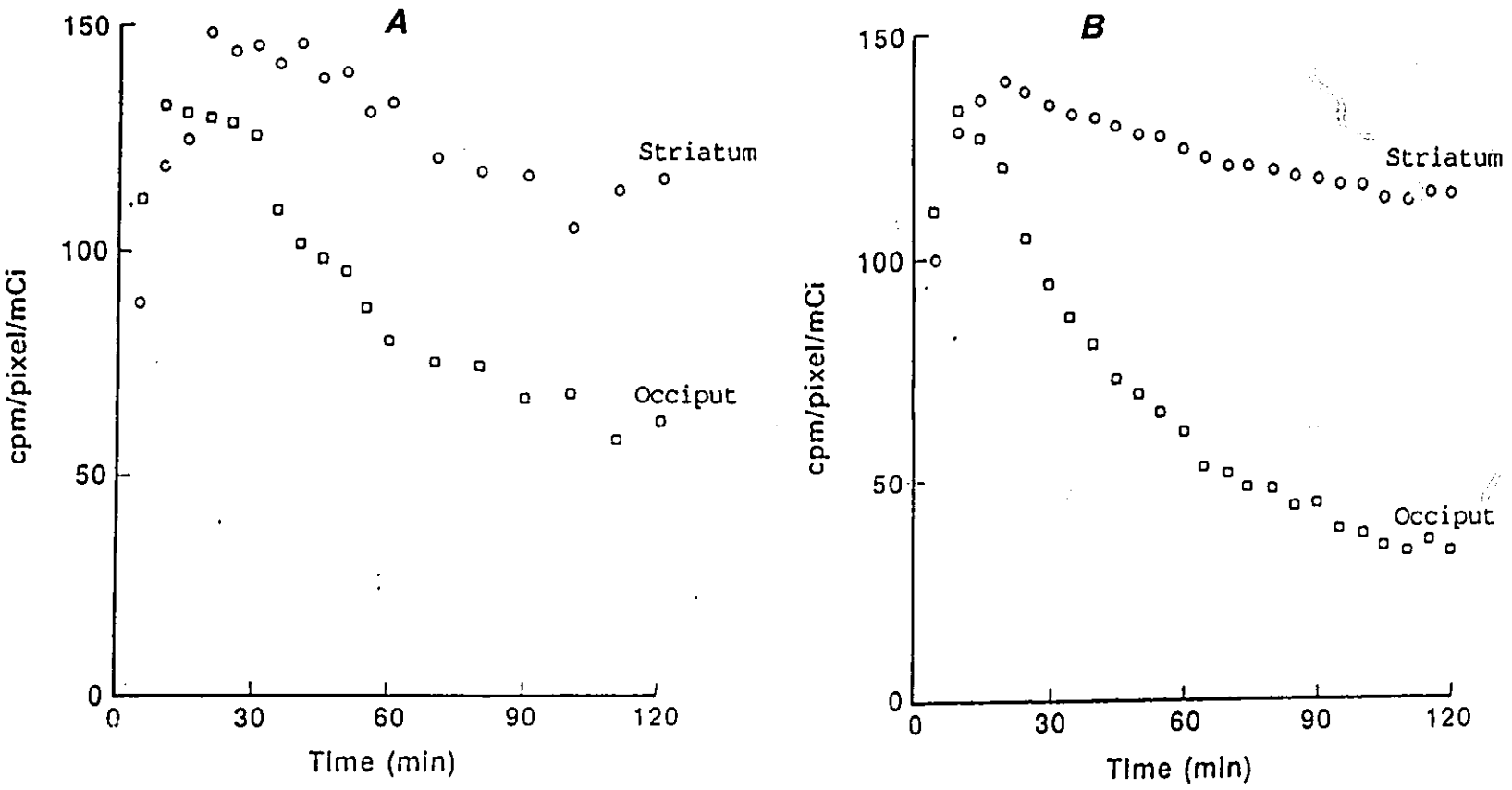
A
150
100
50
0
cpm/pixel/mCi
Striatum
Occiput
0
30
60
90
120
Time (min)
B
150
100
50
0
cpm/pixel/mCi
Striatum
Occiput
0
30
60
90
120
Time (min)

Figure 9.7 PET study of a Parkinsonian patient two hours after the injection (A) [^{18}F]6-fluorodopa and (B) [^{18}F]fluoro-L-m-tyrosine. This cross section is at the level of striatum. In figure 9.7 the person's nose is towards the top and his left is on the reader's right. The pink colour represents maximum accumulation of [^{18}F], followed by the red, yellow, green and blue.

TOP

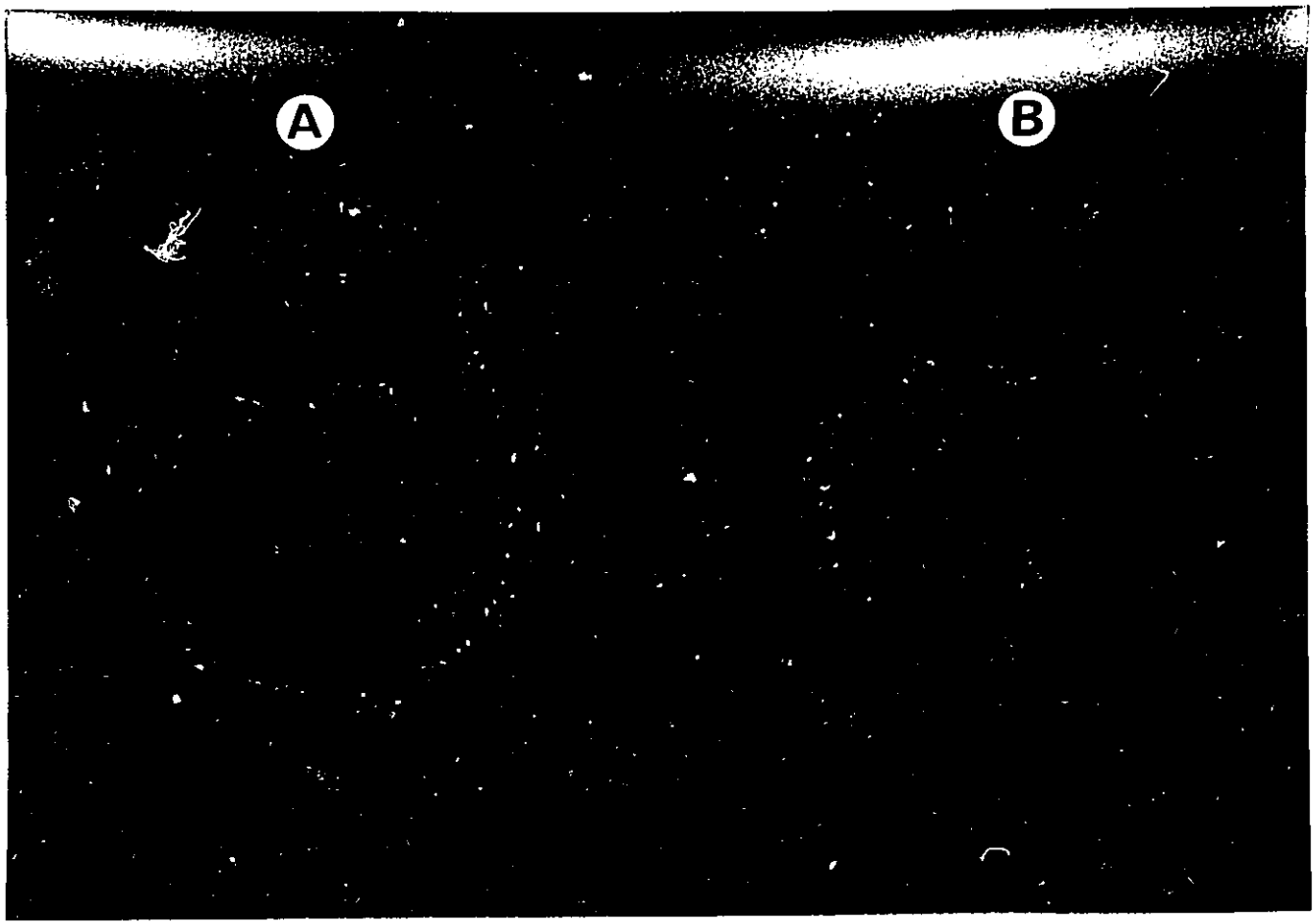

BOTTOM

Figure 9.8 PET study of a normal individual two hours after the injection (A) [^{18}F]fluoro-3-hydroxyphenylacetic acid and (B) striatal and occipital regions of interest defined from figure 9.6 b and transposed to this study. In figure 9.8 the person's nose is towards the top and his left is on the reader's right. The pink colour represents maximum accumulation of [^{18}F], followed by the red, yellow green and blue.

TOP

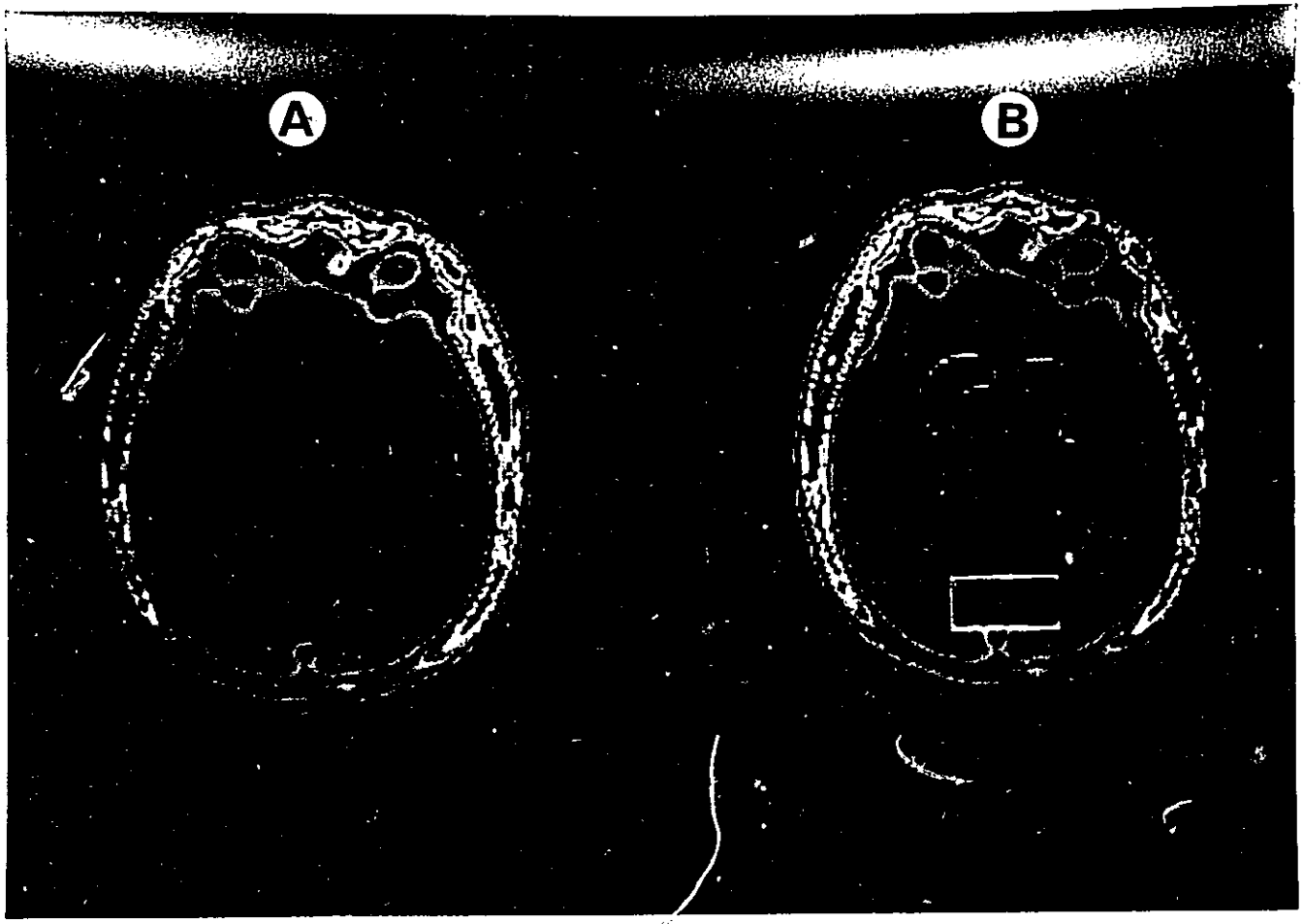

BOTTOM

Figure 9.9 PET study of a normal individual two hours after the injection (A) 3-methoxy-[^{18}F]6-fluorodopa and (B) striatal and occipital regions of interest defined from figure 9.6 a and transposed to this study. In figure 9.9 the person's nose is towards the top and his left is on the reader's right. The pink colour represents maximum accumulation of [^{18}F], followed by the red, yellow, green and blue.

TOP

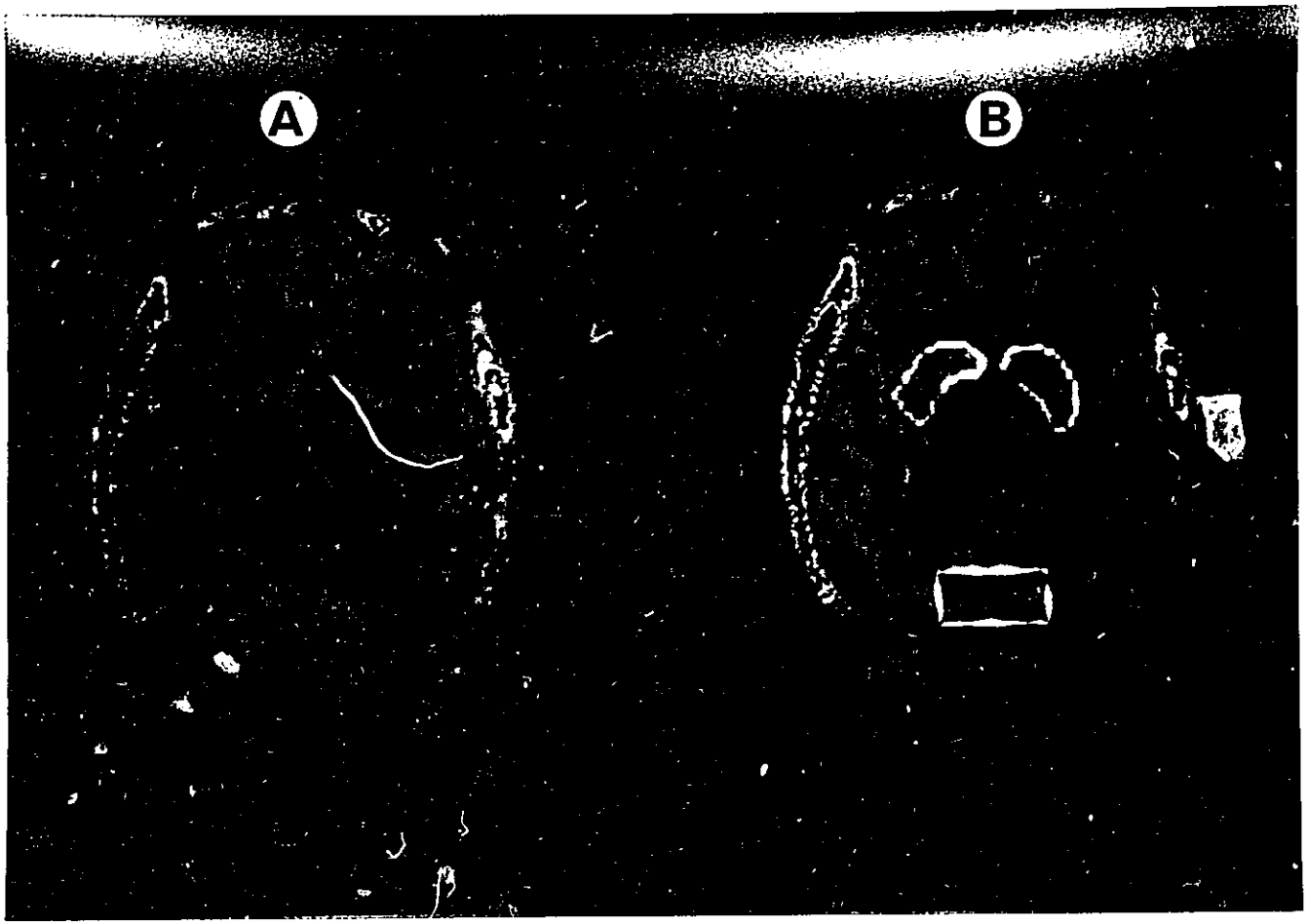

BOTTOM

[^{18}F]fluoro-3-hydroxyphenylacetic acid. Figure 9.8 b shows the extent of the striata in the same individual defined from the [^{18}F]fluoro-L-m-tyrosine study and transposed to this study. There is very little ^{18}F activity in any region of the brain after [^{18}F]fluoro-3-hydroxy-phenylacetic acid.

Figure 9.9 a shows the distribution of ^{18}F in the brain of the same individual 1 hour after injection of a similar dose of 3-methoxy-[^{18}F]6-fluorodopa. Figure 9.9 b shows the extent of the striata. In this case there is a generalized accumulation of ^{18}F in grey matter after 3-methoxy-[^{18}F]6-fluorodopa.

4. [^{18}F] Containing Metabolites in the Brain and Plasma of Monkey

Figure 9.10 shows the distribution of the major ^{18}F containing metabolites in the brain and plasma of monkeys injected with the mixture of [^{18}F]fluoro-L-m-tyrosine. In addition to the fluoro-m-tyrosine, [^{18}F]fluoro-m-tyramine, its sulphate conjugate and [^{18}F]fluoro-3-hydroxyphenyl acetic acid were found. In all tissues there was a progressive decrease in the proportion of [^{18}F]fluoro-L-m-tyrosines and a progressive increase in the proportion of [^{18}F]fluoro-3-hydroxyphenyl acetic acid. In the occiput and in the plasma

Figure 9.10 Distribution of [^{18}F] containing metabolites in the Monkey brain and plasma after the injection of [^{18}F]fluoro-L-m-tyrosine.

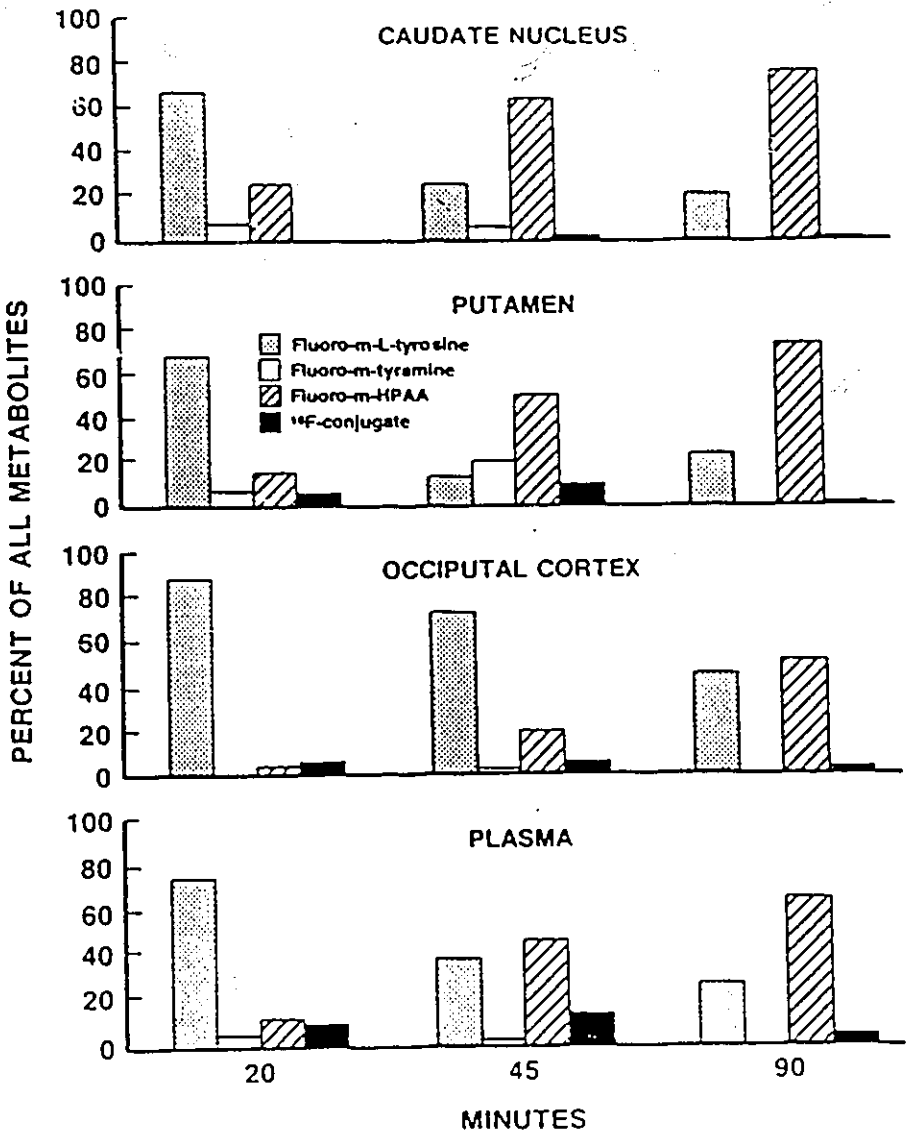
CAUDATE NUCLEUS
PUTAMEN
OCCIPUTAL CORTEX
PLASMA
Fluoro-m-L-tyrosine
Fluoro-m-tyramine
Fluoro-m-HPAA
¹⁸F-conjugate
PERCENT OF ALL METABOLITES
100
80
60
40
20
0
20
45
90
MINUTES

almost no [^{18}F]fluoro-m-tyramine was found. In the striatum, a small amount (less than 5%) was found at 20 and 45 minutes but none was found at 90 minutes.

C. DISCUSSION

The dopaminergic system has been the target of radiotracer development since the early 1970s. Although 6-fluorodopa was developed and successfully applied to the study of presynaptic dopaminergic systems in humans, its metabolism, particularly the formation of 3-O-methyl-6-fluorodopa (Scheme 9.1) complicates the quantitative analysis of PET data. It is therefore desirable to develop an alternate tracer to this end. The use of [^{18}F]fluorotyrosine and [^{18}F]fluoro-m-tyrosine to study the dopamine metabolism has been investigated.

1. [^{18}F]2- and 3-Fluorotyrosine as Tracers for Tyrosine Hydroxylase

Examination of the synthesis of dopamine (Scheme 9.2 below) indicates that an ^{18}F-labelled tyrosine may be a better tracer than [^{18}F]fluorodopa to study dopamine metabolism because the rate determining step in the synthesis of dopamine is the conversion of tyrosine to L-DOPA by tyrosine hydroxylase(step 1, Scheme 9.2). Results from autopsy studies showed a decreased level of tyrosine hydroxylase in the

striatum of patients with Parkinson's disease at a time when the levels of aromatic acid decarboxylase were unaffected.

Scheme 9.2

DOPAMINE METABOLISM

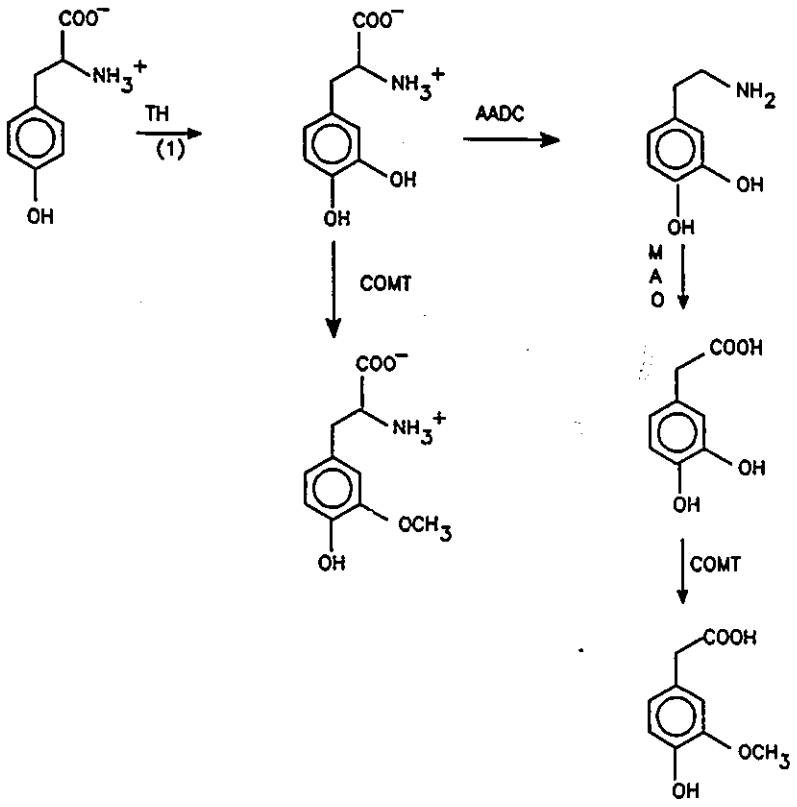

After the injection of either of the [^{18}F]fluorotyrosines, PET studies showed no specific accumulation of [^{18}F] in the striatum, a portion of the brain that is rich in tyrosine hydroxylase because of its dopaminergic nerve terminals

(Figure 9.2 and 9.3). This result may be explained as follows: It is known that tyrosine is a major component of protein and therefore [^{18}F]-labelled tyrosine will be used for protein synthesis throughout the brain. In fact, Coenen *et al.*[178] have demonstrated the use of [^{18}F]2-fluorotyrosine as a tracer to measure cerebral protein synthesis. PET may not be sensitive enough to detect the small additional amount of [^{18}F]fluorotyrosine that is used for L-DOPA synthesis against the much larger amounts of [^{18}F] from [^{18}F]2-fluorotyrosine that are incorporated into proteins. Furthermore, it is not known what the effect of fluorine substitution at carbons 2- or 3- of the aromatic ring of tyrosine will be on the specificity of the reaction with tyrosine hydroxylase. The action of tyrosine hydroxylase with 3-fluorotyrosine should produce 5-fluorodopa which has been shown to accumulate in rat striatum. The action of tyrosine hydroxylase with 2-fluoro-tyrosine should produce either 2- or 6-fluorodopa. If appreciable amounts of [^{18}F]2-fluorodopa were produced, then no specific retention of [^{18}F] in the striatum can be expected because Solin *et al.*[169] reported that there is no striatal accumulation of ^{18}F in man after the injection of [^{18}F]2-fluorodopa. It is also known that 2-fluorodopa enters the brain at approximately 1/3 the rate of 6-fluorodopa and that the rate of decarboxylation of 2-fluorodopa is 16 times slowerthan that of 6-fluorodopa.[179] Unlike [^{18}F]2-fluorodopa,

[^{18}F]6-Fluorodopa does accumulate in the striatum. Therefore some specific accumulation of ^{18}F in the striatum might be expected if appreciable amounts of [^{18}F]6-fluorodopa are produced from [^{18}F]2-fluorotyrosine.

2. [^{18}F]Fluoro-m-tyrosine as a Tracer for Aromatic Acid Decarboxylase

Since the [^{18}F]fluorodopa technique largely assesses the aromatic acid decarboxylase activity (AADC) and since m-tyrosine is a substrate for AADC, [^{18}F]fluoro-L-m-tyrosine could be used to study the levels of activity of this enzyme, and hence the neurone's capacity to synthesize dopamine. In addition, fluoro-m-tyrosine, like m-tyrosine, is not a substrate for COMT and therefore its metabolism will be simpler than that of 6-fluorodopa. When [^{18}F]fluoro-L-m-tyrosine is injected into monkeys, the distribution of ^{18}F within the brain at autopsy (Table 9.1) reflects the known intracerebral distribution of aromatic L-amino acid decarboxylase[180] and m-tyramine in man.[181]

When [^{18}F]fluoro-L-m-tyrosine is injected into man the same preferential striatal accumulation of ^{18}F can be demonstrated by PET (Figure 9.5 b) and is very much like that seen after [^{18}F]6-fluorodopa (Figure 9.5 a). Similarly, the contralateral reduction in putamenal aromatic L-amino acid

Table 9.1 Distribution of ^{18}F in Monkey Brain after Inter Venous Injection of [^{18}F]Fluoro-L-m-tyrosine[a]

Brain Region	20 minutes	90 minutes
Caudate nucleus	127	105
Putamen	106	88
Thalamus	83	44
Hypothalamus	73	45
Sustantia nigra	63	58
Occipital cortex	67	19
Parietal cortex	66	22
Cingulate cortex	68	16

[a] Regional concentration of ^{18}F given as percent of dose of ^{18}F/g tissue/g body weight.

decarboxylase that is characteristic of unilateral Parkinson's disease[153,182] can also be demonstrated by [^{18}F]fluoro-L-m-tyrosine (Figure 9.7 b).

Although [^{18}F]6-fluorodopa and [^{18}F]fluoro-L-m-tyrosine produce comparable images in control subjects and Parkinsonian patients (Figures 9.5 and 9.7), Figure 9.6 shows that the ^{18}F associated with these agents follows different time courses in the cerebral tissues. Thus, the ratio striatum : occiput at 120 min. is 4.4 : 1 in the case of the [^{18}F]fluoro-L-m-tyrosine (Figure 9.6 b) and only 1.7 : 1 with [^{18}F]6-fluorodopa (Figure 9.6 a). Figure 9.5 also shows that the better striatum : occiput ratio with the [^{18}F]fluoro-L-m-tyrosine is not the result of improved striatal retention of ^{18}F but is a consequence of the much lower retention of isotope in non-dopaminergic tissues.

Analysis of the [^{18}F] metabolites in the monkey brain and plasma indicate that when [^{18}F]fluoro-L-m-tyrosine is injected intravenously, some of the amino acid is decarboxylated and then oxidatively deaminated by peripheral monoamine oxidase. Thus, at later times the blood contains varying proportions of [^{18}F]fluoro-L-m-tyrosine and [^{18}F]fluoro-3-hydroxyphenylacetic acid, (Figure 9.10). When [^{18}F]fluoro-3-hydroxyphenylacetic acid is injected alone almost no ^{18}F enters the brain (Figure

9.8 b). Peripherally formed [^{18}F]fluoro-3-hydroxyphenylacetic acid can therefore contribute very little ^{18}F to any part of the brain. These results confirm that the metabolism of fluoro-L-m-tyrosine (Scheme 9.3) is simpler than that of fluorodopa (Scheme 9.1).

Scheme 9.3

METABOLISM OF FLUORO-m-TYROSINE

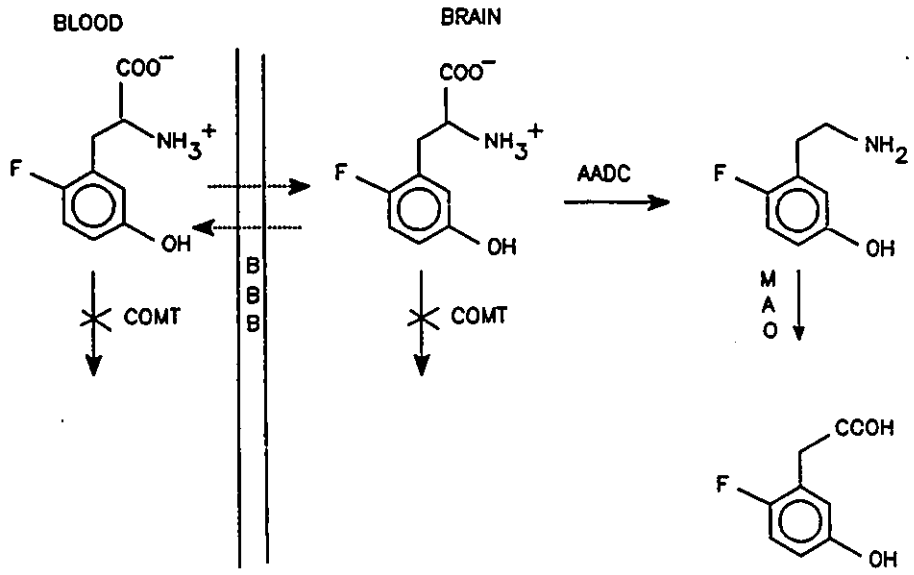

After an intravenous injection of [^{18}F]6-fluorodopa, the situation is very different. [^{18}F]Fluorodopa in the blood is O-methylated by catechol-O-methyl transferase and it is claimed that, in man, given the peripheral decarboxylase

inhibitor carbidopa, that 3-methoxy-fluorodopa is the only intravascular metabolite of fluorodopa.[152] When 3-methoxy-[^{18}F]fluorodopa is injected intravenously it, unlike [^{18}F]fluoro-3-hydroxyphenylacetic acid, enters the brain where it is retained (Figure 9.9). Measurement of the [^{18}F] distribution in the striatum and occiput, using [^{18}F]fluoro-3-hydroxyphenyl-acetic acid and 3-methoxy-[^{18}F]6-fluorodopa, show that relative to [^{18}F]fluoro-3-hydroxyphenylacetic acid, the intracerebral concentration of ^{18}F after an equivalent dose of 3-methoxy-[^{18}F]fluorodopa is at all times 20 fold greater. It can be concluded that this non-specific accumulation of the O-methylated metabolite of [^{18}F]fluorodopa accounts for some of the retention of ^{18}F in non-dopaminergic tissue and hence the lower striatum : occiput ratio in PET images obtained after [^{18}F]fluorodopa.

When the time activity curve of striatal ^{18}F after injection of [^{18}F]fluoro-L-m-tyrosine in Figure 9.5 b is replotted according to the method of Patlak *et al.*,[183] the graph of A(T)striatum/Cp(T) in the normalized time interval 40 to 150 min. is a straight line with a positive slope, 1.6 x 10^{-2} min^{-1} (Figure 9.11). This implies that [^{18}F]fluoro-L-m-tyrosine leaves the blood, and enters what Patlak calls an "irreversible region". This implication is supported by the analyses of brain parts from monkeys presented in Figure 9.10

Figure 9.11 Graphical analysis of the time activity curve for the striatum of a normal brain after the injection of [^{18}F]fluoro-L-m-tyrosine.

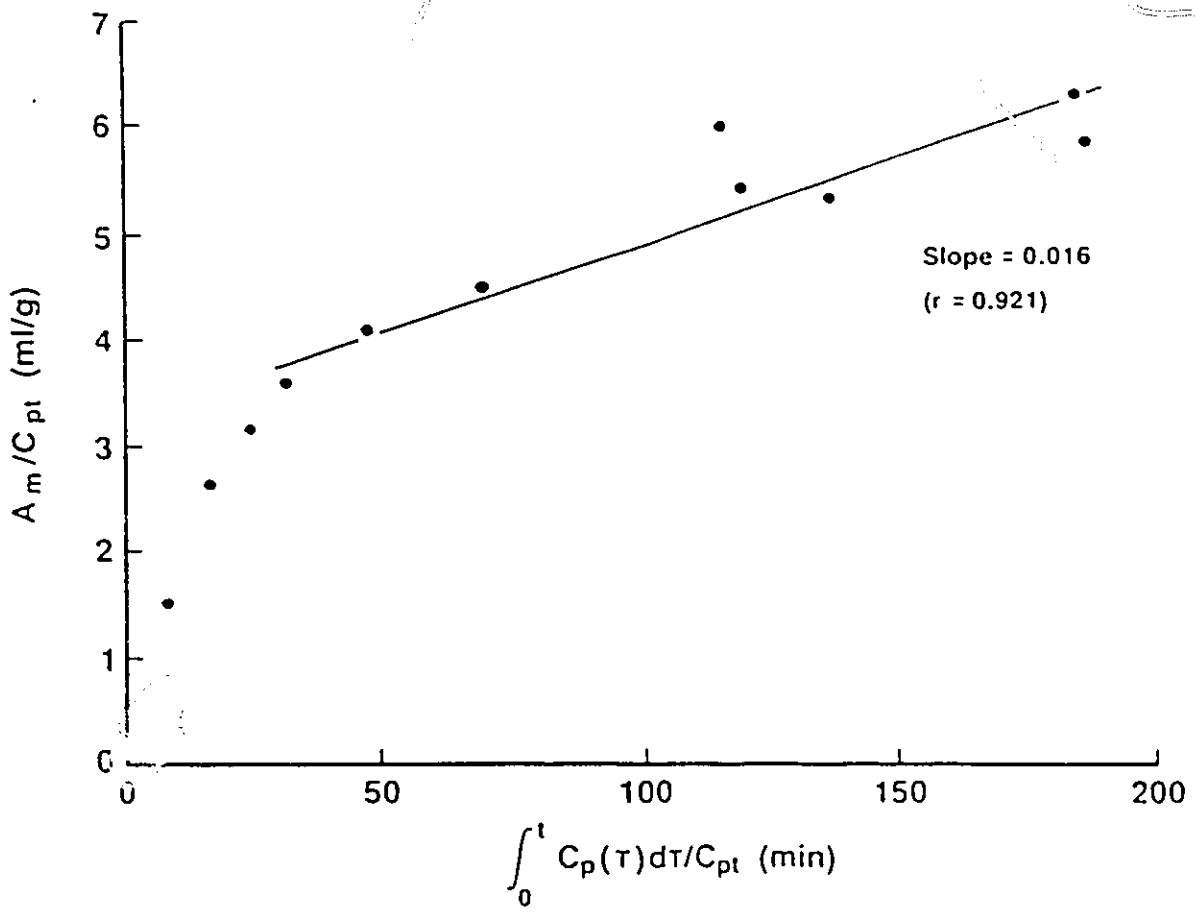
7
6
5
4
3
2
1
0
0
50
100
150
200
A_m/C_{pt} (ml/g)
$\int_0^t C_p(\tau)d\tau/C_{pt}$ (min)
Slope = 0.016
(r = 0.921)

where it is seen that the predominant intracerebral ^{18}F containing species after inter venous injection of [^{18}F]fluoro-L-m-tyrosine is [^{18}F]fluoro-3-hydroxy- phenylacetic acid. In rats, similar results have been reported when [^{18}F]4-fluoro-L-m-tyrosine was given.[72]

Conclusions

Results from the present work confirm that [^{18}F]fluoro-m-tyrosine can be used as a tracer to study striatal aromatic acid decarboxylase activity. Further, because of its simpler metabolic pathway and its much more favourable striatum to occiput [^{18}F] accumulation, [^{18}F]fluoro-L-m-tyrosine will probably supersede [^{18}F]fluorodopa as a tracer for the dopaminergic pathway in man.

REFERENCES

1. M. Henri Moissan, Le Fluor et ses Composés, Paris, G. Steinheil, 1900.
2. H.G. Bryce, "Industrial and Utilitarian Aspects of Fluorine Chemistry" in Fluorine Chemistry J.H. Simons Ed. Academic Press. N.Y. (1964), Vol. 5, Chap.4
3. P.Leveque and H. Goenvec, Bull. Soc. Chim. France (1955) p. 1213.
4. H.W. Newson, Phys. Rev. (1935) 48, 790.
5. A.H. Snell, Proc. Am. Phys. Soc. (1936) 51, 143.
6. Sir. H. Davy, Phil. Trans. (1813) 103, 263.
7. H.R. Crane, L.A. Delsasso, W.A. Fowler and C.C. Lauristen, Phys. Rev. (1935) 48, 971.
8. C.B. Bigham, K.W. Allen and E. Alanquist, Phys. Rev. (1955) 99, 631.
9. J.A. Worthington Jr. "Radiochemistry and Radiation Chemistry of Fluorine" in Fluorine Chemistry J.H. Simons Ed. Academic Press. N.Y. (1964) Vol. 5, Ch. 3.
10. J.J. Sunderland, O.T. DeJesus, O. Solin and R.J. Nickles, 8th International Symposium on Radiopharmaceutical Chemistry Princeton, N.J. (1990) p. 89.
11. J.M. Winfield, J. Fluorine Chem. (1980) 16, 1.
12. M. Azeem, M. Brownstein and R.J. Gillespie, Can. J. Chem. (1969) 47, 4159.

13. M.Blau, W. Naglar and M.A. Bender, J. Nucl. Med. (1962) 3, 332.

14. T. Jones, D.A. Chester and Ter-Pogossian, Br. J. Radiol. (1976) 49, 339.

15. M.E. Raichle, W.R.W. Martin, P. Herscovitch, M.A. Mintuir and J. Markham, J. Nucl. Med. (1983) 24, 790.

16. R. Filler, J. Fluorine Chem. (1986) 33, 361.

17. G. Firnau, S. Sood, R. Chirakal, C. Nahmias and E.S. Garnett, J. Neurochem. (1987) 48, 1077.

18. G. Firnau, S. Sood, R. Chirakal, C. Nahmias and E.S. Garnett, J. Nucl. Med. (1988) 29, 363.

19. R. Cumming, M. Houser, W.R.W. Martin, J. Grierson, M.J. Adam, T.J. Ruth and E.G. McGreer, Biochem. Pharmacol. (1988) 37, 247.

20. G. Baltz and G. Schiemann, Ber. (1927) 60B, 1186.

21. A.J. Palmer, J.C. Clark and R.W. Goulding, "Radiopharmaceuticals and Other Labelled Compounds With Short-Lived Radionuclides". M.J. Welch (ed.), Pergamon Press, New York, N.Y. (1977) p. 53.

22. R.M. Hoyte, S.S. Lin, D.R. Christman, H.L. Atkins, W. Hanser and A.P. Wolf, J. Nucl. Med. (1971) 12, 280.

23. A.J. Palmer, J.C. Clark, R.W. Goulding and M. Roman, "Radiopharmaceuticals and Labelled Compounds". IAEA, Proc. Ser. Vienna (1977) Vol. 1, p. 275.

24. H.L. Atkins, D.R. Christman, J.S. Fowler, W. Hanser, R.M. Hoyle, J.F. Klopper, S.S. Lin and A.P. Wolf, J. Nucl. Med. (1972) 13, 713.

25. G. Firnau, C. Nahmias and E.S. Garnett, J. Appl. Radiat. Isot. (1973) 24, 182.

26. O. Wallach, Ann. Chem. (1888) 235, 255.

27. T.J. Tewson and M.J. Welch, J. Chem. Soc. Chem. Commun. (1979) 1149.

28. M.R. Kilbourn, M.J. Welch, C.S. Dence, T.J. Tewson, H. Saji and M. Maede, J. Appl. Radiat. Isot. (1984) 85, 591.

29. R. Chirakal, G. Firnau and S. Sood, unpublished results.

30. M.S. Berridge and T.J. Tewson, J Appl. Radiat. Isot. (1986) 37, 685.

31. F. Cacace, M. Sperenza, A.P. Wolf and F.S. Fowler, J. Label. Compound Radiopharm. (1981) 18, 1721.

32. F. Cacace, M. Sperenza, A.P. Wolf and R.R. MacGregor, J. Fluorine Chem. (1982) 21, 145.

33. C.Y. Shiue, M. Watanabe, A.P. Wolf, J.S. Fowler and P. Salvadori, J. Label. Compound Radiopharm. (1984) 21, 533.

34. M.S. Berridge, C. Crouzel and D. Comar, J. Label. Compound Radiopharm. (1985) 22, 687.

35. M.R. Kilbourn, "F-18 Labelling of Radiopharmaceuticals" Nuclear Science Series NAS-NS-3203 (1990) National Academy Press, Washington, D.C.

36. C.Y. Shiue, J.S. Fowler, A.P. Wolf, M. Watanabe and C.D. Arnett, J. Nucl. Med. (1985) 26, 181.

37. U.S. Berridge and T.J. Tewson, 6th International Symposium on Radiopharmaceutical Chemistry, Boston (1986), p. 67.

38. T. Irie, F. Fukushi, T. Ido, T. Nozaki and Y. Kasida, J. Appl. Radiat. Isot. (1984) 35, 517.

39. K. Hamachar, H.H. Coenen and G. Stocklin, J. Nucl. Med. (1986) 23, 1047.

40. K.O. Christe, J. Fluorine Chem. (1983) 22, 519.

41. M. Cartwright and A.A. Wolf, J. Fluorine Chem. (1984) 25, 263.

42. K.O. Christe, J. Fluorine Chem. (1984) 25, 269.

43. M.M. Eakins and S. Somaia, J. Label. Compound Radiopharm. (1979) 16, 149.

44. R.E. Ehrenkaufer and R.R. MacGregor, J. Appl. Radiat. Isot. (1983) 34, 613.

45. N. Satyamurthy, G.T. Bida, J.R. Barrio and M.E. Phelps, J. Nucl. Med. (1984) 25, 23.

46. F. Oberdofer, E. Hofman and W. Maier-Frost, J. Label. Compound Radiopharm. (1988) 25, 999.

47. R. Chirakal, G. Firnau, G.J. Schrobilgen, J. McKay and E.S. Garnett, J. Appl. Radiat. Isot. (1984) 35, 401

48. G.J. Schrobilgen, G. Firnau, R. Chirakal and E.S. Garnett, J. Chem. Soc. Chem. Commun. (1981) 198.

49. G. Firnau, R. Chirakal and S. Sood, J. Label. Compdound Radiopharm. (1981) 18, 7.

50. G. Firnau, R. Chirakal and S. Sood, Can. J. Chem. (1980) 58, 1149.

51. S. Rozen, O. Lerman and M. Kol, J. Chem. Soc. Chem. Commun. (1981) 443.

52. C.Y. Shiue, P.A. Salvadori, A.P. Wolf, J.S. Fowler and R.R. MacGregor, J. Nucl. Med. (1982) 23, 899.

53. D.M. Jewett, J.F. Potocki and R.E. Ehrenkaufer, J. Fluorine Chem. (1984) 24, 477.

54. R. Chirakal, G. Firnau, J. Couse and E.S. Garnett, J. Appl. Radiat. Isot. (1984) 35, 651.

55. M.J. Adam, T.J. Ruth, J.R. Grierson, B.Abeysekera and B.D. Pate, J. Nucl. Med. (1986) 27, 1462.

56. H.H. Coenen, K. Franken, S. Metwally and G. Stocklin, 6th International Symposium on Radiopharmaceutical Chemistry, Boston (1986) p. 151.

57. H.H. Coenen, P. Kling and G. Stocklin, J. Nucl. Med. (1988) 29, 754.

58. M.J. Adam, J. Appl. Radiat. Isot. (1986) 37, 811.

59. H.H. Coenen and S. Morelein, J. Fluorine Chem. (1987) 36, 63.

60. A. Luxen, J.R. Barrio, G.T. Bida and N. Satyamurthy, J. Label. Compound. Radiopharm. (1986) 23, 1066.

61. J.R. Barrio, M.M. Perlmulter, A. Luxen, W.P. Melega, S.T. Grafton, S.C. Huang, J.M. Hoffman, G. Van Moffaert, J.C. Maziotta and M.E. Phelps, J. Nucl. Med. (1989) 30, 752.

62. D.L. Gildersleeve, M.E. VanDort, K.C. Rosenspire, S. Toorongian and D.M. Wieland, J. Nucl. Med. (1989) 30, 752.

63. W.A. Sheppard and C.M. Sharts, "Organic Fluorine Chemistry". W.A. Benjamin Inc., N.Y., (1969) p. 602.

64. C.M. Sharts, J. Chem. Educ. (1968) 45, 187.

65. L.A. Bigelow and N. Fukuhara, J. Am. Chem. Soc. (1941) 63, 788, 2792.

66. R.J. Lagow and J.L. Margrave, Prog. Inorg. Chem. S.J. Lippard (ed.) (1979) 26, 161.

67. F. Cacace and A.P. Wolf, J. Am. Chem. Soc. (1978) 100, 3639.

68. R. Chirakal, G. Firnau and E.S. Garnett, J. Nucl. Med. (1986) 27, 417.

69. J.H. Tong, C. Petitclerc, A. D'Iorio and N.L. Benoiton, Can. J. Biochem. (1971) 49, 877.

70. V. Casella, T. Ido, A.P. Wolf, J. Fowler, MacGregor and T.J. Ruth, J. Nucl. Med. (1980) 21, 750.

71. J. Szabo and W.M. Cowan, J. Comp. Neurology (1984) 222, 265.

72. W.P. Melega, M.M. Perlmutter, A. Luxen, C.H.K. Nissenson, S.T. Grafton, S. Huang, M.E. Phelps and J.R. Barrio, J. Neurochem. (1989) 53, 311.

73. C. Nahmias, Nucl. Instrum. and Methods (1984) 221, 113.

74. C. Nahmias, G. Firnau and E.S. Garnett, IEEE Trans. Nucl. Sci. (1984) NS-31, 637.

75. C. Nahmias, D.B. Kenyon and E.S. Garnett (1982) NS-29, 1.

76. D.F. Shriver, P.W. Atkins and C.H. Langford, "Inorganic Chemistry" (W.H. Freeman and Co., NY.) 1990, P.42

77. (a) J.E. Huheey, "Inorganic Chemistry" Second ed.,Harper and Row: New York, N.Y. 1978, Chap. 17. (b) A.E. Reed and P.Von R. Schleyer, J. Am. Chem. Soc. (1990) 112, 1434.

78. G.A. Olah, G. Klopman and R.H. Schlosberg, J. Am. Chem. Soc. (1969) 91, 3261.

79. G.A. Olah, P.W. Westerman, Y.K. Mo and G. Klopman, J. Am. Chem. Soc. (1972) 94, 7859.

80. C.T. Goetschel, V.A. Campanile, R.M. Curtis, K.R. Loos, C.D. Wagner and J.N. Wilson, Inorg. Chem. (1972) 11, 1696.

81. I.J. Solomon, J.N. Keith and A. Snelson, J. Fluorine Chem. (1972/73) 2, 129.

82. J.N. Keith, I.J. Solomon, I. Sheft and H. Hyman, Inorg. Nucl. Chem. Suppl. (1976) 143.

83. G.A. Olah, D.J. Donovan, J. Shen and G.J. Klopman, J. Am. Chem. Soc. (1975) 97, 3559.

84. R.W. Johnson and E.R. Holm, J. Am. Chem. Soc. (1977) 99, 8077.

85. J.N. Murrell and C.E. Scollary, J. Chem. Soc. Dalton Trans. (1976) 818.

86. F. Keil and W. Kutzelnigg, J. Am. Chem. Soc. (1975) 97, 3623.

87. G. Morosi and M. Simonetta, Chem. Phys. Lett. (1977) 47, 396

88. C.S. Ewig and J.R. Van Wazer, J. Am. Chem. Soc. (1989) 111, 4172.

89. H.H. Michels and J.A. Montgomery, Abstracts of Air Force High Energy Density Materials Contractors' Conference; Long Beach, California. Feb., 1990.

90. H.S. Winchell, D.K. Wells, J.F. Lamb and S.B. Beavdy, U.S. Patent (1976) 3, 981, 769.

91. J.R. Dhal, R.E. Bigler, B. Small and J.E. Aber, J. Appl. Radiat. Isot. (1983) 34, 693.

92. T.J. Tewson and M.J. Welch, J. Nucl. Med. (1980) 21, 559.

93. M.J. Welch, J.F. Lifton and P.P. Gaspar, J. Nucl. Med. (1971) 12, 405 (Abstract).

94. R.M. Lambercht, R. Neirineck and A.P. Wolf, J. Appl. Radiat. Isot. (1978) 29, 175.

95. K.O. Christe, J.P. Guertin, A.E. Pavalath and W. Sawodny, Inorg. Chem. (1967) 6, 533.

96. C.S. Ewig and J.R. Van Wazer, J. Am. Chem. Soc. (1990) 112, 109.

97. K.O. Christe, C.J. Shack and R.D. Wilson, Inorg. Chem. (1976) 15, 1275.

98. K.O. Christe, W.W. Wilson and R.D. Wilson, Inorg. Chem. (1980) 19, 1494.

99. K.O. Christe, R.D. Wilson and I.B. Goldberg, Inorg. Chem. (1979) 18, 2572.

100. G.J. Schrobilgen, private communication

101. N.N. Greenwood and A. Earnshaw, "Chemistry of The Elements" Pergamon Press. New York, N.Y. 1986.

102. O. Ruff and R. Keim, Z. Anorg. Allg. Chem. (1930) 193, 176.

103. G.J. Schrobilgen and J.C.P. Sanders, private communication.

104. J.G. Malm, H. Selig and S. Fried, J. Am. Chem. Soc. (1960) 82, 1510.

105. O. Glemser, H.W. Roesky, K.H. Hellberg and H.U. Werther, Chem. Ber. (1966) 99, 2652.

106. A.A. Timakov, V.N. Prusakov, Yu.V. Drobyshevskii, Dokl. Chem. (1986) 291, 442.

107. C.E. Fogle and R.T. Rewick, U.S. Patent 3, 615, 206 (1971).

108. R.J. Gillespie and G.J. Schrobilgen, Inorg. Chem. (1974) 13, 1230.

109. K.O. Christe, Inorg. Nucl. Chem. Lett. (1972) 8, 741.

110. K.O. Christe, Inorg. Chem. (1973) 12, 1580.

111. K.O. Christe and W.W. Wilson, Inorg. Chem. (1989) 28, 3275.

112. K.O. Christe and H. Oberhammer, Inorg. Chem. (1981) 20, 296.

113. R. Bougon, Bull. Inf. Sci. Tech. Commis. Energ. At. (Fr) (1971) 161, 9.

114. M.T. Rogers and J.J. Katz, J. am. Chem. Soc. (1952) 74, 1375.

115. R.C. Adams, R.B. Bernstein and J.J. Katz, J. Chem. Phys. (1954) 22, 13.

116. J.Shamir in "Structure and Bonding" Springer Verlag New York, N.Y. (1979) 37, 141.

117. E.D. Whitney, R.O. MacLaren, C.E. Fogle and T.J. Hurley, J. Am. Chem. Soc. (1964) 86, 2583.

118. H.J. Emeleus and A.G. Sharpe, J. Chem. Soc. (1949) 2206.

119. K.O. Christe, W.W. Wilson and R.D. Wilson, Inorg. Chem. (1989) 28, 675.

120. K.O. Christe and W.W. Wilson, Inorg. Chem. (1983) 22, 1950.

121. A.R. Boate, J.R. Morton and K.R. Preston, Inorg. Chem. (1975) 14, 3127.

122. D. Pilipovich, W. Maya, E.A. Lawton, H.F. Bauer, D.F. Sheehan, N.N. Ogimachi, R.D. Wilson, F.C. Gunderloy and B.E. Bedwell, Inorg. Chem. (1967) 6, 1918.

123. M. Alexandre and P. Rigny, Can. J. Chem. (1974) 52, 3676.

124. R.J. Gillespie, "Molecular Geometry", Van Nostrand Reinhold Co., London, 1972.

125. P. Goulet, R. Jurek and J. Chanussot, J. Phys. (1976) 37, 495.

126. R.T. Boere and R.G. Kidd, Annu. Rep. on NMR Spectrosc., (1982) 13, 320.

127. C.J. Jameson and H.J. Osten, J. Am. Chem. Soc. (1985) 107, 4158.

128. K.O. Christe, J.F. Hon and D. Pilipovich, Inorg. Chem. (1973) 12, 84.

129. W. Gombler, Z. Naturforsch. (1985) 40B, 782.

130. C.J. Jameson, J. Chem. Phys. (1977) 66, 4983.

131. G.M. Begun, W.H. Fletcher and D.F. Smith, J. Chem. Phys. (1965) 42, 2236.

132. A.G. Robiette, R.H. Bradley and P.N. Brier, J. Chem. Soc. Chem. Commun. (1971) 1567.

133. J.C.P. Sanders and G.J. Schrobilgen, private communication.

134. W.B.Fox, J.S. MacKenzie, E.R. McCarthy, J.R. Holmes, R.F. Small and R.Juurik, Inorg. Chem. (1968) 7, 2064.

135. N. Bartlett, J. Passmore and E.J. Wells, Chem. Commun. (1966) 213.

136. K.O. Christe, W.W. Wilson, R.V. Chirakal, J.P.Sanders and G.J. Schrobilgen, Inorg. Chem. (1990) 29, 3504.

137. G. Litzka, Klin Wochschr (1936) 15, 1568 (C.A., 31, 3567)

138. G.C. Finger, Chem. Met. Eng. (1944) 51, 101

139. G. Schiemann and W. Winkelmuller, J. Prakt. Chem. (1932) 135, 101.

140. A.J. Palmer, J.C. Clark, R.W. Goulding and M. Roman, "Radiopharmaceuticals and Labelled Compounds" IAEA Proc. Ser. Vienna (1973) Vol. 1, p. 275.

141. D.M. Taylor and M.F. Cottrail "Symposium on New Developments in Radiopharmaceuticals and Labelled Compounds" Copenhagen, Mar. 26-30 (1973).

142. E. Breitmeuer and W. Voelter (1974) "^{13}C NMR Spectroscopy", Hans F. Ebel (editor), Verlag Chemie GmbH, Weinheim/Bergstr, p. 171.

143. T. Birchall, A.N. Bourns, R.J. Gillespie and P.J. Smith, Can. J. Chem. (1964) 42, 1433

144. G.A. Olah and Y.K. Mo, J. Org. Chem. (1973) 38, 353.

145. D.M. Brouwer, E.L. Mackor and C. Maclean. Rec. Trav. Chim. (1966) 27, 417.

146. H.H.Coenen, K. Franken, P. Kling and G. Stocklin, J. Appl. Radiat. Isot. (1988) 39, 1243.

147. S. Misaki, J. Fluorine Chem. (1981) 17, 159.

148. S. Misaki, J. Fluorine Chem. (1982) 21, 191.

149. F. Cacace and A.P. Wolf, J. Am. Chem. Soc. (1978) 100, 3639.

150. E.S. Garnett, G. Firnau and C. Nahmias, Nature (1983) 305, 137.

151. G. Firnau, S. Sood, R. Chirakal, C. Nahmias and E.S. Garnett, J. Nucl. Med. (1988) 29, 363.

152. B.E. Boyes, P. Cumming, W.R.W. Martin, and E.G. McGeer, Life Sci. (1986) 39, 2243.

153. E.S. Garnett, A.E. Lang, R. Chirakal, G. Firnau and C. Nahmias, Can. J. Neurosci. (1987) 14, 444.

154. H. Blaschko and T.L. Chrusciel, J. Physiol. (1960) 151, 272.

155. W. Oldendorf, Arch. Neurol. (1973) 28, 45.

156. H.C. Guldberg, C.A. Marsden, Pharmacol. Rev. (1975) 27, 135.

157. O.T. DeJesus, J. Mukherjee and E.H. Appelman, 7th International Symposium on Radiopharmaceutical Chemistry, Groningen, The Netherlands, July 4-8 (1988).

158. M.Clark and J.S. Thrasher, J. Chem. Educ. (1990) 67, 235.

159. E. Gil-Av, A. Tishbee and P.E. Hare, J. Am. Chem. Soc. (1980) 102, 5115.

160. D.M. Brouwer, E.L. Mackor and C. MacLean, Recuil. (1966) 85, 1090.

161. H. Hogveen, A.F. Bickel, C.W. Hilbers, E.L. Mackor and C. MacLean, J. Chem. Soc. Chem. Commu. (1966) 898.

162. S. Rozen, Acc. Chem. Res. (1988) 21, 307.

163. M.J. Adam, J.R. Frierson, T.J. Ruth, and S. Jivan, Appl. Radiat. Isot. (1986) 37, 877.

164. O.T. DeJesus, J.H. Sunderland. J.R. Nickles, J. Mukherjee and E.H. Appelman, J.Appl. Radiat. Isot. (1990) 41, 433.

165. O.T. DeJesus, D. Murali, C.A. Chen, J.J. Sunderland, M. Weiler and R.J. Nickles, 8th International Symposium on Radiopharmaceutical Chemistry, Princeton, NJ. June 24-29 (1990) (Abstract).

166. O.T. DeJesus, J. Mukherjee and E.H. Appelman, J. Label. Compound. Radiopharm. (1989) 26, 189.

167. C. MacLean and E.L. Mackor, Discussions. Faraday Soc. (1962) 34, 165.

168. E.C. Taylor, F. Kiengle, R.L. Robey, A. McKillop and J.D. Hunt, J. Am. Chem. Soc. (1971) 93, 4845.

169. M.J. Adams, UBC/TRIUMF, Vancouver, B.C., Canada (Personal Communication).

170. O.Solin, G. Firnau, M. Haaparanta, R. Chirakal, H. Sipila, E.S. Garnett and C. Nahmias, 6th International Symposium on Radiopharmaceutical Chemistry, Boston, June-29 - July 4, 1986.

171. R.D. Howells and J.D. McCowan, Chem. Rev., (1977) 77, 69.

172. P.J. Stang and M.R. White, Aldrichimica Acta (1983)16,15.

173. R.F. Childs and B.E. George, Can. J. Chem. (1987) 66, 1343.

174. L.L. Iversen, Lancet (1982) 914.

175. O. Hornykiewicz, In "Movement Disorders" (C.A. Marsden and S. Fahn Eds.) Butterworth Scientific, London. 1982.

176. W.R.W. Martin, M.R.Palmer, C.S. Patlak and D.B. Calne, Ann. Neurol. (1989) 26, 535.

177. G.V. Sawle, J.G. Colebatch, A. Shah, D.J. Brooks, C.D. Marsden and R.S.J. Frackowiak, Ann. Neurol. (1990) 28, 799.

178. H.H. Coenen, P. King and G. Stocklin, J. Nucl. Med. (1989) 30, 1367.

179. P. Cuming, M. Houser, W.R.W. Martin, J. Grierson, M.J. Adam, T.J. Ruth and E.G. McGreer, Biochem Pharmacol. (1988) 37, 247.

180. K.G. Lloyd and O. Hornykiewicz, J. Neurochem. (1972) 19, 1549.

181. S.R. Philips, R. Rozdilsky and A.A Boulton, Biol. Psychiatry. (1978) 13, 51.

182. S.J. Kish, K. Shannak and O. Hornykiewiez, N. Engl. J. Med. (1988) 318, 876.

183. C.S. Patlak, R.G. Blasberg and J.D. Fenstermacher, J. Cereb. Blood Flow and Metab. (1983) 3, 1.